

**CONTROL OF NOZZLE AND CAVITY PRESSURE
DURING FILLING AND PACKING IN
THERMOPLASTICS INJECTION MOLDING**

by

DIB I. ABU FARA

**A Thesis Submitted to the Faculty of Graduate Studies
and Research in Partial Fulfillment of the
Requirements for the Degree of
Doctor of Philosophy**

**Department of Chemical Engineering
McGill University
Montreal**

© August 1988

ABSTRACT

Thermoplastics injection molding involves plastication followed by the injection of the melt into a cold cavity. Packing is employed to compensate for shrinkage due to cooling. Ultimately, the solidified part is ejected from the mold without damage. The successful operation of an injection molding machine requires control of the process variables during each of the consecutive stages in addition to correctly identifying the points of transition from one stage to the next.

Pressure and its variation during the injection molding cycle play an important role with regard to productivity, product quality, and product reproducibility. From the practical point of view, it is necessary to consider simultaneously hydraulic pressure, nozzle pressure, and the distribution of pressure in the cavity. Control of each phase of the injection molding process is best achieved by controlling one or a combination of the above pressure parameters. The present work describes a comprehensive study of the dynamics and control of pressure during each stage of the injection molding cycle.

Deterministic models were obtained for cavity gate pressure during the filling and packing stages. Dynamic model predictions were in good agreement with experimental data. The response of cavity gate pressure exhibited nonlinear behavior which was investigated and rectified by a gain scheduling control strategy. Stochastic models were obtained for cavity gate pressure response in the filling stage for the purpose of comparison and future design of more advanced control algorithms.

The dynamic models were employed to design and evaluate control schemes for the injection molding cycle. Nozzle and cavity pressures were used in conjunction with PI, PID and Dahlin controllers. The hydraulic system of the injection

molding machine was redesigned to incorporate two servovalves in order to achieve control over the cavity pressure-time profile during the packing stage as well as over peak cavity and hold pressures. The control loops were designed through a simulation study which also gave good indications of system limitations.

On the basis of this study, very good and reliable integrated control over the filling, packing, and holding stages was achieved by a general control scheme which allows the transfer of control from one variable to another during the various stages of the process.

R E S U M E

Le moulage par injection des thermoplastiques comprend la plastification de la matière d'un état solide, suivi de l'injection du polymère fondu dans la cavité froide du moule. Le compactage est utilisé pour compenser le retrait dû au refroidissement. A la fin du cycle, presque toute la pièce est solidifiée, permettant ainsi son éjection avant le prochain cycle. La conduite satisfaisante de la machine à injection réclame le contrôle des variables du procédé pendant chacune des étapes consécutives, en plus d'identifier correctement les points de transition d'un stage à l'autre.

La valeur de la pression d'injection et ses variations au cours du cycle joue un rôle important vis à vis de la productivité et de la qualité du produit fini. Du point de vue pratique, il est nécessaire de considérer en même temps les pressions hydraulique et en buse et également la distribution des pressions dans le moule. Le contrôle de chacune des phases du procédé est mieux exécuté par le contrôle d'une ou d'une combinaison de plusieurs de ces pressions. Cette thèse présente une étude globale de la dynamique et du contrôle de la pression pendant chaque étape du cycle d'injection.

Des modèles déterministiques ont été obtenus pour des pressions au seuil de la cavité durant les phases de remplissage et de compactage. Les prédictions du modèle dynamique montre un bon recoupage avec les données expérimentales. Une stratégie de contrôle prédéterminé du gain a permis de rectifier, après investigation, le comportement non-linéaire de la réponse en pression au seuil du moule. Des modèles stochastiques ont été obtenus pour la réponse en pression au seuil lors de la phase de remplissage, dans le but d'être utilisés comme moyen de comparaison et de vérification.

Les modèles dynamiques ont été utilisés afin d'évaluer des schémas de contrôle pour le cycle d'injection. Le système hydraulique de la machine a été modifié en vue d'obtenir un contrôle du profil de pression de la cavité au cours du temps pendant le compactage, ainsi qu'un contrôle de sa pression maximale et de maintien.

Un schéma de contrôle général a permis de réaliser, sur la base de cette étude, un contrôle intégré performant et sûr pour les phases de remplissage, de compactage et de maintien, ce qui permet de passer du contrôle d'une variable à celui d'une autre au cours des différentes phases du procédé.

ACKNOWLEDGEMENTS

I wish to express my sincere gratitude to my research directors, Professor and Chairman Musa R. Kamal and Professor W. Ian Patterson for their advice and guidance throughout the course of this work. I would also like to convey my appreciation for their critical review of the thesis which instilled some measure of clarity and completeness in this work. I am grateful to my research committee: Professor O.M. Fuller, Mr. M. Perrier, Mr. V. Gomes, and Mr. R. DiRaddo for their helpful comments and suggestions.

I wish to thank Mr. A. Krish and the staff of the machine workshop for their assistance in modifying the experimental equipment. My thanks extend to Mr. J. Dumont, Mr. L. Cosmitch, and Mr. N. Habib for their help in supplying the research facilities and instrumentation.

I wish to thank Mr. A. Kallos and Miss S. Nassehi for their help in using the VAX computer and the Applicon system.

I wish to thank my colleagues in the polymer group in particular O. Khennache, P. Singh, M. Samara, T. Mutel, E. Chu, G. Ruscitti, and H. Musa for their valuable discussions and comments throughout the project. Special thanks to Mr. Khennache for translating the French abstract.

I like to thank The University of Jordan for financial support in the form of a scholarship which enabled the achievement of this study.

I wish to thank DuPont of Canada, for supplying the material used in this study.

The financial support from the Department of Chemical Engineering at McGill University, the Natural Science and Engineering Research Council of Canada, and the Ministère de l'Education du Gouvernement du Québec is also acknowledged. The financial support of my dear friend A. Amro is not to be forgotten.

Last, but certainly not least, I would like to express my deepest gratitude to my family, in particular my wife, for their unlimited love, support and encouragement.

TABLE OF CONTENTS

ABSTRACT	i
RESUME	iii
ACKNOWLEDGMENTS	v
TABLE OF CONTENTS	vii
LIST OF TABLES	xii
LIST OF FIGURES	xiv
 1. INTRODUCTION	 1
 2. RESEARCH OBJECTIVES	 6
 3. GENERAL BACKGROUND	 10
3.1 Introduction	10
3.2 Process Modelling and Identification	11
3.2.1 Theoretical Modelling	12
3.2.2 Experimental Modelling	12
3.2.2.1 Deterministic Identification	14
3.2.2.2 Stochastic Identification	15
3.2.2.2.1 Off-Line Identification	19
3.2.2.2.2 On-Line Identification	20
3.3 Application of Process Modelling to the Injection Molding Process	22
3.3.1 Mathematical Modelling of Injection Molding	22
3.3.1.1 Modelling of the Plastication Stage	22
3.3.1.2 Modelling of the Filling and Packing Stages	23
3.3.1.3 Applications of Mathematical Models	24
3.3.2 Interactions Between Process Variables	25
3.3.3 Dynamic Models and Control Applications to the Injection Molding Process	31

3.4	Sequential Control	47
3.4.1	Switching Based on Ram Position	47
3.4.2	Switching Based on Hydraulic Pressure	48
3.4.3	Switching Based on Cavity Pressure	49
3.4.4	Switching Based on Mold Separation	50
4.	EXPERIMENTAL	52
4.1	Equipment	52
4.1.1	Injection Molding Machine	52
4.1.2	Instrumentation	55
4.1.3	Microcomputer System	58
4.2	Material	61
4.3	Experimental Procedure	61
5.	DYNAMIC MODELLING OF THE FILLING STAGE	65
5.1	Machine Operation and Characterization	65
5.1.1	Injection Start-Up Stage	67
5.1.2	Filling Stage	67
5.1.3	Filling to Packing Transition	74
5.1.4	Packing Stage	77
5.1.5	Summary	82
5.2	Dynamic Modelling of Cavity Gate Pressure	83
5.2.1	Deterministic (Step) Tests	83
5.2.1.1	Results and Discussions	84
5.2.2	Stochastic (PRBS) Tests	99
5.2.2.1	Results and Discussion	100
5.2.2.2	Comparison Between the Deterministic and Stochastic Models	116
5.2.3	Summary	116
5.3	Dynamics of Cavity Pressure Gradient	118

6.	CONTROL OF THE FILLING STAGE OF THE INJECTION CYCLE . . .	123
6.1	Discrete-Time Control Algorithms	123
6.1.1	PID Controller	124
6.1.2	Dahlin Controller	128
6.2	Discrete Dynamic Models	130
6.2.1	Hydraulic Pressure Model	131
6.2.2	Nozzle Pressure Model	134
6.2.3	Cavity Pressure Model	137
6.3	Control Loop Design	140
6.3.1	Controller Tuning	140
6.3.2	Sampling Interval	144
6.4	Control Loop Simulation	147
6.4.1	Hydraulic Pressure Control Loop Simulation . .	148
6.4.2	Nozzle Pressure Control Loop Simulation . .	155
6.4.3	Cavity Pressure Control Loop Simulation . .	176
6.4.4	Summary	183
6.5	Filling Stage Control Experiments	185
6.5.1	Experimental Nozzle Pressure Control . . .	186
6.5.2	Experimental Cavity Pressure Control . . .	191
6.5.3	Summary	197
7.	DYNAMIC MODELLING OF THE PACKING STAGE	198
7.1	Feasibility of Packing Pressure Control	199
7.1.1	Modification of the Hydraulic System	199
7.2	Packing Stage Dynamics : Experiments and Models . .	201
7.2.1	Cavity Gate Pressure	204
7.2.2	Nozzle Pressure Model	213
7.2.3	Hydraulic Pressure Model	217
7.2.4	Summary	220
7.3	Analysis of the Dynamic Behavior of Cavity Pressure During Packing Stage	223

8.	CONTROL OF THE PACKING AND HOLDING STAGES, AND PEAK CAVITY PRESSURE	235
8.1	Design of the Control loop for Packing stage	235
8.1.1	Cavity Pressure Discrete Model	235
8.1.2	Combinations of the Supply and Relief Valve Opening	238
8.1.3	Simulation of the Control Loop	240
8.2	Control Experiments	242
8.2.1	Sequential Control	242
8.2.2	Control of Peak Cavity and Hold Pressures	245
8.2.3	Control of the Overall Injection Molding Cycle	247
8.3	Summary	263
9.	CONCLUSIONS AND RECOMMENDATIONS	264
9.1	Conclusions	264
9.1.1	Dynamic Studies	264
9.1.2	Control Studies	265
9.2	Recommendations	267
9.3	Claims of Original Work	268
	REFERENCES	269
APPENDIX A:	Modelling of Injection Molding Process	
	3.A.1 Plastication Stage	
	3.A.2 Filling and Packing Stages	
	3.A.3 Product Quality Studies	
APPENDIX B:	Specifications of the Transducers and the Calibration Procedure	
APPENDIX C:	Specification of the Servovalves	
APPENDIX D:	Derivation of Hydraulic Pressure Discrete Model	

APPENDIX E:	Derivation of Nozzle Pressure Discrete Model
APPENDIX F:	Derivation of Cavity Pressure Discrete Model
APPENDIX G:	Derivation of Dahlin Controller for Nozzle Pressure
APPENDIX H:	Listing of the Computer Simulation Programs
APPENDIX I:	Listing of Overall Control Program for the Injection Molding Cycle

LIST OF TABLES

<u>Table</u>	<u>Caption</u>	<u>Page</u>
4.1	Injection Molding Machine Specifications	55
4.2	Calibration Equations for the Transducers used on the Injection Molding Machine	59
4.3	Physical Properties of the Resin Used in the Study . .	63
5.1	Values of the Parameters for the Cavity Pressure Model : First Order Plus Ramp	91
5.2	Parameters for the Cavity Pressure Model Obtained from Tests Performed at 1.2 sec After the Start of Injection	93
5.3	Parameters for the Cavity Pressure Model Obtained from Tests Performed at Different Times After the Start of Injection	96
5.4	Parameters for the Cavity Pressure Model Obtained from Tests Performed at the Same Percent of Cavity Filled	98
5.5	Parameters of the ARX Model for Cavity Pressure Response	105
5.6	Parameters of the ARMAX Model for Cavity Pressure Response	106
5.7	Parameters of Box-Jenkins Models for Cavity Gate Pressure Response	114
5.8	Parameters for the Cavity Pressure Gradient Model . .	120
6.1	Minimum Error Integral Tuning Formulas for Set Point Changes	143
6.2	Discrete Models for the Hydraulic Pressure Response .	149
6.3	Initial Controller Parameter Values Calculated by ITAE for the Hydraulic Pressure Control Loop	150

6.4	Discrete Models for the Nozzle Pressure Response . . .	156
6.5	Initial Controller Parameter Values Calculated by ITAE for the Nozzle Pressure Control Loop	157
6.6	Parameters of the Dahlin Controller for Nozzle Pressure	167
6.7	Dahlin Controller Equations for Nozzle Pressure Control Loop Using Equation 4.5.38 with Different Sampling Time, T, and Different Tuning Parameter, L	168
6.8	Dahlin Controller Equations for Nozzle Pressure Control Loop Using Equation 4.5.39 with Different Sampling Time, T, and Different Tuning Parameter, L	169
6.9	Performance Indices of Nozzle Pressure Control Simulation Using Dahlin Controller with Different Tuning Parameter, L, and Sampling Interval, T = 0.005 sec.	172
6.10	Performance Indices of Nozzle Pressure Control Simulation Using Dahlin Controller with Different Sampling Interval, T, and Tuning Parameter, L = 0.008	174
6.11	Discrete Models for the Cavity Pressure Response . . .	177
6.12	Initial Controller Parameter Values Calculated by ITAE for the Cavity Pressure Control Loop	178
7.1	Values of the Parameters for the Cavity Gate Pressure Model : First Order	211
7.2	Values of the Parameters for the Cavity Gate Pressure Model at Different Values of Cavity Pressure	214
7.3	Values of the Parameters for the Nozzle Pressure Model : First Order	218
7.4	Values of the Parameters for the Hydraulic Pressure Model : First Order	224
8.1	Initial Controller Parameter Values Calculated by the ITAE for Cavity Gate Pressure During the Packing Stage	243

LIST OF FIGURES

<u>Figure</u>	<u>Caption</u>	<u>Page</u>
1.1	Cavity Pressure Representation of the Injection Molding Cycle	3
3.1	Process and Noise Model	17
3.2	Representation of the Injection Molding Variables	27
3.3	Control Alternative for Injection Molding Process	29
3.4	Transfer Functions for the Ram Velocity Control Loop [105,106].	32
3.5	Ram Velocity Step Response Calculated by Equation (3.10) [107].	34
3.6	Comparison Between Calculated Ram Velocity (Equation 3.10) and Fitted First Order Model (Equation 3.11).	36
3.7	Comparison Between Experimental and Calculated Filling Rate [113].	41
3.8	Comparison Between Experimental and Simulated Cavity Pressure Profile [113].	43
3.9	Comparison Between Experimental Ram Velocity and the Simulation Results [114].	44
4.1	Danson Metalmic Injection Molding Machine and the Microprocessor System	53
4.2	The Hydraulic System of the Machine	56
4.3	The Instrumented Mold Cavity, PT = Pressure Transducer, TC = Thermocouple	57
4.4	Machine - Microcomputer Interface	62
5.1	Pressure-Time Profiles for Cavity Pressure, Nozzle Pressure, and Hydraulic Pressure During the Injection Molding Cycle	66

5.2	Pressure - Time Profile for Hydraulic, Nozzle, and Cavity Gate Pressure at the Start of the Injection Cycle	68
5.3	Pressure - Time Profiles for Hydraulic, Nozzle, and Cavity Gate Pressure During the Filling Stage	69
5.4	Relationship Between Nozzle Pressure (P_N) and Hydraulic Pressure (P_H) in the Filling Stage	70
5.5	Relationship Between Cavity Gate Pressure (P_C) and Nozzle Pressure (P_N) in the Filling Stage	72
5.6	Schematic Representation of the Flow Patterns During the Filling of a Rectangular Mold Cavity	73
5.7	Pressure - Time Profiles for Hydraulic, Nozzle, and Cavity Gate Pressure in the Transition Period from Filling to Packing	75
5.8	Relationship Between Nozzle Pressure (P_N) and Hydraulic Pressure (P_H) in the Transition Period from Filling to Packing	76
5.9	Relationship Between Cavity Gate Pressure (P_C) and Nozzle Pressure (P_N) in the Transition Period from Filling to Packing	78
5.10	Pressure - Time Profiles for Hydraulic, Nozzle, and Cavity Gate Pressure in the Packing Stage	79
5.11	Relationship Between Nozzle Pressure (P_N) and Hydraulic Pressure (P_H) in the Packing Stage	80
5.12	Relationship Between Cavity Gate Pressure (P_C) and Nozzle Pressure (P_N) in the Packing Stage	81
5.13	Cavity Gate Pressure Response to 30 - 40 % and 40 - 30 % Step Changes in Valve Opening	85
5.14	Cavity Gate Pressure Response to 30 - 45 % and 45 - 30 % Step Changes in Valve Opening	86
5.15	Cavity Gate Pressure Response to 40 - 50 % and 50 - 40 % Step Changes in Valve Opening	87
5.16	Comparison of Experimental Cavity Gate Pressure Response to Fitted Model	89
5.17	Comparison of Experimental Cavity Gate Pressure Response to Fitted Model	90

5.18	Percent of Cavity Filled at the Time of the Step Change for Different Initial Valve Opening	92
5.19	Response of Cavity Gate Pressure to 30 - 40 % Valve Opening Change at Different Injection Times . . .	95
5.20	Response of Cavity Gate Pressure to 30 - 40% Step Change 2 sec. and to 40 - 30% Change at 1.2 sec	97
5.21	Response of Cavity Gate Pressure to PRBS Input Signal to the Servovalve	101
5.22	Differenced Response of Cavity Gate Pressure to PRBS Input Signal	102
5.23	Frequency Response of Cavity Gate Pressure	103
5.24	Auto-Correlation and Cross-Correlation of the Residuals for the ARMAX Model [1211]	107
5.25	Auto-Correlation and Cross-Correlation of the Residuals for the ARMAX Model [1311]	108
5.26	Auto-Correlation and Cross-Correlation of the Residuals for the ARMAX Model [1321]	109
5.27	Comparison Between the Bode Plots of the ARMAX Models and the Spectral Analysis Estimates of the Experimental Data	111
5.28	Comparison Between the Experimental Data and the ARMAX Models Predictions	112
5.29	Auto-Correlation and Cross-Correlation of the Residuals for Box-Jenkins Model [11211]	115
5.30	Cavity Gate Pressure Gradient Response to 30 - 40% and 40-30% Changes in the Servovalve Opening	119
5.31	Cavity Pressure Gradient for a Static Experiment . . .	121
5.32	Comparison of Experimental Cavity Pressure Gradient Response to Fitted Data	122
6.1	Simplified Digital Control Loop	125
6.2	Dahlin Control Block Diagram	129
6.3	Hydraulic Pressure Response to a Step Change in the Set-point with a PI Controller	152

6.4	Hydraulic Pressure Response to a Step Change in the Set-point with a PID Controller	153
6.5	Comparison of Hydraulic Pressure Response with PI and PID Controllers	154
6.6	Nozzle Pressure Response to a Step Change in the Set-point with a PI Controller	159
6.7	Nozzle Pressure Response to a Step Change in the Set-point with a PID Controller	160
6.8	Nozzle Pressure Response to a Step Change in the Set-Point with PI and PID Controllers	161
6.9	Nozzle Pressure Response to a Set-Point Pressure-Time Profile with the PI and PID Controllers	162
6.10	Nozzle Pressure Response to a Set-Point Pressure-Time Profile with the PI and PID Controllers	163
6.11	Nozzle Pressure Response to a Set-Point Pressure-Time Profile with the PI and PID Controllers	164
6.12	Control of Nozzle Pressure Using Dahlin Controller with Different Tuning Parameter, Lambda	170
6.13	Control of Nozzle Pressure Using Dahlin Controller with Different Sampling Interval	173
6.14	Control of Nozzle Pressure Using Dahlin and PID Controllers	175
6.15	Cavity Gate Pressure Response to a Step Change Plus Ramp in the Set-Point with a PI Controller	180
6.16	Cavity Gate Pressure Response to a Step Change Plus Ramp in the Set-Point with a PID Controller	181
6.17	Cavity Gate Pressure Response to a Step Change Plus Ramp in the Set-Point with PI and PID Controller	182
6.18	Cavity Gate Pressure Response to a Step Change Plus Ramp in the Set-Point with PI and PID Controller	184
6.19	Experimental Nozzle Pressure Control Using PI Controller	188
6.20	Experimental Nozzle Pressure Control Using PID Controller	189

6.21	Experimental Nozzle Pressure Control Using Dahlin Controller	190
6.22	Experimental Cavity Gate Pressure Control Using PI Controller	192
6.23	Gain Scheduling Adaptive Control	194
6.24	Experimental Cavity Gate Pressure Control Using PI Controller	195
6.25	Experimental Cavity Gate Pressure Control Using PID Controller	196
7.1	Hydraulic System of the Injection Molding Machine . . .	200
7.2	Simplified Schematic of the Hydraulic System of the Injection Molding Machine	202
7.3	The New Design of the Hydraulic System of the Injection Molding Machine	203
7.4	Step Changes in the Supply and Relief Valves Opening in the Packing Stage	205
7.5	Response of Cavity Gate Pressure in Packing Stage to Step Change Composed of 40-60% in the SSV and 30-20% in the RSV Opening	206
7.6	Response of Cavity Gate Pressure in Packing Stage to Step Change Composed of 40-60% in the SSV and 30-10% in the RSV Opening	207
7.7	Response of Cavity Gate Pressure in Packing Stage to Step Change Composed of 40-60% in the SSV and 30-0% in the RSV Opening	208
7.8	Comparison Between Experimental Cavity Gate Pressure and Fitted First and Second-Order Models . . .	209
7.9	Cavity Gate Pressure Response to Step Changes Introduced at Different Times	212
7.10	Nozzle Pressure Response to Step Change in the Valves Openings During Packing Stage	215
7.11	Comparison Between Experimental Nozzle Pressure and Fitted First and Second-Order Models	216
7.12	Hydraulic Pressure Response to Step Change in the Valves Openings During the Packing Stage	219

7.13	Comparison Between Experimental Hydraulic Pressure and Fitted First and Second-Order Models	221
7.14	Variation of Density of polyethylene Resins with Pressure [160]	230
7.15	Variation of $d(\mu/\beta)/dP$ as a Function of Pressure for a Polyethylene Resin	231
8.1	Control Scheme for Supply and Relief Servoalves Using Two PI Controllers	239
8.2	Control Scheme for Nozzle Pressure, Cavity Pressure, and Peak Cavity and Hold Pressure	241
8.3	Control Simulation of Cavity Gate Pressure During Packing and Holding Stages Using a PI Controller	244
8.4	Peak Cavity and Hold Pressure Control Scheme Using Two Separate PI Controllers	246
8.5	Control of Peak Cavity and Hold Pressure Using a PI Controller	248
8.6	Control of Peak Cavity Pressure and a Variable Hold Pressure Using a PI Controller	249
8.7	Improved Control of Peak Cavity and Hold Pressure Using a PI Controller	250
8.8	Control Scheme with One Controller for Both Servoalves	252
8.9	Nozzle, Cavity, Peak Cavity and Hold Pressure Control Using a PI Controller	254
8.10	Control of Injection Molding Cycle with Readjusted Hold Pressure Controller	256
8.11	Control of Injection Molding Cycle Using a PI Controller with Full Scale Operation of Supply and Relief Valves	257
8.12	Reproducibility of the Control of Injection Molding Cycle	258
8.13	General Control Strategy for the Injection Molding Cycle	261
8.14	Control of Injection Molding Cycle Using a General Control Strategy	262

CHAPTER 1

INTRODUCTION

Injection molding is a process whereby a solid polymeric material is heated until it reaches a state of fluidity; it is then transferred under pressure (injected) into a closed space (mold cavity) and then cooled in the mold until it solidifies, conforming in shape and dimensions to the mold cavity.

Injection molding is accomplished in an injection molding machine which basically consists of two components: the injection unit and the clamping unit. The injection unit serves to heat the raw material to a molten state and to transfer it under pressure into the closed mold which is held by the clamping unit. Melting is achieved with the help of external heaters and by mechanical heating produced when the granular raw material is compressed and worked.

Over the past two decades, injection molding has played a major role in the fabrication of plastic parts for both thermoplastic and thermosetting materials. Its outstanding versatility and ability to produce parts with intricate shapes to extremely tight specifications have been the key reasons for its wide spread use. Injection molding is also highly cost effective, especially in large volume operations. The chief drawback of injection molding

is the inherent difficulty of controlling the ultimate properties of the molded parts to high degrees of precision. Because of the spatial nonuniformity of the temperature and pressure fields, the complete thermo-mechanical history is unevenly distributed in the cavity, leading to structural inhomogeneity of molded parts. Although not necessarily a major concern in conventional molding, this could cause serious problems in the molding of high precision parts, as for example integrated circuit boards, lenses, and fiber-optic connectors. Thus the production of intricate parts with extremely high tolerances and quality finish imposes stringent manufacturing and process control requirements.

The injection molding process is cyclic with a short cycle time, typically of the order of a minute or less. Therefore, to ensure good quality and consistency of the product from cycle to cycle, efficient and reliable control is necessary. Ideally, control of any aspect of the process must be based on understanding of the phenomena involved.

The sequence of events taking place in the cavity can be depicted in terms of the variation of the cavity pressure with time, as shown in Figure 1.1. It includes the following consecutive stages: filling, packing, holding and cooling.

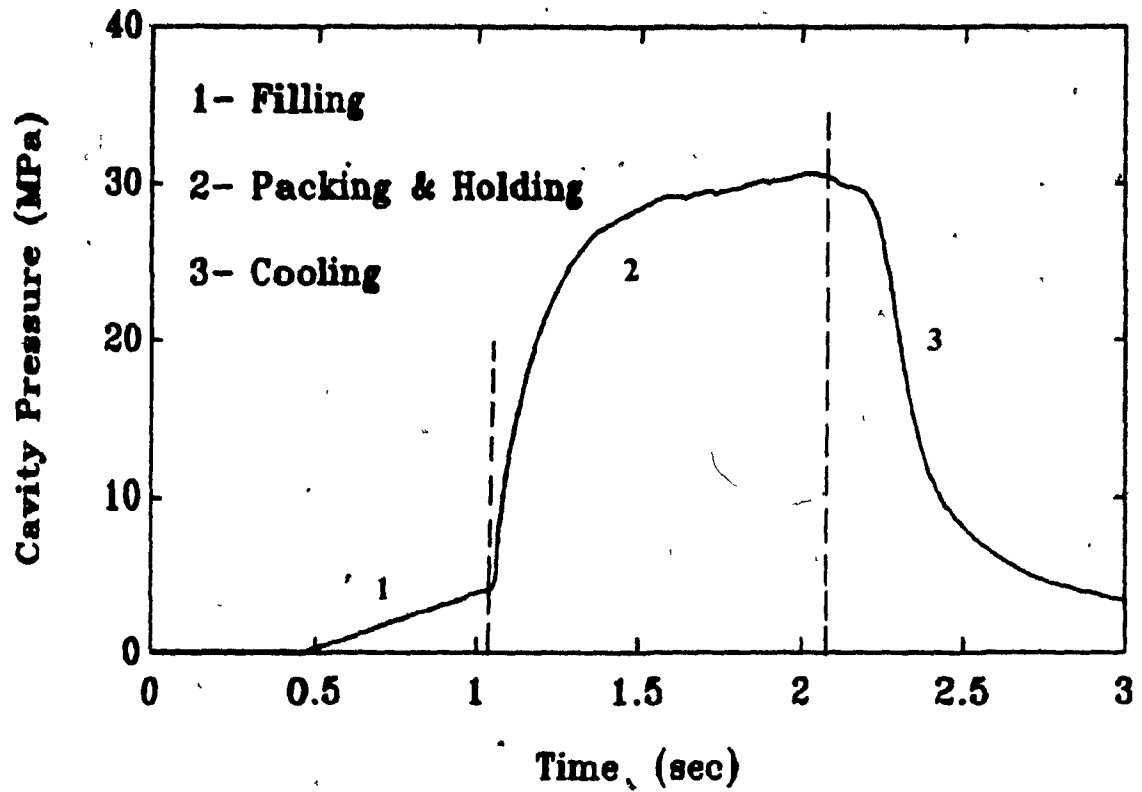


Figure 1.1 Cavity Pressure Representation of Injection Molding Cycle.

During the filling stage, the pressure in the mold cavity rises slowly, as the molten, non-Newtonian, polymer spreads to fill the empty cold cavity. After the filling stage is completed, more material has to be packed into the mold cavity to compensate for the shrinkage of the material. In this stage, the pressure in the cavity rises sharply within a short time to reach its peak. Sometimes, the pressure is maintained at a high level or allowed to decrease only slowly at the holding stage, subsequent to the packing stage. Cooling, however, through heat exchange with the solid walls of the cold mold, causes the molding to solidify. Thus, in the cooling stage, a continuous decrease in cavity pressure is observed. No flow should take place in this stage, but the rate of cooling plays a major role in determining some of the final properties of the molded article.

The successful operation of an injection molding machine requires control of the process variables during each of the consecutive phases in addition to correctly identifying the points of transition from one phase to the next.

In recent years, improvements in injection molding control have relied on refinements in equipment and the use of computers. Developments in equipment such as hydraulic components have led to considerable improvements in the

performance and reliability of injection molding machines [1,2]. Application of computer control to the injection molding process has been addressed by many authors [3-14]. Even with the best equipment and computer hardware, it is the control strategies and the quality of the dynamic models describing the process that determine the quality of process control. Dependable control and dynamic modelling schemes should therefore be employed to fully exploit the advantages offered by the improved equipment.

This research concentrates on the study of the dynamics of the injection molding process during the filling and packing stages as well as the dynamic behavior of the peak cavity pressure. The dynamic models obtained are employed in controlling the injection molding cycle.

CHAPTER 2

SCOPE AND OBJECTIVES

The present work represents a part of a general research program in the field of injection molding, which has been in progress for the last two decades in the Chemical Engineering Department at McGill University. Recently, a significant part of this effort has been in the area of injection molding process control.

The effective control of the injection molding process is closely associated with controlling cavity pressure [15-20]. The importance of cavity pressure arises due to its close interactions with most of the process variables and its influence on important microstructural and final product characteristics, such as orientation, crystallinity, surface properties, sink marks, and mechanical properties [18-20]. This role of cavity pressure furnishes the incentive for the present study.

The objective of the present study was to obtain dynamic models and achieve control over cavity pressure, cavity pressure gradient, and peak cavity pressure. The work involves phenomenological analysis and takes note of theoretical models and considerations.

The specific objectives of the present work were :

- (1) To develop dynamic models for cavity gate pressure and cavity pressure gradient during the filling stage through the analysis of dynamic experimental data.
- (2) To develop a dynamic model for cavity gate pressure during the packing stage and to study the dynamics of peak cavity pressure.
- (3) To design control schemes utilizing the dynamic models obtained in (1) and (2) above and to evaluate different controllers through simulation studies.
- (4) To evaluate different strategies for switching from one stage to the next in the injection molding cycle.
- (5) To modify the injection molding machine so as to perform the appropriate dynamic and control experiments.
- (6) To employ the chosen controllers and the modified hydraulic system to experimentally control the consecutive stages of the injection molding cycle.

The present work incorporates the results of a large number of experiments. Although an effort will be made, in this work, to explain some of the observed phenomena, it should be emphasized that a complete quantitative explanation is possible only by the application of detailed mathematical models of the injection molding process and related phenomena. The main aim of the present work is presented in the context of obtaining detailed experimental data relating to the dynamics of some parameters of the injection molding process and achieving control over these parameters. The explanation of these data on the basis of an analysis of the complex flow and thermo-mechanical phenomena is not attempted. The latter task awaits the results of work currently in progress in this laboratory.

The text is divided into nine chapters. Chapter 1 introduces the injection molding process and the need for process control. This chapter contains the scope and objectives of the present study. Chapter 3 presents a general background of the study. It includes a description of different methods of process identification and the application of process modelling to the injection molding process. The chapter ends with a discussion of different strategies for the switching from one stage to the next in the injection molding cycle. Chapter 4 describes the injection molding machine and the experimental set-up. Chapter 5 presents the dynamic modelling of cavity gate

pressure and cavity pressure gradient during the filling stage using both deterministic and stochastic experiments. Chapter 6 demonstrates the control of the filling stage using different process variables in conjunction with various controllers. Chapters 7 and 8 deal with the dynamics and control of the packing stage. Chapter 9 summarises the conclusions and the original contributions of this work and offers some recommendations for future work.

CHAPTER 3

GENERAL BACKGROUND

3.1 Introduction

The studies concerned with the injection molding process can be divided into the following major categories:

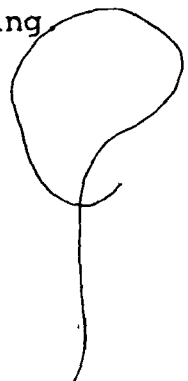
- (1) Mathematical modelling of the various stages of the injection molding cycle,
- (2) Functional description of the interactions between the process parameters,
- (3) Dynamic modelling and control of the injection molding cycle,
- (4) Temperature control in the injection molding process,
- (5) Characterization of the injection molded product,
- (6) Optimization and management through the application of computers,
- (7) Mold design optimization,
- (8) Machinery development.

In the light of the objectives of the present research

study, the bulk of this chapter deals with a detailed review of the dynamic modelling and control studies relating to the injection molding process. A brief review of the mathematical modelling and functional studies is presented. Before discussing the modelling of the injection molding process, it is worthwhile to address the various approaches to process modelling.

3.2 Process Modelling and Identification

The goal of an automatic control system is to force selected process variables to follow a specified pattern or profile and/or to compensate for disturbances in the process. The rational design of a control system therefore, requires an accurate dynamic model(s) of the process variable(s) to be controlled. These models can be obtained by either theoretical analysis or experimentation. A detailed discussion of the principles of model building and of the practical aspects encountered in this process is presented by Fasol and Jorgl [21] and Isermann [22]. The following sections briefly describe the theoretical and experimental approaches for process modeling.



3.2.1 Theoretical Modelling

Theoretical process models are obtained by solving the relevant momentum, energy, and mass balance equations. Solutions of the coupled ordinary / partial differential equations usually involve considerable computational effort. Theoretical models are thus not well suited for real-time control applications. The advantage of theoretical models is that they can be developed for a process or a plant that is not yet built or available for experimentation. Moreover, they can be used via simulation to evaluate different control strategies before applying them to the real process. In many cases, essential knowledge gained from theoretical models, especially in relation to critical aspects of the process, prevents costly failures in the operation of the plant.

3.2.2 Experimental Modelling

Experimental modeling avoids many of the difficulties and hypotheses necessary in theoretical modeling, at the expense of performing experiments. It involves selection of some of the process variables and observing the transient response of the process output to changes in these

variables. The experimental determination of the dynamic behavior of a process from input-output signals is referred to as system identification. Techniques for system identification have been extensively studied in recent years. Relevant reviews have been published by Astrom and Eykhoff [23], Nieman et.al.[24] and Gustavsson et.al. [25].

The techniques used for identification depend on the final goal of the process model. In general, this may be one or more of the following : verification of theoretical models, controller parameter tuning, computer-aided design of digital control algorithms, self-tuning control, and process failure detection. The identification procedure involves several steps such as : the selection of a model to describe the process, specifying the input signal, and criteria to test the adequacy of the model. Detailed identification procedures are given by Isermann [22] and Franklin and Powell [26].

Identification methods can be classified using a number of criteria. The classification into deterministic or stochastic methods is used in the following sections.

3.2.2.1 Deterministic Identification Methods

Classical identification methods are based on deterministic perturbations of the input signal such as step, pulse and sinusoidal changes [27,28]. The step function is used most widely since it is easy to generate and the process response can be described by simple models, using relatively few parameters. The response of a process to a step input often has a S-shape for a wide range of processes. A first-order plus delay or a second-order system plus delay is assumed and the time constants, the time delay and the process steady-state gain are estimated graphically or by a non-linear regression fitting of the model to the data. The amplitude of the step input must be chosen with some care. It should be sufficiently large so that the output data are distinguished from the process noise but small enough to keep the system in the linear range. Several positive and negative step changes of different amplitude are generally performed to check the linearity of the system.

A disadvantage of the deterministic tests is that they are useful only when the system has small amounts of noise. Moreover, it is difficult to discriminate between system models of second and third or higher order. Thus, in practice, some features of the process may not be adequately described.

3.2.2.2 Stochastic Identification Methods

Variables in most processes are subject to random disturbances (noise) which cannot be described by deterministic modeling. Stochastic identification methods provide a noise model in addition to the process model by applying the theory of stochastic processes. Therefore, the estimates of the process model parameters are more reliable.

The system is assumed to be described by a linear difference equation of the form [29]:

$$Y_u(k) + a_1 Y_u(k-1) + \dots + a_m Y_u(k-m) = b_1 U(k-d-1) + \dots + b_n U(k-d-n) \quad (3.1)$$

Where: $U(k)$ and $Y_u(k)$ are respectively the deviations of the input and undisturbed output signals from their steady-state values,

- k : the sampling instant
- d : the discrete deadtime
- m & n : the process order
- a_i, b_i are the model coefficients

The Z-transformation of equation (3.1) gives [29] :

$$\begin{aligned}
 G_p(Z) &= \frac{Y_u(Z)}{U(Z)} = \frac{B(Z^{-1})}{A(Z^{-1})} Z^{-d} \\
 &= \frac{b_1 Z^{-1} + \dots + b_m Z^{-m}}{1 + a_1 Z^{-1} + \dots + a_n Z^{-n}} Z^{-d} \quad (3.2)
 \end{aligned}$$

where G_p is the process discrete transfer function. The measured output $Y_u(k)$, as shown in ~~Figure 3.1~~, is assumed to be contaminated by noise $n(k)$ to give :

$$Y(k) = Y_u(k) + N(k) \quad (3.3)$$

The disturbance signal $N(k)$ is assumed to be stationary and described by an Autoregressive Moving Average signal process (ARMA) [29] :

$$\begin{aligned}
 N(k) + c_1 N(k-1) + \dots + c_p N(k-p) = \\
 v(k) + d_1 v(k-1) + \dots + d_q v(k-q) \quad (3.4)
 \end{aligned}$$

where c_i and d_i are the model coefficients. $v(k)$ is a nonmeasurable, normally distributed, discrete white noise [30] with :

$$E \{ v(k) \} = 0$$

$$E \{ v(k) v(k+t) \} = \sigma_v \delta(\tau)$$

where σ_v is the variance and $\delta(\tau)$ is the Kronecker delta

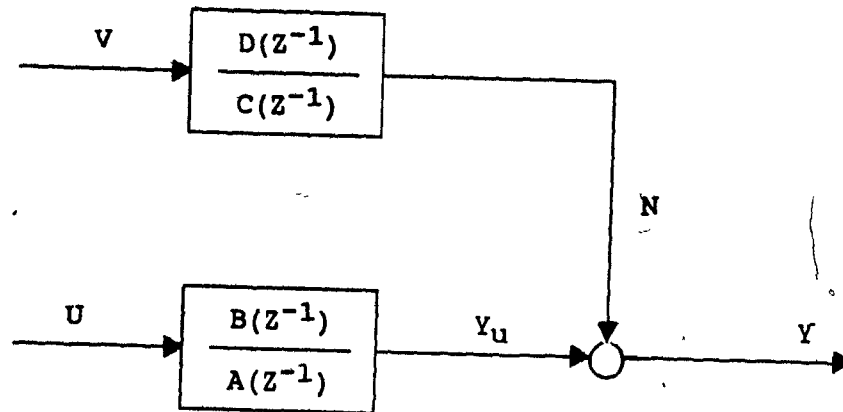


Figure 3.1 Process and Noise Model

function and E is the expectation operator. The Z -transfer function of the noise filter is :

$$G_V(Z) = \frac{N(Z)}{V(Z)} = \frac{D(Z^{-1})}{C(Z^{-1})} = \frac{1+d_1 Z^{-1}+\dots+d_q Z^{-q}}{1+c_1 Z^{-1}+\dots+c_p Z^{-p}} \quad (3.5)$$

The combination of equations (3.2) and (3.5) yields the combined general (Box-Jenkins) process and noise model:

$$Y(Z) = \frac{B(Z^{-1})}{A(Z^{-1})} Z^{-d} U(Z) + \frac{D(Z^{-1})}{C(Z^{-1})} V(Z) \quad (3.6)$$

The objective of parameter estimation is then to estimate the process parameters in the polynomials $A(Z^{-1})$ and $B(Z^{-1})$ and noise parameters in $C(Z^{-1})$ and $D(Z^{-1})$, from the measured signals $U(k)$ and $Y(k)$. It is often assumed that the model orders m , n , p and q are known apriori. The noise $n(k)$ is assumed to be stationary, i.e. the roots of the polynomial $C(Z^{-1})$ lie within the unit circle in the Z -plane.

The parameter estimation methods described in the following section differ in the assumptions regarding the structure of the noise filter, which must be made for convergent parameter estimates. The general model described by equation (3.6) is often limited to two subclasses of

models [30]:

- (1) The Least-Squares (LS); or ARX model :

$$Y(Z) = \frac{B(Z^{-1})}{A(Z^{-1})} Z^{-d} U(Z) + \frac{1}{A(Z^{-1})} V(Z) \quad (3.7)$$

- (2) The Maximum Likelihood (ML) model, also called ARMAX :

$$Y(z) = \frac{B(Z^{-1})}{A(Z^{-1})} Z^{-d} U(z) + \frac{D(Z^{-1})}{A(Z^{-1})} V(Z) \quad (3.8)$$

Stochastic identification methods may also be classified as "off-line" or "on-line". The on-line recursive identification forms an integral part of the adaptive control techniques which is beyond the objectives of this study. However, the next subsections describe very briefly both identification methods.

3.2.2.2.1 Off-Line Identification Methods

A modelling technique that is widely used has been developed by Box and Jenkins [30]. It combines the computations of the weights of the impulse response function with statistical tests and the maximum likelihood

technique to estimate the process and noise parameters and structure. It is well suited to determine model order (or number of parameters), the time delay and parameter values for an unknown process. The iterative procedure consists of three main steps :

- (1) tentative identification of the order of the process transfer function and noise model,
- (2) estimation of the model parameter values, and
- (3) diagnostic verification of the model and repetition of the process if the model is not statistically acceptable.

3.2.2.2.2 On-Line Identification Methods

A number of steps are usually involved in the development of a control system using the off-line identification methods. These steps involve :

- (i) experimentation to collect data on the system,
- (ii) identification of a suitable dynamic model, and
- (iii) design of the controller using this model.

Often, one of the main benefits from performing such an exercise comes from improved understanding gained about the

behavior of the process and the nature of the disturbances. However, as a procedure for developing a controller the above steps can be time consuming and demand a level of expertise sometimes not available in industry. Furthermore, if the process changes with time (for example, due to production rate changes, raw material properties, etc.) then the process model parameters must be periodically reestimated and the controller parameters readjusted. The attempt to overcome the above difficulties leads to the idea of on-line identification and adaptive control schemes. Extensive work has been reported in the literature on the use and evaluation of on-line recursive identification methods [31 - 35].

3.3 Application of Process Modelling to the Injection Molding Process

The study of the injection molding of thermoplastics has received considerable attention in recent years. A number of studies have been concerned with the phenomenological modelling of the various phases of the injection molding process. The following sections summarize the theoretical and experimental modelling studies on the injection molding of thermoplastics.

3.3.1 Mathematical Modelling of Injection Molding

3.3.1.1 Modelling of the Plastication Stage

Mathematical models of the plastication phase of the injection molding cycle is of great value to determine the effect of the machine and processing parameters such as dimensions and shape of the screw, temperature of barrel surface, screw rpm and back pressure on the melting performance, the melt temperature and the pressure profile in the barrel. Melt temperature and residence time are of primary consideration in the plasticating analysis. A proper choice of plasticating parameters can significantly

improve melt mixing without greatly increasing the melt temperature. A fair amount of work has been done to study the conversion of solid polymer granules to polymer melt by the combined effect of external heating of the barrel and the mechanical work done by the rotation of the screw [36-45]. A brief review of these studies is given in Appendix A.

3.3.1.2 Modelling of the Filling and Packing Stages

These studies usually deal with the flow and cooling of the polymer, mainly in cavities having simple geometry such as round disks and rectangular cavities. Mold filling has been studied as an independent operation without considering the interaction between mold cavity filling and other operations occurring simultaneously or prior to filling. Different models, of varying complexity, depending on the simplifying assumptions and the nature of the rheological constitutive equations and other relationships, have been proposed [46-88]. The models can be treated in two respects : firstly, with regard to the potential to predict the thermomechanical history, particularly flow and thermal conditions during the process and, secondly, the potential to predict some of the microstructure properties of the molded article. A review of these modeling studies is given in Appendix A.

3.3.1.3 Applications of Mathematical Models

The theoretical models for the various stages of the injection molding cycle represent attempts to predict the distributions of polymer pressure, temperature, and velocity in the cavity and the barrel and their dependence on resin properties, cavity shape, screw design and processing conditions. Some of these models can also yield information regarding the relationships between resin properties, molding conditions, the thermomechanical history of the resin and the microstructure and ultimate properties of the molded article. Due to the complexity of the resulting equations, numerical solutions are usually required with considerable computational effort.

On the other hand, models for control purposes must be simple, so that the necessary calculations can be accomplished quickly using a small computer. Such models should reflect the dynamic nature of the process by providing relations between the time-varying distributions of process and product parameters and the relevant machine and material variables. The following sections summarize the available relationships and dynamic models developed for the injection molding process.

3.3.2 Interactions Between the Process Parameters

The injection molding process involves, as previously described, a number of phases with interaction between the process variables. The nature of the interactions between the variables is complex, hence, for a detailed study of the process, it is convenient to divide the variables into smaller groups. The injection molding process at any time can be defined by combinations of:

- (1) Variables pertaining to the material being processed at every point within the machine such as thermal properties, composition, rheological behavior, density and molecular weight.
- (2) Variables pertaining to the machine such as hydraulic pressure, back pressure (hydraulic pressure during plastification phase), screw velocity, screw rotational speed (RPM), barrel temperature, and mold temperature.
- (3) Variables pertaining to the material being processed (process variables) such as melt pressure at the nozzle, melt temperature at the nozzle, cavity pressure, cavity pressure gradient, and melt temperature in the mold cavity.

(4) Variables pertaining to the microstructure development and the final product properties such as orientation, crystallinity (degree of crystallinity and distribution), density, dimensions, tensile strength, impact strength, optical properties, and surface quality.

(5) Disturbances such as pump/valve leakage, voltage fluctuations, electrical noise, change in ambient conditions, ...etc.

The above system characteristics are illustrated in Figure 3.2. They suggest the following options for injection molding control :

Control of Material Variables

Control of Machine Variables

Control of Process Variables

Control of Microstructure and Final Product

Properties

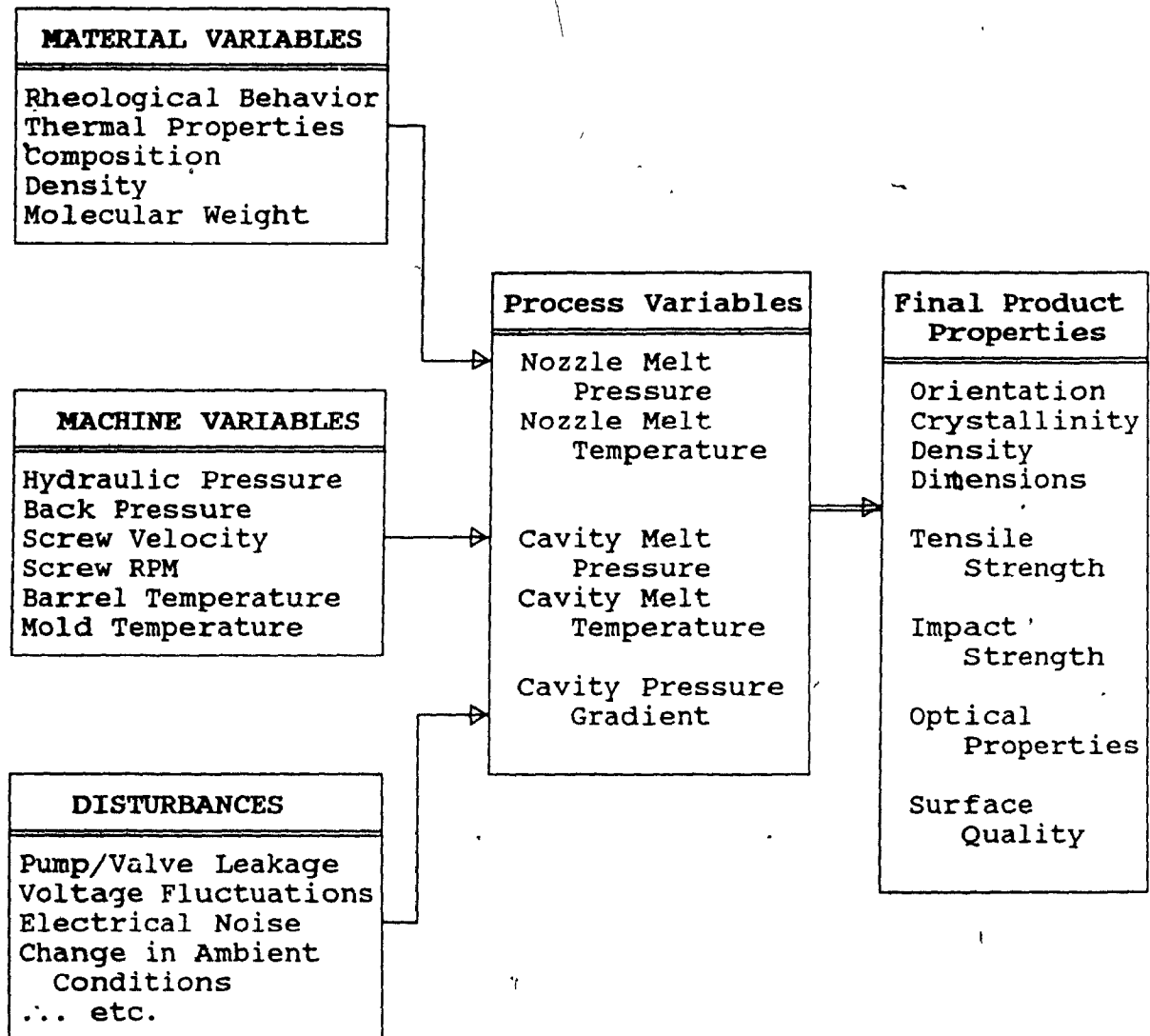
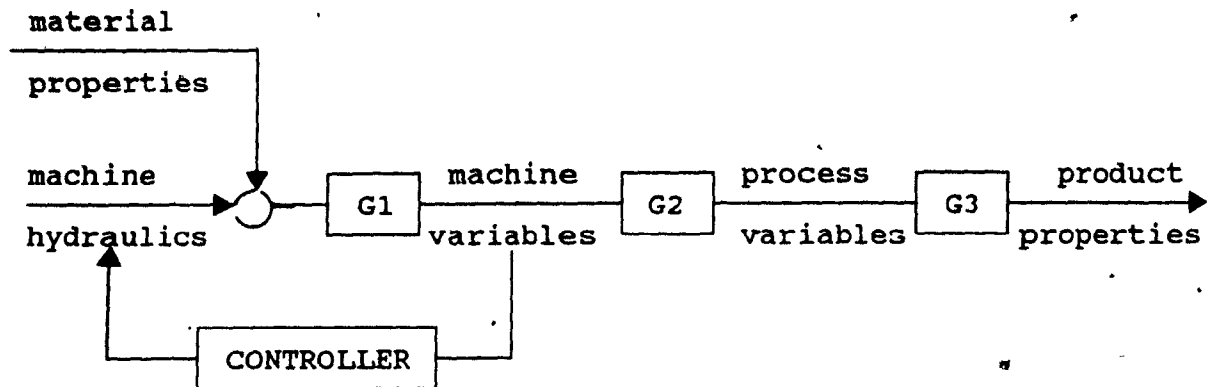


Figure 3.2 Relationships of the Injection Molding Variables

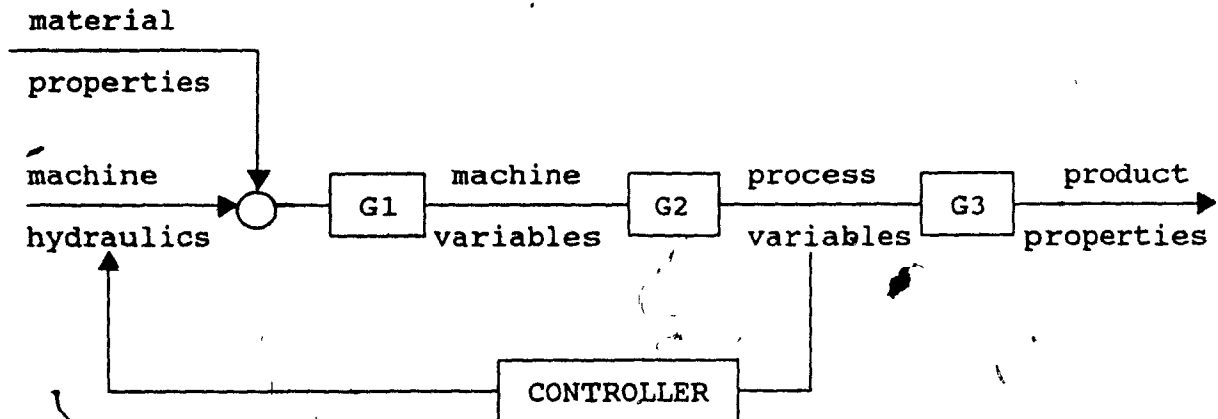
The ultimate goal of injection molding control is to optimize the quantity and the quality of the product, i.e. the option shown in Figure 3.3.C. Such a control loop is difficult to achieve since it requires on-line measurements or estimates of the microstructure characteristics or final product properties. Practical and dependable sensors for such measurements are yet not developed, and the relationships, G_3 , between the process variables and the product properties are very complex. Only qualitative and, in most instances, steady state studies have been reported on this issue [reviewed in Appendix A]. Control of material variables or properties upstream might present a useful option. However, these properties are somewhat remote from the product. Moreover, upstream material properties are generally influenced by process variables. They are also difficult to measure within the short cycle time available. Therefore, upstream material variables do not represent a suitable basis for injection molding process control.

The second alternative is to control the machine variables (Figure 3.3.A). The drawback of this method is that the machine variables are too remote from the product. Moreover, the relations between machine variables and product quality are not easily established and are interrupted by the process variables.

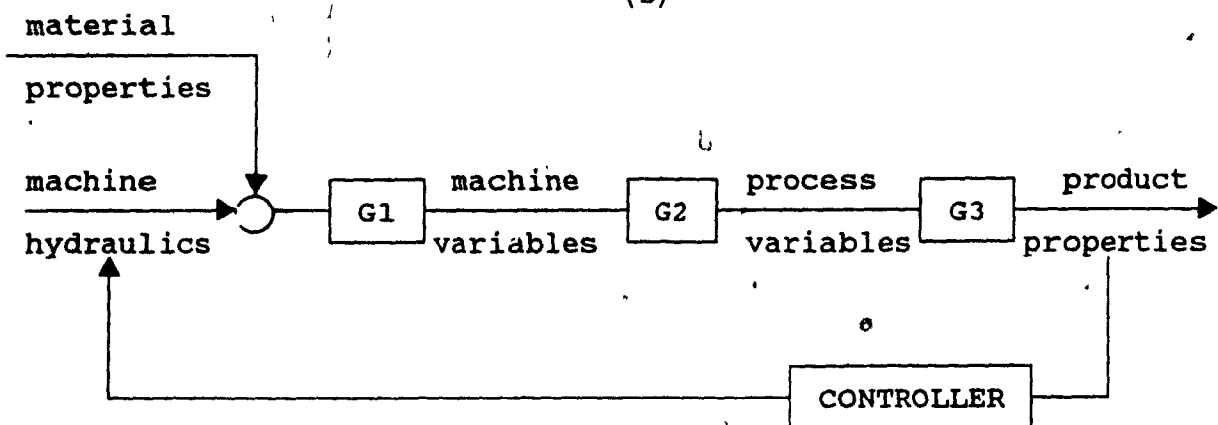
5



(A)



(B)



(C)

Figure 3.3 Control Alternatives for Injection Molding Process

In view of the above arguments, the control of the process variables represents a plausible approach to injection molding process control (Figure 3.3.B).

Several workers have attempted to develop descriptive (functional) relationships between the various groups of injection molding variables [89-103]. A review of these studies and others has been given in reference [104]. The reported relationships, although useful in examining the interactions between these variables, are generally static in nature and do not reflect the dynamic effects that result when the variables are changing in response to a time - variable forcing function. Dynamic models are thus required to furnish the basic information needed to develop dependable control strategies for the injection molding process.

The remaining part of this chapter presents a review of the work relating to application of process dynamic modelling to the injection molding process.

3.3.3 Dynamic Models and Control Applications to the Injection Molding Process

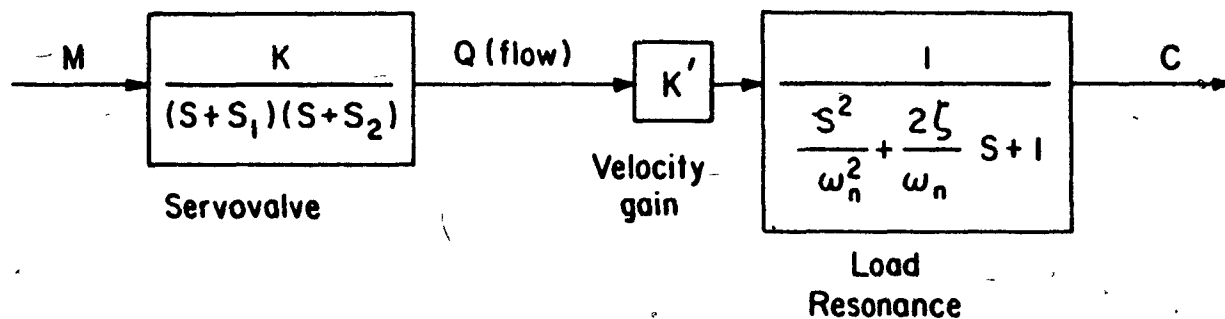
Process identification techniques have been applied to the injection molding process to develop dynamic models for the various parameters of the process.

Davis [105] combined a typical servovalve transfer function given by Thayer [106] with a force balance on the injection ram to propose transfer function models for injection velocity and hydraulic pressure control. Compressibility of the oil and viscous friction of the polymeric material were considered. His results, using closed loop control, showed an improvement in repeatability over the open loop experiments.

Wang et.al. [107] combined the transfer functions proposed by Davis [105] and Thayer [106] for the injection velocity and the servovalve (Figure 3.4) to derive a model for the injection ram velocity. The model is written in the transfer function form as :

$$G(S) = \frac{C(S)}{M(S)} = \frac{2.144 \times 10^{11}}{(S+125)(S+1138)((S+383)^2 + (1135)^2)} \quad (3.9)$$

OR



$$\omega_n = \sqrt{\frac{B}{mV} (k_1 b + A^2)} \quad (\text{rad/sec})$$

$$\zeta = \frac{1}{2} \frac{k_1 m + \frac{V}{B} b}{\sqrt{\frac{V}{B} m (k_1 b + A^2)}}$$

Figure 3.4 Transfer Functions for the Ram Velocity Control Loop [105,106].

$$\frac{C(S)}{M(S)} = \frac{1}{4.7 \times 10^{-12} S^4 + 9.5 \times 10^{-9} S^3 + 11.0 \times 10^{-6} S^2 + 8.9 \times 10^{-3} S + 0.9} \quad (3.10)$$

Where :

$C(S)$ = the change in ram velocity

$M(S)$ = the change in the control valve opening

The ram velocity calculated from the continuous and the discrete forms of Equation (3.10) is shown in Figure 3.5. No experimental data were reported to test the adequacy of the derived model. The simulation results apparently fit a first order plus time delay response. Therefore, the calculated data were fitted (in this study) with a first order model of the form :

$$C(t) = K (1 - \exp(-(t-t_d)/\tau)) \quad (3.11)$$

or in a transfer function form :

$$\frac{C(S)}{M(S)} = \frac{K e^{-t_d}}{\tau S + 1} \quad (3.12)$$

Where :

K = the process gain = 1.067 in/ms. %

τ = the process time constant = 8.759 ms

t_d = the time delay = 1.885 ms

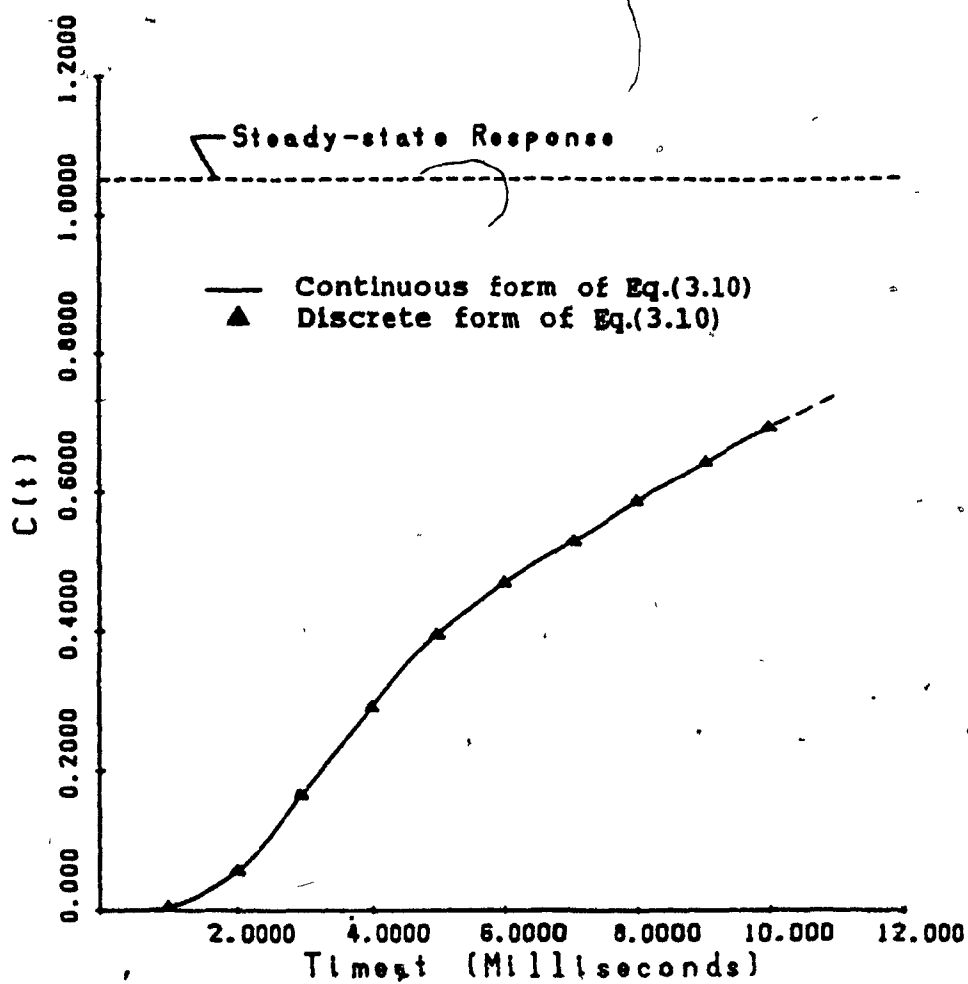


Figure 3.5 Ram Velocity Step Response Calculated by Equation (3.10) [107].

Figure 3.6 shows a good agreement between the ram velocity calculated by Equation (3.10) and the fitted first order model (Equation 3.11). The discrete form of Equation (3.10) was used in conjunction with a recursive parameter estimation technique for on-line identification of the process parameters, but no results were published.

Pandelidis and Agrawal [108] used the transfer function proposed by Wang et.al [107] to design a self-tuning regulator for the ram velocity. Their simulation results demonstrated the feasibility of such a control scheme for injection velocity control.

Kamal et.al. [109] utilized the transfer function approach to develop dynamic models relating the variations in the hydraulic pressure and nozzle pressure to changes in the opening of the servovalve which controls the flow of oil to the injection cylinder. Deterministic and stochastic models were obtained by employing step and pseudo-random binary sequence (PRBS) input functions to the manipulated servovalve opening. The hydraulic pressure response was best modelled by a delayed first order plus oscillatory component, as given by :

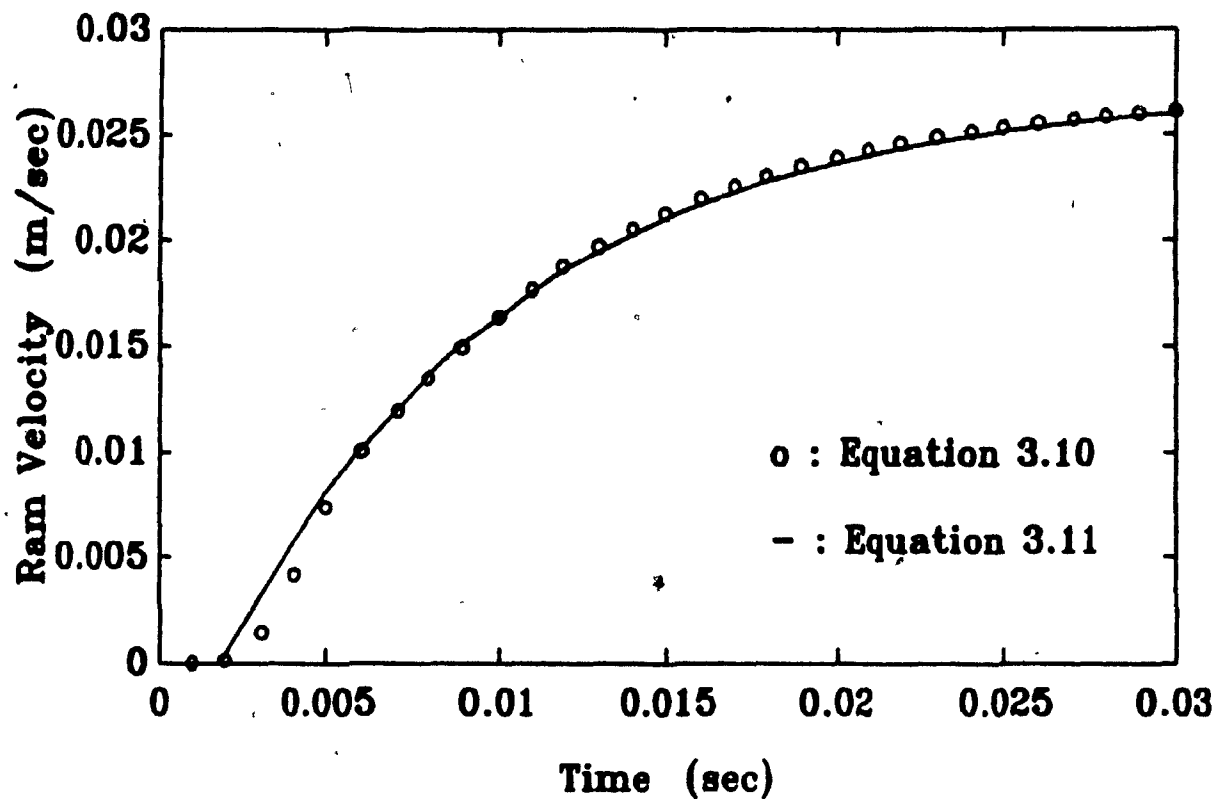


Figure 3.6 Comparison Between Calculated Ram Velocity (Equation 3.10) and Fitted First Order Model (Equation 3.11).

$$P_H(t) = K_1 (1 - e^{-(t-D)/\tau}) + K_2 \left[\frac{1}{(1 - \zeta^2)^{1/2} \tau_1} e^{-\zeta t / \tau_1} \sin\left((1 - \zeta^2)^{1/2} \frac{t}{\tau_1}\right) \right] \quad (3.13)$$

where :

- P_H = hydraulic pressure, Pa
- K_1, K_2 = process gains, Pa/% change in Valve opening
- τ, τ_1 = time constants, sec.
- D = time delay, sec.
- ζ = damping factor, dimensionless

The first term of Equation (3.13) accounts for the delayed first order of the response while the second term is an oscillatory, servovalve-induced component. A first order plus time delay model and an overdamped second order model were fitted to the nozzle pressure response. The fits for both models were equally good and justified the use of the simpler first order model to represent the nozzle pressure response as:

$$P_N(t) = K (1 - e^{-(t-D)/\tau}) \quad (3.14)$$

where P_N is nozzle pressure, Pa.

Stochastic transfer function-noise models were also obtained for the nozzle pressure and ram velocity [104,109]

of the form :

$$P_N(k) = \frac{w_0 - w_1 B}{1 - \delta_1 B} U(k-2) + \frac{1}{1 - \phi_1 B} a(k) \quad (3.15)$$

$$V(k) = w_0 U(k-1) + (1 - \theta B) a(k) \quad (3.16)$$

where: $a(k)$ = random noise value at sample time, k

B = backwards difference operator defined as

$$U(k-1) = B U(k)$$

$\delta_1, w_0, w_1, \phi_1$, and θ are the model coefficients.

The best parameters for the fitted equations (3.13 - 3.16) are given in references [104,109]. The model predictions were in good agreement with the experimental data. The linearity assumption implied by the transfer function approach was verified for the hydraulic pressure, nozzle pressure and ram velocity models [104]. The stochastic models were compared to the corresponding deterministic models, and satisfactory agreement was obtained. The above results showed that the responses of the three variables were rapid and were thus good candidates for controlling the injection phase of the injection molding cycle.

Conley [110] obtained deterministic and stochastic models relating the responses of cavity gate pressure and

the pressure gradient in the cavity to changes in the servovalve opening. Both responses were best fit with a delayed first order model superimposed on a constantly increasing component. The ramping component was due to the natural rise of cavity gate pressure with time. The ramping component in the pressure gradient model did not seem to correspond to expectations based on a physical analysis of the problem, since the pressure gradient was expected to reach a constant steady state level. The cavity pressure response exhibited significant nonlinear behavior which was not explained.

A time series model for cavity pressure has been identified by Sanschagrin [111] as :

$$P_C(k) = 0.87 P_C(k-1) + 6.8 P_H(k) + 5.7 P_H(k-1) \quad (3.17)$$

where $P_C(k)$ = cavity pressure at the kth instant,
 $P_H(k)$ = hydraulic pressure at the kth instant.

No validation tests of the model or comparison with experimental data were reported. Haber and Kamal [112] identified a similar time series model for peak cavity pressure. Their model suggested that peak cavity pressure during given cycle could be statistically related to the peak cavity pressure in the previous cycles. They concluded that improved repeatability of peak cavity pressure could

be achieved by improving the design of the hydraulic system of the injection molding machine.

The above two studies [111,112] provide quantitative relationships for cavity pressure and peak cavity pressure from cycle to cycle. However, they do not furnish the basis for the design of a control system for the injection molding cycle.

Shankar and Paul [113] combined single analytical models for the dynamics of individual machine elements in a simulation of overall machine dynamics for a conventional molding machine with manually adjustable flow control valves. They employed the equations of conservation of mass, momentum and energy for the oil in the hydraulic injection cylinder, the polymer melt in the barrel and the polymer in the mold cavity. Their major assumptions were that the mold cavity could be represented by a single lumped parameter model and the filling and packing stages were isothermal. A comparison between the experimental ram position and the simulation results is shown in Figure 3.7. The experimental and predicted values agree at the start of the injection then the cavity fill predicted by the model is more rapid than the experimental data. This is believed to be due to the isothermal assumption in the filling stage, while in reality, the cooling of polymer during filling increases the resistance to flow. The effect of this assumption is also observed in the mold cavity

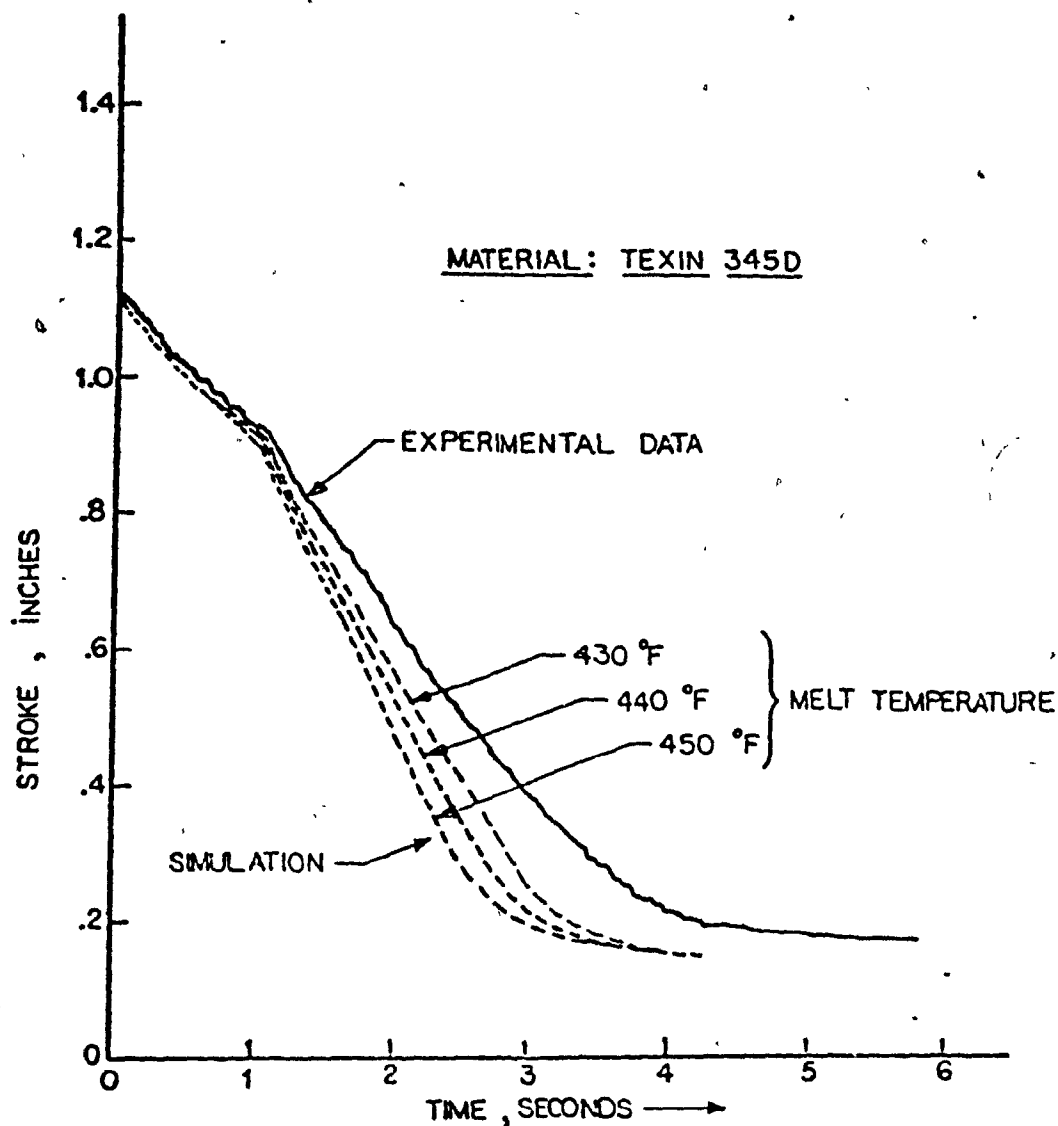


Figure 3.7 Comparison Between Experimental and Calculated Filling Rate [113].

pressure profile given in Figure 3.8, which compares the experimental and calculated cavity pressure values. Since the pressure transducer was not located at the gate, polymer cooling resulted in a lower experimental pressure readings. Better agreement between the model and experimental data can be obtained by including the effect of cooling of the polymer during the filling stage. This requires a large computational effort to solve a complex set of nonlinear partial differential equations.

Wang et.al. [114] in a recent study used an approach similar to that of Shankar and Paul [113] in a simulation study of injection ram velocity. They simulated air shots to eliminate the effects of mold geometry and flow phenomena in the mold in an effort to identify the important machine parameters. Furthermore, the flow in the nozzle area was assumed to be steady-state, incompressible and isothermal. They wrote differential equations to describe the pump flow rate, pressure in the hydraulic line between the pump and the servovalve, servovalve flow rate, pressure in the injection cylinder, ram velocity, and nozzle pressure. Simple Couette flow was used for determining the viscous shear force between the screw and the barrel. This assumption agrees with the results of Kama! et.al [103] for the relation between hydraulic and nozzle pressure. Figure 3.9 shows a comparison between Wangs' experimental data and the simulated ram velocity,

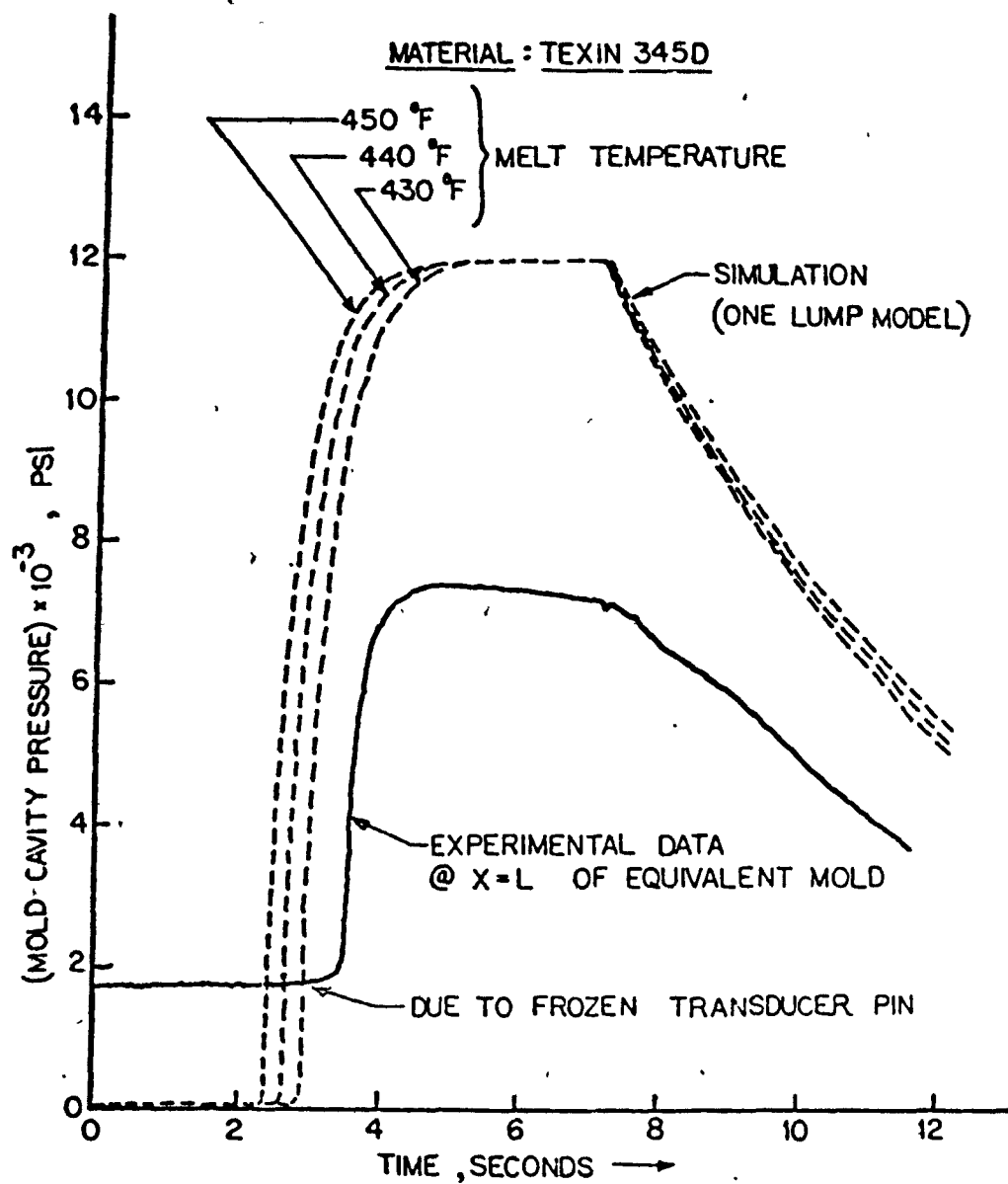


Figure 3.8 Comparison Between Experimental and Simulated Cavity Pressure Profile [113].

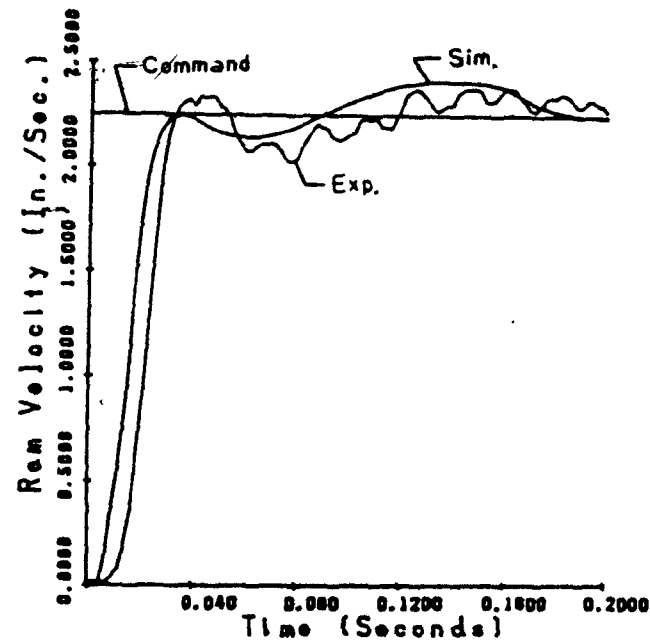


Figure 3.9 Comparison Between Experimental Ram Velocity and the Simulation Results [114].

using the derived set of equations in conjunction with an integral controller. The results show a fast response of the ram speed to reach the set point. The simulation and the experimental responses exhibit similar trends. The results show that the calculated velocity response leads the experimental response. This difference might be due to some initially significant static friction between the ram and the fixed machine parts which was neglected in the derivation of the model. The gradual overshoot after approximately 80 ms was attributed to the relatively slow response of the variable displacement hydraulic pump to changes in the flow demand. An accumulator in the line between the pump and the servovalve would minimize this problem, but a high-pressure accumulator usually requires additional safety and cost considerations. In this simulation, numerous parameters must be known, and some of these can only be determined experimentally. The simulation could be simplified by an analysis of the sensitivity of the dynamic behavior of the process to parameter variations. Such analysis would allow many of the parameters to be fixed or some dynamic elements to be omitted, if they have no significant effect on the overall system behavior. Selective simplification is necessary if injection molding machine dynamics are to be generalized to a practical degree. A study is currently in progress in this laboratory to obtain detailed understanding of the

characteristics of the hydraulic system of the injection molding machine and of the relationships between hydraulic pressure and the flow phenomena of the polymer in the barrel and nozzle [115].

A recent review of studies relating to the control of the injection molding process is given in reference [116].

The successful operation of an injection molding machine requires control of the process variables during the different consecutive phases. Moreover, it is necessary to correctly identify the points of transition from one phase to the next. The following sections discuss different strategies employed for sequential control in the injection molding cycle.

3.4 Sequential Control

Sequential control is the heart of an automated cyclic process and is essential to the operation of injection molding machines. The filling to packing and packing to holding phase transitions should take place at appropriate times reflecting the completion of filling and packing stages. The transition to the hold pressure is rather critical. Delaying this transition results in over-packing, which causes flash and/or difficulties in ejection of the part. On the other hand, early transition results in under-packed parts.

It is possible to achieve open loop control of the transitional sequential actions. Such actions are typically triggered by limit switches to detect the position of different machine parts together with electromechanical relays which determine the various phases of the injection operation and timers which control the phase duration. This method does not explicitly take into account the compression of the melt or its viscosity. It also ignores variations in the hydraulic pressure which can result in changes of the screw position and consequently of the corresponding strokes (plastication stroke, injection stroke). The result is a large variability of part quality, particularly in its weight and the dimensions of the molded

part. For these reasons, a time-dependent switching strategy is not desirable.

Recently, different closed loop strategies have been suggested and evaluated to determine the transition points [117,118]. The following parameters have been employed in these strategies:

- (i) ram position and velocity
- (ii) hydraulic pressure
- (ii) cavity pressure
- (iv) mold separation

3.4.1 Switching Based on Ram Position and Velocity

The use of ram position at the end of filling and packing tends to be an unreliable method of triggering the transition to holding, unless no cushion is used [119]. The use of a cushion, by its nature, implies that the ram position at the end of the filling and packing phases will vary from shot to shot. This variation makes ram position unsuitable for determining the point of switching to holding pressure. The use of zero cushion risks under-pack or even short shots and is generally avoided by most molders.

3.4.2 Switching Based on Hydraulic Pressure

The use of hydraulic pressure for switch-over control can be misleading since large pressure peaks can occur early in the filling phase, particularly when profiled ram velocity control is employed. Moreover, the relationship between the hydraulic pressure and the pressure in the mold cavity is too remote to be precisely correlated [120]. The hydraulic pressure is most suitable for transition detection when it rises steadily as the mold is filled and packed. Obviously, this condition does not hold for all moldings unless relatively long (hence uneconomic) filling times are used.

A combination of ram position and hydraulic pressure has been suggested as a working strategy [119]. This requires that the hydraulic pressure is ignored until the ram has almost completed the filling process. The transition is then triggered by the hydraulic pressure. Large pressure peaks early in the filling phase, due to ram velocity profiling, do not cause premature transition to the packing or holding phase.

3.4.3 Switching Based on Cavity Pressure

In recent years, cavity pressure-dependent switch-over has been successfully used [120]. A number of studies have shown that pressure transfer based on peak cavity pressure improves the repeatability of the injection molding process [15-20]. The switch-over is actuated when cavity pressure at a given location reaches a preset value. Although there is no clear location for melt pressure sensor placement, sensors placed in the cavity near the gate have been shown to be the most effective [121,122]. The influence of the screw stroke is eliminated. The use of cavity pressure to trigger the transition works well when the pressure transducer is correctly placed in the cavity wall.

3.4.4 Switching Based on Mold Separation

The packing phase is accompanied by high cavity pressure which causes the mold to open slightly because of the compliance of its clamping mechanism. The separation of the mold halves is small ($<100 \mu\text{m}$), but measurable. The measurement of mold separation is, in effect, an indirect measure of the cavity pressure and can be used to determine the transition to the holding phase [19]. The transducer is mounted externally on the mold and is a less costly

alternative to modifying the cavity to accept a pressure transducer. Although this method requires the installation of an additional transducer (compared to the other three strategies) it offers the possibility of manipulating the holding/cooling phase and appears to be the preferable strategy for a fully instrumented and controlled machine when the installation of a cavity pressure transducer is impossible or impractical [19].

Investigation of the different switch-over techniques has shown that significant differences in molded part weight repeatability are observed when the different techniques are employed [122]. It appears that strategies based on cavity pressure are the most effective.

The present study has investigated the feasibility of a new switch-over technique based on the change in the slope of cavity gate pressure-time profile. This technique represents a general method which is not restricted to any specified equipment geometry or limited by the processing conditions.

CHAPTER 4

EXPERIMENTAL4.1 Equipment4.1.1 Injection Molding Machine

The experimental work was carried out on a Danson-Metalmec reciprocating screw injection molding machine, Figure 4.1. Detailed machine specifications are given in Table 4.1. The machine can be operated either in the manual or semi-automatic mode. The original machine sequencing control uses timers, limit switches and relays. The injection, holding and cooling times are set by the corresponding timers on the machine. The limit switches are used to determine when certain machine movements, such as mold closing, carriage advancement, plastication, and mold opening are complete. The screw rotation speed is set manually by adjusting a hand wheel on the screw speed valve. The barrel is equipped with two electric heating bands : the front zone (near the nozzle) and the rear zone (near the hopper). The analog control of barrel temperatures is accomplished by Gulton model JPC on-off controllers. The mold is cooled with tap water.

National Library
of Canada

Canadian Theses Service

Bibliothèque nationale
du Canada

Service des thèses canadiennes

NOTICE

THE QUALITY OF THIS MICROFICHE
IS HEAVILY DEPENDENT UPON THE
QUALITY OF THE THESIS SUBMITTED
FOR MICROFILMING.

UNFORTUNATELY THE COLOURED
ILLUSTRATIONS OF THIS THESIS
CAN ONLY YIELD DIFFERENT TONES
OF GREY.

AVIS

LA QUALITE DE CETTE MICROFICHE
DEPEND GRANDEMENT DE LA QUALITE DE LA
THESE SOUMISE AU MICROFILMAGE.

MALHEUREUSEMENT, LES DIFFERENTES
ILLUSTRATIONS EN COULEURS DE CETTE
THESE NE PEUVENT DONNER QUE DES
TEINTES DE GRIS.






FIGURE 4.1 Danson Metalmic Injection Molding Machine

Table 4.1

Injection Molding Machine Specifications

Machine Model	: Danson Metaltec 60-SR
Capacity	: 2 1/3 oz (66.1 g)
Screw Diameter	: 1.375 in (0.035 m)
Screw L/D Ratio	: 15/1
Screw RPM	: 40-150
Clamping Force	: 60 T (53386 KN)
Hydraulic Pump	: Sperry-Vickers Vane Pump
Pump Capacity	: 8 gpm (1.82 cu.m/hr) flow at 2000 psi (13.8 MPa) Pressure
Electric Motor	: 20 hp (14.92 KW), 3 phase, 50 Hz
Servo valve	: Moog A076-103, 10.gpm (2.28 cu.m/hr) flow at 1000 psi (6.9 MPa)

The hydraulic system of the machine was redesigned to include an electrically controlled servovalve [123]. The electro-hydraulic servovalve installed is a Moog type A076-103, with a 10 U.S. gallon (37.85 L) per minute capacity at a rated pressure drop of 1000 psi (6.2 MPa). It is located in the line which feeds oil to the back of the injection ram. Figure 4.2 depicts the modified hydraulic system of the machine. A simplified version of the full schematic showing the components essential to this work is shown in Figure 7.2.

4.1.2 Instrumentation

Nine Dynisco pressure transducers were used in this study. Two pressure transducers were mounted in the hydraulic system. The first transducer was mounted on the output of the pump while the second transducer was installed just before the servovalve. A third was mounted on the injection cylinder to measure the hydraulic pressure. One was located in the nozzle to measure the nozzle pressure. Four transducers were installed in the mold cavity, as depicted in Figure 4.3, to measure the pressure and pressure gradient(s) in the mold cavity. The ninth pressure transducer was located on the clamping cylinder to measure the hydraulic clamping pressure.

- 1 Electric Motor
- 2 Pump
- 3 Safety Valve
- 4 Ball Valve
- 5 Main Pressure Distributor
- 6 Hydraulic Safety Pilot Operated
- 7 Injection Relief Valve
- 8 Clamp Speed Adjusting Valve
- 9 Clamp Cylinder
- 10 Main Pressure Relief Valve With Two Pilots
- 11 Accumulator
- 12 Filter
- 13 Servovalve
- 14 Hydraulic Motor
- 15 Injection Cylinder
- 16 Carriage Cylinder
- 17 Injection Speed And Screw Back Pressure Regulating Valve
- 18 Pressure Transducer
- 19 Check Valve
- 20 Injection Carriage Forward and Return Valve
- 21 Screw Drive Regulating Valve
- 22 Heat Exchanger

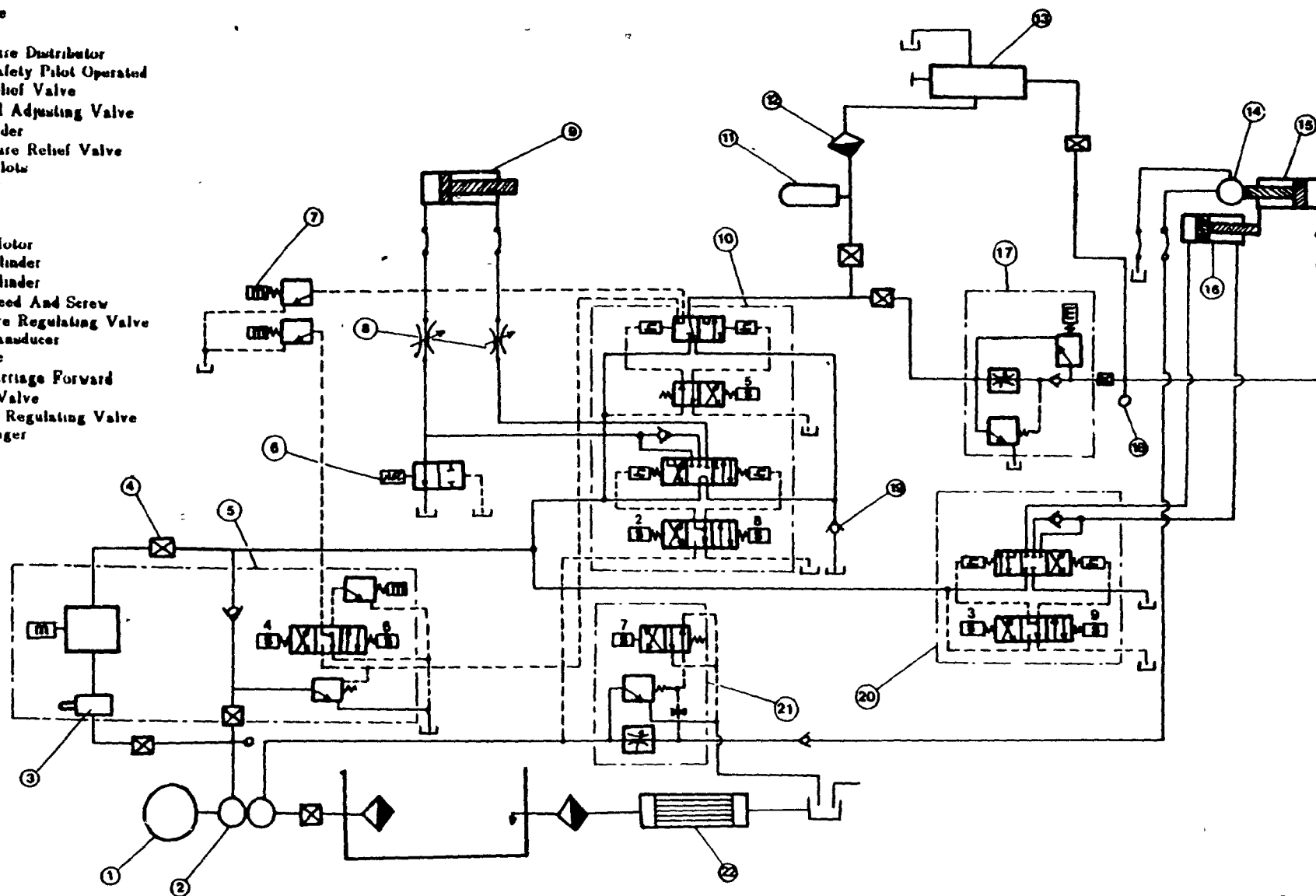


Figure 4.2 The Hydraulic System of the Machine.

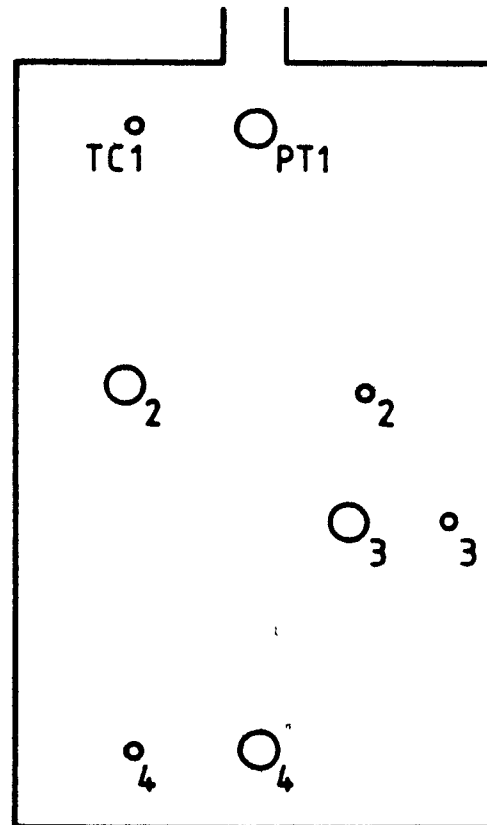


Figure 4.3 The Instrumented Mold Cavity, PT = Pressure Transducer, TC = Thermocouple.

A linear displacement transducer, manufactured by Markite (Model 4709) was used to measure the ram displacement as a function of time during the injection molding cycle. A linear velocity transducer, TRANS-TEK (Model 112-001), was installed to measure the screw linear velocity.

All the transducers were calibrated prior to installation to verify their gauge factors and linearity. The model numbers and calibration equations are given in Table 4.2. The calibration data and descriptions of the calibration procedures are given in Appendix B.

A grounded junction thermocouple (3 mm diameter) projecting into the polymer melt (about 7 mm immersion) from the screw tip and positioned at the centre of the screw, parallel to the flow direction, was installed for melt temperature measurement [124]. The front and rear zone barrel temperatures were measured by means of two type J thermocouples, installed at approximately the mid-plane of each zone. The mold temperature was measured by four thermocouples flush mounted in the mold cavity at the positions shown in Figure 4.3.

4.1.3 Microcomputer System

The injection molding machine has been interfaced with a microcomputer system to achieve the following tasks :

TABLE 4.2
Calibration Equations for the Transducers used
on the Injection Molding Machine

Transducer	Equation
Hydraulic Pressure	$P = 43.24 \times (\text{mV}) - 27.15 \text{ psi}$
Nozzle Pressure	$P = 462.92 \times (\text{mV}) + 51.2 \text{ psi}$
Cavity Pressure (1)	$P = 284.33 \times (\text{mV}) - 133.24 \text{ psi}$
Cavity Pressure (2)	$P = 424.34 \times (\text{mV}) - 208.04 \text{ psi}$
Clamping Pressure	$P = 28.51 \times (\text{mV}) - 59.50 \text{ psi}$
System Pressure (1)	$P = 149.56 \times (\text{mV}) - 189.37 \text{ psi}$
System Pressure (2)	$P = 146.98 \times (\text{mV}) - 121.39 \text{ psi}$
Linear Displacement	$L = 0.6147 \times (\text{mV}) - 1.2265 \text{ cm}$
Linear Velocity	$V = 0.209 \times (\text{mV}) - 0.004 \text{ mm/s}$

$$1 \text{ Pa} = 1.45 \times 10^{-4} \text{ psi}$$

- (1) Data acquisition
- (2) Machine sequencing control
- (3) Control of the different stages of the injection cycle

The heart of the microcomputer system is a Z-80 based Cromemco Single Card Computer with a resident Monitor and Control BASIC Interpreter. The computer has available 13 K (k=1024 bytes) of random access memory (RAM) and 12 K of read only memory (ROM). There are seven 8 bit parallel input-output ports, and four serial ports. The peripherals connected to the system are :

- (1) A CRT terminal (TeleVideo Model 912 C),
- (2) A Burr-Brown 12 bit, 8 channel, analog to digital converter (A/D) (SDM-856),
- (3) A Burr-Brown amplifier, a sample and hold and an 8-channel multiplexer circuit with the A/D converter,
- (4) An 8 bit digital to analog converter (D/A) with amplifier interfaced to the servovalve,
- (5) 8-channel, optically isolated, digital input/output modules (Opto 22). These modules interface the computer to the machine limit switches and solenoid valves.

The microcomputer system lacked sufficient random access memory (RAM) and a permanent mass storage facility. It was

therefore connected to a VAX-780 computer available in the department to store the data and for further data processing. A schematic of the machine, instrumentation, and computer interface is shown in Figure 4.4.

4.2 Material

An injection molding grade high density polyethylene resin, designated as EX2 and supplied by DuPont of Canada, was used in this study. This resin has been employed in a large number of injection molding studies carried out in the Department of Chemical Engineering, McGill University [125,126]. A substantial amount of data is available regarding the fundamental properties and molding characteristics of this resin. Some of these properties are given in Table 4.3.

4.3 Experimental Procedure

The experimental procedure is outlined at the start of each specific experimental section. The general operating conditions which were kept constant for all experiments are:

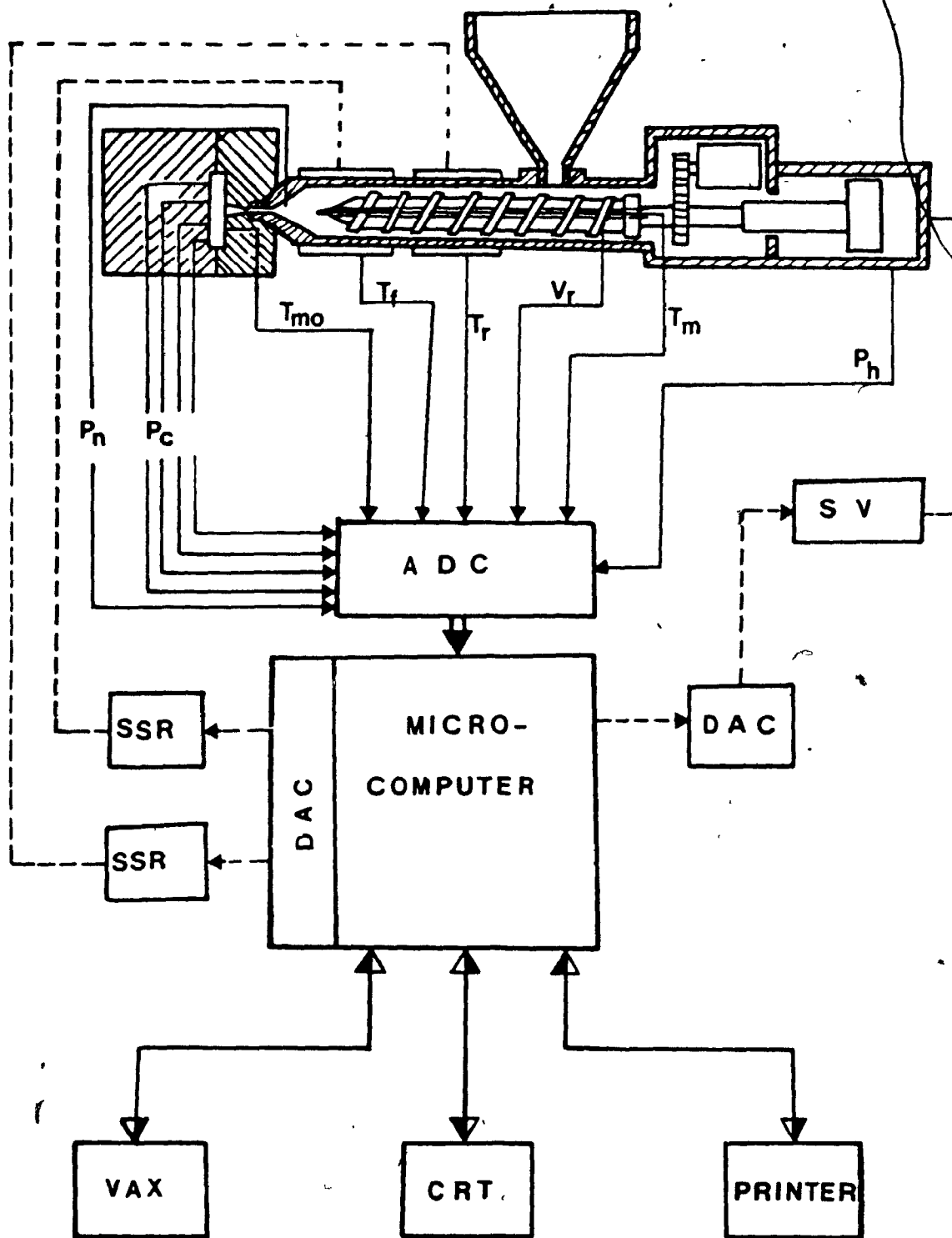


Figure 4.4 Machine - Microcomputer Interface.

Table 4.3

Physical Properties of the Resin Used in this Study [125]

Type of Resin	: EX 2 (HDPE)
MW (Kg/Kmole)	: 74500
MN	: 22300
MW/MN	: 3.33
Density (Kg/m ³)	: 962
Melt Index (g/10 min)	: 7.4
Melting Range, K	: 386-419
Average Specific Heat	: 2543 (solid)
(J/Kg.K)	2459 (melt)
Average Thermal Conductivity	: 0.35 (solid)
(J/m.s.K)	0.26 (melt)
Rheological Characterization	: $\eta = A \exp (E/RT) (\dot{\gamma})^{(n-1)}$
Power Law Index, n	: 0.822
E/R, (K)	: 2167.4
A (Kg.s ⁽ⁿ⁻²⁾ /m)	: 13.99

- (1) Barrel temperatures were maintained at 465 ± 3 K and 430 ± 3 K for the front and rear zones respectively.
- (2) The machine was operated without a check valve on the injection screw.
- (3) The data sampling interval for the static and dynamic experiments was 0.01 sec.

CHAPTER 5

DYNAMIC MODELLING OF THE FILLING STAGE5.1 Machine Operation and Characterization

This section will examine the behavior of the various process variables during the injection molding cycle. The purpose of this investigation is to determine the physical limitations of the machine and to establish working regions for the various dynamic tests. Quantitative relationships between the variables will be obtained from experiments.

Figure 5.1 shows the pressure - time profiles, during a typical injection molding cycle, for cavity gate pressure (P_C), nozzle pressure (P_N) and hydraulic pressure (P_H). It shows clearly the consecutive stages of the cycle : filling, packing and holding, and cooling. The following discussion furnishes a detailed presentation of the behavior of the machine and process variables in the consecutive stages of the cycle.

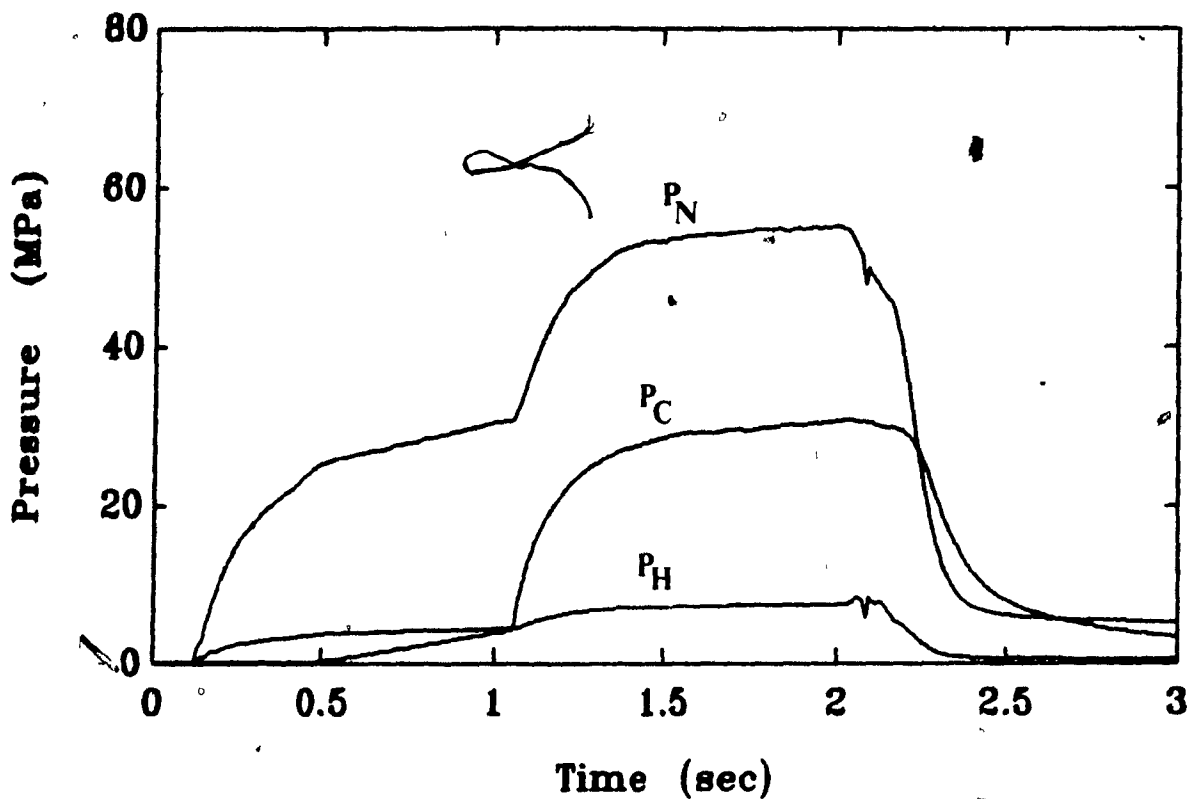


Figure 5.1 Pressure - Time Profiles for Cavity Pressure, Nozzle Pressure, and Hydraulic Pressure During the Injection Molding Cycle.

5.1.1 Injection Start-up Stage :

Figure 5.2 shows the pressure-time profiles for hydraulic, nozzle and cavity gate pressure during the early stages of the filling step. Hydraulic and nozzle pressure profiles in this stage reflect the dynamic behavior of the hydraulic system of the machine including the pump and the servovalve (These dynamics will be discussed and modelled later). The figure shows that hydraulic and nozzle pressures build up significantly before the pressure at the cavity gate starts to increase. This period of time corresponds to the filling of the delivery system. It also indicates that cavity gate pressure cannot be used as a control variable during this period.

5.1.2 Filling Stage :

The three pressure profiles (P_H , P_N , P_C) in the filling stage are depicted in Figure 5.3. It can be seen that after the start-up period, hydraulic and nozzle pressures follow the same trend and that there is a linear relationship between them with a constant P_N/P_H ratio, as shown in Figure 5.4. The linear P_N - P_H relationship is expected because of the direct pressure transmission between the injection piston and the tip of the screw.

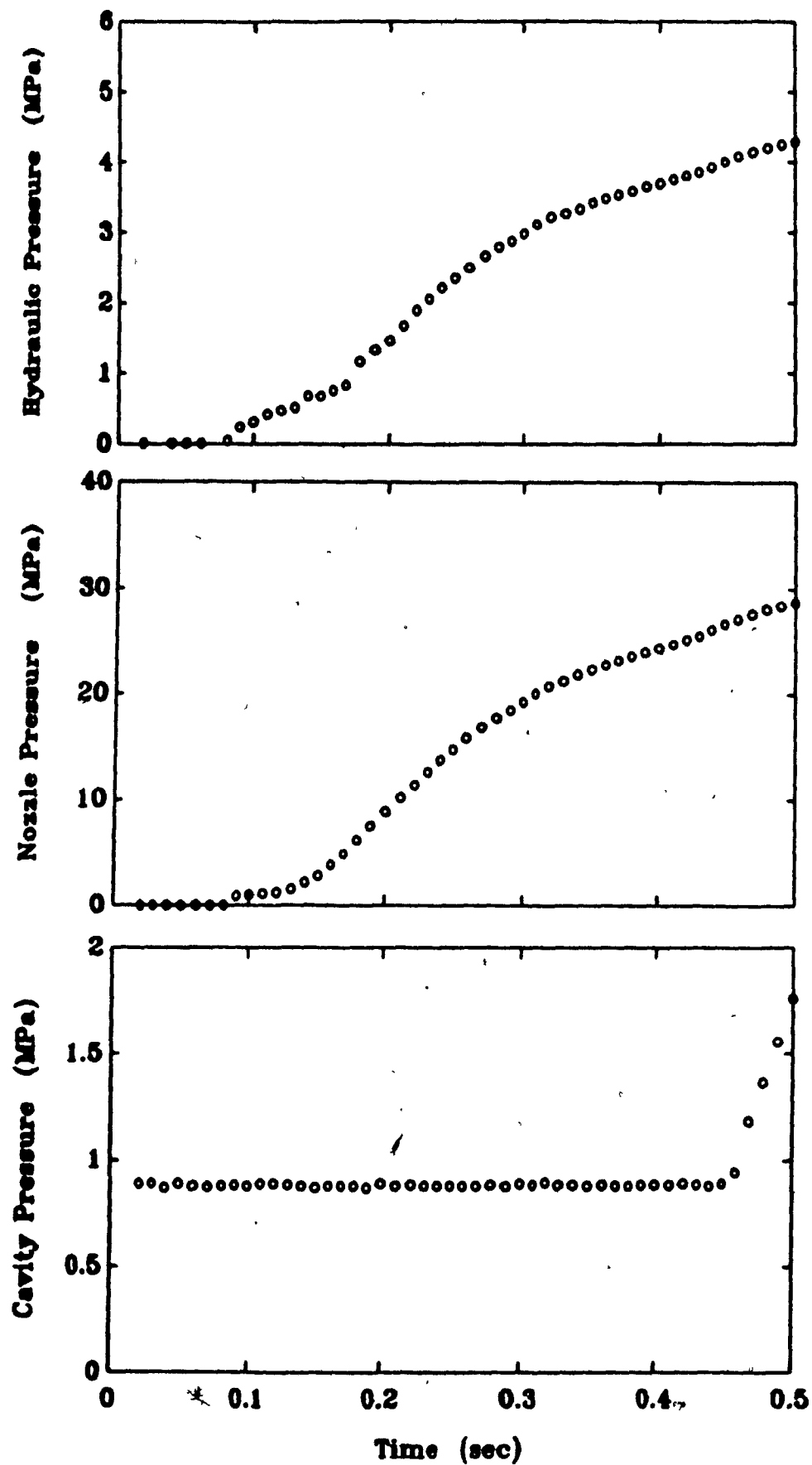


Figure 5.2 Pressure - Time Profile for Hydraulic, Nozzle, and Cavity Gate Pressure at the Start of the Injection Cycle.

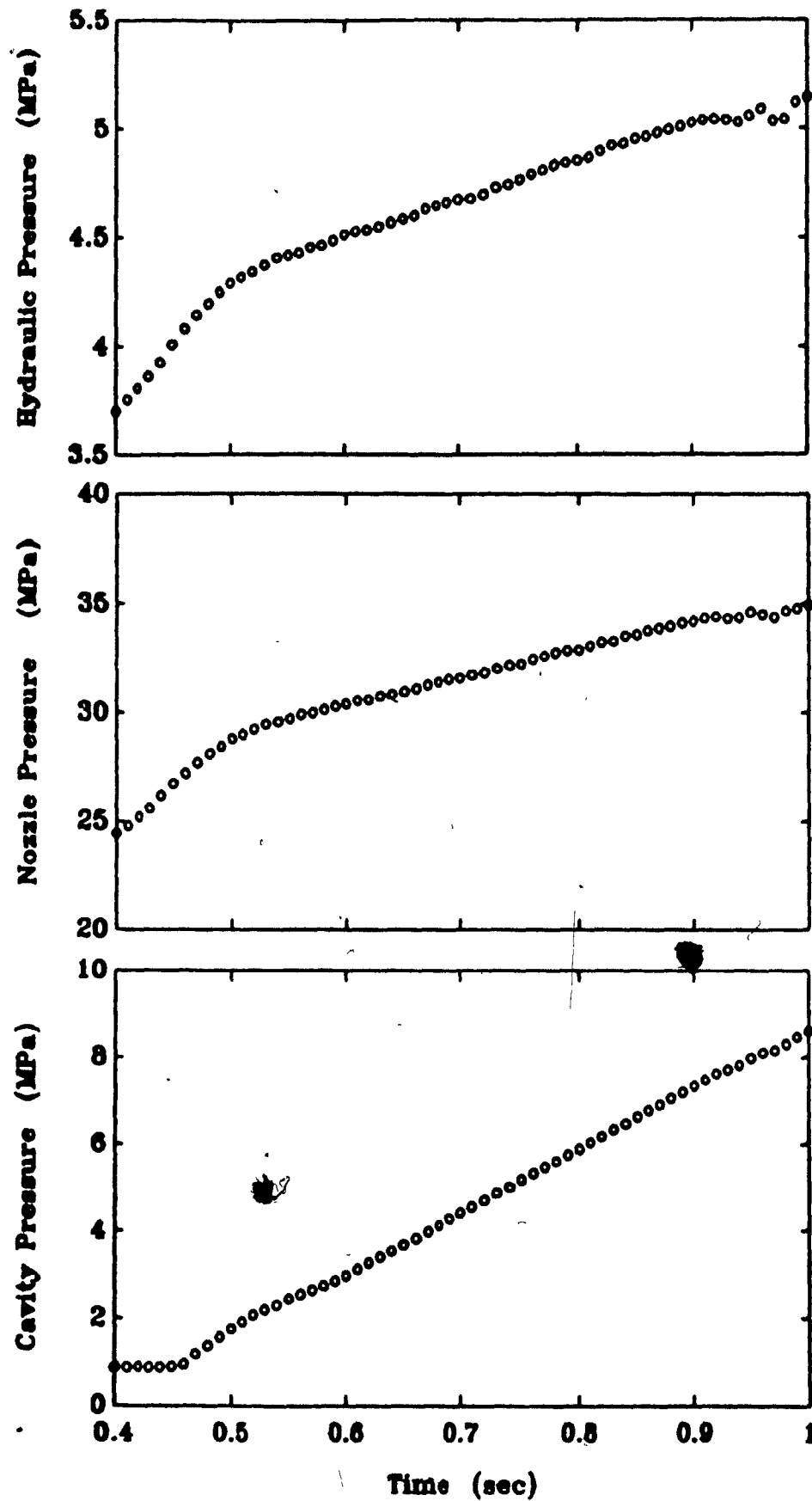


Figure 5.3 Pressure - Time Profiles for Hydraulic, Nozzle, and Cavity Gate Pressure During the Filling Stage.

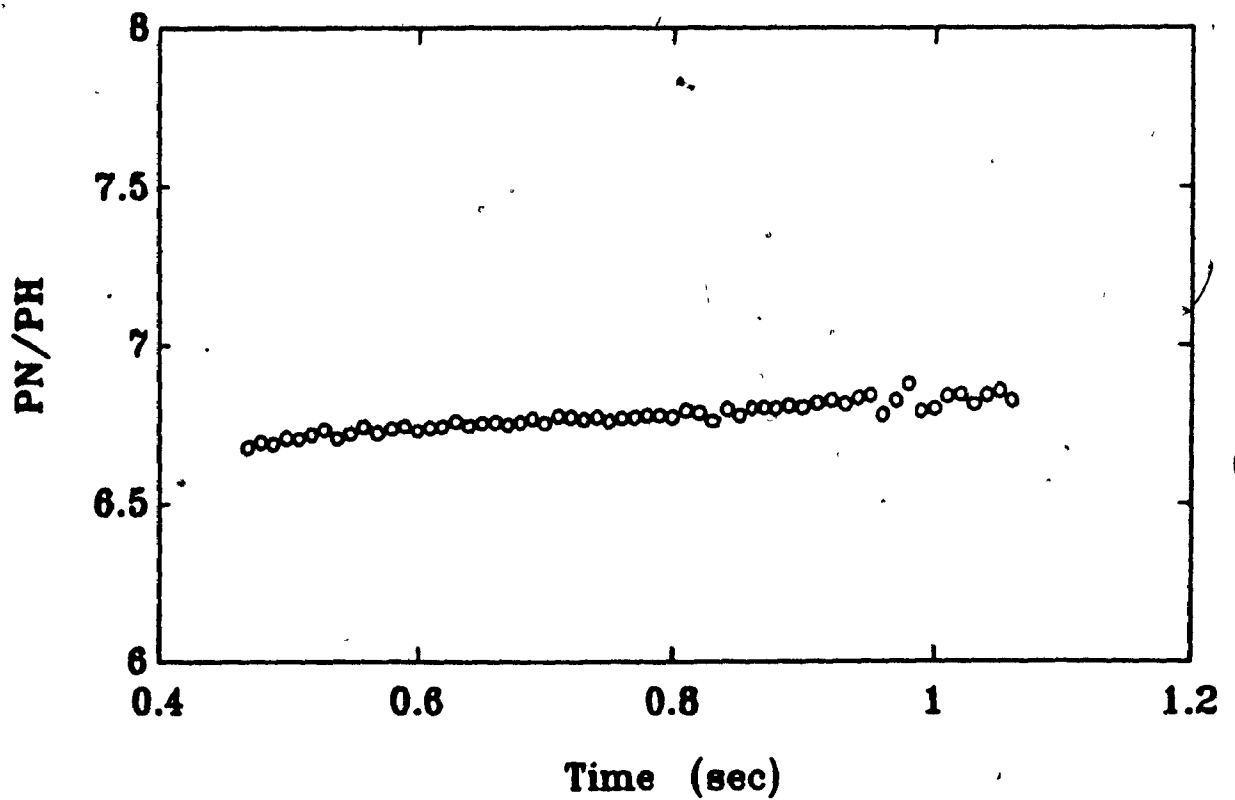
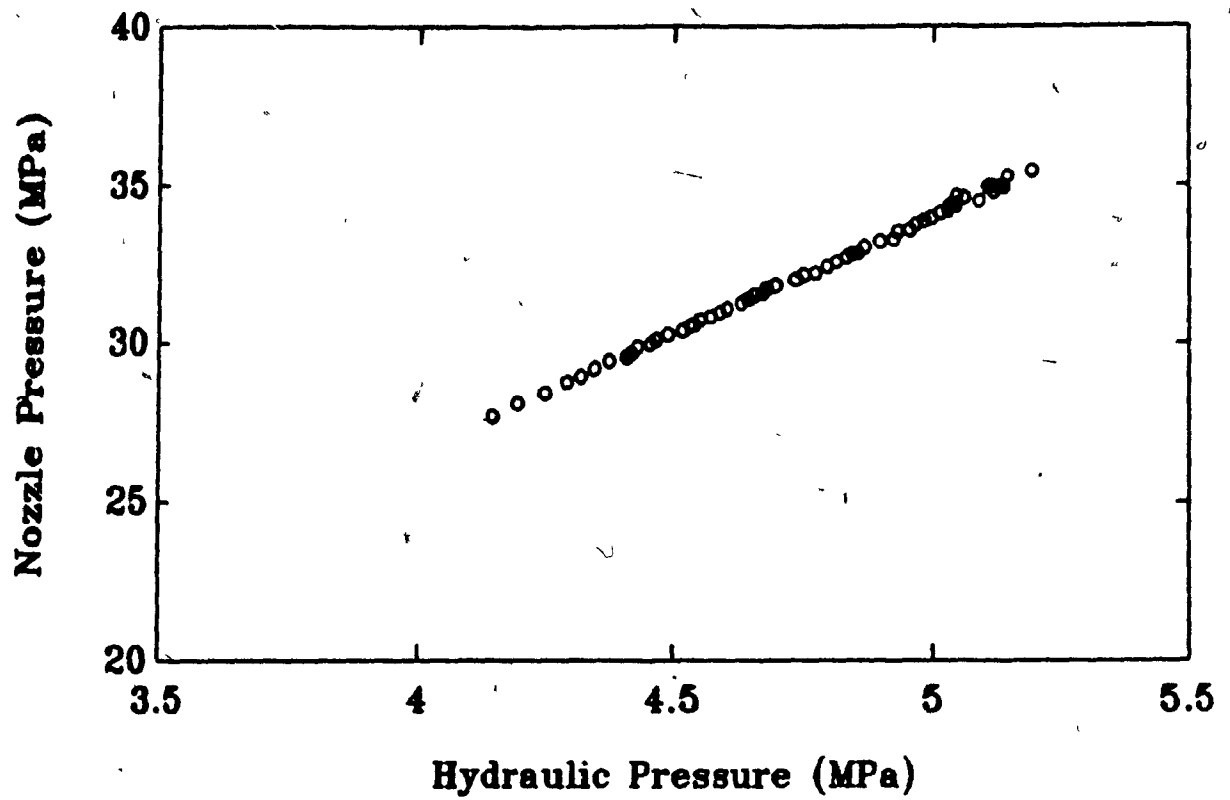


Figure 5.4 Relationship Between Nozzle Pressure (P_N) and Hydraulic Pressure (P_H) in the Filling Stage.

Figure 5.5 shows a nonlinear relationship between nozzle pressure and cavity gate pressure. The nonlinearity is introduced by the varying resistance to the polymer flow in the cavity. This resistance is a function of the polymer rheological behavior, its temperature, amount of polymer in the cavity, and the geometric shape of the delivery system and the cavity. Two regions can be distinguished in Figure 5.5 (A) with different values for the slope of the $P_C - P_N$ curve. This can be related to the corresponding flow regions in the mold cavity as shown in Figure 5.6. The slope of $P_C - P_N$ curve starts to increase in region 2 because the melt reaches the side walls of the cavity and, hence contributes an increase in the shear force [127].

The increase in P_C/P_N ratio with injection time, as shown in Figure 5.5 (B), can be explained as follows :

$$P_N = P_C + P_D \quad (5.1)$$

Where: P_N = nozzle pressure,

P_C = cavity gate pressure,

P_D = pressure drop between the nozzle and the gate

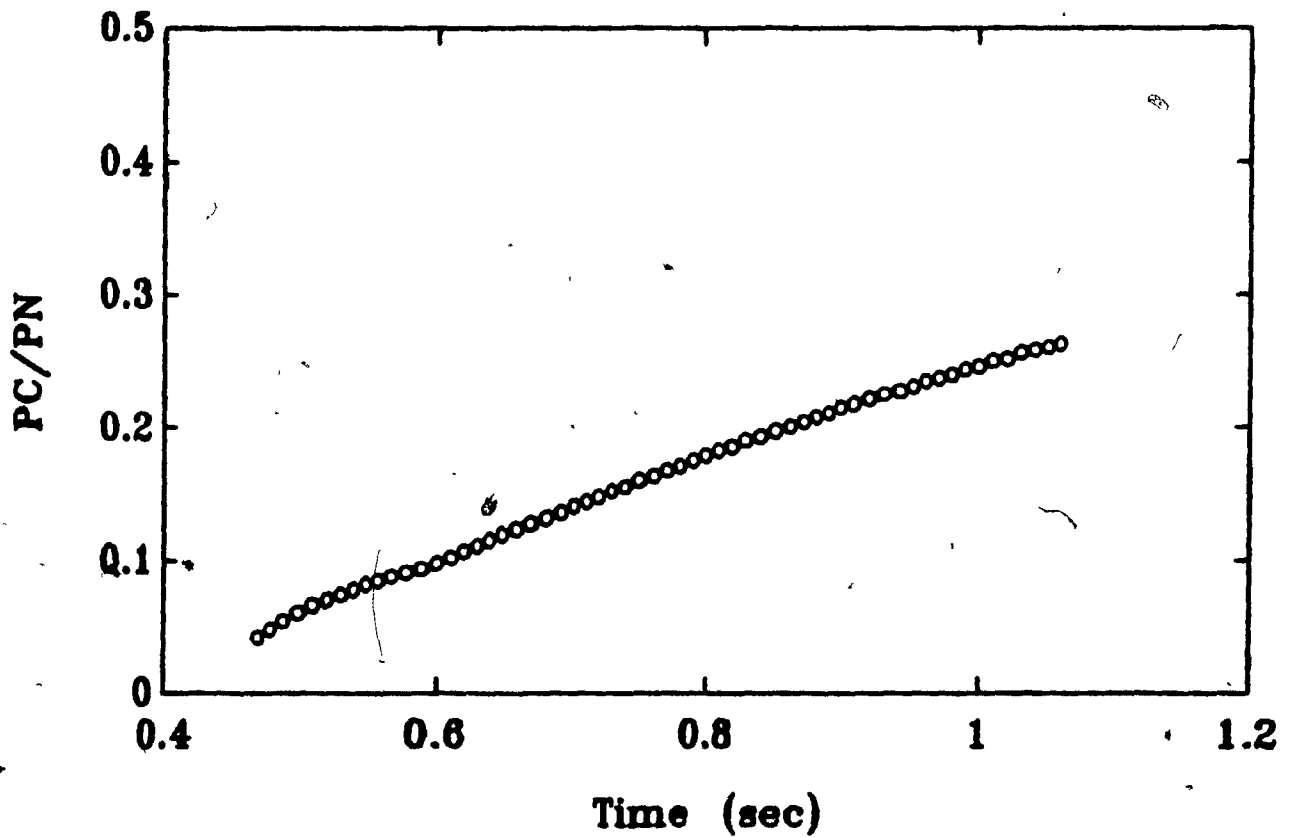
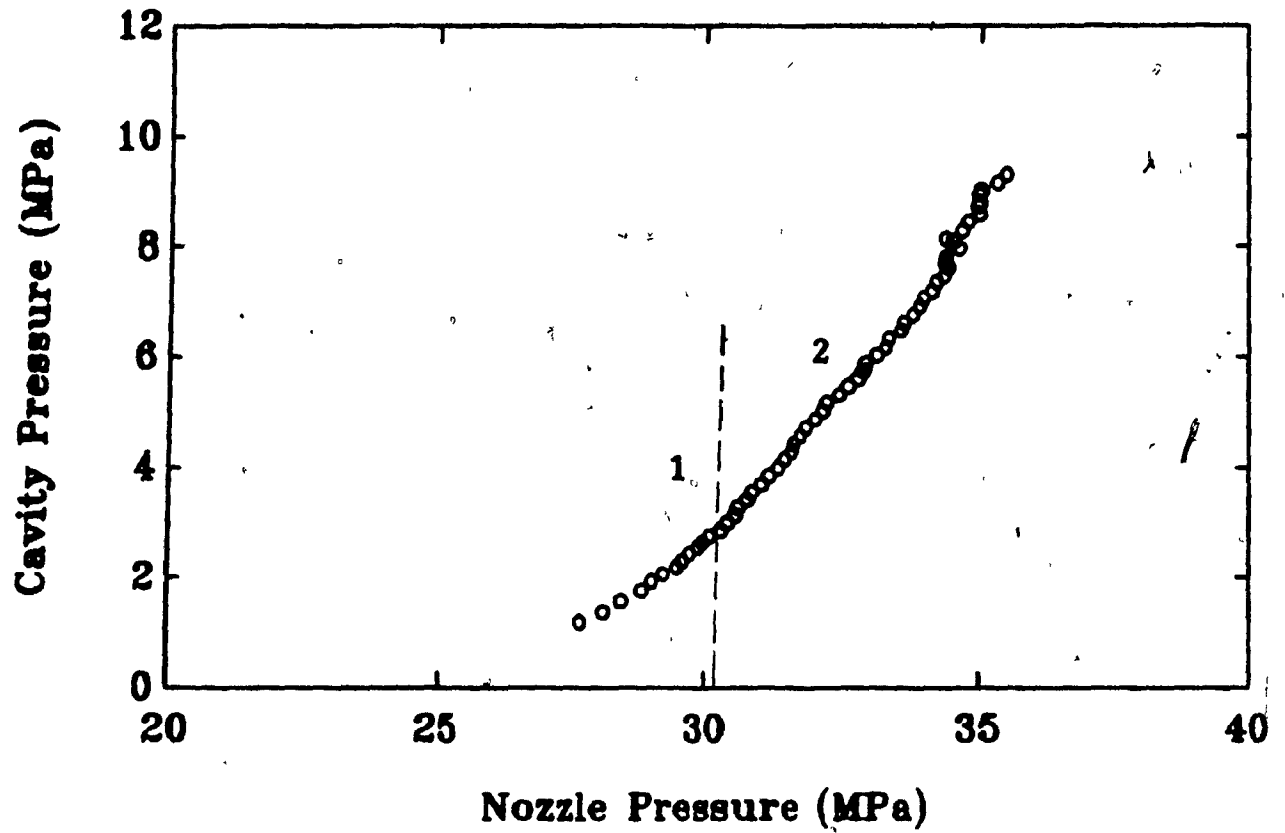


Figure 5.5 Relationship Between Cavity Gate Pressure (P_C) and Nozzle Pressure (P_N) in the Filling Stage.

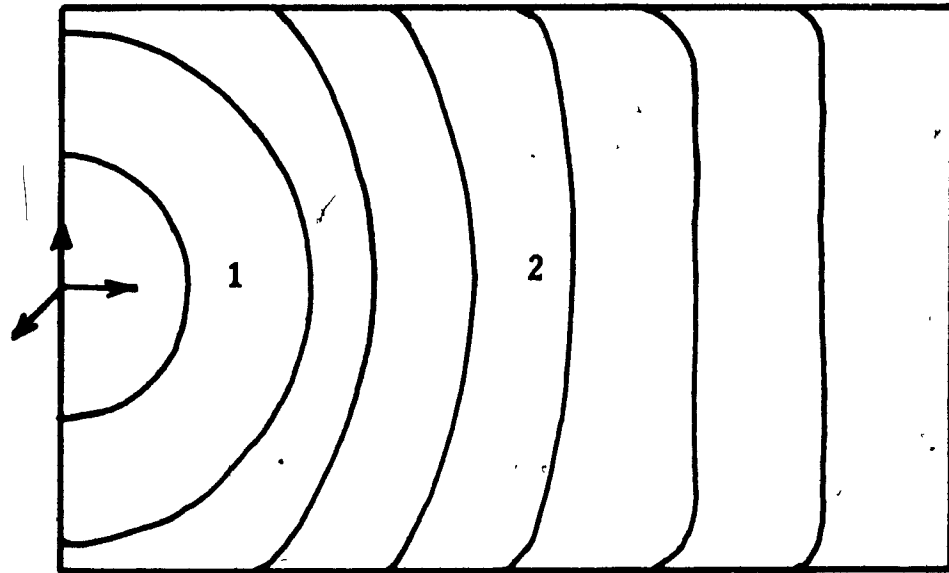


Figure 5.6 Schematic Representation of the Flow Patterns During the Filling of a Rectangular Mold Cavity.

Equation (5.1) can be written as :

$$\frac{P_C}{P_N} = \frac{P_C}{P_C + P_D} \quad (5.2)$$

OR

$$\frac{P_C}{P_N} = \frac{1}{1 + P_D/P_C} \quad (5.3)$$

For a constant flow rate between the nozzle and the cavity gate, $P_D \approx \text{constant}$, and hence, P_D/P_C decreases as P_C increases. Therefore, P_C/P_N ratio increases and this agrees with the experimental results shown in Figure 5.5 (B). For long filling times the rate of decrease of P_D/P_C decreases, and the ratio P_C/P_N approaches a limiting value of 1.0 for very large cavities. This trend is observed in the latter stage of filling (second region).

5.1.3 Filling to Packing Transition :

The hydraulic, nozzle, and cavity gate pressure profiles during the transition period from filling to packing are shown in Figure 5.7. The transition is reflected by the simultaneous sudden increase in the three pressures. (Figure 5.8 shows that the relationship between

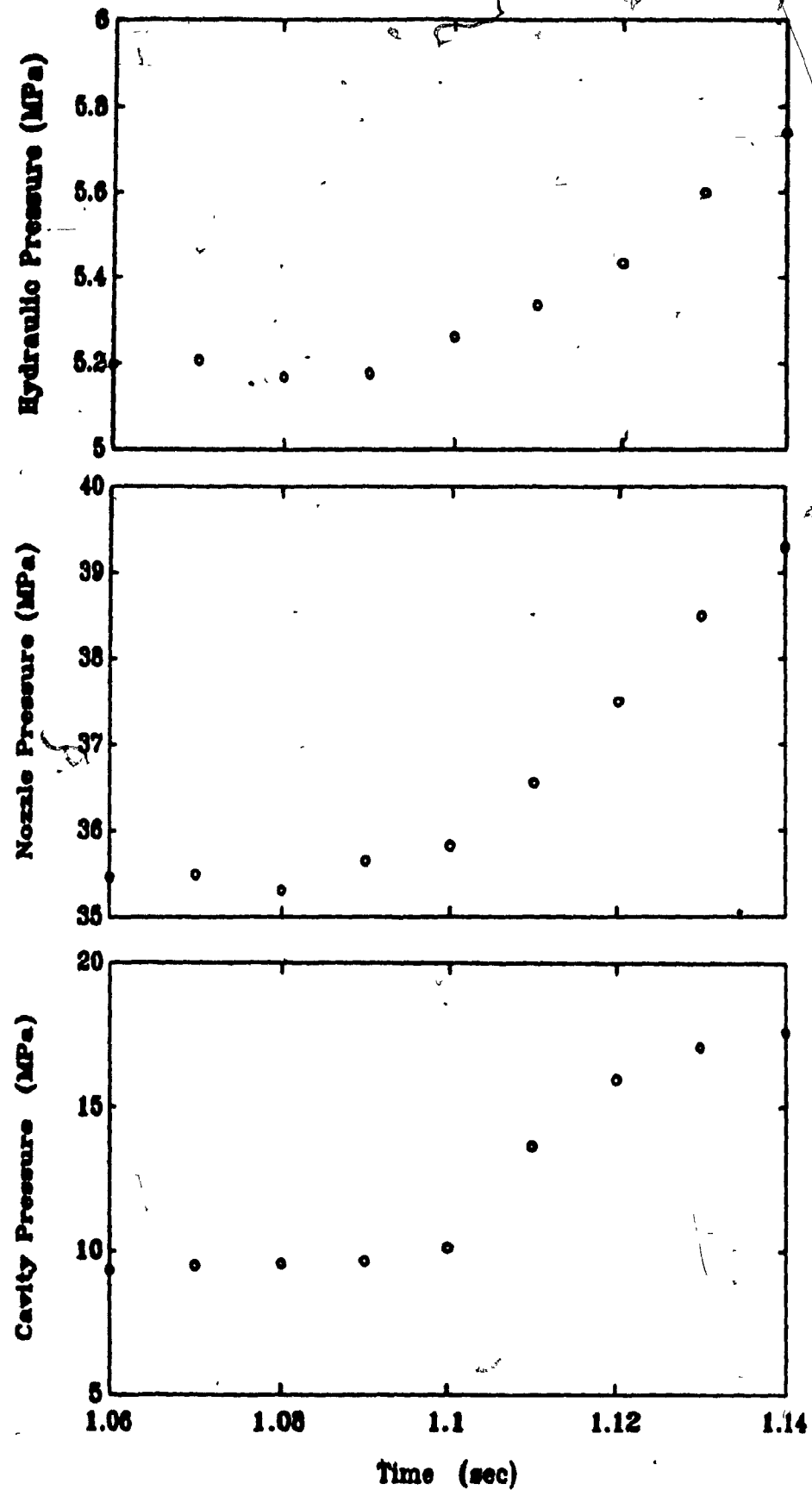


Figure 5.7 Pressure - Time Profiles for Hydraulic, Nozzle, and Cavity Gate Pressure in the Transition Period from Filling to Packing.

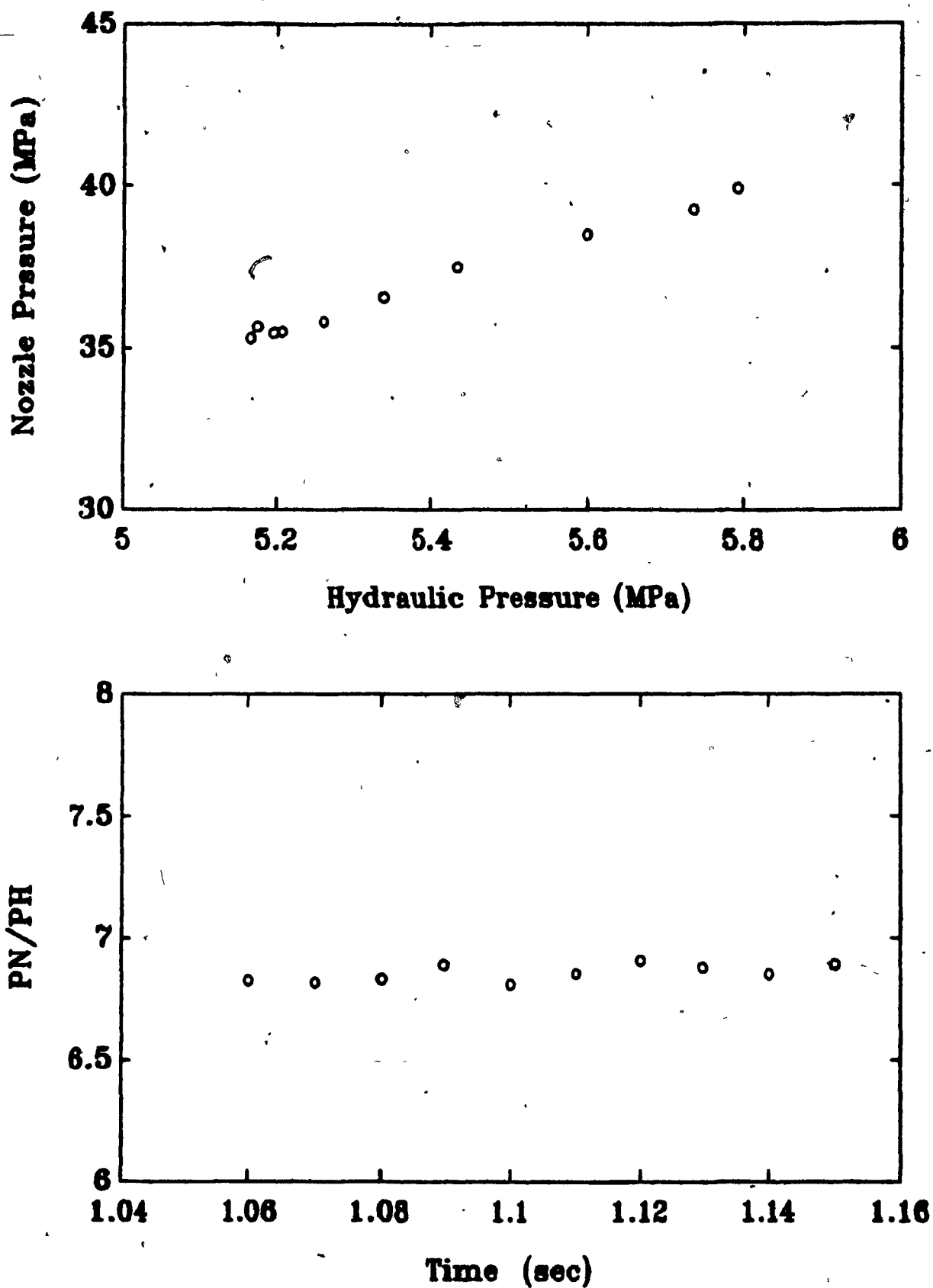


Figure 5.8 Relationship Between Nozzle Pressure (P_N) and Hydraulic Pressure (P_H) in the Transition Period from Filling to Packing.

nozzle and hydraulic pressure remains linear with almost the same P_N/P_H ratio as in the filling stage. The ratio between cavity gate pressure and nozzle pressure exhibits a step change during the transition from the filling to packing as can be seen from Figure 5.9. This ratio increases rapidly initially, and the rate of increase decreases substantially after a fraction of a second. It should be noted that P_C/P_N is not equal to 1.0 during the packing stage. In fact, it is in the range of 0.5 during most of the packing stage.

5.1.4 Packing Stage :

Figure 5.10 shows that hydraulic, nozzle, and cavity gate pressure follow similar trends during the packing stage. Again a linear relationship is observed between nozzle and hydraulic pressure as shown in Figure 5.11. Thus, the P_N-P_H relationship is linear throughout the injection cycle. However, the relationship between cavity gate pressure and nozzle pressure (P_C/P_N), as shown in Figure 5.12, continues to be nonlinear.

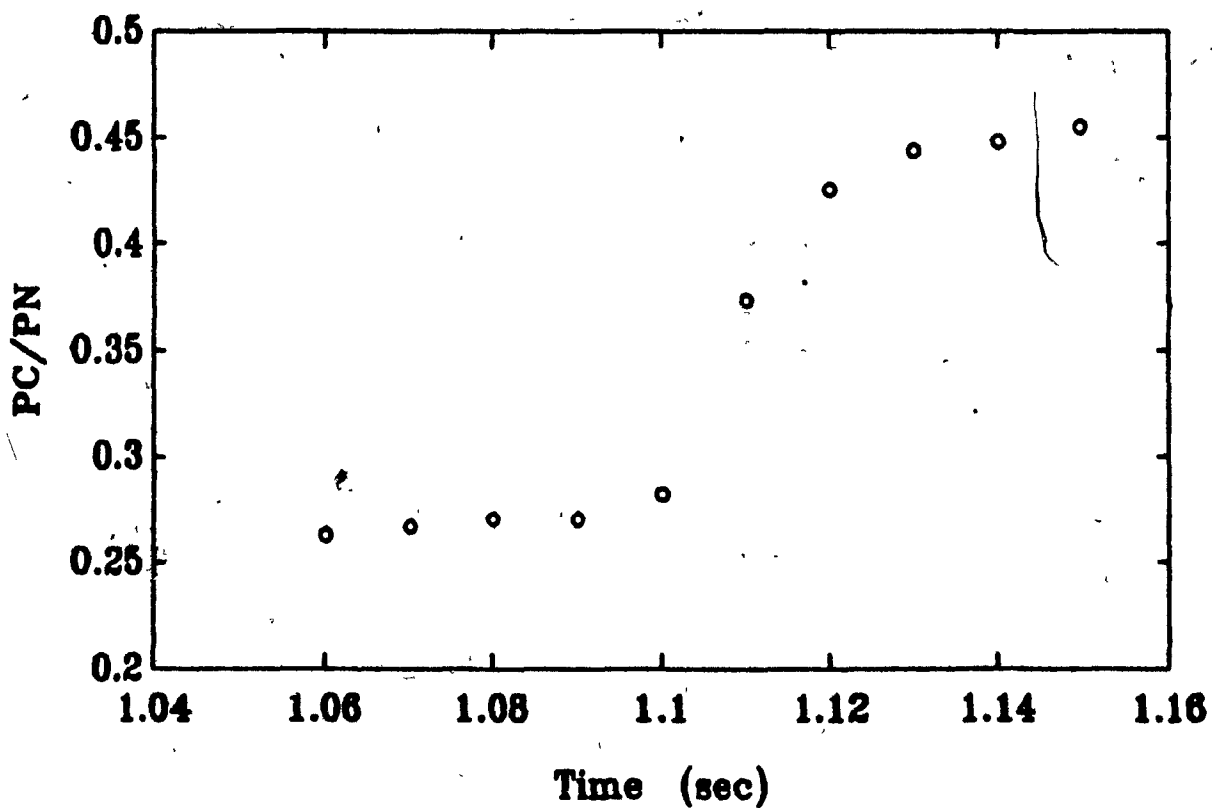
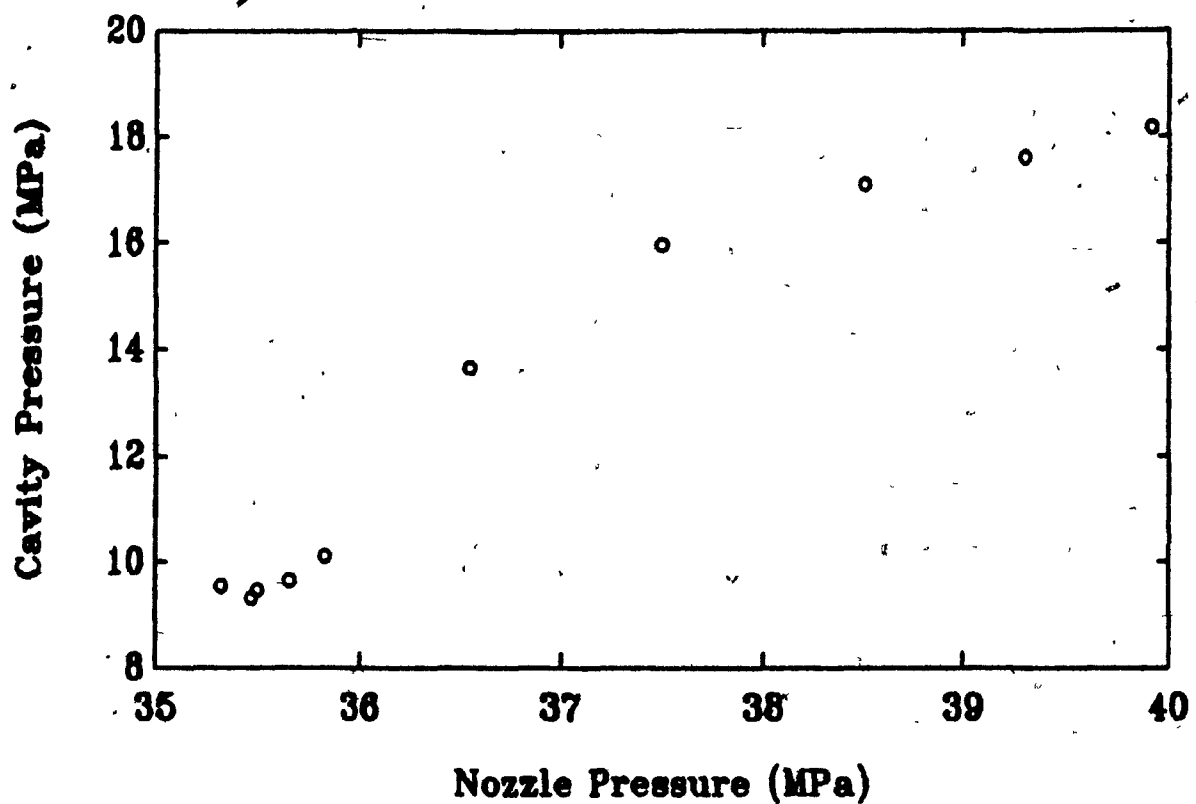


Figure 5.9 Relationship Between Cavity Gate Pressure (P_C) and Nozzle Pressure (P_N) in the Transition Period from Filling to Packing.

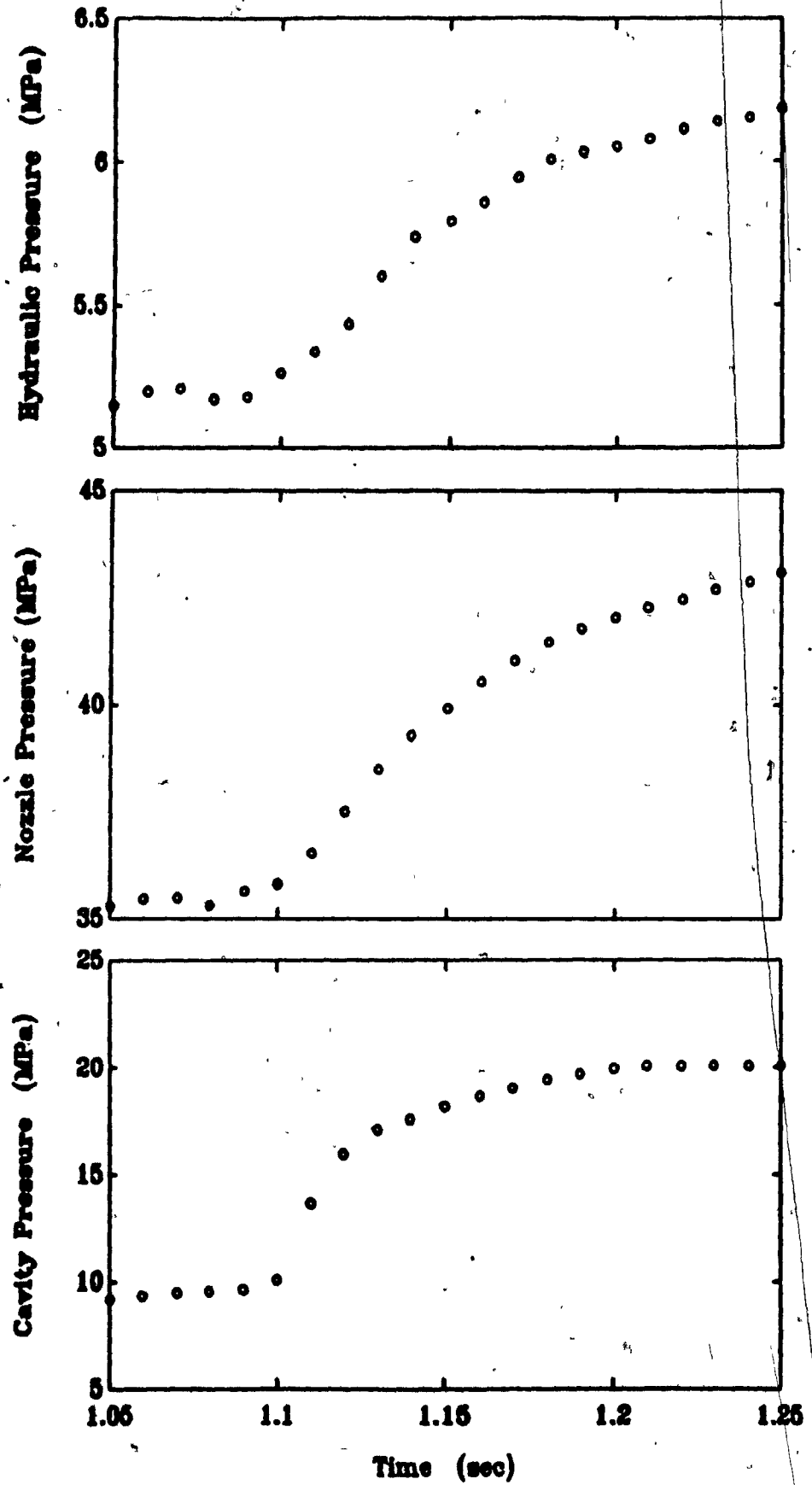


Figure 3.10 Pressure-Time Profiles for Hydraulic, Nozzle, and Cavity Gate Pressure During the Packing Stage.

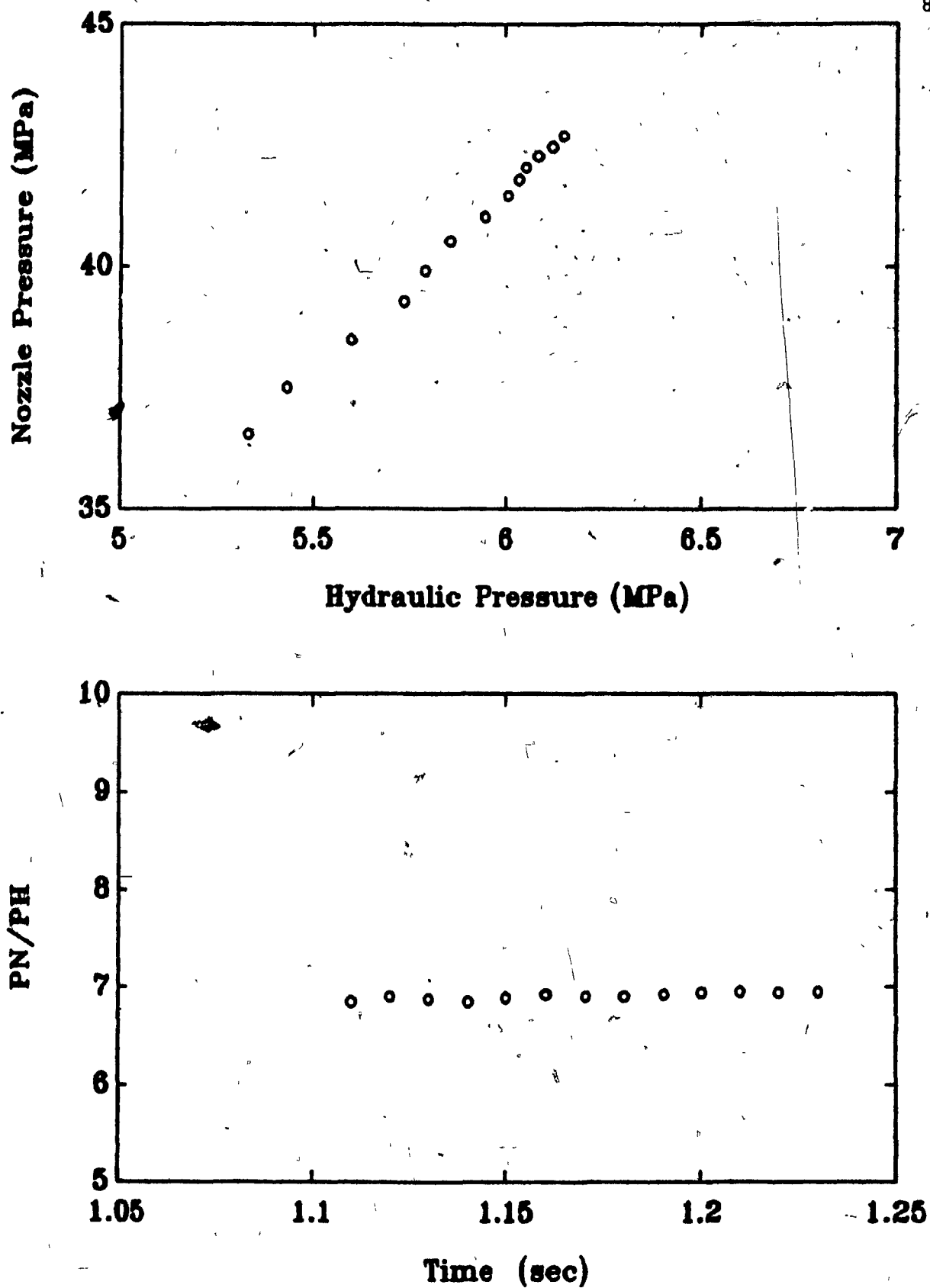


Figure 5.11 Relationship Between Nozzle Pressure (P_N) and Hydraulic Pressure (P_H) During the Packing Stage.

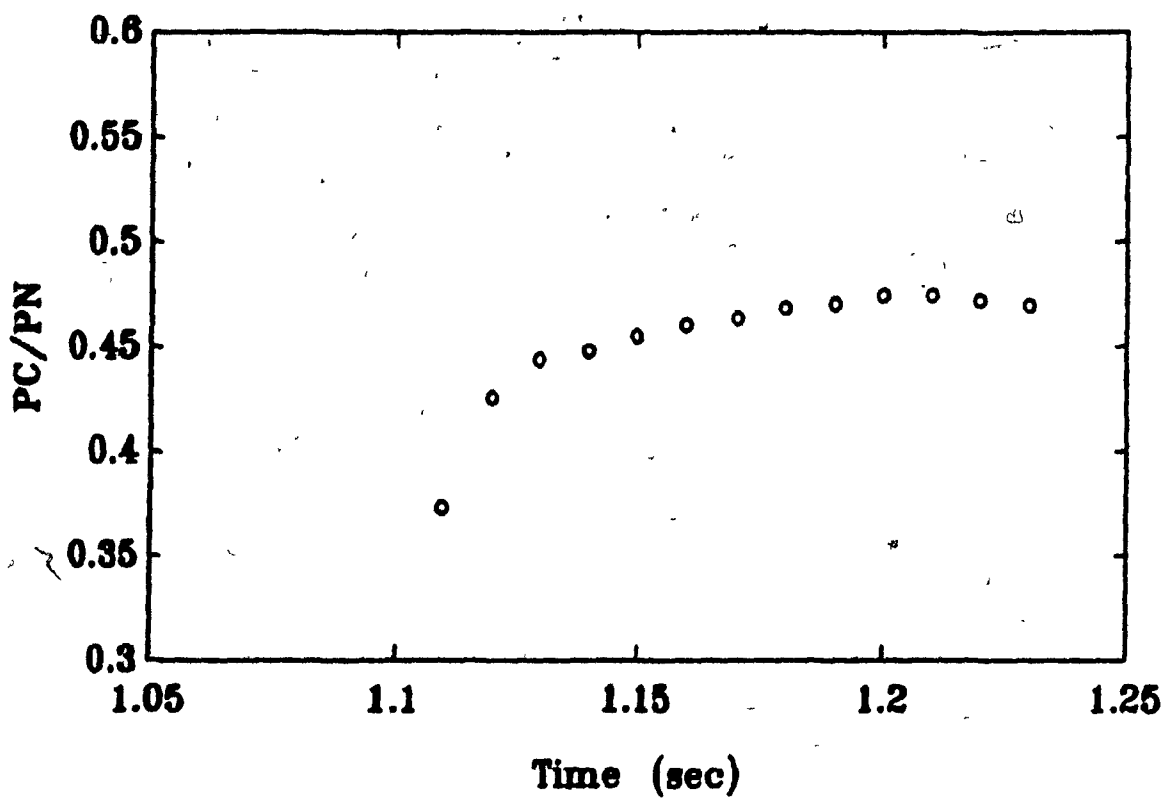
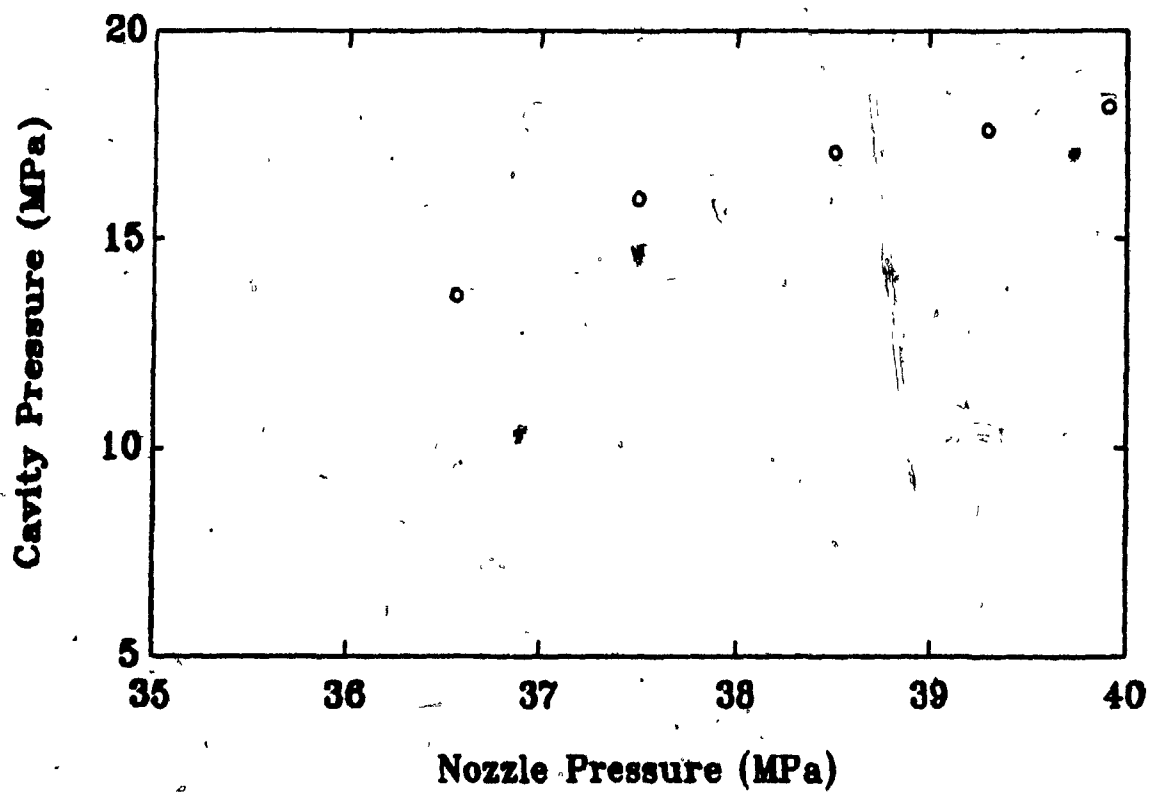


Figure 5.12 Relationship Between Cavity Gate Pressure (P_C) and Nozzle Pressure (P_N) During the Packing Stage.

5.1.5 Summary

The following conclusions can be drawn :

- 1- The relationship between nozzle and hydraulic pressure is linear throughout the injection cycle.
- 2- The relationship between cavity gate pressure and nozzle pressure is not linear during the filling and packing stages.
- 3- The $P_C - P_N$ ratio exhibits a step change during the transition from filling to packing.
- 4- Cavity gate pressure cannot be used as the controlled variable at the start of the filling stage.

5.2 Dynamic Modelling of Cavity Gate Pressure

This section presents the experimental development of the dynamic models for cavity gate pressure during the filling stage. Two experimental modelling techniques were employed : deterministic (step) and stochastic (PRBS) tests.

5.2.1 Deterministic (Step) Tests

Step tests of magnitudes ± 10 , ± 15 and ± 20 percent change in the servovalve opening (0% closed, 100% fully open) were performed during the filling stage of the injection molding cycle. The steps were introduced at different times during the filling stage to investigate the linearity of the developed models and the behavior of the model parameters as a function of the filling time or the filled fraction of the cavity. Steps were also introduced within different ranges of the valve opening (20 - 60%). Cavity pressure at the gate, cavity pressure at the second transducer location (Figure 4.3), nozzle pressure, hydraulic pressure, ram velocity, ram linear displacement, melt temperature at the nozzle, and mold temperature were recorded.

5.2.1.1 Results and Discussion

The response of cavity gate pressure to various step changes in the servovalve opening is shown in Figures 5.13 - 5.15. Examination of the results indicates that there is a delay in the response of about two sampling intervals (sampling interval = 0.01 sec). The delay in the response could be attributed to the distance between the position at which the step is introduced (the servovalve) and the location of the cavity pressure transducer. After the transient period, the response has a steady slope equal to that observed for an unperturbed equivalent valve opening.

The response of cavity gate pressure to step changes in the servovalve opening was modeled by a first-order plus time delay model superimposed on a constantly increasing (ramp) pressure component of the form :

$$P_C(t) = K_1 t + K_2 (1 - e^{-(t-D)/\tau}) \quad (5.4)$$

Where :

- P_C = cavity gate pressure, psi
- K_1 = ramping slope, psi/sec
- K_2 = process gain, psi/% change in valve opening
- τ = process time constant, sec
- D = time delay, sec

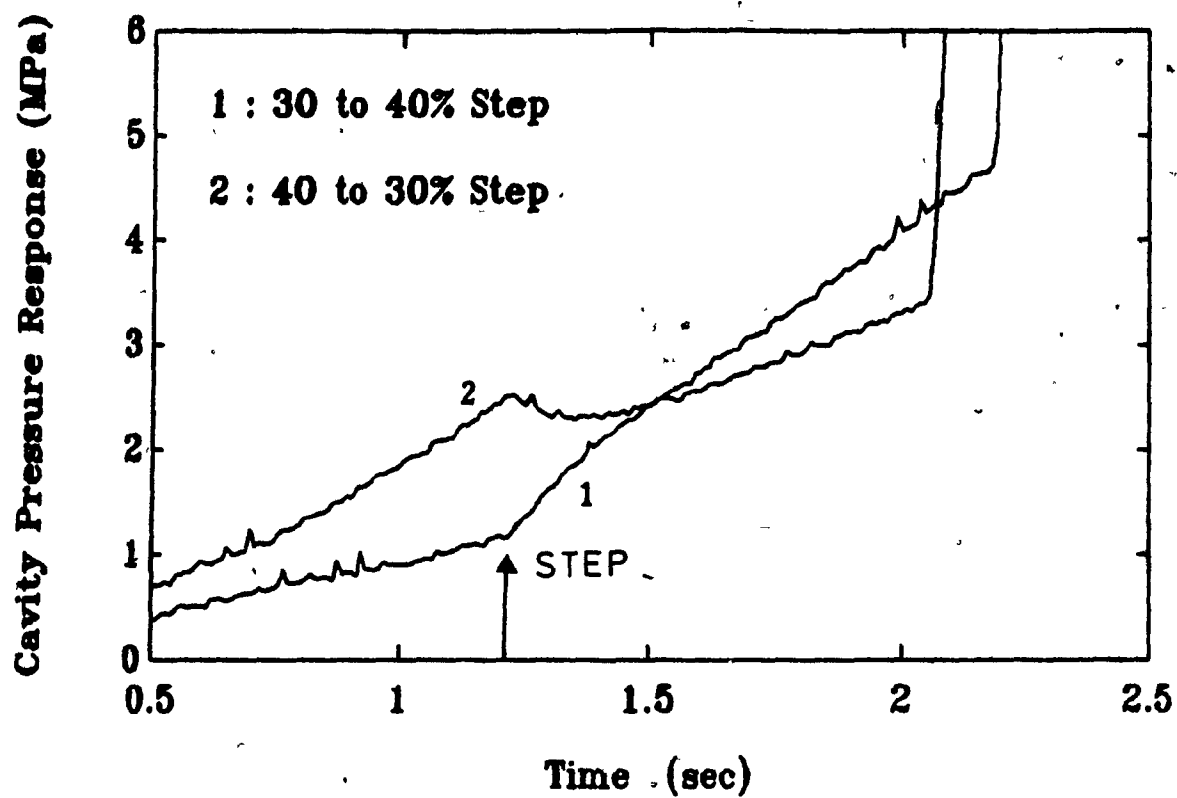


Figure 5.13 Cavity Gate Pressure Response to 30 - 40% and 40 - 30 % Step Changes in Valve Opening.

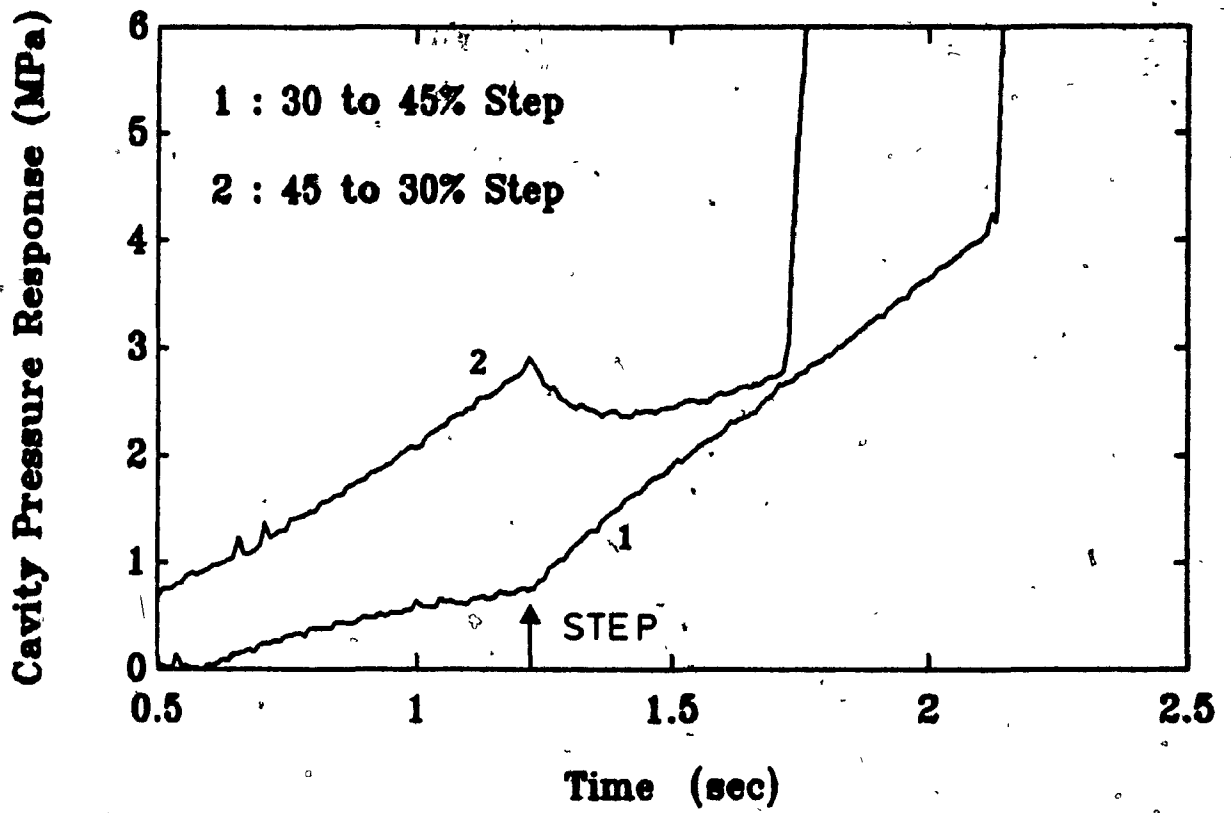


Figure 5.14 Cavity Gate Pressure Response to 30 - 45% and 45 - 30% Step Changes in Valve Opening.

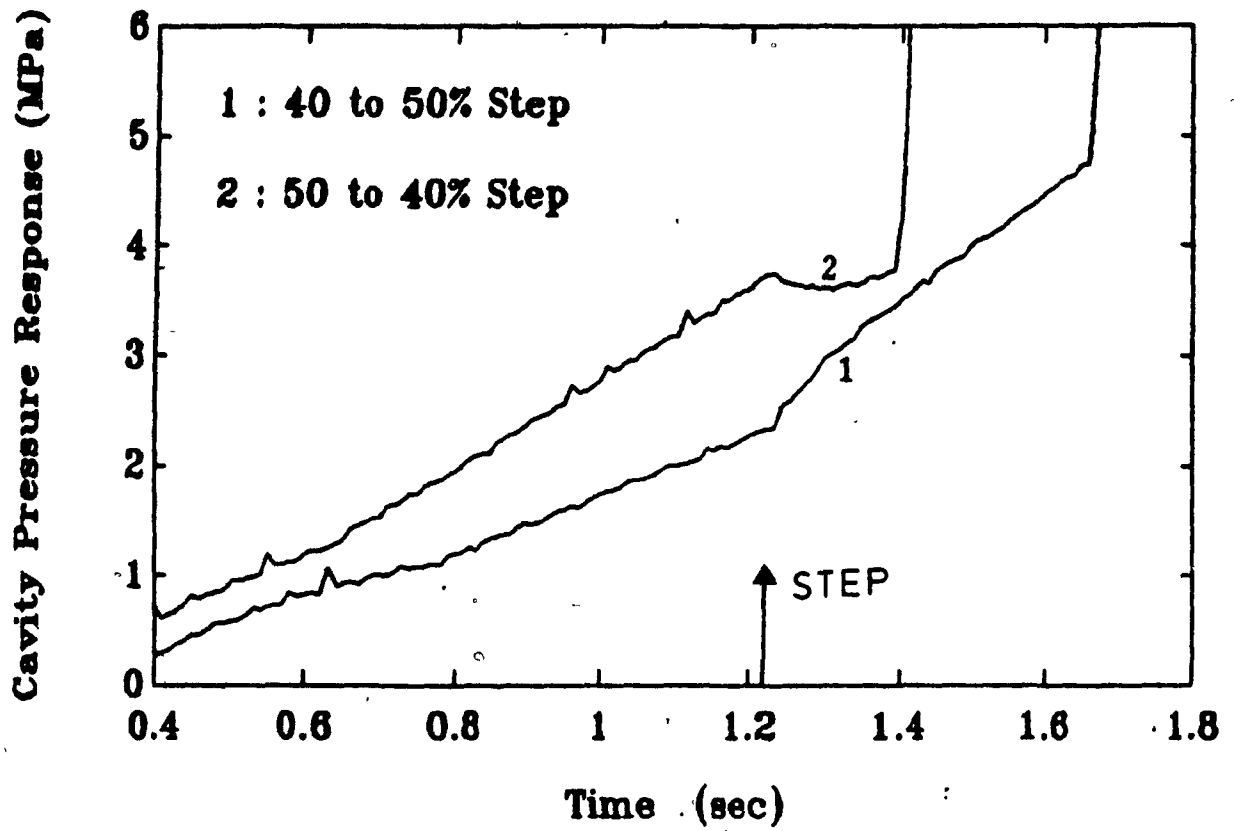


Figure 5.15 Cavity Gate Pressure Response to 40 - 50% and 50 - 40% Step Changes in Valve Opening.

Model fitting was done using the NONLINWOOD [128] computer program. An overdamped second-order with time delay model plus a ramp component was also fitted to the data. The fits for both the first and second order models appeared to be equally good, but comparison of the two models using the sum of squares of the residuals (SQR) indicated that the second-order model was a slightly better fit. The improvement in SQR was not large, and the simpler first-order model was thus preferred. Figures 5.16 and 5.17 show the agreement between the experimental results and the first-order model predictions. The parameters for Equation (5.4) are given in Table 5.1. As it can be seen from Table 5.1, the process gain indicates that cavity gate pressure has a nonlinear response to changes in the servovalve opening.

The results show that the change in the process gain for different step magnitudes (40 - 50% and 40 - 55%) is less than its change to the same step magnitude with different initial valve openings before the step (30 - 40% and 30 - 45%). This is attributed to the effect of the amount of polymer present in the cavity at the time of the step change. Figure 5.18 and the corresponding Table 5.2 show that the process gain increases from 28.96 to 58.07 by increasing the initial valve opening from 30 to 40 percent.

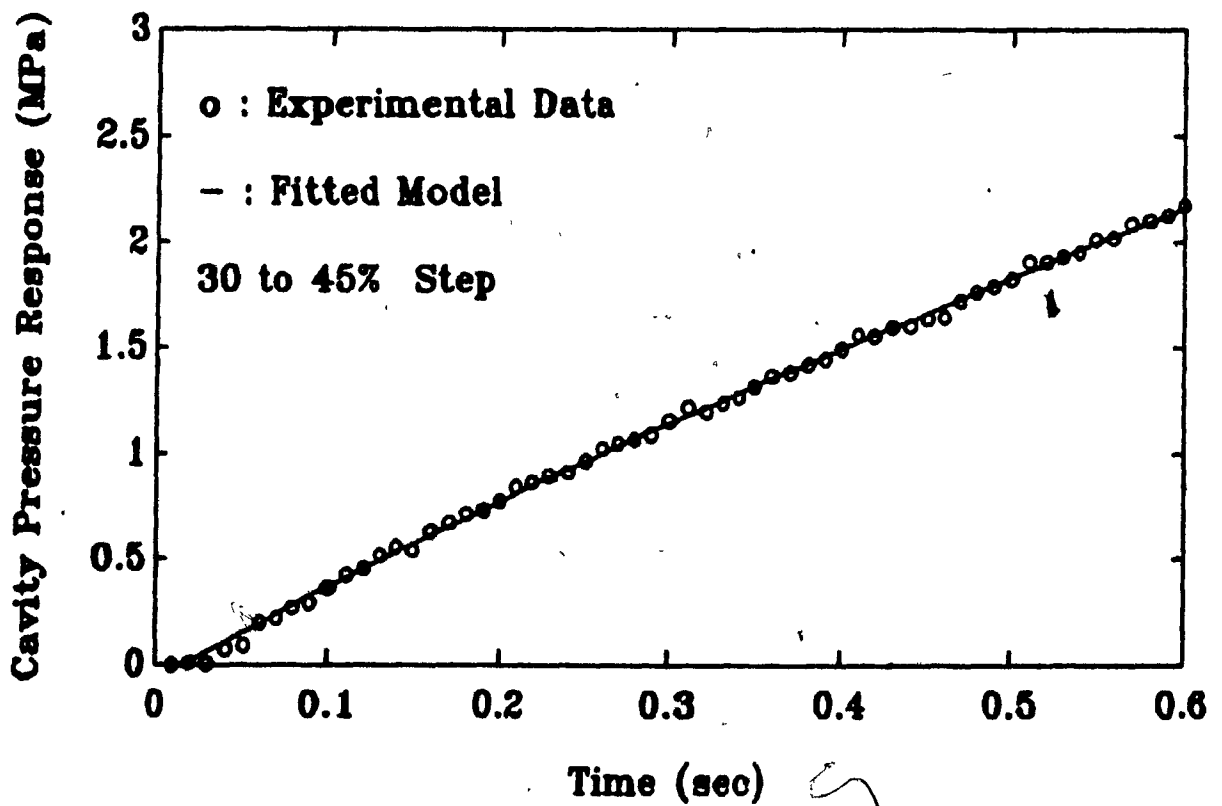
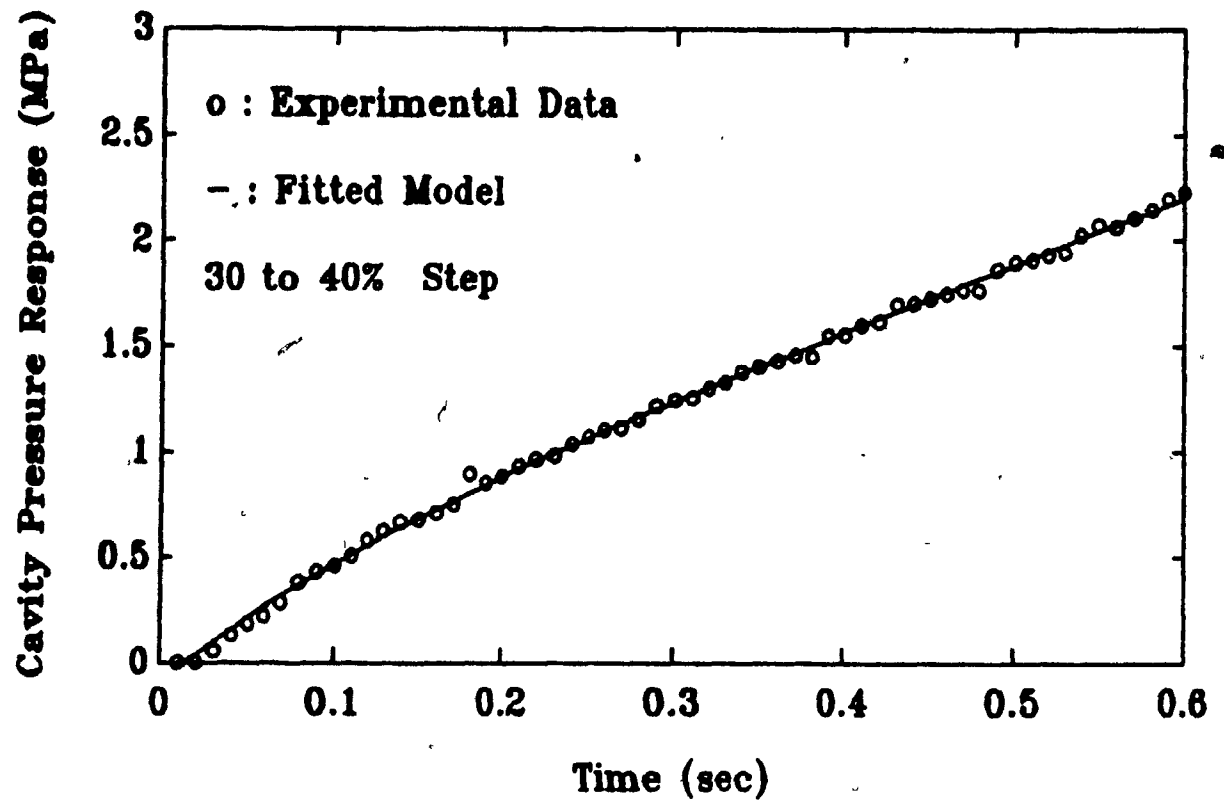


Figure 5.16

Comparison of Experimental Cavity Gate Pressure Response to Fitted Model. Step at $t=0.0$

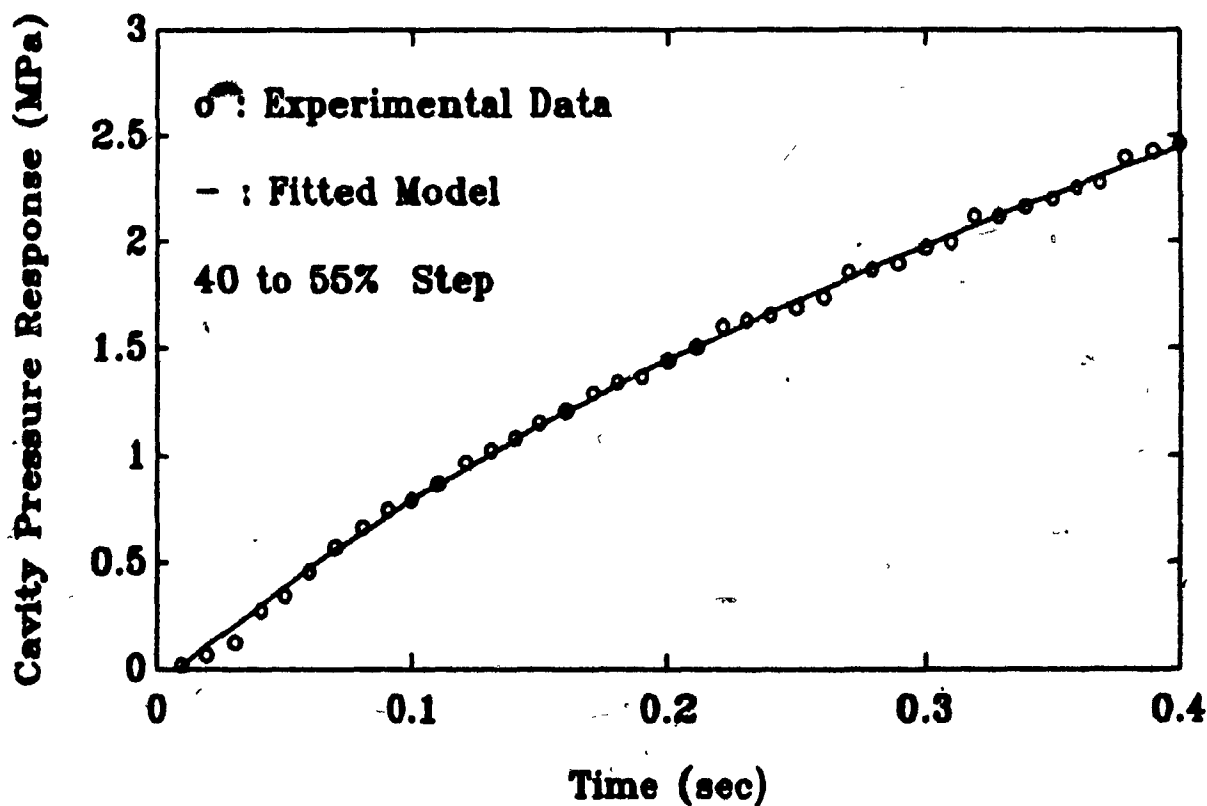
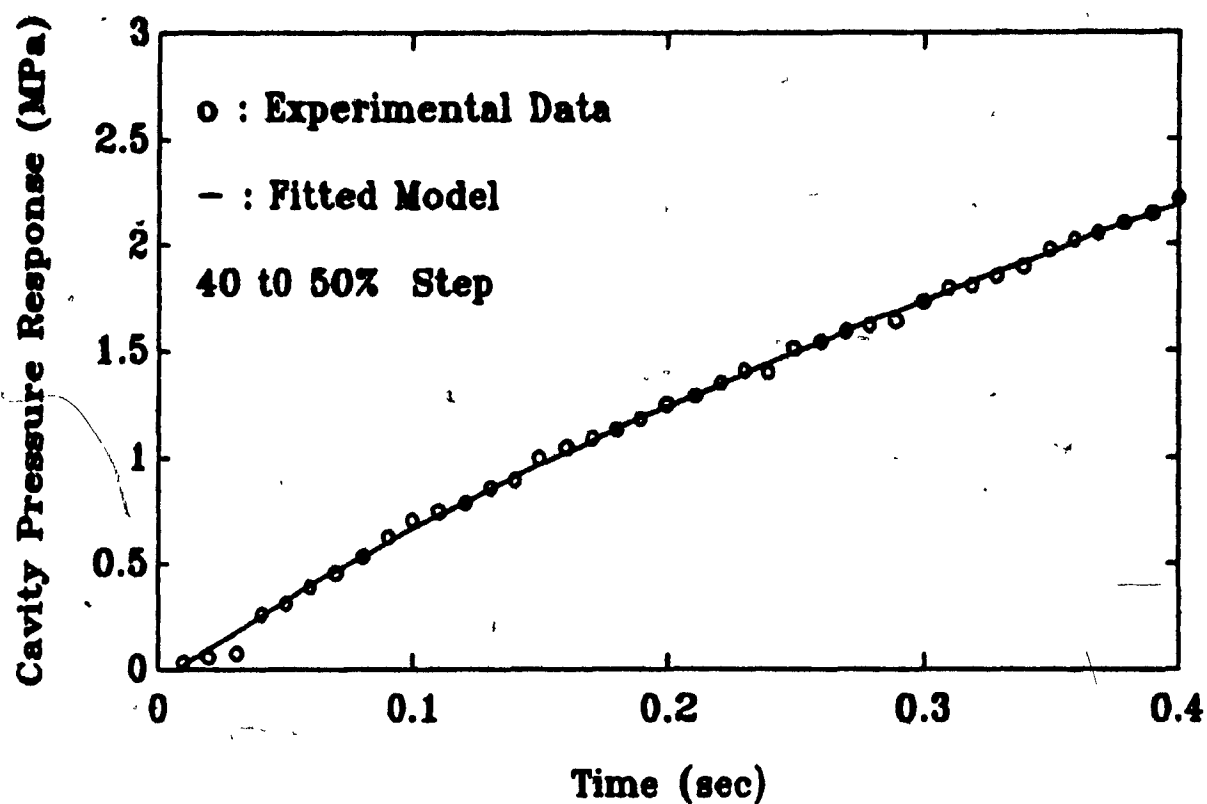


Figure 5.17 Comparison of Experimental Cavity Gate Pressure Response to Fitted Model. Step at $t=0.0$

TABLE 5.1
Values of the Parameters for the Cavity Pressure
Model : First Order Plus Ramp

Change in Valve Opening, %	Ramp Slope K_1 , KPa/sec.%	Process Gain K_2 , KPa/%	Time Constant τ , sec	Time Delay D , sec
30 - 40	79.38 ± 5.37	36.34 ± 1.17	0.122 ± 0.05	0.022 ± 0.008
40 - 50	104.5 ± 2.62	54.62 ± 5.10	0.135 ± 0.11	0.016 ± 0.009
40 - 55	72.76 ± 2.68	62.20 ± 5.38	0.162 ± 0.11	0.016 ± 0.007

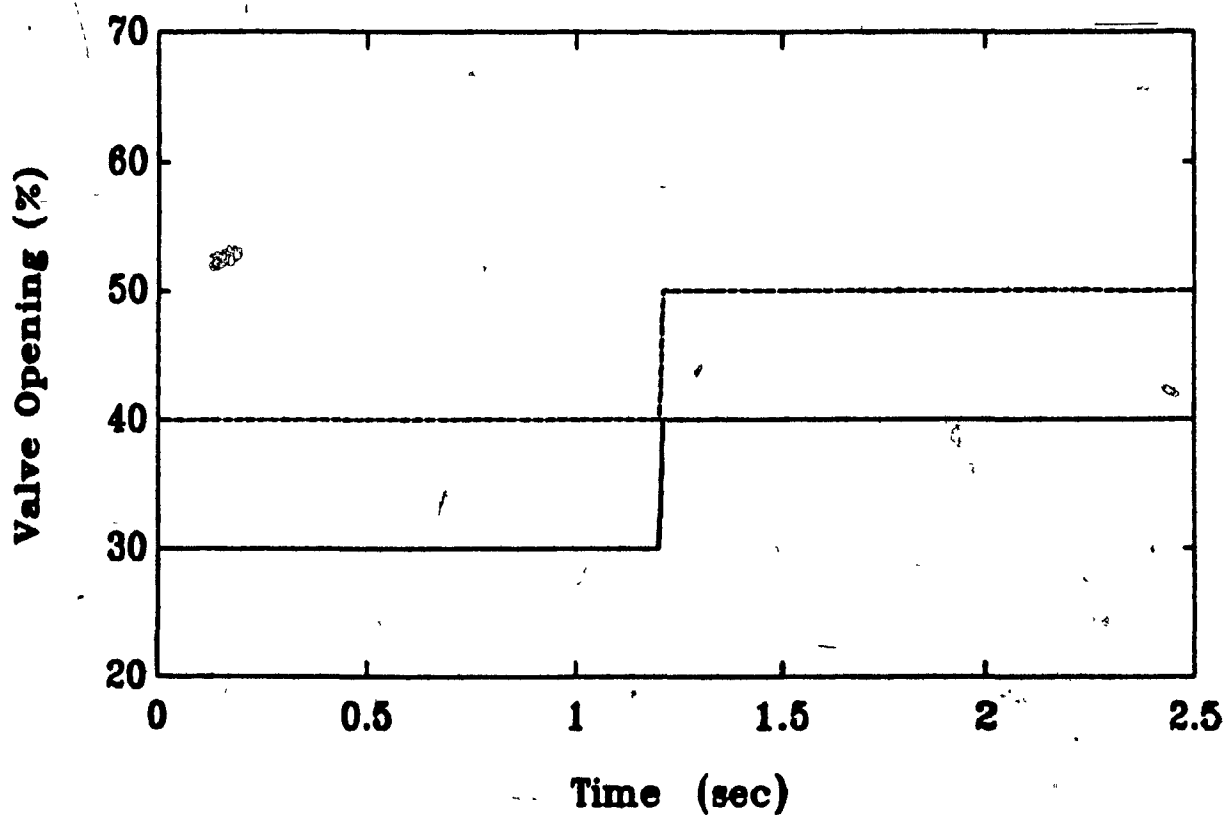
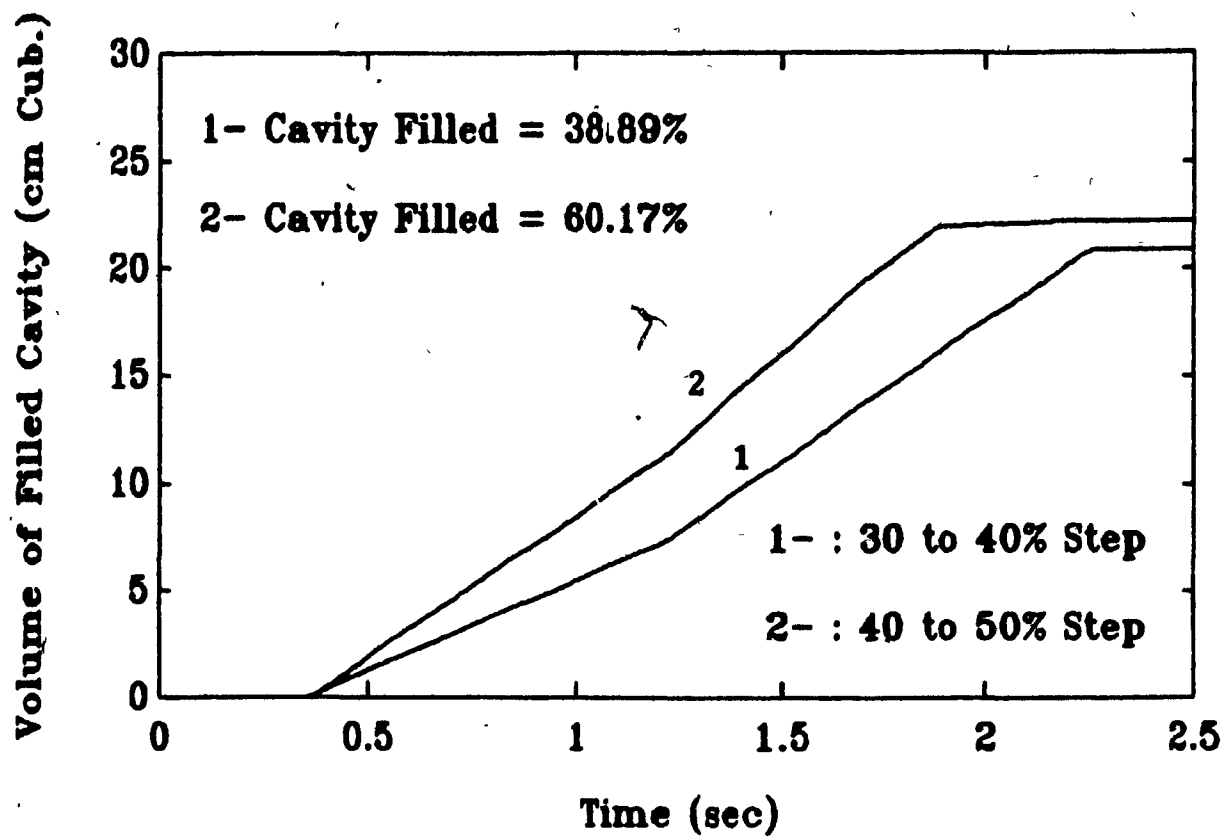


Figure 5.18 Percent of Cavity Filled at the Time of the Step Change for Different Initial Valve Opening.

TABLE 5.2

Parameters for the Cavity Pressure Model
Obtained from Tests Performed at 1.2 sec
After the Start of Injection

Change in Valve Opening %	% Volume of Cavity Filled	Process Gain K_2 , KPa/%
30 - 40	38.89	28.96
40 - 50	60.17	58.07

$$V_2/V_1 = 60.17/38.89 = 1.5$$

$$K_2/K_1 = 58.07/28.96 = 2.0$$

The volume of polymer in the cavity was calculated, using the measured ram linear velocity, by the equation :

$$\frac{dV}{dt} = A \left(\frac{dv_i}{dt} \right) \quad (5.5)$$

Where : V = volume of polymer in the cavity
 v_i = injection ram linear velocity
 A = cross-sectional area of the barrel

The effect of degree of filling on the process gain was then investigated by performing step changes with the same step magnitude and the same initial valve opening but at different times after the injection started. The responses of cavity gate pressure to 30 - 40% step change introduced at different times after the injection started are shown in Figure 5.19. The process gain, as given in Table 5.3 shows the same nonlinear behavior as in the case of different step magnitudes.

Figure 5.20 presents a cross validation of the above results. Different initial valve openings were used with the step introduced at different times but at the same percent of the cavity filled. The results yield the same value for the process gain as shown in Table 5.4.

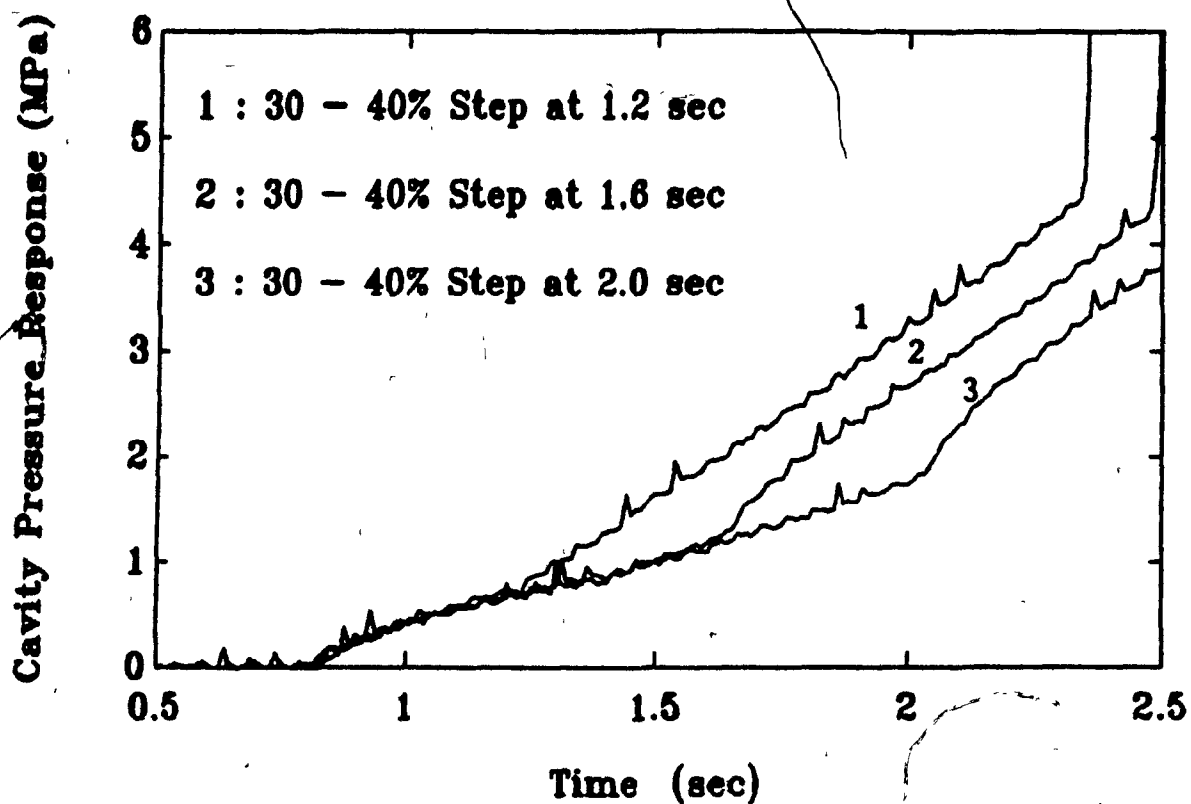


Figure 5.19 Response of Cavity Gate Pressure to 30 - 40% Valve Opening Change at Different Injection Times.

TABLE 5.3

Parameters for the Cavity Pressure Model
 Obtained from Tests Performed at Different
 Times After the Start of Injection

Change in Valve Opening %	Time of Change sec	% Volume of Cavity Filled	Process Gain K_2 , KPa/%
30 - 40	1.6	38	25.03
30 - 40	2.0	59	62.83

$$\frac{V(2)}{V(1.6)} = \frac{59}{38} = 1.5$$

$$\frac{K_2(2)}{K_2(1.6)} = \frac{62.83}{25.03} = 2.5$$

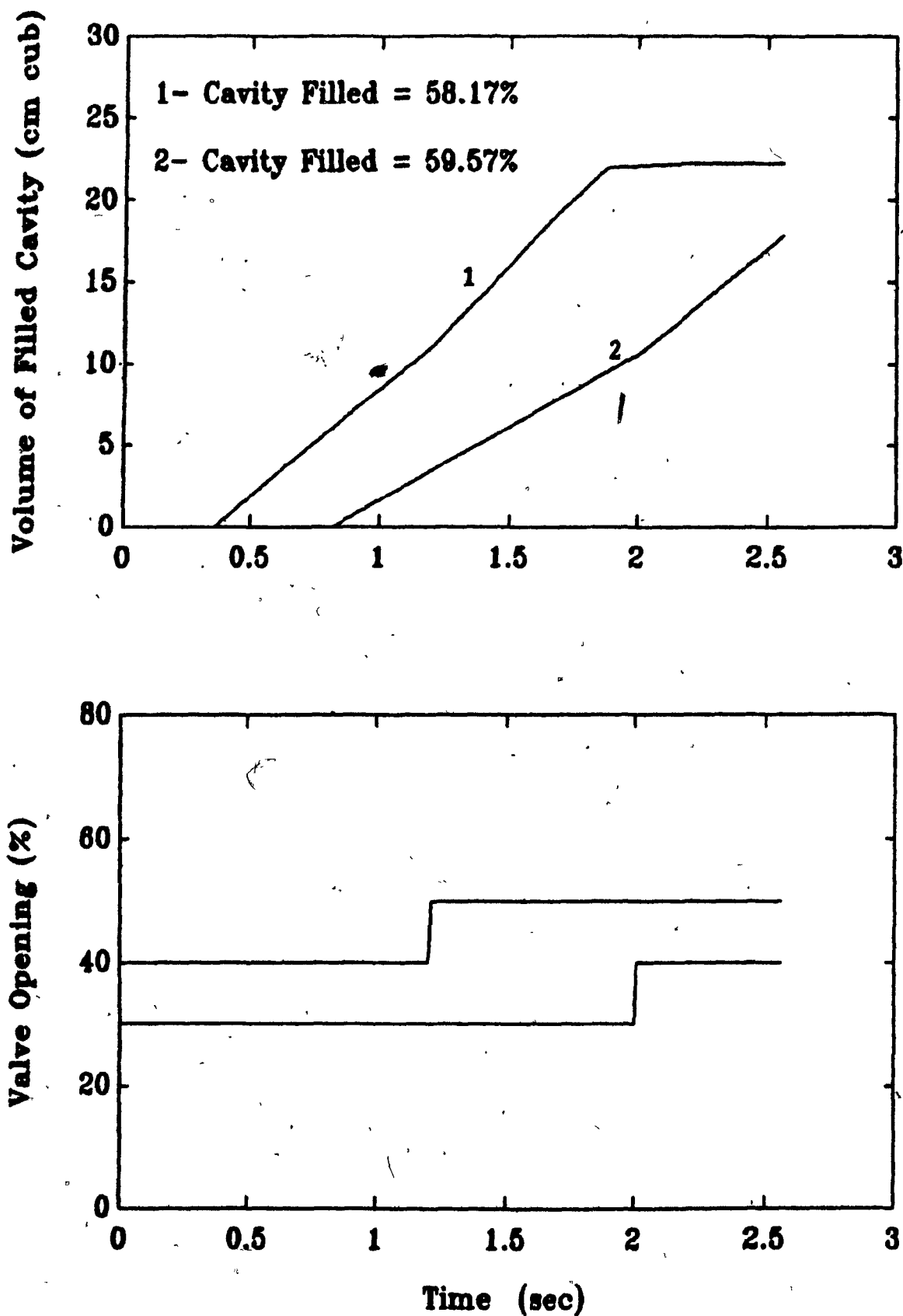


Figure 5.20. Response of Cavity Gate Pressure to 30 - 40% Step Change at 2 sec. and to 40 - 50% Change at 1.2 sec.

TABLE 5.4
Parameters for the Cavity Pressure Model
Obtained from Step Tests Performed at the Same
Percent of Cavity Filled

Change in Valve Opening %	Time of Change sec	% Volume of Cavity Filled	Process Gain K_2 , KPa/%
30 - 40	2.0	59	62.83
30 - 40	1.2	58	58.07

5.2.2 Stochastic Modelling

The objectives of the stochastic experiments were :

- (1) To develop a stochastic model for cavity gate pressure which could be used in designing controllers for the injection molding process.
- (2) To obtain intermediate dynamic relationships between cavity pressure, nozzle pressure, and hydraulic pressure to improve the understanding of the interactions between the process variables.

The stochastic experiments were performed by applying a pseudo-random binary sequence signal (PRBS) to the servovalve opening. The sequence length was 63 intervals with a sampling period of 10 ms and servovalve change amplitudes of ± 5 , ± 10 , and $\pm 15\%$ were examined. Three sequences were applied to cover the filling and packing stages. Cavity gate pressure, nozzle pressure, hydraulic pressure, screw linear velocity and linear displacement were recorded along with the melt temperature at the nozzle and the mold temperature.

5.2.2.1 Results and Discussion

The analysis of the stochastic, experimental data was performed using the identification procedure outlined by Ljung [129] and utilizing the PC-MATLAB identification package [130]. Figure 5.21 shows the response of cavity gate pressure to the PRBS input signal during the filling stage. The response is non-stationary (its mean is not constant in time) [30] because the cavity gate pressure constantly increases as the filling progresses. The nonstationarity was removed by a first order differencing [30]. Figure 5.22 shows the PRBS input signal and the differenced cavity pressure response in deviation form.

The spectral analysis of the data is shown in Figure 5.23. The high frequency asymptote of the amplitude has a slope of about -1, indicating a first order system, and the phase shift suggests a time delay [129].

An ARX model was first used to estimate the time delay in the response. The model equation is :

$$A(q) y(t) = B(q) U(t-nk) + e(t) \quad (5.5)$$

Where: $A(q) = 1 + a_1 q^{-1} + \dots + a_{na} q^{-na}$

$B(q) = b_1 q^{-1} + \dots + b_{nb} q^{-nb}$

q^{-1} = backwards difference operator defined as
 $U(k-1) = q^{-1} U(k)$. [Same operator as B in Equation 3.16]

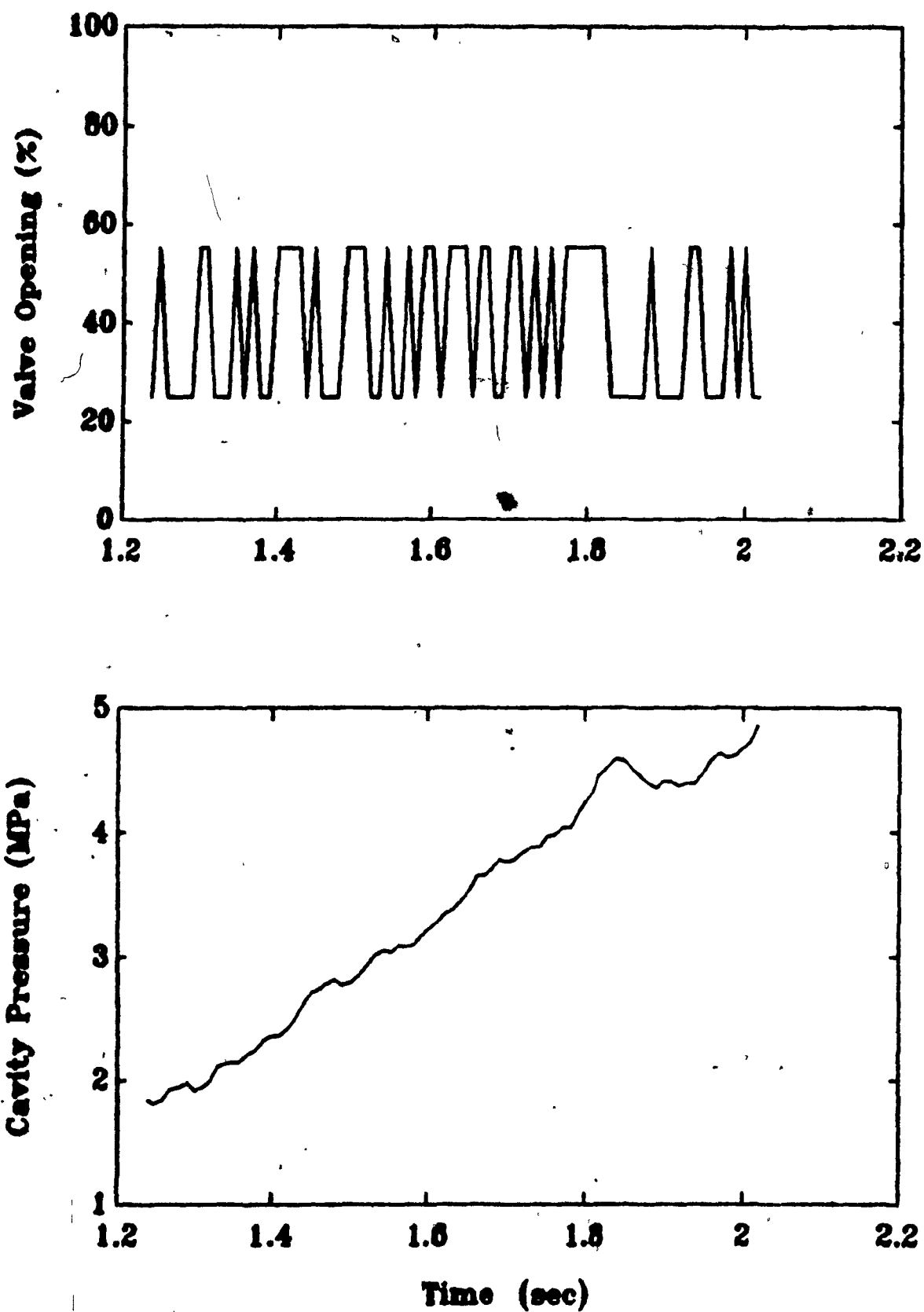


Figure 5.21 Response of Cavity Gate Pressure to PRBS Input Signal to the Servovalve.

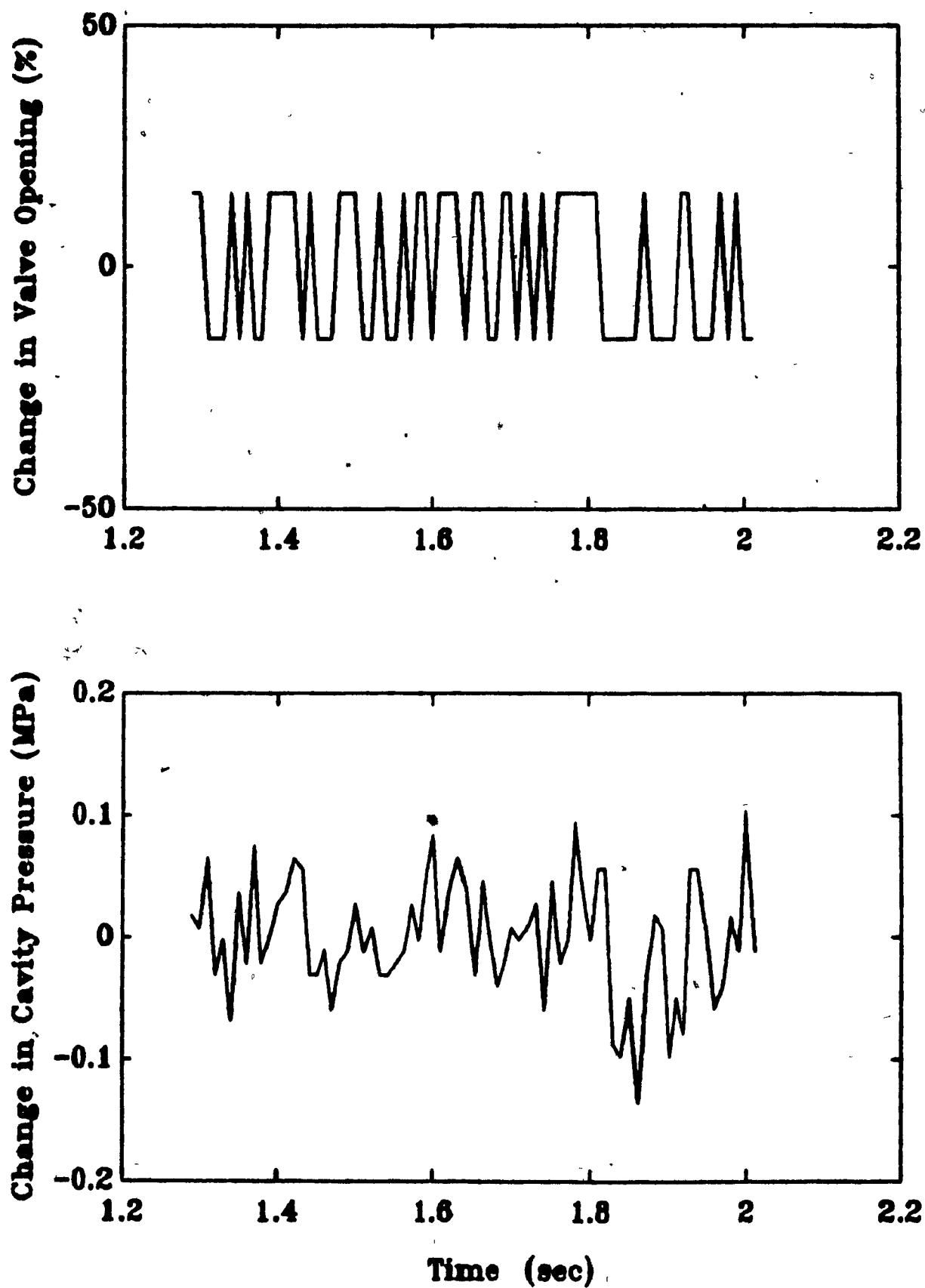


Figure 5.22 Differenced Response of Cavity Gate Pressure to PRBS Input Signal.

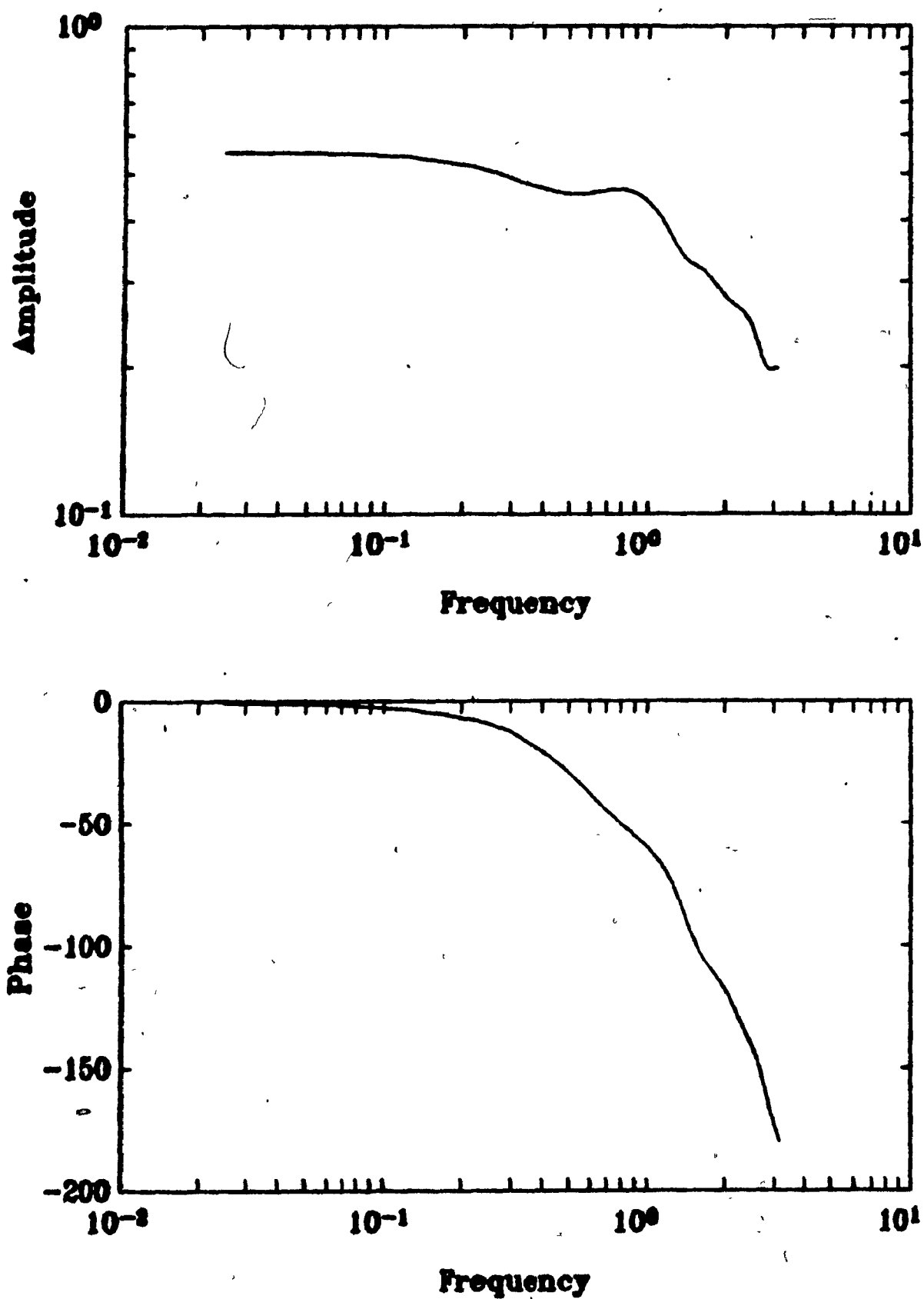


Figure 5.23 Frequency Response of Cavity Gate Pressure.

The values of the parameter estimates and their standard deviations as well as the Akaike's (AIC) values are given in Table 5.5. From the Table, it is clear that the model ARX [1 1 1] gives the best values for the parameter estimates, on the basis of the standard deviations and the lowest AIC value. Therefore, a time delay of one sampling interval was considered for further model identification.

The more general ARMAX model was investigated. This model (5.6) includes a noise term, $C(q)$.

$$A(q) Y(t) = B(q) U(t-nk) + C(q) e(t) \quad (5.6)$$

Different orders of the model were examined. The parameter estimates and the AIC values are given in Table 5.6. The standard deviations of the parameters and the values of the AIC indicated that models [1111], [1121] and [1131] were the best candidates for further investigation.

The auto-correlation function of the residuals and the cross correlation function between the residuals and the input were examined. The results confirmed the choice of the above three ARMAX models. As it can be seen from Figures 5.24 - 5.26, the three models gave no auto-correlation between the residuals. Furthermore, the three models gave identical insignificant cross correlation between the residuals and the input.

TABLE 5.5

Parameters of the ARX Model for Cavity Pressure Response
 where: na=order of "A" polynomial, nb=order of "B" polynomial
 nk=time delay

Run #	Model ARX [na,nb,nk]	"A" Parameters & standard Deviations		"B" Parameters & Standard Deviations			AIC
1	[1 1 0]	1	-0.575	0.153			39.31
		0	0.094	0.074			
	[1 1 1]	1	-0.498	0	0.301		33.19
		0	0.069	0	0.069		
	[1 1 2]	1	-0.661	0	0	- 0.167	39.29
		0	0.105	0	0	0.084	
2	[1 1 0]	1	-0.569	0.083			46.79
		0	0.096	0.081			
	[1 1 1]	1	-0.549	0	0.378		33.79
		0	0.082	0	0.068		
	[1 1 2]	1	-0.635	0	0	- 0.132	46.57
		0	0.108	0	0	0.091	
3	[1 1 0]	1	-0.608	0.178			36.34
		0	0.088	0.071			
	[1 1 1]	1	-0.534	0	0.291		31.67
		0	0.068	0	0.068		
	[1 1 2]	1	-0.762	0	0	- 0.249	34.87
		0	0.098	0	0	0.081	

TABLE 5.6

Parameters of the ARMAX Model for Cavity Pressure Response

ARMAX [na,nb,nc,nk]

MODEL	"A" Parameters		"B" Parameters				"C" Parameters				AIC
[1111]	1.0	-0.28	0.0	0.31			1.0	-0.36			22.11
	0.0	0.10	0.0	0.07			0.0	0.15			
[1121]	1.0	-0.31	0.0	0.32			1.0	0.44	0.15		21.72
	0.0	0.08	0.0	0.05			0.0	0.14	0.12		
[1131]	1.0	-0.30	0.0	0.33			1.0	0.41	0.18	0.74	21.99
	0.0	0.08	0.0	0.03			0.0	0.15	0.13	0.21	
[1211]	1.0	-0.09	0.0	0.33	0.09		1.0	-0.21			22.11
	0.0	0.28	0.0	0.04	0.10		0.0	0.30			
[1221]	1.0	-0.19	0.0	0.32	-0.05		1.0	-0.34	0.13		22.19
	0.0	0.25	0.0	0.04	0.09		0.0	0.28	0.12		
[1231]	1.0	-0.15	0.0	0.33	-0.08		1.0	-0.33	0.12	-0.14	22.06
	0.0	0.24	0.0	0.03	0.05		0.0	0.26	0.14	0.13	
[1311]	1.0	0.17	0.0	0.33	0.17	0.04	1.0	0.05			22.56
	0.0	0.86	0.0	0.03	0.27	0.10	0.0	0.87			
[1321]	1.0	-0.09	0.0	0.33	0.08	0.02	1.0	-0.22	0.11		22.88
	0.0	0.87	0.0	0.03	0.28	0.11	0.0	0.87	0.16		
[1331]	1.0	-0.88	0.0	0.31	-0.17	-0.17	1.0	-1.25	0.32	0.27	19.31
	0.0	0.11	0.0	0.03	0.06	0.03	0.0	0.16	0.18	0.13	

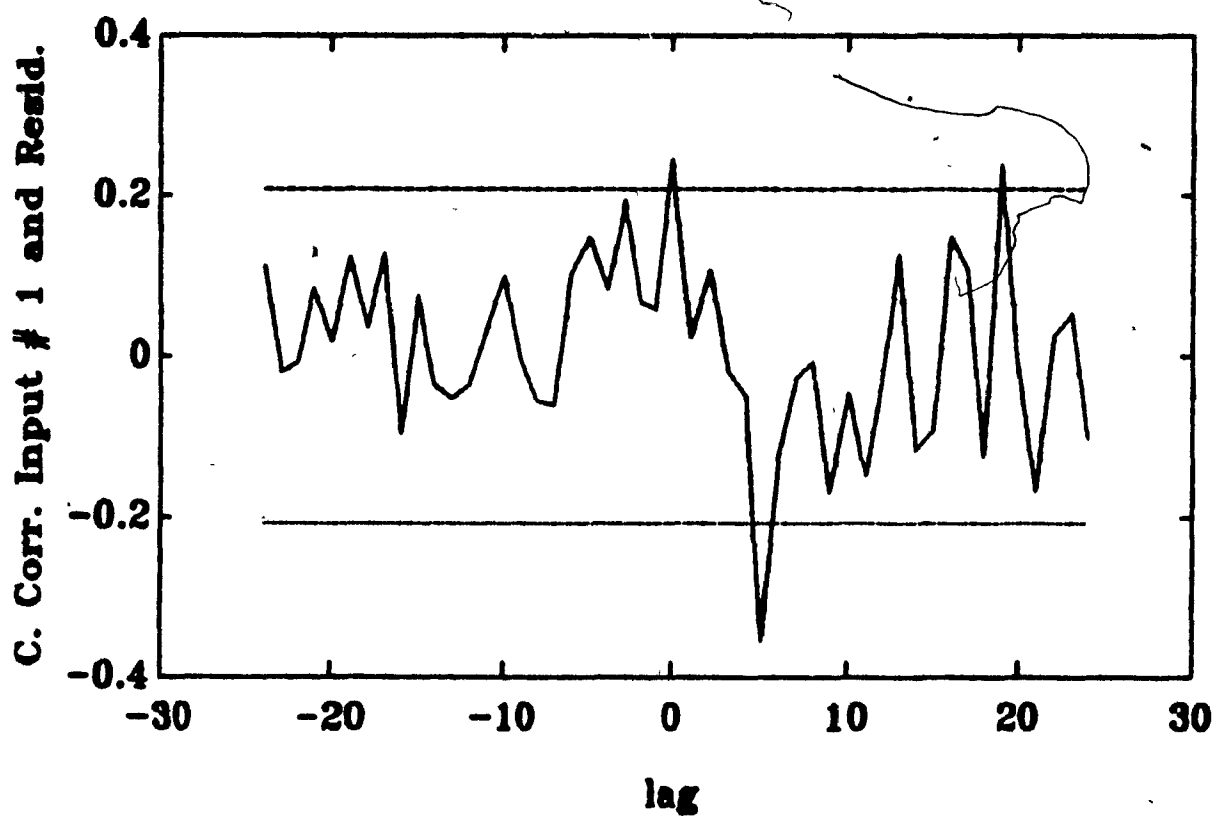
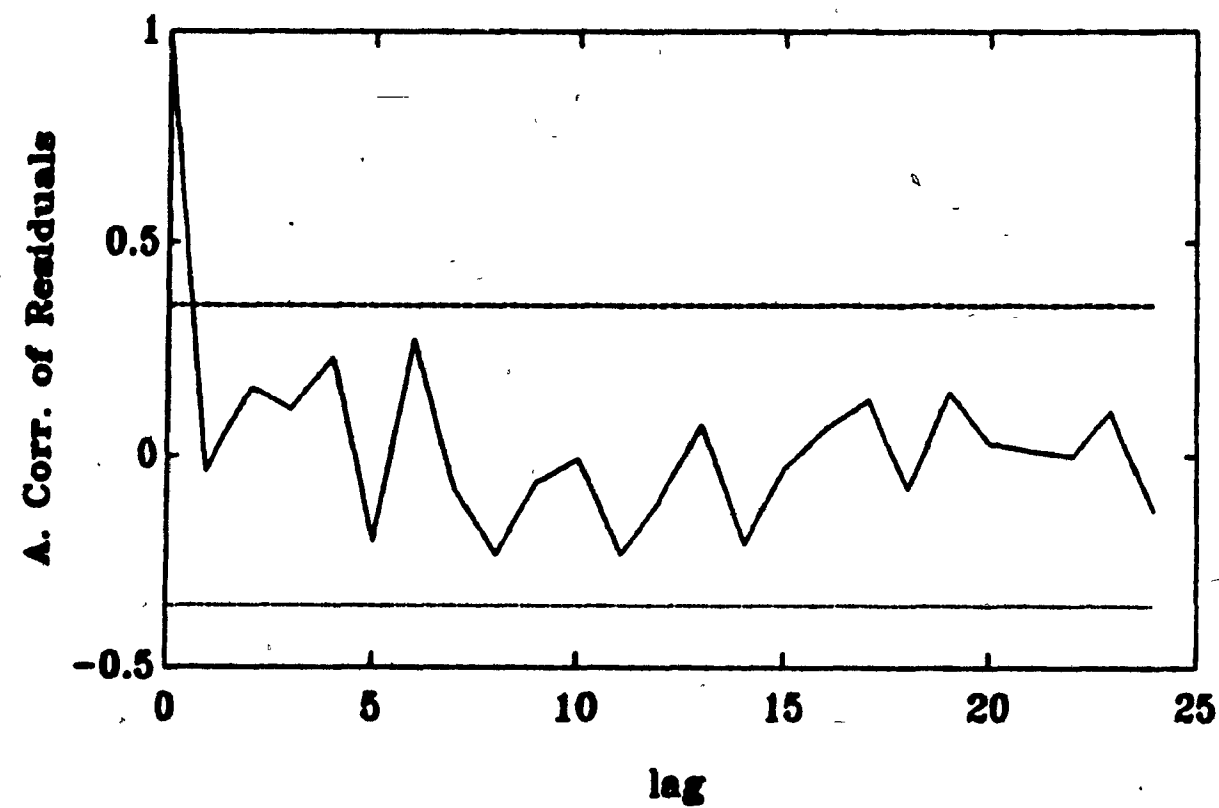


Figure 5.24 Autocorrelation and Cross Correlation of the Residuals for Model ARMAX [1111].

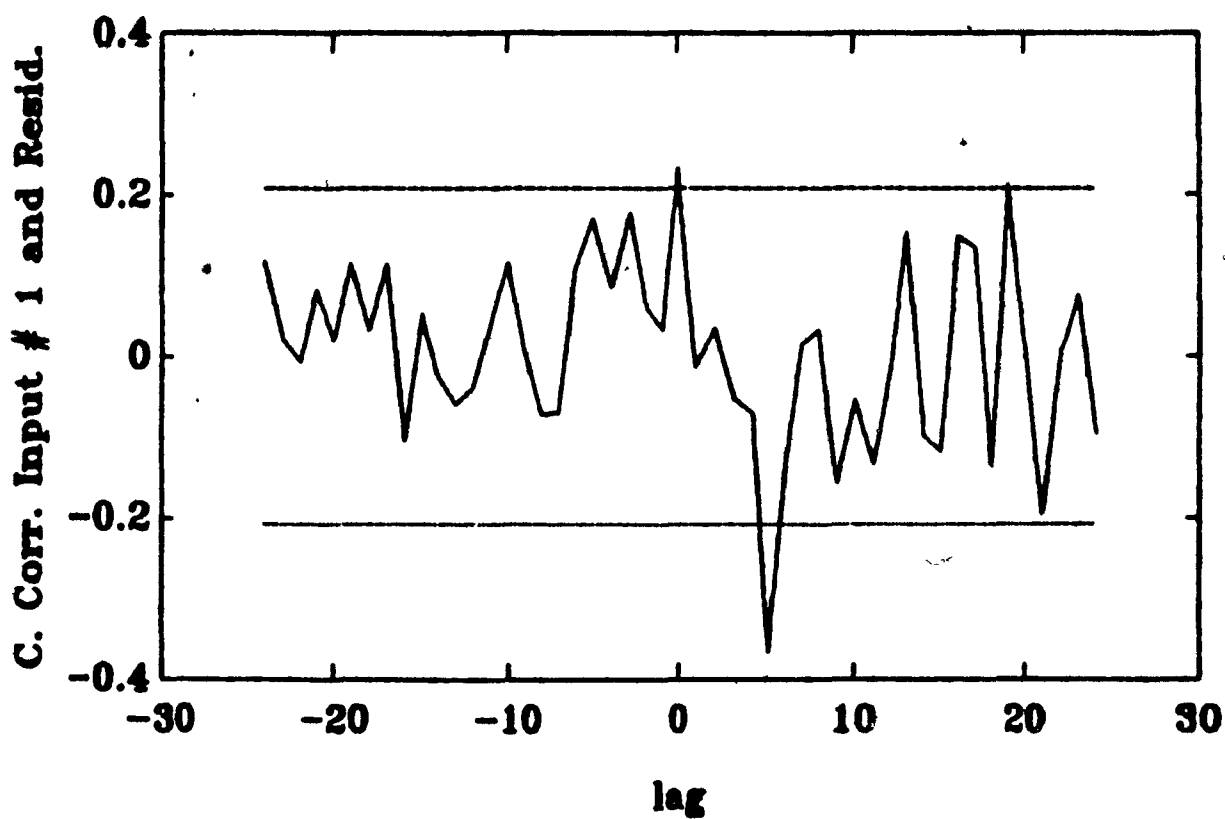
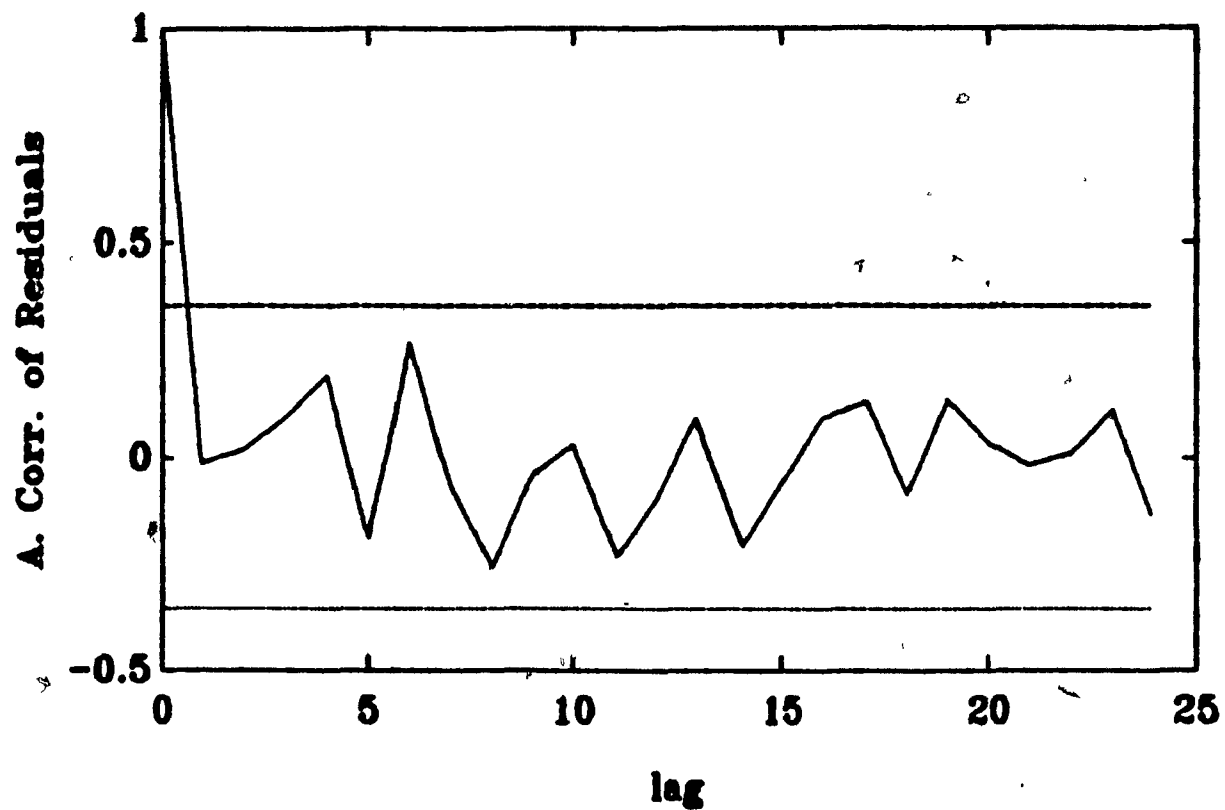


Figure 5.25 Autocorrelation and Cross Correlation of the Residuals for Model ARMAX [1121].

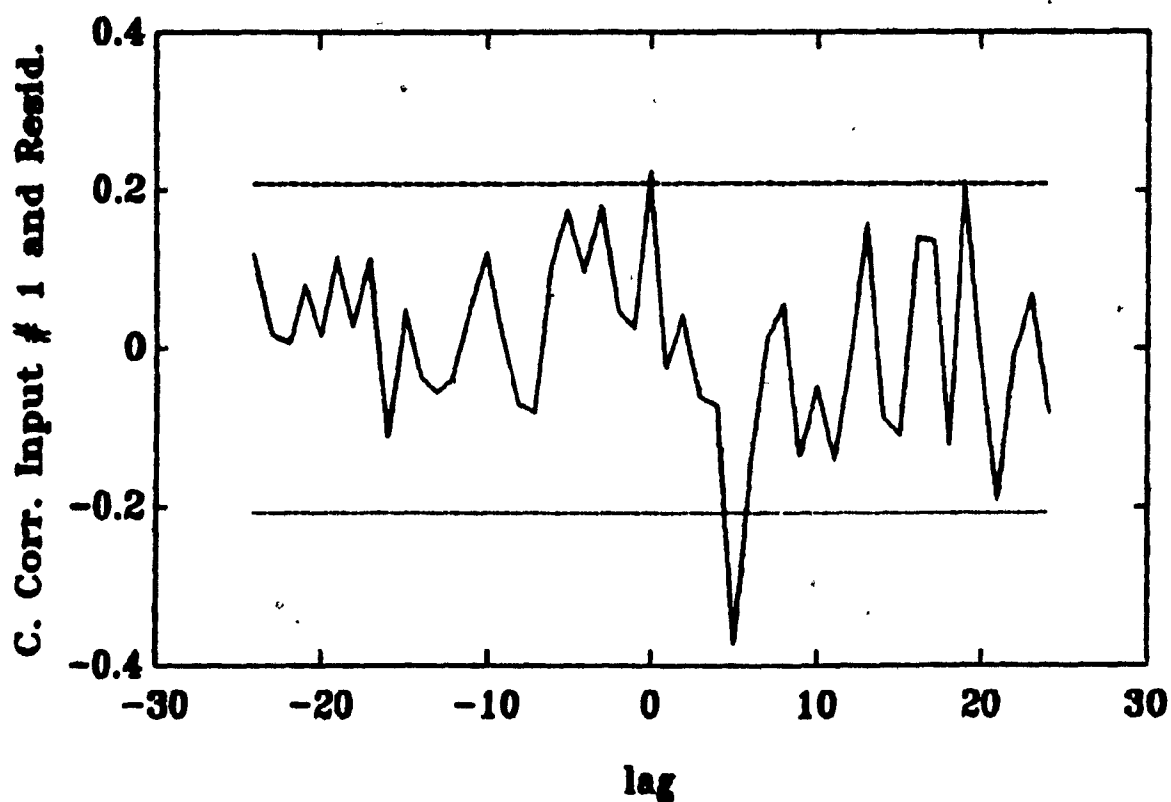
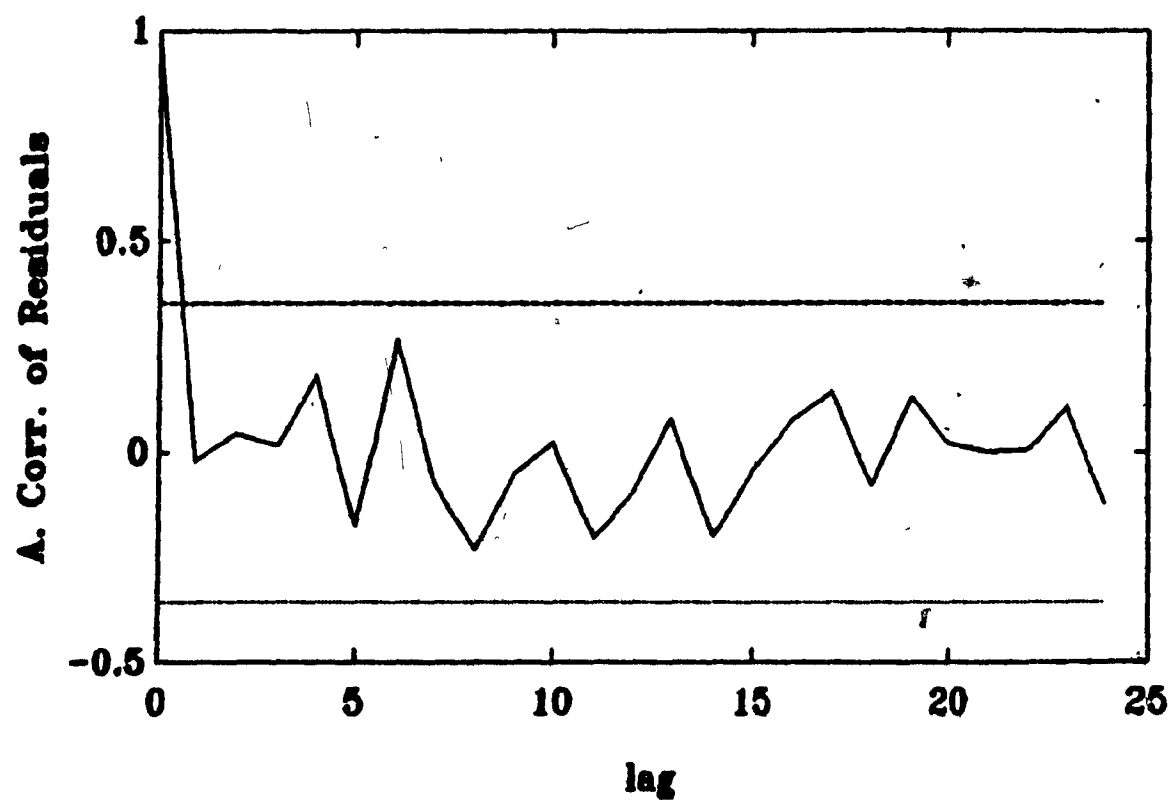


Figure 5.26 Autocorrelation and Cross Correlation of the Residuals for Model ARMAX [1131].

The Bode plots of the three models were compared to the spectral analysis estimates of the experimental results. As shown in Figure 5.27, the three models gave equally good results. Model [1121] was chosen since it gave the lowest AIC value (Table 5.6). Figure 5.28 shows a good agreement between the simulation results using this model and a fresh set of experimental data.

Based on the results of the above investigations, the model ARMAX [1121] was chosen to represent the relationship between the cavity gate pressure response and the servovalve opening. This model can be written as follows :

$$(1-q^{-1}) P_C(t) = \frac{0.32}{1-0.31q^{-1}} U(t-1) + \frac{1-0.44q^{-1}+0.15q^{-2}}{1-0.31q^{-1}} e(t) \quad (5.7)$$

Where :

- $P_C(t)$ = cavity gate pressure at sampling instant, t
- $U(t)$ = servovalve opening at sampling instant, t
- q^{-1} = backwards difference operator defined as

$$U(k-1) = q^{-1} U(k)$$

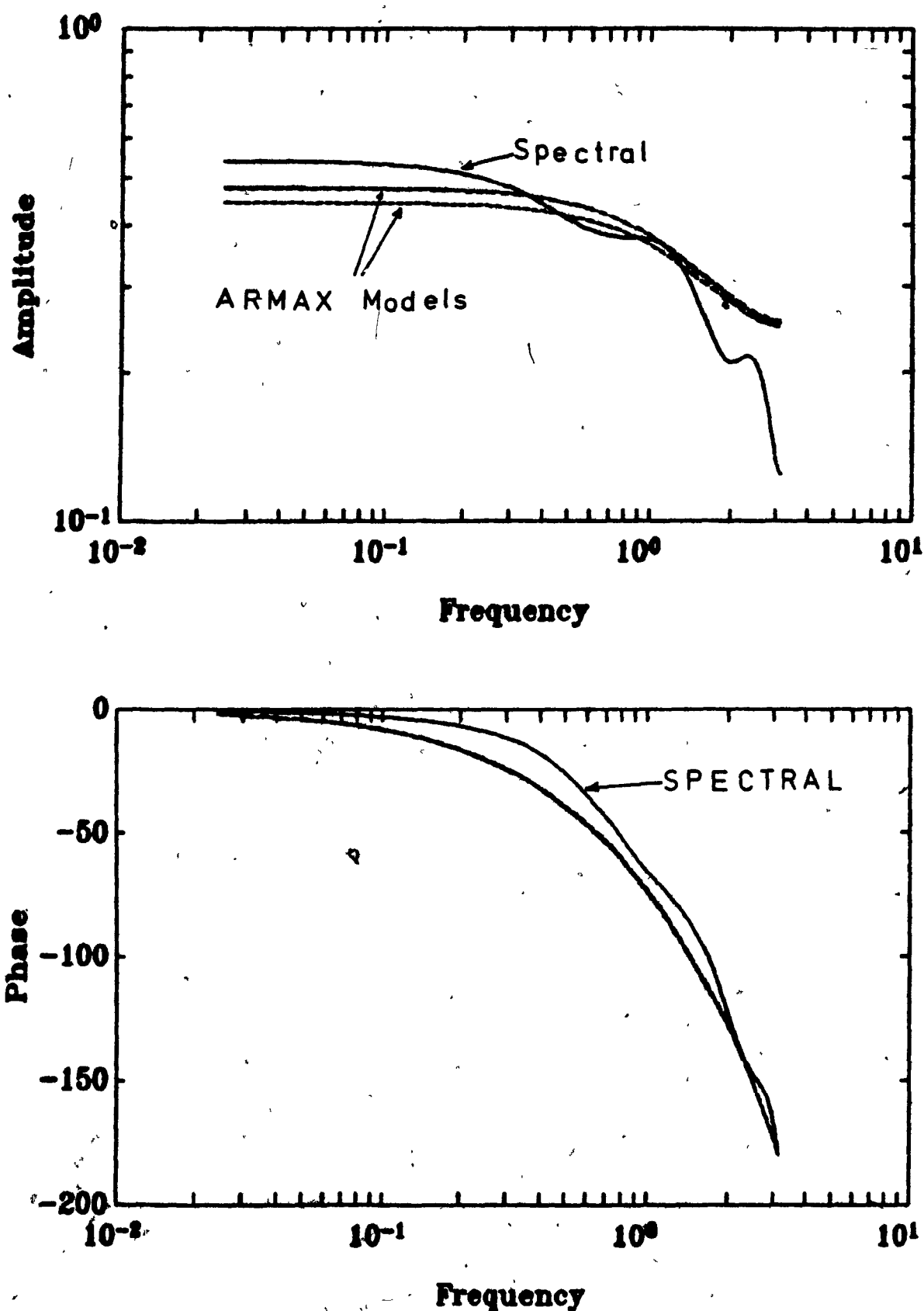


Figure 5.27 Comparison Between the Bode Plots of the ARMAX Models and the Spectral Analysis Estimates of the Experimental Data.

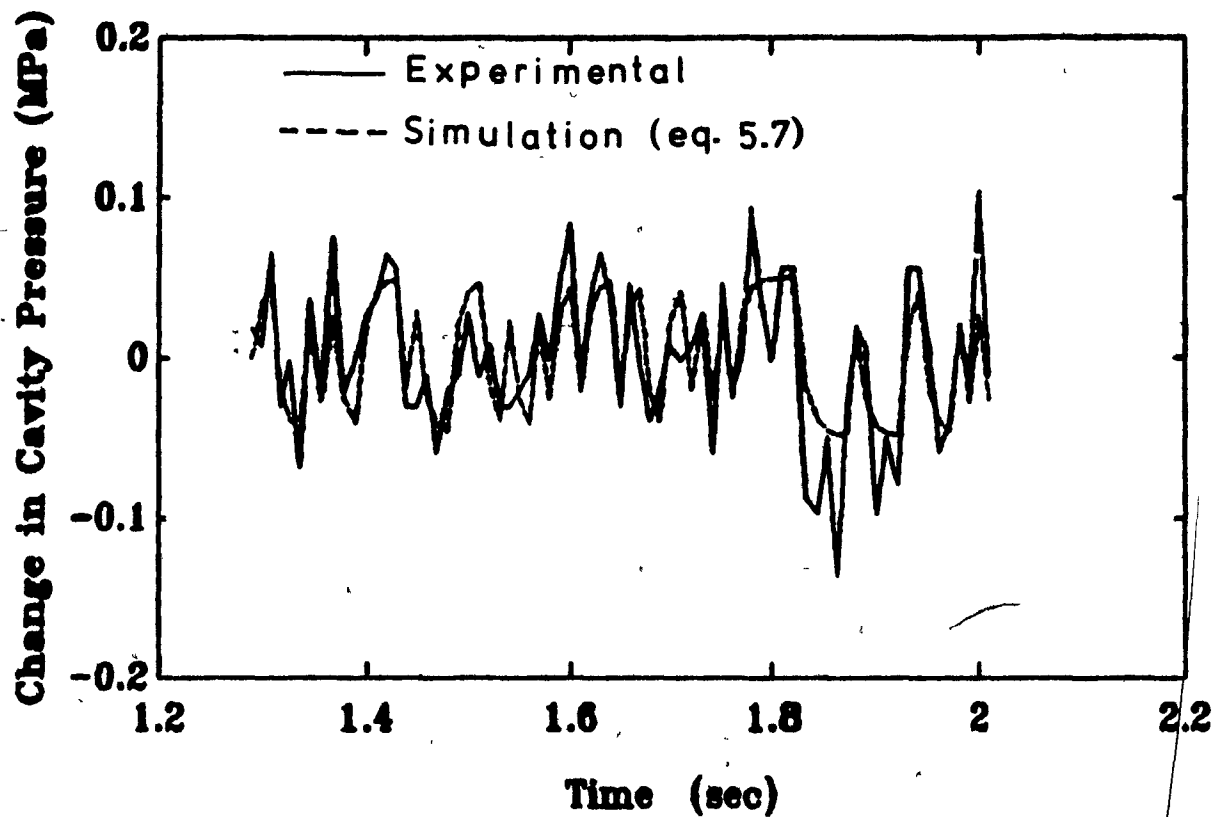


Figure 5.28 Comparison Between the Experimental Data and the ARMAX [1121] Model Predictions.

Another investigation included a Box-Jenkins model of the form :

$$Y(t) = \frac{B(q)}{F(q)} U(t-nk) + \frac{C(q)}{D(q)} e(t) \quad (5.8)$$

Various structures were tried with different orders of the polynomials B, F, C and D. The parameter estimates of the various models are shown in Table 5.7. An identification procedure identical to that followed in investigating the ARMAX models revealed that the most reasonable Box-Jenkins formula was the model BJ[11211]. The correlation function plot for the model BJ[11211] is shown in Figure 5.29. Using the parameter estimates given in Table 5.7, the model can be written as follows :

$$(1-q^{-1}) P_C(t) = \frac{0.31}{1-0.42q^{-1}+0.15q^{-2}} U(t-1) + \frac{1-0.78q^{-1}}{1-0.87q^{-1}} e(t) \quad (5.9)$$

As a conclusion, both the ARMAX and Box-Jenkins models gave a satisfactory results. The ARMAX model gave a slightly lower AIC value. Therefore, the simpler ARMAX model was chosen to describe the dynamic behavior of the cavity gate pressure response to the change in the servovalve opening.

TABLE 5.7
Parameters of Box-Jenkins Models for Cavity Gate Pressure Response

MODEL	"B"		"C" Parameters			"D" Parameters			"F" Parameters				AIC
11111	0	0.32	1	0.78		1	0.89		1	-0.28			21.72
	0	0.03	0	0.22		0	0.01		0	0.09			
11121	0	0.31	1	0.78		1	0.87		1	-0.42	0.15		21.67
	0	0.03	0	0.26		0	0.20		0	0.11	0.10		
11131	0	0.32	1	0.72		1	0.83		1	-0.35	0.06	0.22	20.97
	0	0.03	0	0.31		0	0.24		0	0.11	0.13	0.10	
11211	0	0.32	1	0.77		1	0.82	-0.06	1	-0.28			22.33
	0	0.03	0	0.26		0	0.29	0.15	0	0.09			
11221	0	0.31	1	0.79		1	0.88	0.01	1	-0.42	0.15		22.28
	0	0.03	0	0.31		0	0.34	0.15	0	0.10	0.10		
11231	0	0.32	1	0.77		1	0.92	0.05	1	-0.37	-0.02	0.21	21.40
	0	0.03	0	0.39		0	0.42	0.18	0	0.11	0.13	0.10	
11311	0	0.33	1	-0.48		1	-0.37	-0.16 -0.09	1	-0.29			22.62
	0	0.03	0	0.59		0	0.60	0.14 0.15	0	0.09			
11321	0	0.31	1	-0.47		1	-0.26	-0.09 -0.22	1	-0.53	0.27		21.70
	0	0.03	0	0.46		1	0.45	0.14 0.12	1	0.09	0.09		
11331	0	0.33	1	-0.48		1	-0.24	-0.17 -0.19	1	-0.38	0.06	0.19	21.03
	0	0.03	0	0.39		0	0.39	0.14 0.13	0	0.12	0.14	0.10	
12111	0	0.32	1	0.84	0.06	1	0.89		1	-0.29			22.34
	0	0.03	0	0.21	0.14	0	0.18		0	0.09			
12121	0	0.31	1	0.79	0.01	1	0.87		1	-0.42	0.15		22.30
	0	0.03	0	0.28	0.14	0	0.15		0	0.11	0.10		
12131	0	0.32	1	-1.05	0.52	1	-0.67		1	-0.35	-0.05	0.19	20.05
	0	0.03	0	0.13	0.11	0	0.13		0	0.11	0.14	0.09	
13111	0	0.30	1	0.94	0.03 -0.22	1	0.84		1	-0.28			23.07
	0	0.03	0	0.16	0.17 0.13	0	0.12		0	0.10			
13121	0	0.32	1	-1.16	0.21 -0.05	1	-0.99		1	-0.43	0.14		23.20
	0	0.03	0	0.38	0.20 0.12	0	0.36		0	0.11	0.10		
13131	0	0.32	1	-1.03	0.31 0.21	1	-0.71		1	-0.36	0.07	0.19	19.85
	0	0.03	0	0.18	0.19 0.15	0	0.15		0	0.11	0.14	0.09	

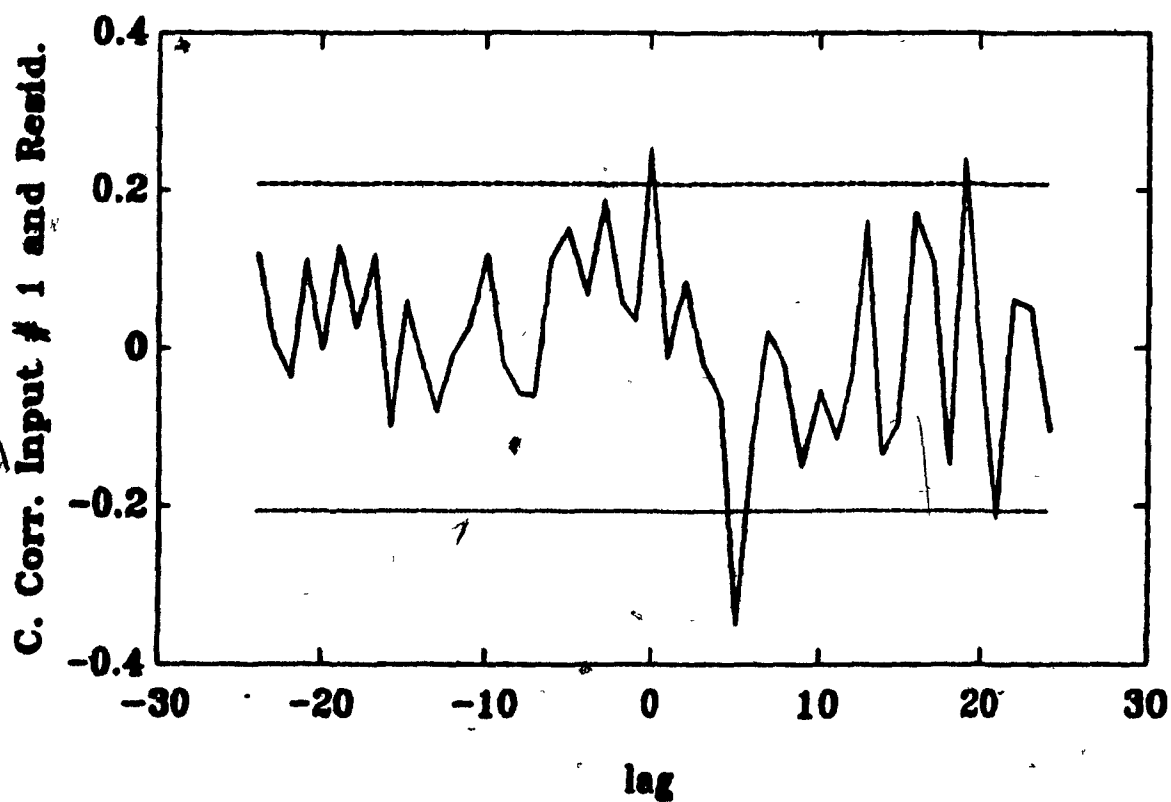
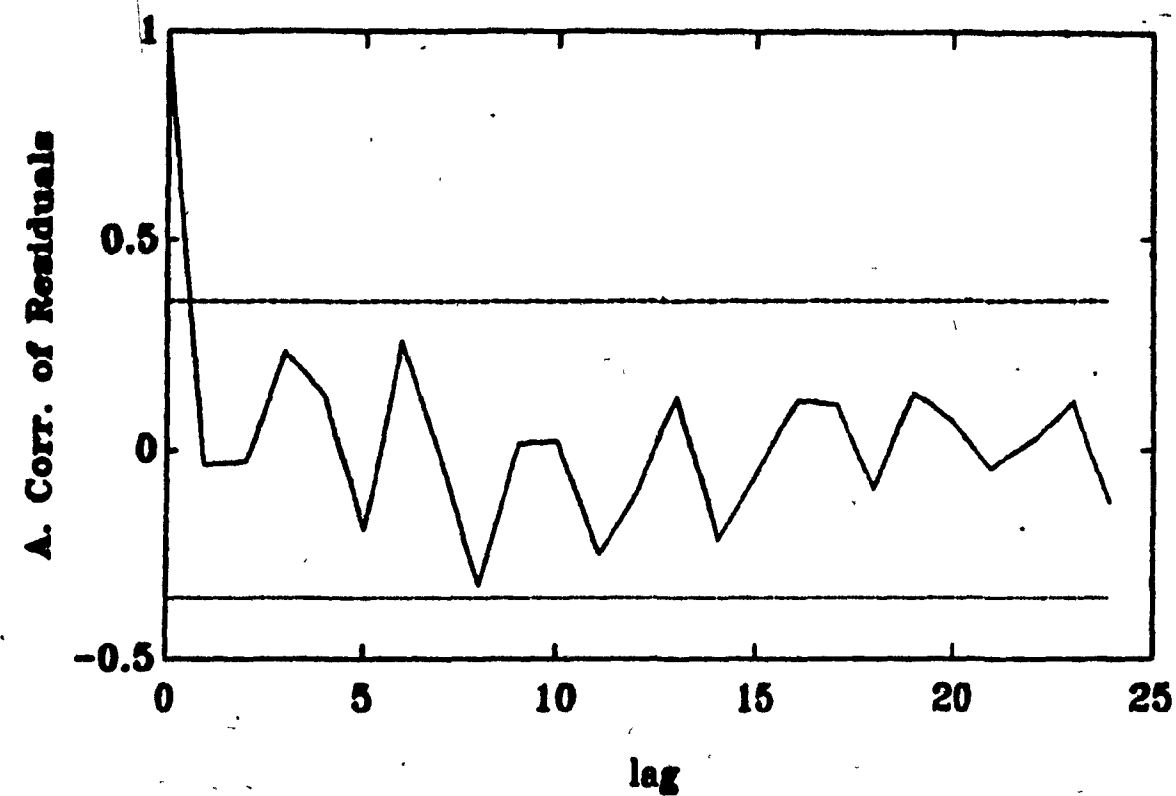


Figure 5.29 Autocorrelation and Cross-Correlation Functions of Residuals for BJ[115] Model.

5.2.2.2 Comparison Between the Deterministic and the Stochastic Models

The ramp part of the response (Equation 5.4) is shown in the differencing operator $(1-q^{-1})$ in both Equations (5.7) and (5.9).

The first order response part (Equation 5.4) is an average over the increasing and decreasing steps in the PRBS. Hence it was not possible to compare between the parameters of the stochastic and deterministic models.

5.2.3 Summary

- (1) Cavity gate pressure response was best modelled by a first-order plus time delay superimposed on a constantly increasing (ramp) pressure component.
- (2) Good agreement was obtained between the experimental data and the fitted model.
- (3) The response exhibited nonlinear behavior in terms of the process gain. The nonlinearity was related to the fraction of the cavity filled at the time of step. The process time constant and the time delay showed very little change.

- (4) The process gain increased with the amount of polymer injected into the cavity at the time that the step is made.
- (5) Stochastic ARMAX and Box-Jenkins models were obtained for cavity gate pressure response. The models were in general agreement with the deterministic models.

5.3 Dynamics of Cavity Pressure Gradient

Step tests with various changes in the servovalve opening were performed to obtain a dynamic model for the pressure gradient in the cavity. The pressure gradient was calculated as the difference between the signals from the pressure transducer mounted at the cavity gate and that at the second position, as shown in Figure 4.3. The response of the pressure gradient in the cavity for both positive and negative step changes in the servovalve opening is shown in Figure 5.30. The response was best fitted by a first order model of the form :

$$P_G = K (1 - e^{-t/\tau}) \quad (5.10)$$

where P_G is the pressure gradient in the cavity. The fitted parameters of the model are given in Table 5.8. The response of the pressure gradient reaches a constant steady state after the step change which agrees with the results of a static experiment as shown in Figure 5.31. Good agreement, as shown in Figure 5.32, was obtained between the experimental data and the model predictions. The noise encountered with the pressure gradient response is due to the subtraction of the two pressure signals.

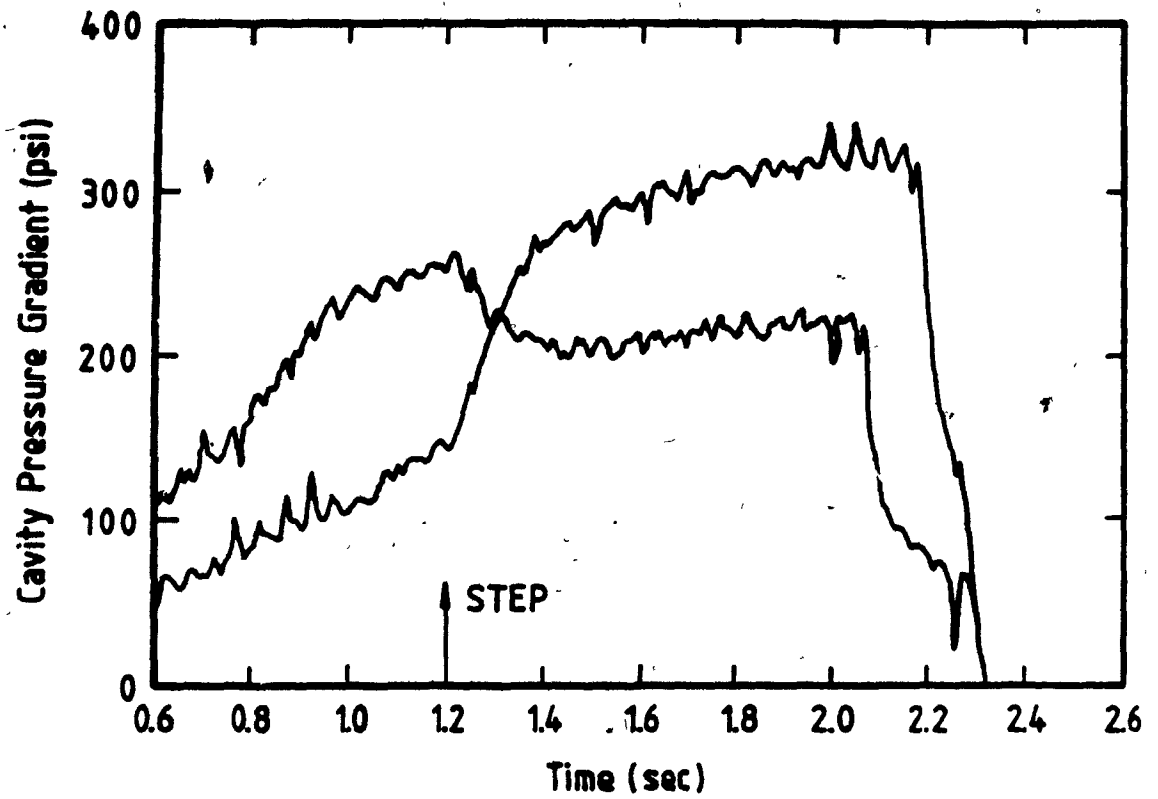


Figure 5.30 Cavity Pressure Gradient Response to 30-40% and 40-30% Changes in the Servovalve Opening.

TABLE 5.8

Parameters for the Cavity Pressure Gradient Model
Equation (5.10)

Change in Valve Opening %	Process Gain K (KPa/%)	Time constant τ (sec)
40 - 50	18.55 ± 1.45	0.097 ± 0.028
40 - 55	15.10 ± 1.65	0.092 ± 0.040
35 - 50	14.41 ± 2.41	0.084 ± 0.044
35 - 55	14.83 ± 2.34	0.094 ± 0.036
50 - 40	13.79 ± 1.72	0.074 ± 0.049
50 - 35	11.03 ± 0.90	0.103 ± 0.040
55 - 40	10.34 ± 0.60	0.060 ± 0.020
55 - 35	10.34 ± 0.48	0.088 ± 0.020

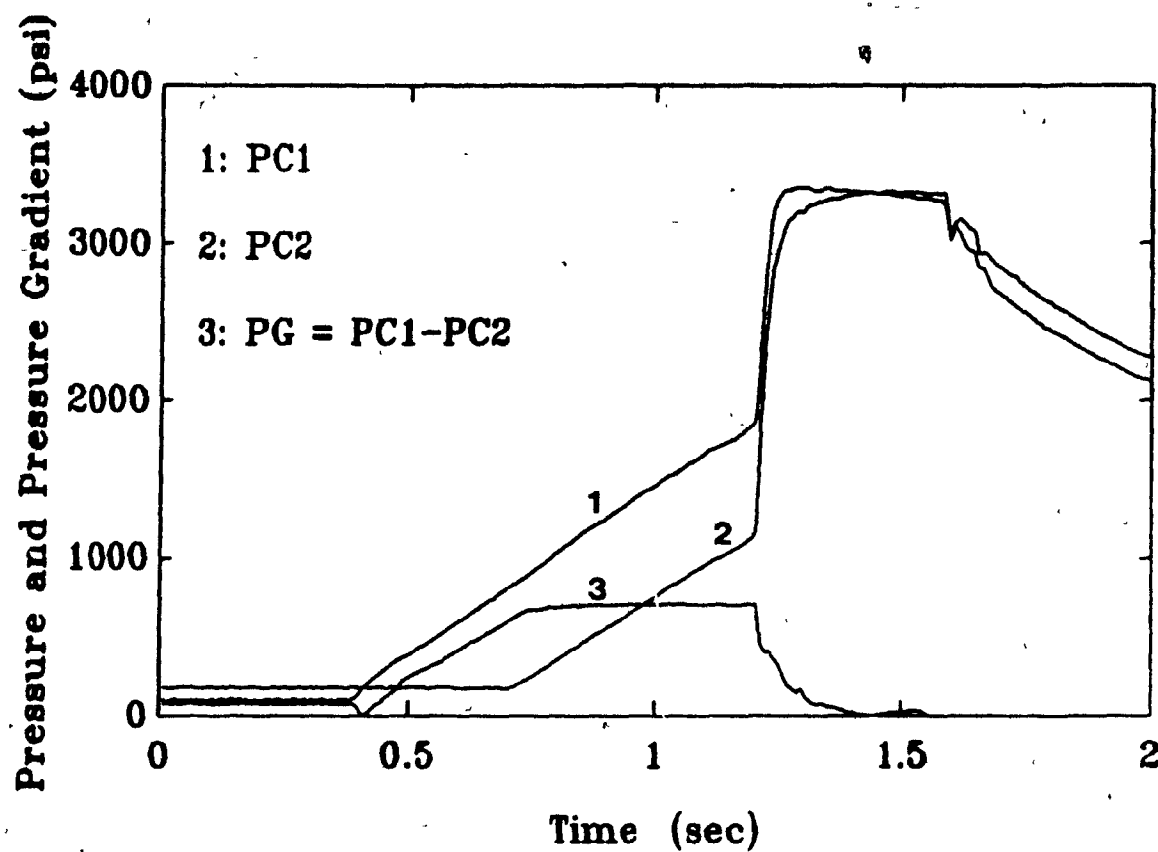


Figure 5.31 Cavity Pressure Gradient for a Static Experiment.

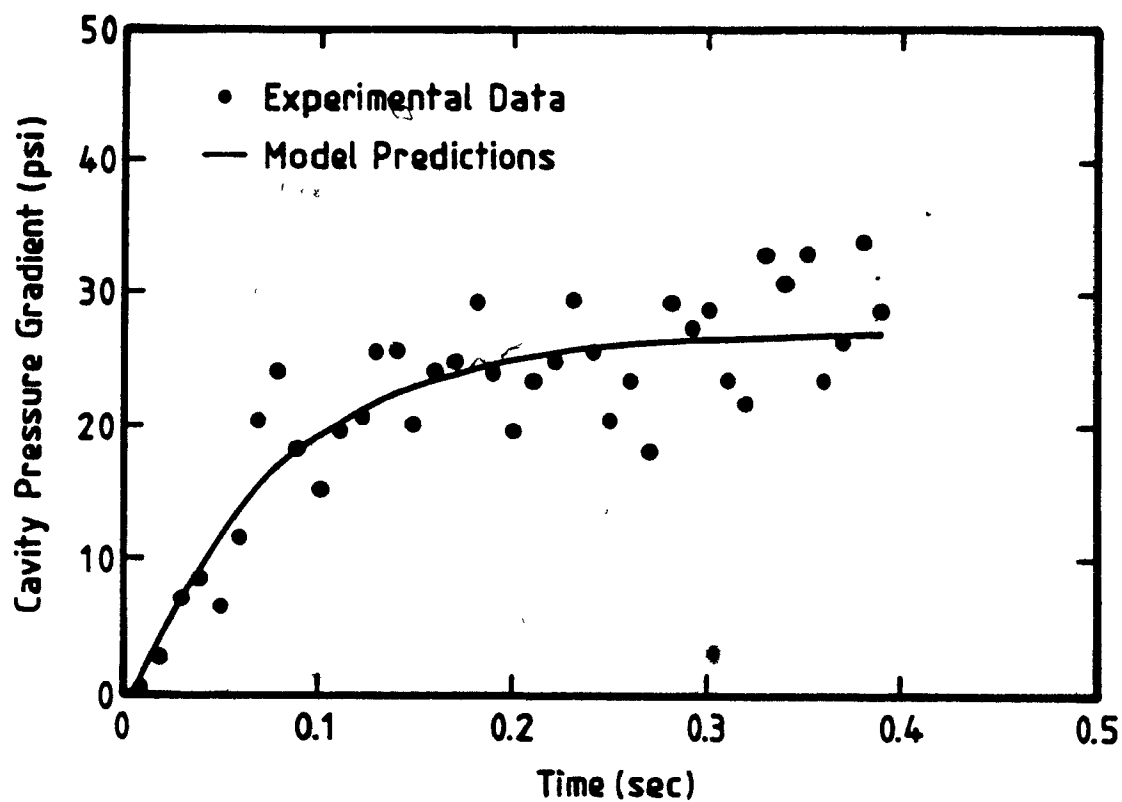


Figure 5.32 Comparison of Experimental Cavity Pressure Gradient Response to Fitted Model.

CHAPTER 6

CONTROL OF THE FILLING STAGE OF THE INJECTION MOLDING CYCLE

The process control problem consists of two parts: first, a mathematical model of the process is identified, then a control strategy is designed based on the knowledge obtained from the modeling stage. The previous chapter presented the modeling of the filling stage of the injection molding cycle. This chapter gives a short description of some widely used classical sampled-data control algorithms and their design procedure followed by a simulation of filling stage control. The last section covers the experimental application of the different controllers to the injection molding process during the filling stage.

6.1 Discrete-Time Control Algorithms

In recent years significant progress has been made in discrete-data and digital control systems. These systems have gained importance in all industries due to advances made in digital computers, and more recently in

microcomputers. Also, there are advantages associated with the use of digital signals. Discrete-data and digital control systems differ from the continuous-data or analog systems in that the signals in one or more parts of the former systems are in the form of either a pulse train or a numerical code. The basic control loop in digital control systems is illustrated in Figure 6.1. Following is a short description of the control algorithms used in this study.

6.1.1 PID Controller

The most commonly used control algorithm in industry is the three-mode proportional-integral-derivative (PID) controller. Its general analog form is given by the equation :

$$M = K_C e + (K_C/\tau_I) \int e dt + K_C \tau_D (de/dt) + C \quad (6.1)$$

Where: M = the controller output or the manipulated variable

K_C = the controller gain

e = the error = (set-point) - (measured variable)

τ_I = the integral or reset time constant

τ_D = the rate time or derivative time constant

C = a constant signal to drive the actuator when the error is zero.

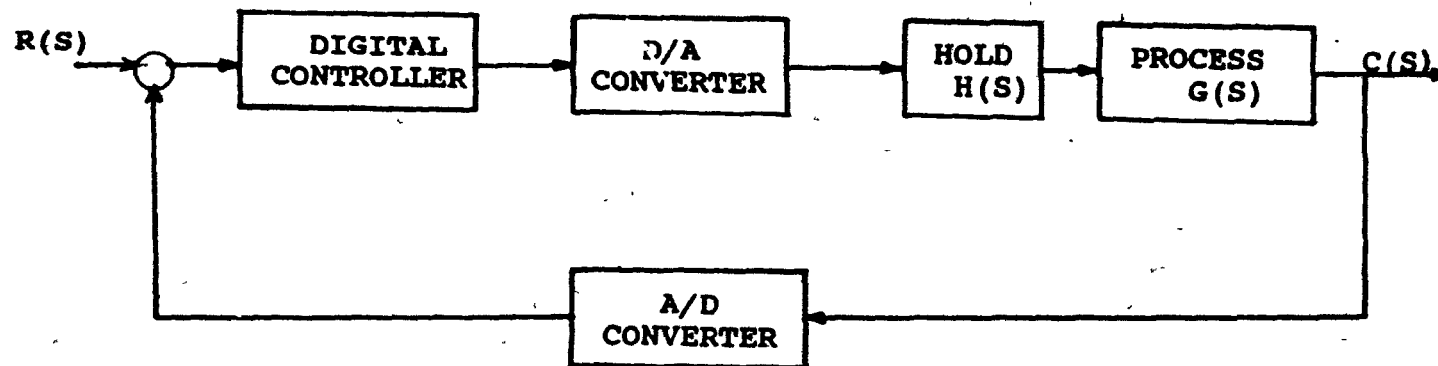


Figure 6.1: Simplified Digital Control Loop

Discrete equivalent forms of the continuous controllers are used in digital computer process control. A discrete PID controller can be obtained by approximating the integral in equation (6.1) by the backwards rectangular integration rule and the derivative by a first order finite difference [131]:

$$M(k) = K_C [e(k) + (T/\tau_I) \sum e(k) + (\tau_D/T) \{e(k) - e(k-1)\}] + C \quad (6.2)$$

Where : T is the sampling period. Equation (6.2) is known as the position form of the PID algorithm, because at each sampling instant it calculates the actual value (absolute) of the controller output signal. An alternative form for the PID control algorithm is the so called velocity form. It calculates the incremental change of the controller output signal with respect to its previous value. Writing equation (6.2) for the k^{th} and the $(k-1)^{\text{th}}$ sampling instants and obtaining the difference gives the velocity form of the controller as follows :

$$M(k) = K_C [\{e(k) - e(k-1)\} + (T/\tau_I) e(k) + (\tau_D/T) \{e(k) - 2e(k-1) + e(k-2)\}] + M(k-1) \quad (6.3)$$

The velocity form of the algorithm is preferred because it has the following advantages over the position form [134]:

- (i) The velocity algorithm unlike, the position form, does not require the steady state value of the actuator position (see equation (6.3)).
- (ii) The position form with its continuous summation of the errors produces "integral windup" and special attention is required. The velocity form, on the other hand, is protected against integral windup for the following reason: The control action changes continuously until it becomes saturated. But as soon the error changes sign, the control action can return within the control range in one sampling period [134].

The discrete transfer function for the PID controller can be written after Z-transformation of equation (6.3) as follows [132]:

$$\frac{M(Z)}{E(Z)} = D(Z) = \frac{a_0 + a_1 Z^{-1} + a_2 Z^{-2}}{1 - Z^{-1}} \quad (6.4)$$

Where :

$$a_0 = K_C [1 + (T/\tau_I) + (\tau_D/T)]$$

$$a_1 = -K_C [1 + 2(\tau_D/T)]$$

$$a_2 = K_C [\tau_D/T]$$

A modified version of equation (6.4) using the trapezoidal rule is given by Isermann [132].

6.1.2 Dahlin Controller

Dahlin [133] proposed that the feedback controller should be designed so that the closed loop response has a first order plus deadtime transfer function. For the continuous loop, the response to a step change in set point would be:

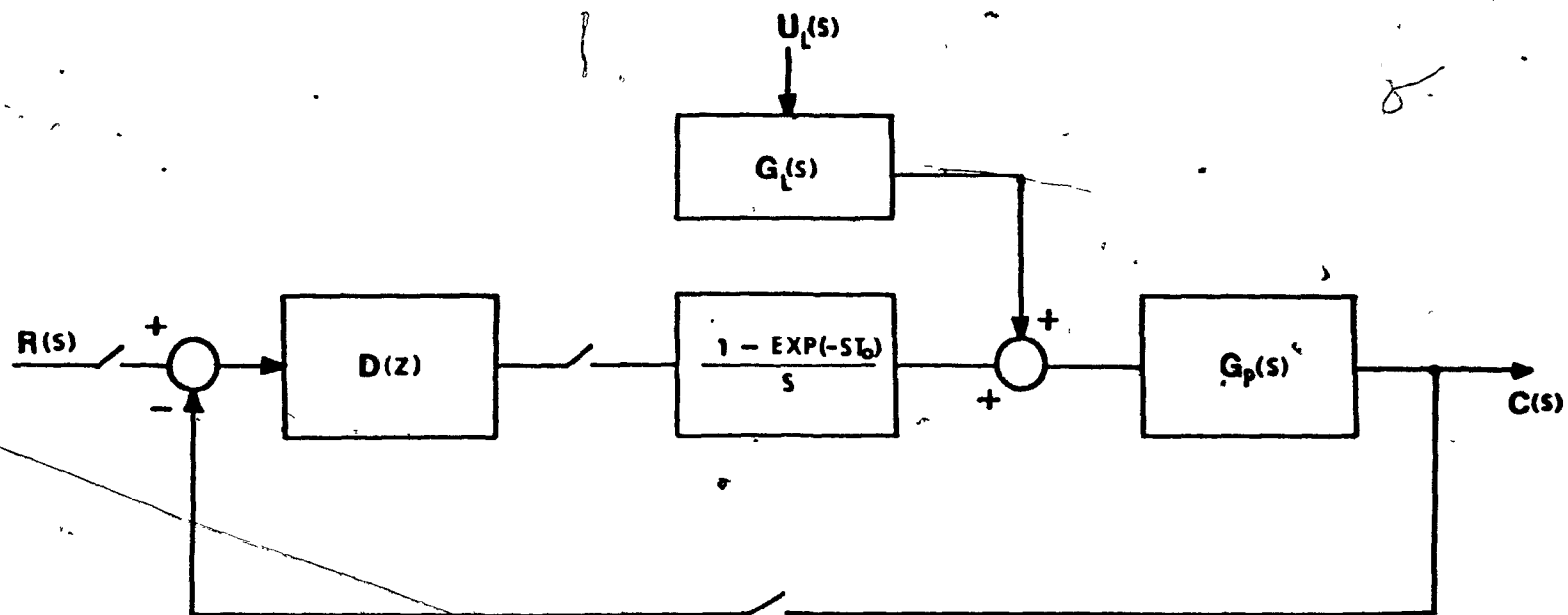
$$\frac{C(s)}{R(s)} = \frac{e^{-Ds}}{\lambda s + 1} \quad (6.7)$$

Where D is the dead-time and λ is the closed-loop tuning parameter. The discrete form of equation (6.7) is given by [132]:

$$\frac{C(Z)}{R(Z)} = \frac{[1 - \exp(-T/\lambda)] Z^{-N-1}}{1 - \exp(-T/\lambda) Z^{-1}} \quad (6.8)$$

Where $N = D/T$ (the nearest integer number of sampling times in D). Considering the control loop block diagram in Figure 6.2, the controller equation can be written as :

$$D(Z) = \frac{C(Z)/R(Z)}{1 - C(Z)/R(Z)} \cdot \frac{1}{HG(z)} \quad (6.9)$$



$$D(z) = \frac{C(z)/R(z)}{[1 - C(z)/R(z)]} \cdot \frac{1}{HG(z)} ; \quad \frac{C(z)}{R(z)} = \frac{[1 - \exp(T_0/\lambda)] z^{-n-1}}{1 - \exp(T_0/\lambda) z^{-1}}$$

Figure 6.2 Dahlin Control Block Diagram.

Where $HG(z)$ is the pulse transfer function. Substituting equation (6.8) into equation (6.9) gives :

$$D(z) = \frac{1 - \exp(-T/\lambda) z^{-N-1}}{1 - \exp(-T/\lambda) z^{-1} - [1 - \exp(-T/\lambda)] z^{-N-1}} \cdot \frac{1}{HG(z)} \quad (6.10)$$

The closed loop deadtime, D , should be at least as long as the actual deadtime [133]. If it is less, the controller will be physically unrealizable because it will contain a time advance term. The Dahlin algorithm, in general, provides reasonable control action and avoids undesirable overshoots or highly oscillatory closed loop response.

6.2 Discrete Dynamic Models

The discrete forms of the dynamic models for injection hydraulic pressure, nozzle pressure, and cavity pressure were derived from the corresponding continuous models utilizing the Z-transform method. The full derivation of the discrete models is presented in Appendices D - F. Two methods were used to deal with the time delay involved in the models : the first method approximates the dead time as

a multiple integer of the sampling interval, while in the second method, a first order Pade approximation was used [134]. Comparison between the two approximations will be presented. The following subsections present the main equations for the injection hydraulic pressure, nozzle pressure and cavity gate pressure.

6.2.1 Hydraulic Pressure Model

The injection hydraulic pressure response was modelled by a delayed first order plus oscillatory component as given by [135] :

$$P_H(t) = K_1 [1 - e^{-(t-D)/\tau}] + K_2 \left[\frac{1}{(1-\zeta^2)^{1/2} \tau_1} e^{-\zeta t / \tau_1} \sin((1-\zeta^2)^{1/2} \frac{t}{\tau_1}) \right] \quad (6.11)$$

Where :

- P_H = injection hydraulic pressure, pa
- K_1, K_2 = process gains, Pa/% change in valve opening
- τ, τ_1 = time constants, sec
- D = time delay, sec
- ζ = damping factor, dimensionless

Let $a = \zeta/\tau_1$

$$C = \frac{1}{(1-\zeta^2)^{1/2} \tau_1}$$

$$w = \frac{(1-\zeta^2)^{1/2}}{\tau_1}$$

Equation (6.11) can be written in a transfer function form for a step change in the manipulated valve opening, M , as follows [134]:

$$G(s) = \frac{P_H(s)}{M(s)} = \frac{K_1 e^{-Ds}}{(\tau s + 1)} + \frac{K_2 C w s}{(s + a)^2 + w^2} \quad (6.12)$$

When a zero-order hold is used, Equation (6.12) becomes :

$$HG(s) = \left(\frac{1 - e^{-Ts}}{s} \right) \left| \frac{K_1 e^{-Ds}}{(\tau s + 1)} + \frac{K_2 C w s}{(s + a)^2 + w^2} \right| \quad (6.13)$$

where T is the sampling time. For $D = nT$, where n is an integer, the discrete transfer function will be as follows [see Appendix D]:

$$HG(Z) = \frac{P_H(Z)}{M(Z)} = \frac{b_1 Z^{-1} + b_2 Z^{-2} + b_3 Z^{-3} + b_4 Z^{-4}}{1 - a_1 Z^{-1} + a_2 Z^{-2} - a_3 Z^{-3}} \quad (6.14)$$

Where :

$$a_1 = \exp(-\zeta T/\tau_1) [2 \cos wT + \sin wT]$$

$$a_2 = \exp(-\zeta T/\tau_1) [2 \exp(T/\tau) \cos wT + \exp(-sT/\tau_1)]$$

$$a_3 = \exp((T/\tau) - 2\zeta T/\tau_1)$$

$$b_1 = K_2 (1-\zeta^2)^{1/2} \tau_1 \exp(-\zeta T/\tau_1) \sin wT$$

$$b_2 = K_1 [1 - \exp(T/\tau)] - b_1 - b_1 \exp(T/\tau)$$

$$b_3 = 2K_1 [1 - \exp(T/\tau)] \exp(-\zeta T/\tau_1) \cos wT \\ - b_1 \exp(T/\tau)$$

$$b_4 = K_1 [1 - \exp(T/\tau)] \exp(-2\zeta T/\tau_1)$$

Thus, the discrete response of the injection hydraulic pressure in the time domain can be expressed as :

$$P_H(k) = a_1 P_H(k-1) - a_2 P_H(k-2) + a_3 P_H(k-3) + b_1 M(k-1) \\ + b_2 M(k-2) - b_3 M(k-3) + b_4 M(k-4) \quad (6.15)$$

Where:

$P_H(k)$ = injection hydraulic pressure at sampling instant k ,
 $M(k)$ = valve opening at sampling instant k , and a_i and b_i
 are the model parameters in terms of process gain, time
 constant, dead time and sampling time.

6.2.2 Nozzle Pressure Model

Nozzle pressure response to a step change in the valve opening was best fit with a first order plus time delay model as in the following equation [135] :

$$P_N(t) = K_p [1 - e^{-(t-D)/\tau}] \quad (6.16)$$

Where :

P_N = nozzle pressure, Pa

K_p = process gain, Pa/% change in valve opening

τ = time constant, sec

D = dead time, sec

Equation (6.16) can be written in the transfer function form using the two methods mentioned above for dead time approximation as follows :

(i) $D = n T$, where n = integer, and T = sampling time

$$G(s) = \frac{P_N(s)}{M(s)} = \frac{K_p e^{-Ds}}{\tau s + 1} \quad (6.17)$$

The discrete pulse transfer function between nozzle pressure and the valve opening is [see Appendix E for derivation]:

$$HG(Z) = \frac{P_N(Z)}{M(Z)} = \frac{K_p (1-a)Z^{-2}}{1 - a Z^{-1}} \quad (6.18)$$

where $a = \exp(-T/\tau)$. Therefore, the nozzle pressure discrete model in the time domain is of the form :

$$P_N(k) = a P_N(k-1) + K_p (1-a) M(k-2) \quad (6.19)$$

(ii) Pade Approximation

Using a first order Pade approximation, the exponential term in Equation (6.17) can be approximated as :

$$e^{-Ds} = \frac{1 - (D/2)s}{1 + (D/2)s} \quad (6.20)$$

Substituting into Equation (6.17) and with $D_1 = D/2$, the transfer function between nozzle pressure response and the valve opening becomes

$$G(s) = \frac{P_N(s)}{M(s)} = \frac{K_p (1 - D_1 s)}{(\tau s + 1)(D_1 s + 1)} \quad (6.21)$$

The discrete pulse transfer function with a zero-order hold as derived in Appendix E is :

$$HG(Z) = \frac{P_N(Z)}{M(z)} = \frac{b_1 Z^{-1} - b_2 Z^{-2}}{1 - a_1 Z^{-1} + a_2 Z^{-2}} \quad (6.22)$$

This transfer function gives the following discrete model in the time domain:

$$P_N(k) = a_1 P_N(k-1) - a_2 P_N(k-2) + b_1 M(k-1) + b_2 M(k-2) \quad (6.23)$$

Where :

$$\begin{aligned} a_1 &= \exp(-T/\tau) + \exp(-T/D_1) \\ a_2 &= \exp(-T/\tau) * \exp(-T/D_1) \\ b_1 &= K(\tau + D_1)(1 - \exp(-T/\tau))/(\tau - D_1) \\ &\quad + 2KD_1(1 - \exp(-T/D_1))/(D_1 - \tau) \\ b_2 &= 2KD_1 \exp(-T/\tau)(1 - \exp(-T/D_1))/(D_1 - \tau) + \\ &\quad K(\tau + D_1) \exp(-T/D_1) * (1 - \exp(-T/\tau))/(\tau - D_1) \end{aligned}$$

6.2.3 Cavity Pressure Model

As presented in Equation (4.1), the response of cavity gate pressure was modeled by a first order plus time delay superimposed on a constantly increasing pressure component of the form :

$$P_C(t) = K_1 t + K_2 [1 - \exp(-(t-D)/\tau)] \quad (6.24)$$

The transfer function form of this equation is

$$G(s) = \frac{P_C(s)}{M(s)} = \frac{K_1}{s} + \frac{K_2 e^{-Ds}}{(\tau s + 1)} \quad (6.25)$$

The discrete transfer function, using a zero-order hold, can be obtained as follows [see Appendix F].

(i) $D = nT$, where n is an integer, T is the Sampling Time

$$HG(Z) = \frac{P_C(Z)}{M(Z)} = \frac{b_1 Z^{-1} - b_2 Z^{-2} - b_3 Z^{-3}}{1 - a_1 Z^{-1} + a_2 Z^{-2}} \quad (6.26)$$

Where :

$$a_1 = 1 + \exp(-T/\tau)$$

$$a_2 = \exp(-T/\tau)$$

$$b_1 = K_1 T$$

$$b_2 = K_1 T \exp(-T/\tau) - K_2 [1 - \exp(-T/\tau)]$$

$$b_3 = K_2 [1 - \exp(-T/\tau)]$$

From Equation (6.26), the discrete response of cavity gate pressure in the time domain can be written as

$$P_C(k) = a_1 P_C(k-1) - a_2 P_C(k-2) + b_1 M(k-1) - b_2 M(k-2) - b_3 M(k-3) \quad (6.27)$$

(ii) Pade Approximation for the Dead Time

Using a first order Pade approximation and letting $D_1 = D/2$, Equation (6.25) becomes

$$G(s) = \frac{K_1}{s} + \frac{K_2 (1 - D_1 s)}{(\tau s + 1)(D_1 s + 1)} \quad (6.28)$$

If a zero-order hold is used, the discrete transfer function can be obtained [derivation is found in Appendix F] :

$$HG(Z) = \frac{P_C(Z)}{M(Z)} = \frac{f_1 Z^{-1} - f_2 Z^{-2} + f_3 Z^{-3}}{1 - h_1 Z^{-1} + h_2 Z^{-2} - h_3 Z^{-3}} \quad (6.29)$$

and the response of cavity gate pressure in the time domain becomes

$$P_C(k) = h_1 P_C(k-1) - h_2 P_C(k-2) + h_3 P_C(k-3) + f_1 M(k-1) - f_2 M(k-2) + f_3 M(k-3) \quad (6.30)$$

Where :

$$h_1 = 1 + c + d$$

$$h_2 = c + d + c d$$

$$h_3 = c d$$

$$f_1 = K_1 T + A(1-c) + B(1-d)$$

$$f_2 = K_1 T + A(1-c)(1+d) + B(1-d)(1+c)$$

$$f_3 = K_1 T c d + A d (1-c) + B c (1-d)$$

$$A = K_2 (\tau + D_1) / (\tau - D_1)$$

$$B = 2 K_2 D_1 / (D_1 - \tau)$$

$$c = \exp(-T/\tau)$$

$$d = \exp(-T/D_1)$$

6.3 Control Loop Design

6.3.1 Controller Tuning

A critical step in the implementation of any controller is the determination of the values of the relevant parameters. It is also necessary to specify the sampling period. The objective of the tuning process is the selection of a combination of controller parameters that give a satisfactory response according to appropriate criteria. The criteria used to select the best response vary, depending on the application and on the process. A number of tuning procedures and formulae have been introduced to tune controllers for various response criteria [136-146]. The commonly used criteria can be classified into two categories :

- (i) simple criteria based on a single response characteristic,
- (ii) more exact criteria based on the entire response.

An example of the first is the $1/4$ decay ratio [136] while an example of the second is the minimum error integral criteria (EIC) [138]. The latter approach has been used in this study.

The error integral criteria include both the error

magnitude and the time over which it occurs. The general form of the EIC is [138]:

$$\text{EIC} = \int f(t, e(t)) dt \quad (6.31)$$

The following formulas have been proposed for the function "f" in the integral of Equation (6.31) [138]:

Integral of the Square Error (ISE)

$$\text{ISE} = \int [e(t)]^2 dt \quad (6.32)$$

Integral of the Absolute value of the Error (IAE)

$$\text{IAE} = \int |e(t)| dt \quad (6.33)$$

Integral of Time multiplied by the Absolute Error (ITAE)

$$\text{ITAE} = \int t |e(t)| dt \quad (6.34)$$

The ISE is relatively insensitive to small errors. Large errors, that usually occur at the beginning of the response, contribute heavily to the value of the integral. Consequently, using ISE as a criterion of performance will result in a response with small overshoot but with a long settling time. The IAE criterion is more sensitive to small errors but less sensitive to the initial large errors. The

ITAE is insensitive to the initial and somewhat unavoidable errors, but it is strongly influenced by errors occurring late in time. Optimum responses defined by ITAE will consequently show shorter total response times and larger overshoots than with either of the other criteria.

The optimum set of controller parameter values is not only a function of which of the three integral definitions is selected, but also of the type of the input (that is, disturbance or set point change) and of its shape, for example, step change, ramp, or others. In terms of the shape of the input, the step change is usually selected because it is the most disruptive type that occurs in practice. The type of the input depends on the aim of the control loop, which could be as a set point tracking or a disturbance rejection. The values of the controller parameters also depend on the dynamic characteristic of the process. If the process is nonlinear, its characteristics change from one operating condition to another. This means that a particular set of tuning parameters produces the desired response at only one operating condition. For operation in a range of conditions, an acceptable set of tuning parameters is necessarily a compromise.

Controllers in this study have been tuned for a set point change using the ITAE criterion with the formulae given in Table 6.1 [147].

TABLE 6.1

Minimum Error Integral Tuning Formulae
for Set-Point Changes [147]

$$\text{Process Model } G(S) = \frac{K e^{-\theta S}}{\tau S + 1}$$

Controller	Controller Parameters		Error Integral	
			IAE	ITAE
PI	$K_C = \frac{a_1}{K} (\theta/\tau)^{b_1}$ $\tau_I = \frac{\tau}{a_2 + b_2(\theta/\tau)}$	a1	0.758	0.586
		b1	-0.861	-0.916
		a2	1.020	1.030
		b2	-0.323	-0.165
PID	$K_C = \frac{a_1}{K} (\theta/\tau)^{b_1}$ $\tau_I = \frac{\tau}{a_2 + b_2(\theta/\tau)}$ $\tau_D = a_3 \tau (\theta/\tau)^{b_3}$	a1	1.086	0.965
		b1	-0.865	-0.855
		a2	0.740	0.796
		b2	-0.130	-0.147
		a3	0.348	0.308
		b3	0.914	0.929

6.3.2 Sampling Interval

The choice of the sampling interval plays an important role in discrete control algorithms. It influences the time-delays and the locations of the discrete system poles and zeros and thereby the closed loop control performance. It is difficult to formulate a general rule for choosing the optimal sampling time since it should reflect the process dynamics, the external disturbance characteristics, and the desired control performance. In general, a long sampling time, relative to the dominant time constant of the process, impairs the overall control performance mainly due to the loss of system information. On the other hand, a short sampling time usually gives better performance at the expense of large excursions of the manipulated variable.

Several practical rules are suggested for selecting the sampling period. When the dominant time constant of the process, τ , is known, the following range has been suggested to ensure satisfactory performance [147]:

$$\tau/20 < T \leq \tau/10 \quad (6.35)$$

For processes with time delay, t_d , of the same order of magnitude as the time constant, τ , the sampling period can be selected as equal to 0.1τ or $0.1t_d$, whichever is smaller [134]. If t_d is much smaller than τ , the dead time can be

neglected and $T = 0.1\tau$. Another criterion for an overdamped process with time delay, t_d , is given by [132]:

$$t_d/8 < T < t_d/4 \quad (6.36)$$

or in terms of settling time

$$t_{st}/12 < T < t_{st}/6 \quad (6.37)$$

where t_{st} is the 95% settling time of the step response [132]. Another rule of thumb suggests obtaining 2 to 4 samples per rise time of the closed loop system response to a step change [148].

When the sample time is of the above order of magnitude, its effect can be taken into consideration in the tuning formulae by adding one-half the sample time to the process dead time [142]. Therefore, the adjusted dead time used in the tuning formulae (Table 6.1) becomes:

$$t_{dc} = t_d + T/2 \quad (6.38)$$

where

t_{dc} = the adjusted dead time

t_d = the dead time of the process

T = the sampling time

As mentioned before, the control performance

deteriorates in case of a long sampling interval. Thus, when the control performance is of primary importance, the sampling time should be as small as possible. However, it cannot be arbitrarily small, because a small sampling time relative to the dominant time constant of the process may result in the overall system being very oscillatory. This mainly results from the fact that the locations of the poles and zeros of a discrete transfer function are partially determined by the sampling time. A small sampling interval produces small numerator coefficients in the transfer function and results in zeros close to the unit circle in the Z -plane, which is the stability limit. On the basis of the above considerations, sample intervals of 5 and 10 ms were selected for the simulation study presented in the next section.

6.4 Control Loop Simulation

A computer simulation study of the control loop was carried out to achieve the following objectives:

- (1) To refine the initial controller parameters obtained by the ITAE tuning criterion.
- (2) To evaluate the performance of the different controllers using the dynamic models derived for hydraulic pressure, nozzle pressure, and cavity gate pressure as described in section 6.2.
- (3) To choose the most appropriate and practical controllers and set point profiles to control the injection molding process.

The controllers were evaluated according to their response to different set point profiles. Five different criteria were used in the evaluation: peak overshoot, damping behavior, rise time, settling time and the integral performance indices. The discrete control equations presented in section 6.1 for the Proportional, PI and PID controllers are listed below.

PI :

$$m(k) = m(k-1) + a_0 e(k) - a_1 e(k-1) \quad (6.39)$$

PID :

$$m(k) = m(k-1) + a_0 e(k) - a_1 e(k-1) + a_2 e(k-2) \quad (6.40)$$

Simulation results of hydraulic pressure, nozzle pressure, and cavity gate pressure control loops are presented in the following subsections. Listings of the computer simulation programs are given in Appendix H.

6.4.1 Hydraulic Pressure Control Loop

The discrete model for the hydraulic pressure response was obtained in a previous section as :

$$HG(Z) = \frac{P_H(Z)}{M(Z)} = \frac{b_1 Z^{-1} + b_2 Z^{-2} + b_3 Z^{-3} + b_4 Z^{-4}}{1 - a_1 Z^{-1} + a_2 Z^{-2} - a_3 Z^{-3}} \quad (6.41)$$

The model parameters a_i and b_i , as defined in section 6.2.1, are functions of the process gain, time constant, dead time and sampling time. The numerical values were calculated using combinations of the process parameters given in reference [135] and various sampling times. The resulting model is presented in Table 6.2. The initial controller parameters for the PI, and PID controllers as calculated by ITAE tuning, are given in Table 6.3.

Table 6.2

Discrete Models for the Hydraulic Pressure Response
(Equation 6.34)

Sampling Time (sec)	Model
0.005	$\frac{P_H(Z)}{M(Z)} = \frac{3.77 Z^{-1} - 3.92 Z^{-2} - 2.39 Z^{-3} + 2.30 Z^{-4}}{1 - 2.68 Z^{-1} + 2.32 Z^{-2} - 0.64 Z^{-3}}$
0.01	$\frac{P_H(Z)}{M(Z)} = \frac{3.19 Z^{-1} + 0.39 Z^{-2} - 6.22 Z^{-3} + 3.14 Z^{-4}}{1 - 2.23 Z^{-1} + 1.65 Z^{-2} - 0.41 Z^{-3}}$

TABLE 6.3

Initial Controller Parameter Values Calculated by ITAE
for the Hydraulic Pressure Control Loop

Controller	K_C	τ_I	τ_D
PI	0.076	0.046	-
PID	0.114	0.059	0.003

Parameters for Discrete P, PI and PID Controllers
for the Hydraulic Pressure Control Loop

Controller	Sampling Time, sec	a_0	a_1	a_2
PI	0.005	0.084	-0.076	-
	0.010	0.093	-0.076	-
PID	0.005	0.215	-0.296	0.091
	0.010	0.179	-0.205	0.046

The response of the controlled hydraulic pressure, using a PI controller, is shown in Figure 6.3. The ITAE tuning criterion gave reasonable initial values for the controller parameters, but the response was improved by adjusting the controller gain, K_C .

The PID controller loop behavior is shown in Figure 6.4 for the same situation. This controller is more sensitive to changes in the controller parameter values (compare with Figure 6.3).

The optimum parameters for the PI and PID controllers, based on minimizing the ITAE criterion, were obtained by using the Nelder-Mead (N-M) optimization routine [149]. The actual process model (Equation 6.11) was used rather than the approximated model used in the formulae of Table 6.1. The optimum settings obtained were as follows :

PI controller: $K_C = 0.029$, $\tau_I = 0.044$

PID controller: $K_C = 0.032$, $\tau_I = 0.046$, $\tau_D = 0.003$

Figure 6.5 compares the hydraulic pressure response for the PI and PID controllers with the (N-M) optimum settings. The PID controller performs slightly better than the PI controller as shown in Figure 6.5. The PID controller, however, is more sensitive to changes in the controller parameters (Figure 6.4). For this reason the PI controller was chosen to control the hydraulic pressure.

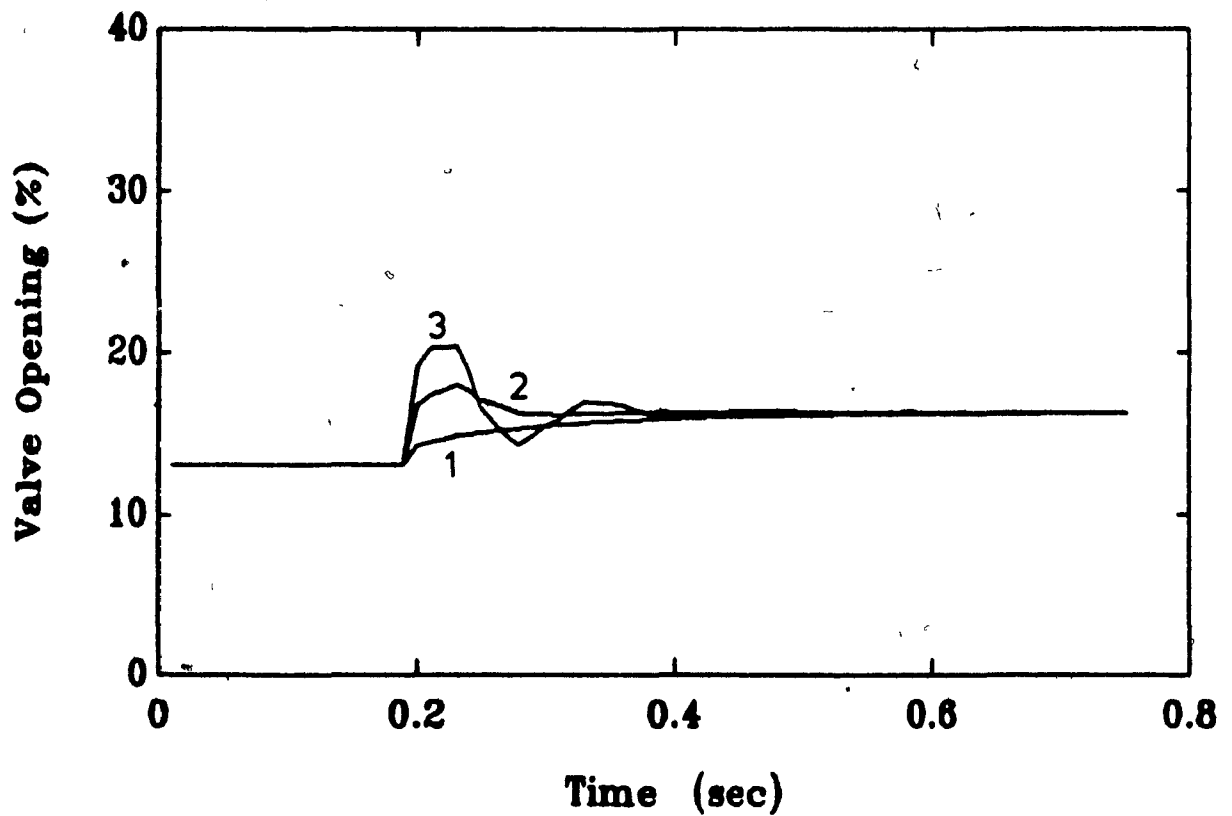
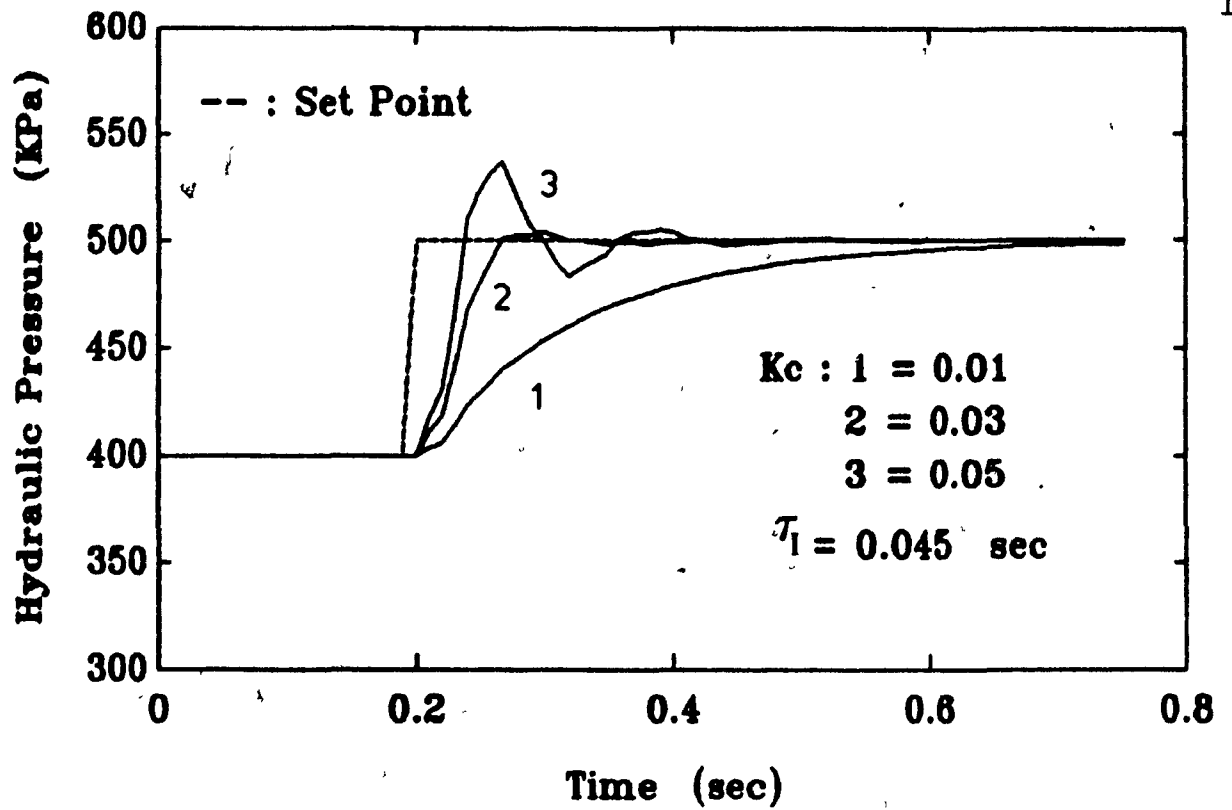


Figure 6.3 Hydraulic Pressure Response Simulation to a Step Change in the Set-Point with a PI Controller.

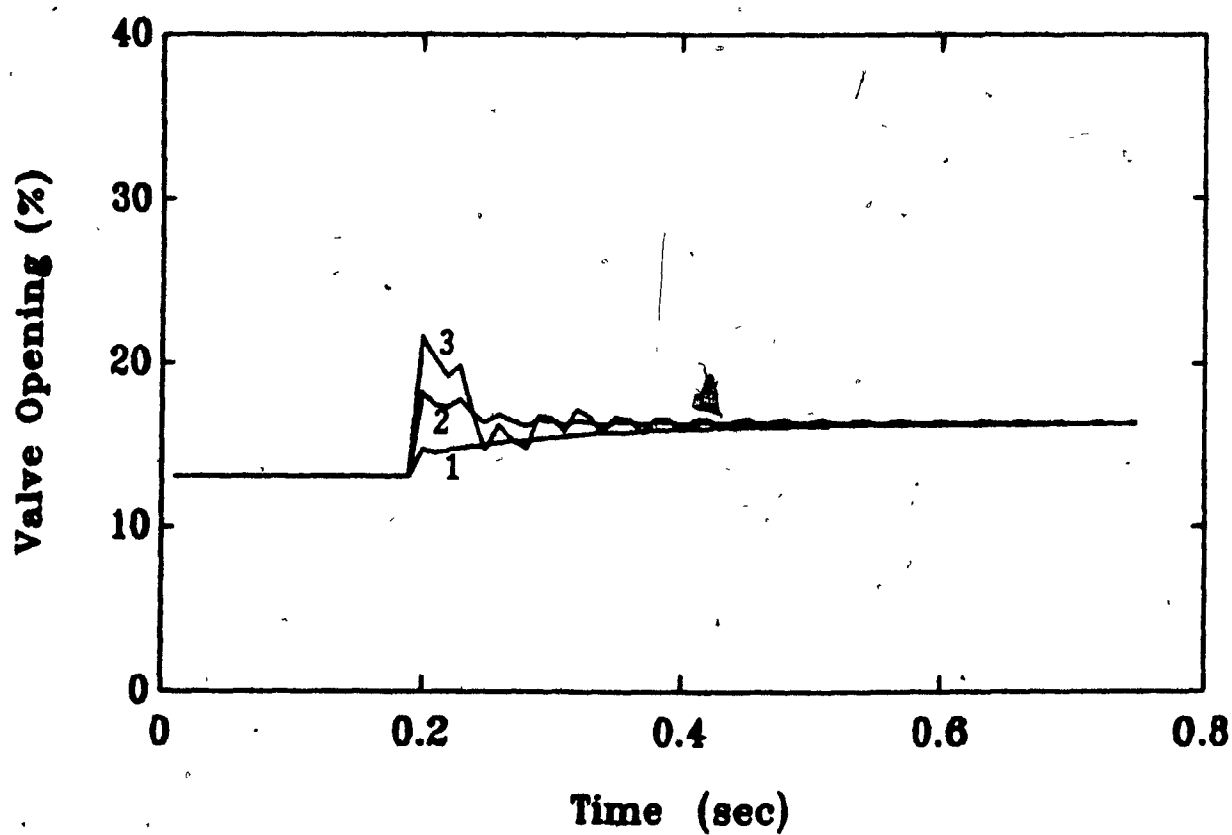
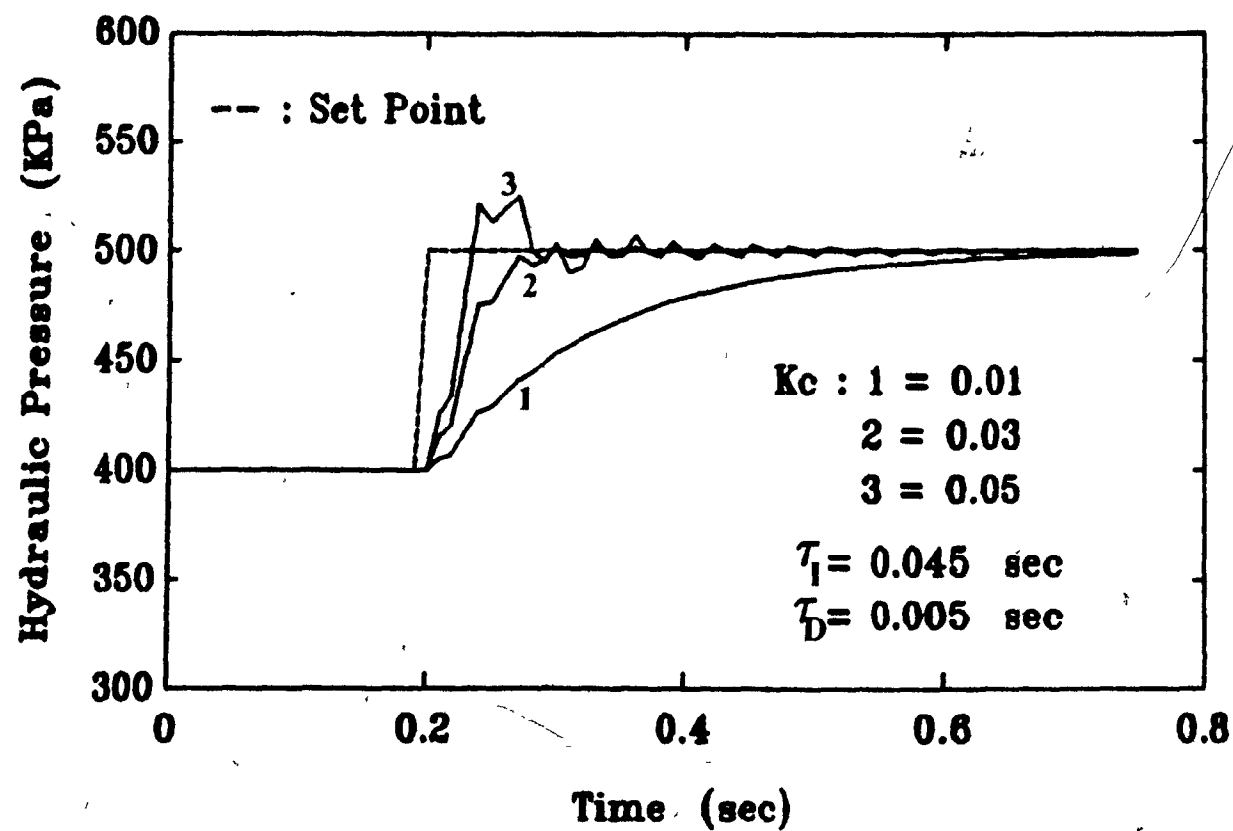


Figure 6.4 Hydraulic Pressure Response Simulation to a Step Change in the Set-point with a PID Controller.

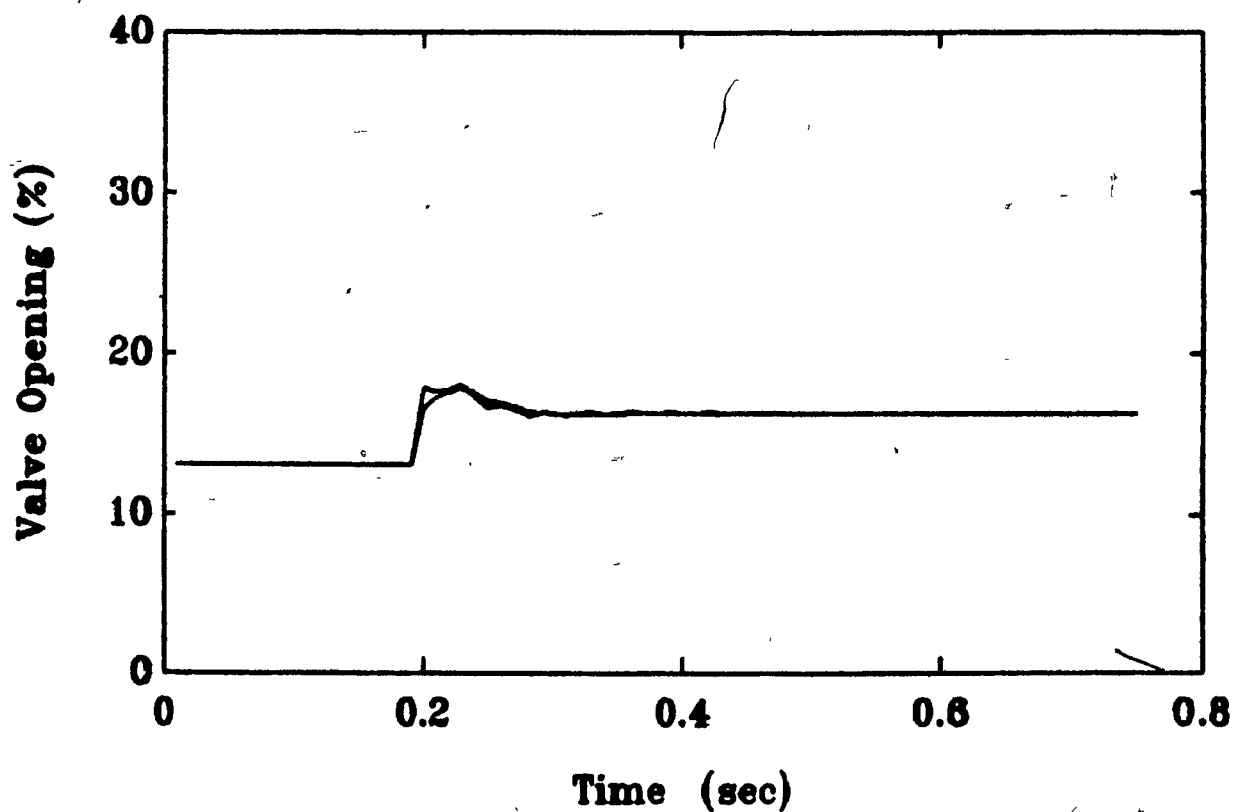
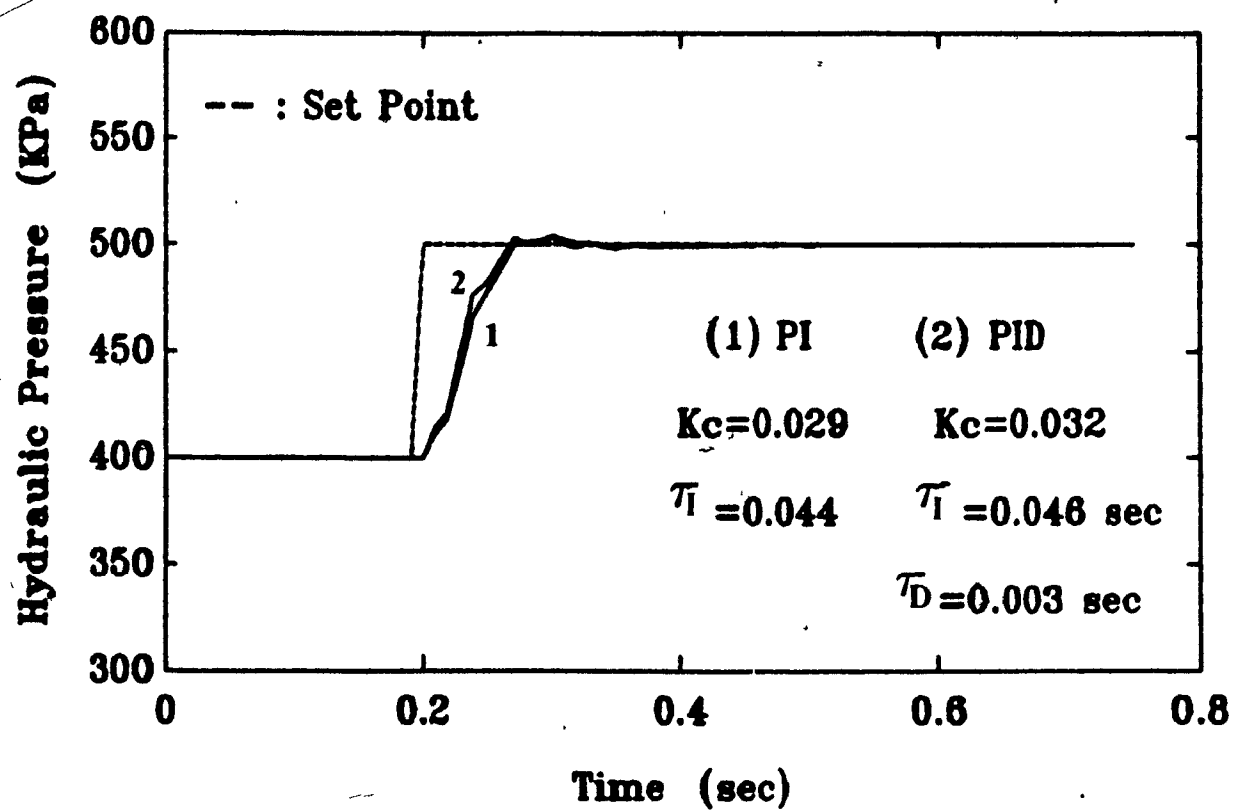


Figure 6.5 Comparison of Hydraulic Pressure Response with the Optimum PI and PID Controllers.

6.4.2 Nozzle Pressure Control Loop

The flow into the mold is more directly related to the nozzle pressure than to the hydraulic pressure. The control of the nozzle pressure directly (rather than via the hydraulic pressure) is of interest. The discrete models derived in a section 2.2.2 for nozzle pressure response using two approximations of the dead time (Equations 6.18 and 6.22) are rewritten below:

$$(i) \quad \frac{P_N(Z)}{M(Z)} = \frac{K_p (1-a) Z^{-2}}{1 - a Z^{-1}} \quad (6.42)$$

$$(ii) \quad \frac{P_N(Z)}{M(Z)} = \frac{b_1 Z^{-1} - b_2 Z^{-2}}{1 - a_1 Z^{-1} + a_2 Z^{-2}} \quad (6.43)$$

The model parameters a , a_i and b_i , as previously defined in section 6.2.2, are functions of the process gain, time constant, dead time and sampling time. The numerical values were calculated using combinations of the process parameters given in [135] and various sampling times. The resulting models are presented in Table 6.4. The initial controller parameters for the proportional, PI, and PID controllers, calculated by the ITAE are given in Table 6.5.

TABLE 6.4

Discrete Models for the Nozzle Pressure Response
(Equations 6.42 and 6.43)

Sampling Time (sec)	Model (1)	Model (2)
0.005	$\frac{P_N(Z)}{M(Z)} = \frac{20.09 Z^{-2}}{1 - 0.90 Z^{-1}}$	$\frac{2.99 Z^{-1} + 14.40 Z^{-2}}{1 - 1.04 Z^{-1} + 0.12 Z^{-2}}$
0.01	$\frac{P_N(Z)}{M(Z)} = \frac{38.28 Z^{-2}}{1 - 0.90 Z^{-1}}$	$\frac{20.51 Z^{-1} + 17.11 Z^{-2}}{1 - 0.83 Z^{-1} + 0.01 Z^{-2}}$

TABLE 6.5

Initial Controller Parameter Values Calculated by ITAE
for the Nozzle Pressure Control Loop

Controller	K_C	T_I	T_D
PI	0.012	0.050	-
PID	0.018	0.065	0.004

Parameters for Discrete PI and PID Controllers
for the Nozzle Pressure Control Loop

Controller	Sampling Time, sec	a_0	a_1	a_2
PI	0.005	0.013	-0.012	-
	0.010	0.015	-0.012	-
PID	0.005	0.034	-0.047	0.015
	0.010	0.028	-0.033	0.007

The responses of nozzle pressure under the control of PI and PID controllers are shown in Figures 6.6 and 6.7. The controller parameters were optimised, based on the ITAE value, using the Nelder-Mead optimization method [149] in conjunction with the actual model for nozzle pressure. The optimum values of the controller parameters were :

PI controller: $K_C = 0.005$, $\tau_I = 0.048$

PID controller: $K_C = 0.006$, $\tau_I = 0.052$, $\tau_D = 0.006$

The responses of the two controllers with the (N-M) optimum settings are given in Figure 6.8. The advantages of the PID controller over the PI controller are stronger than in the case of hydraulic pressure.

Some responses to set-point pressure-time profiles were investigated for the PI and PID controllers. These are presented in Figures 6.9, 6.10 and 6.11. Figure 6.9 shows a simple ramping of the nozzle pressure to a plateau followed by a decrease to the initial pressure. Both the PI and PID controllers perform about equally well in this case. The Profile of Figure 6.10 shows the nozzle pressure increasing at the beginning of injection. At 0.2 seconds, the profile is suddenly increased in a step fashion to correspond to filling a larger mold cross-section. Both PI and PID controllers handle the ramp part of the profile well, but the PID controller gives a better response to the step

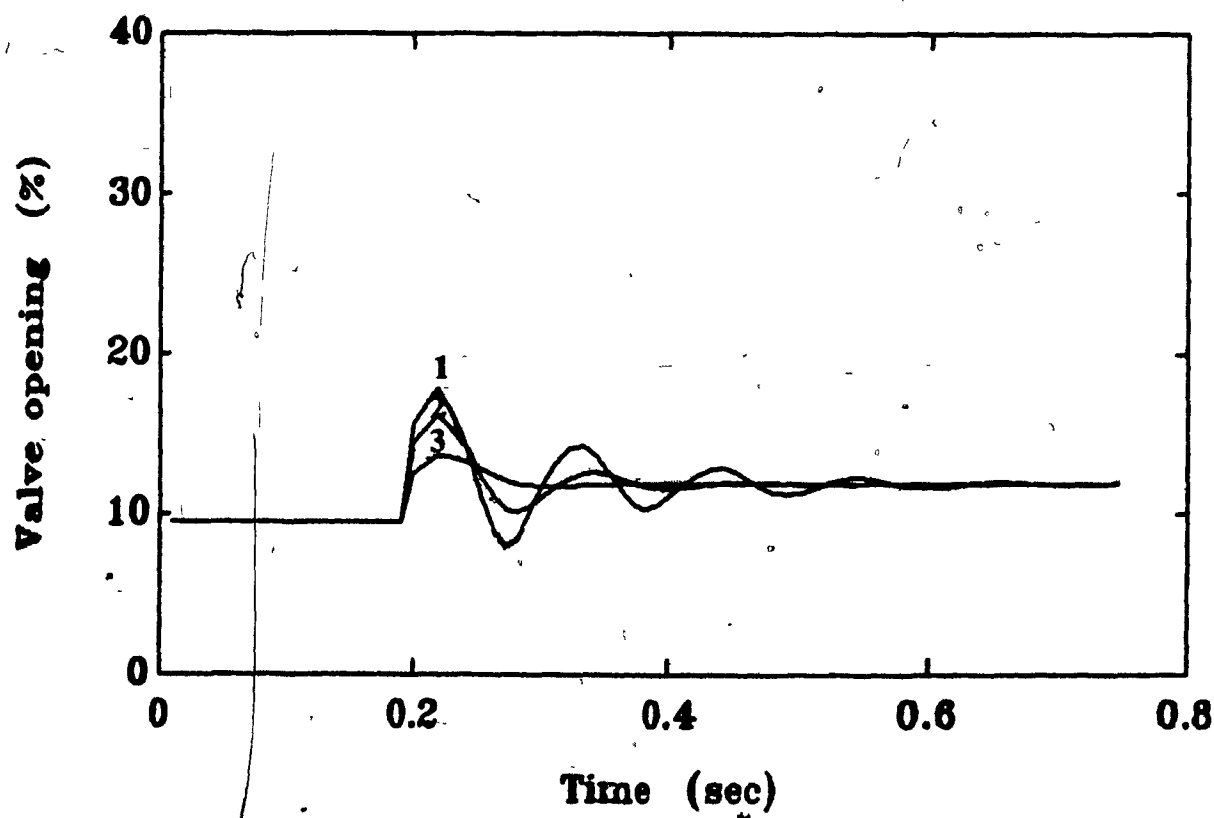
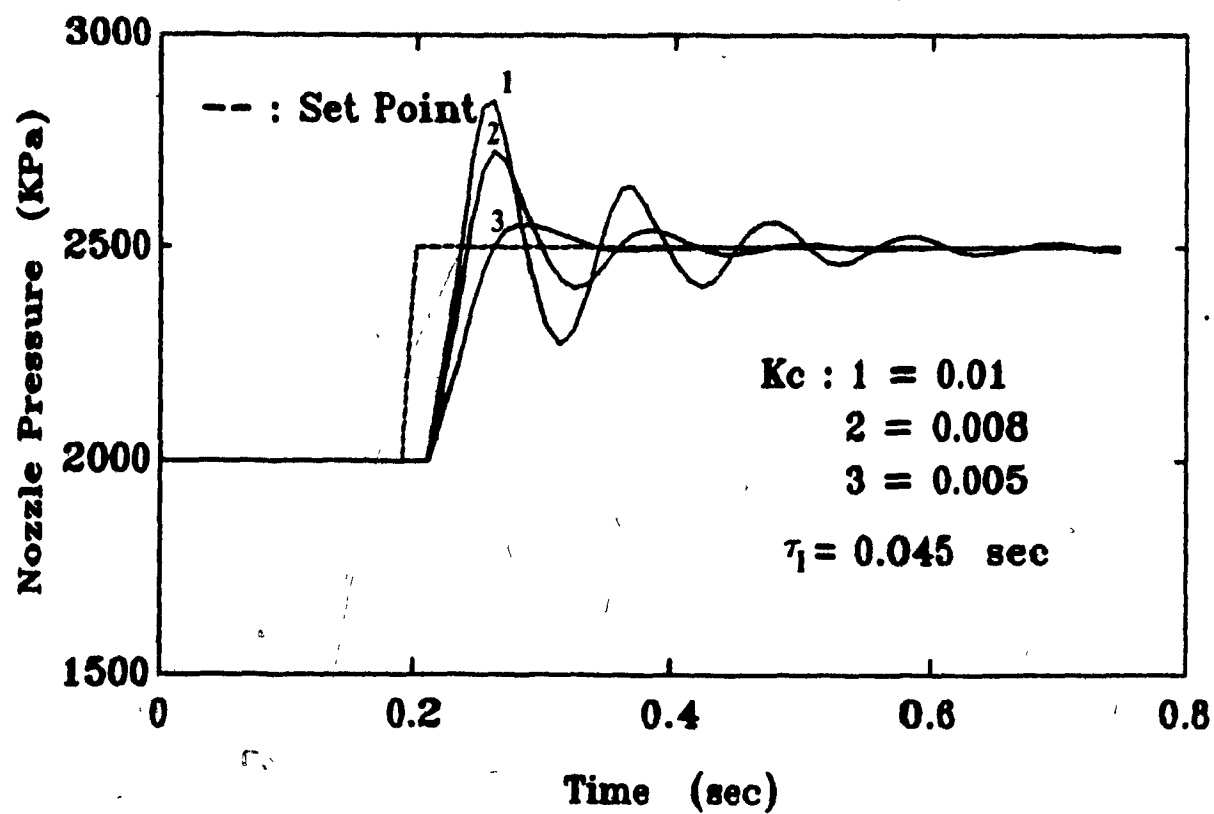


Figure 6.6 Nozzle Pressure Response to a Step Change in the Set-point with a PI Controller.

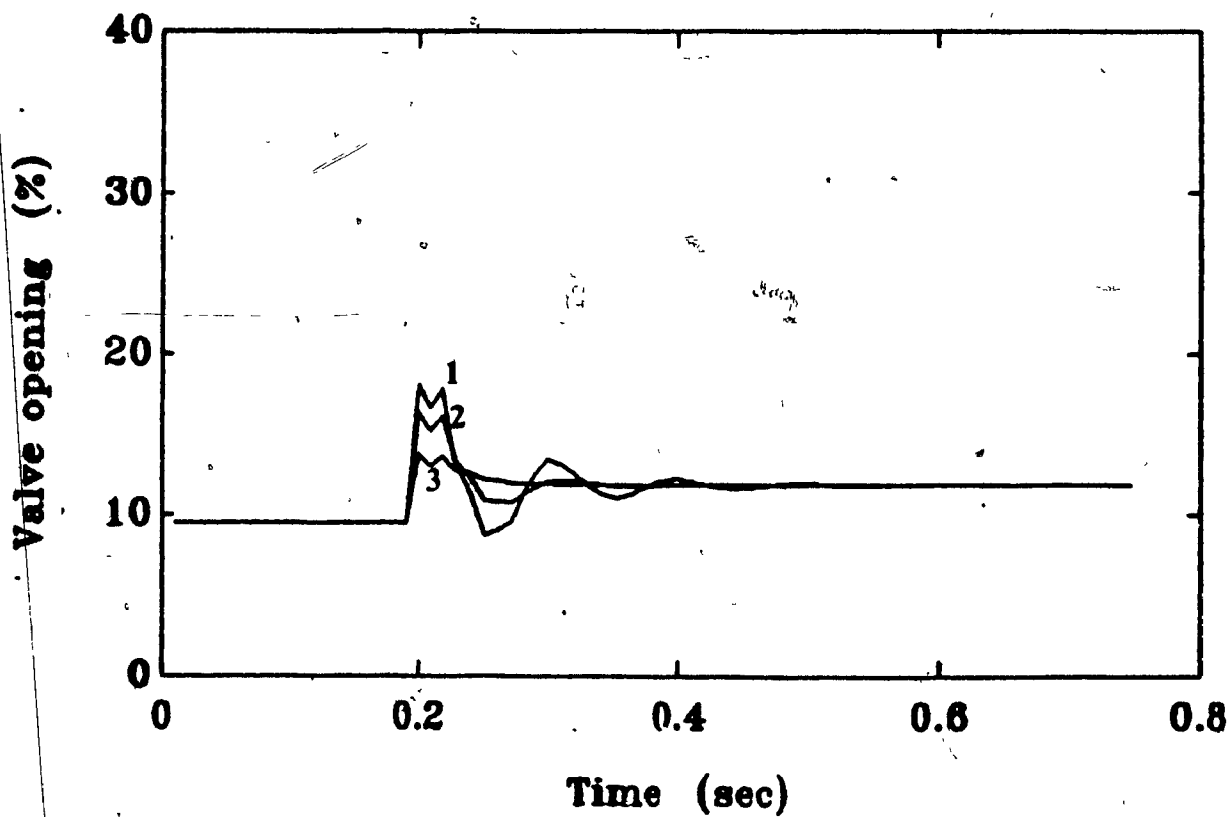
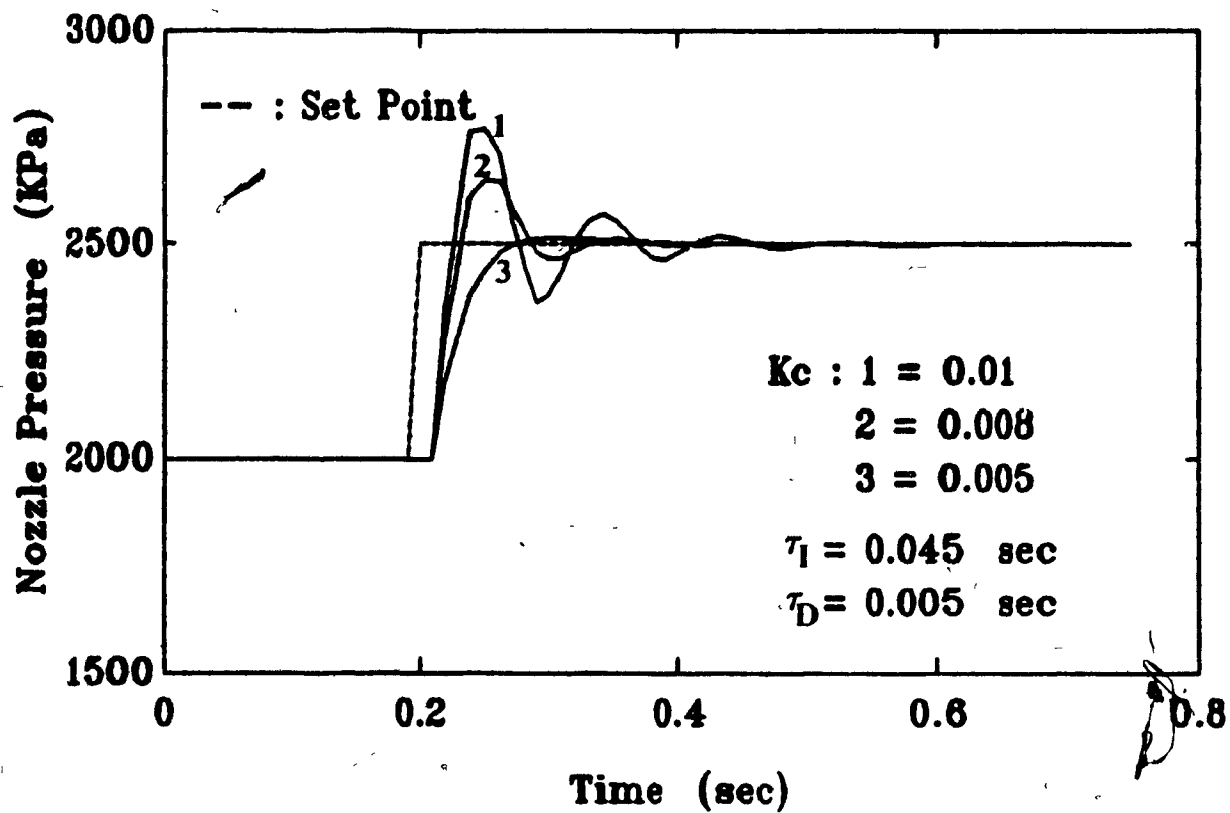


Figure 6.7 Nozzle Pressure Response to a Step Change in the Set-point with a PID Controller.

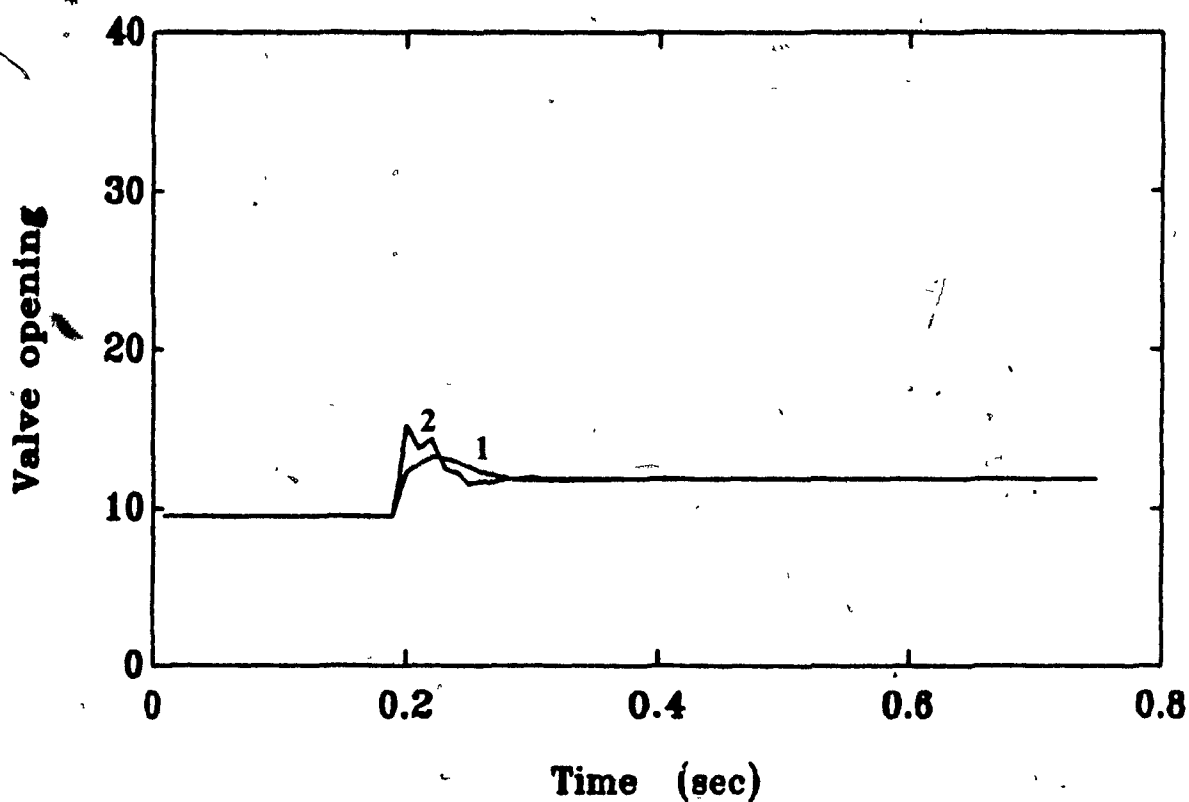
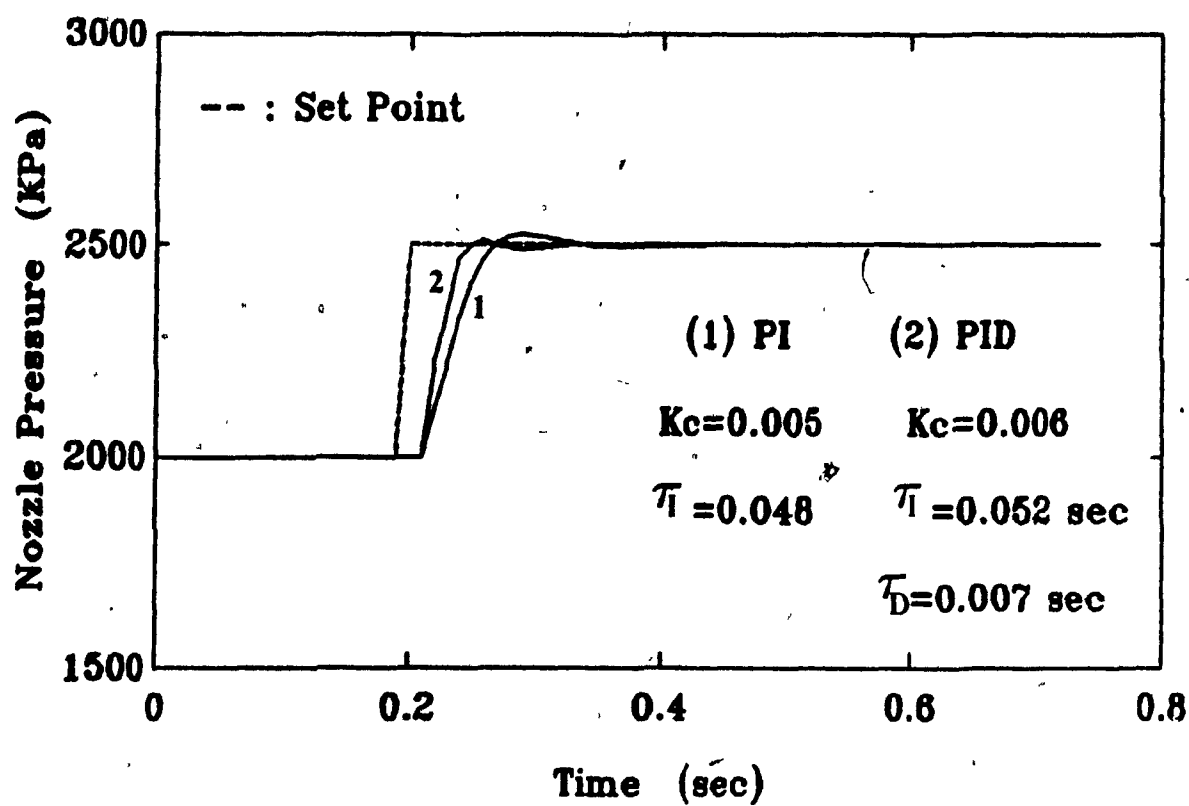


Figure 6.8 Nozzle Pressure Response to a Step Change in the Set-Point with PI and PID Controllers.

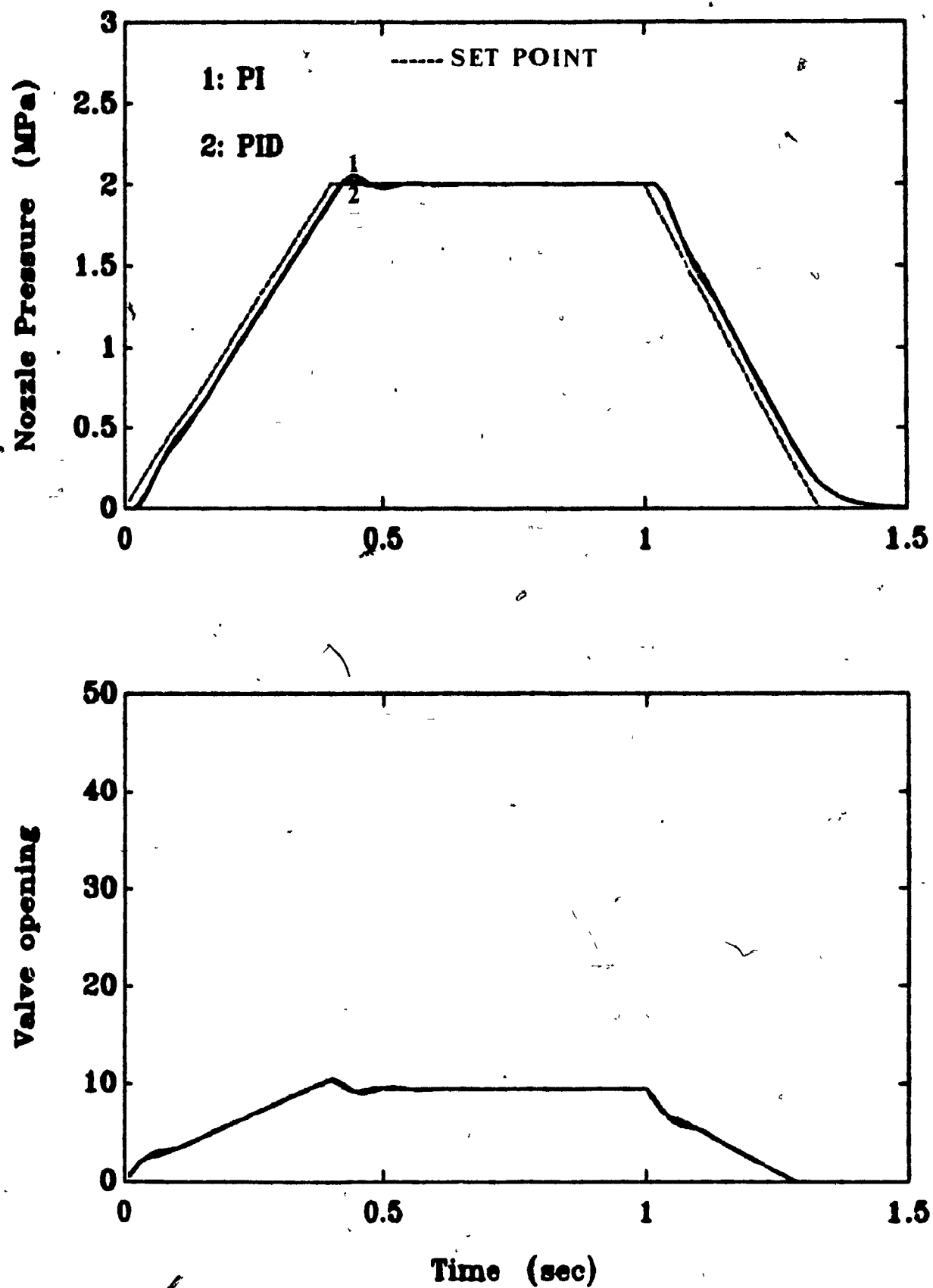


Figure 6.9 Nozzle Pressure Response to a Set-Point Pressure-Time Profile with the PI and PID Controllers.

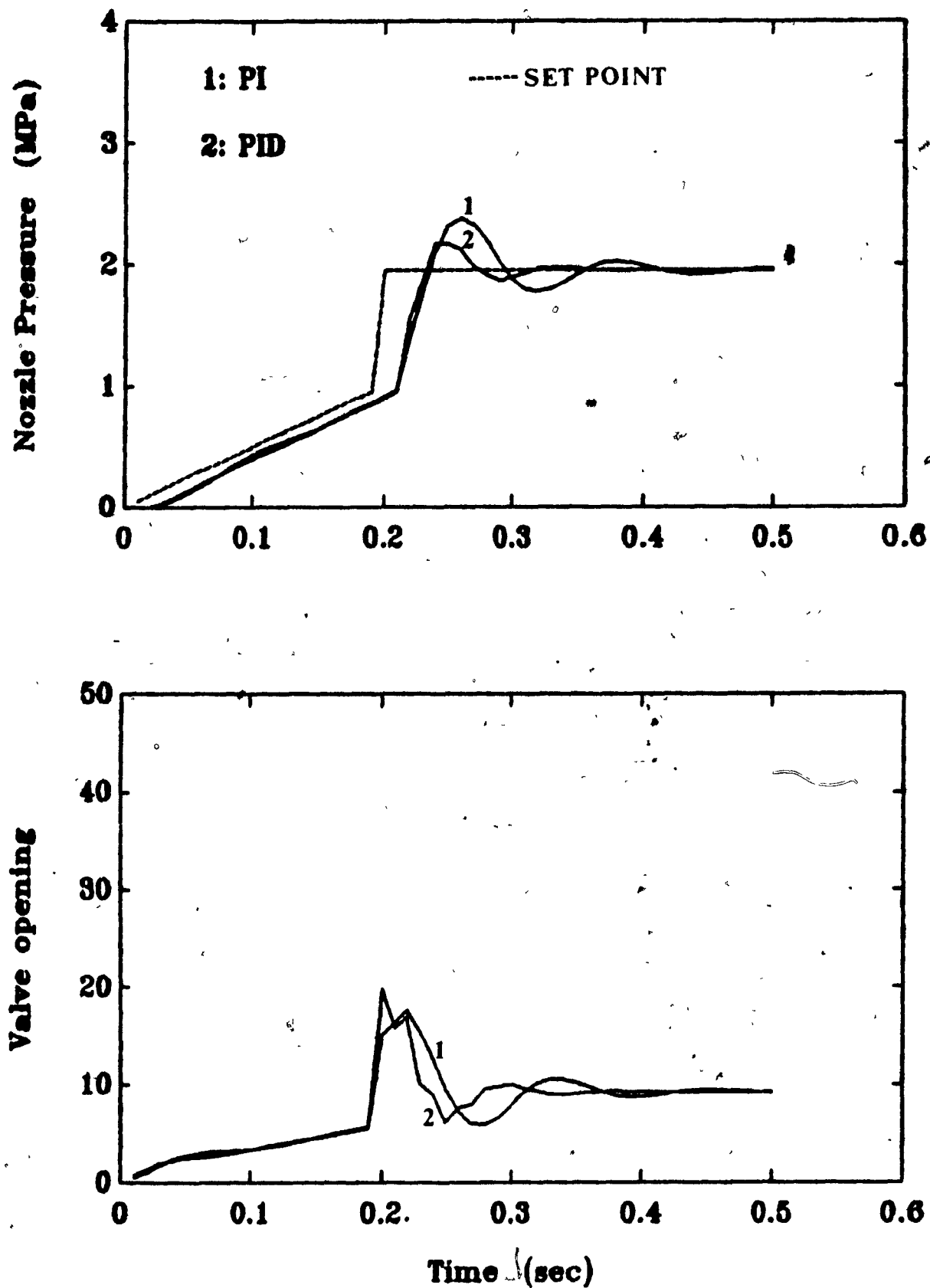


Figure 6.10 Nozzle Pressure Response to a Set-Point Pressure-Time Profile with the PI and PID Controllers.

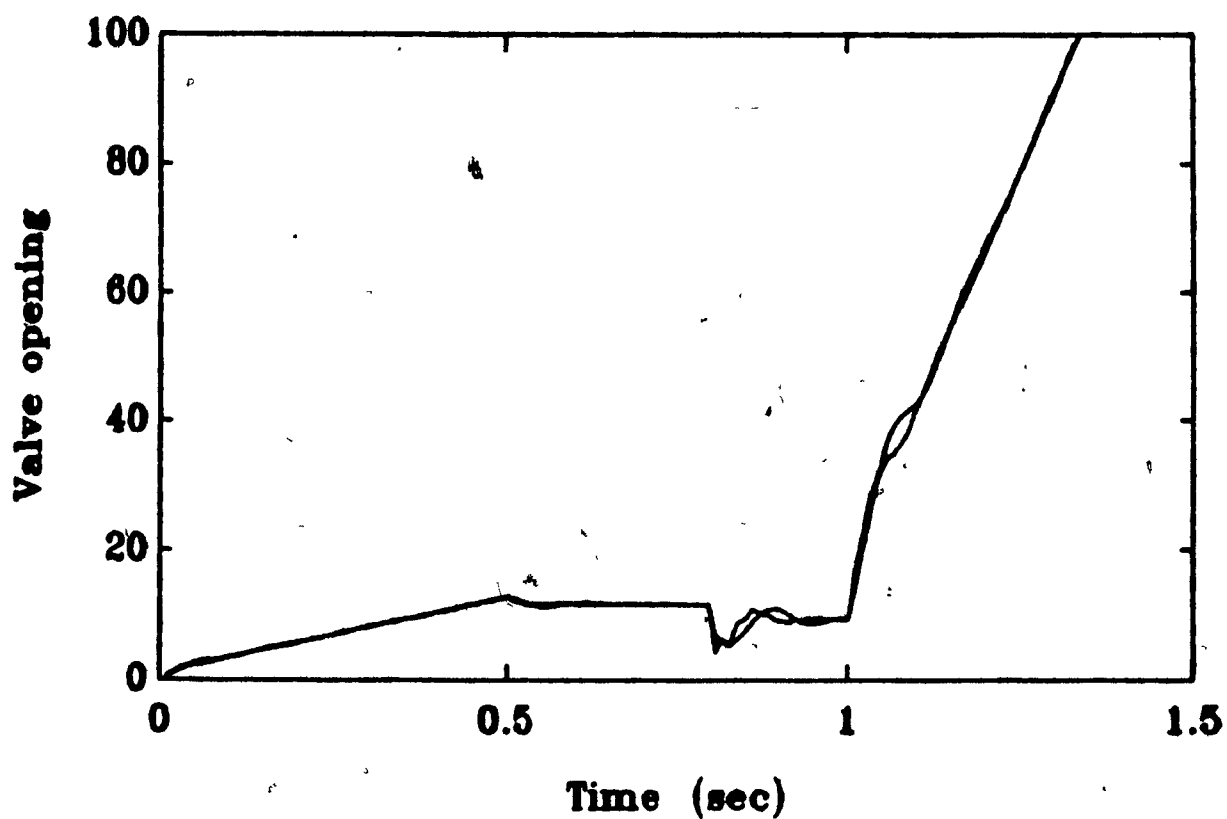
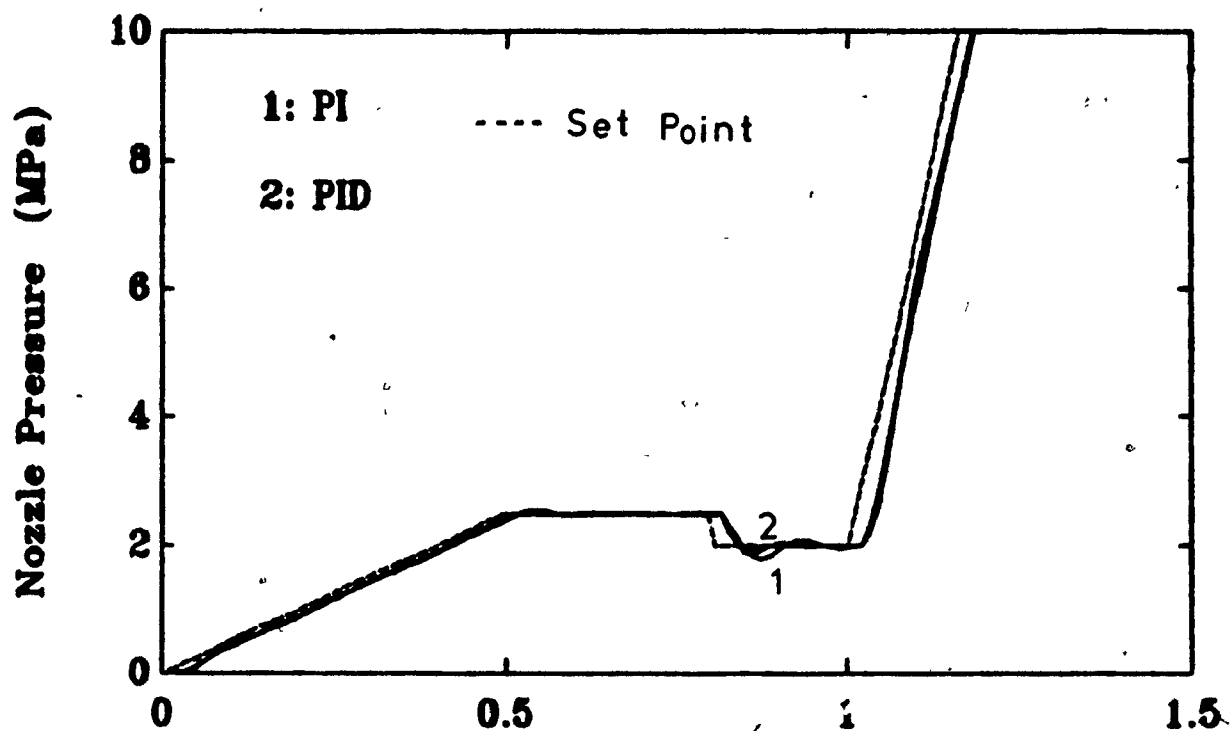


Figure 6.11 Nozzle Pressure Response to a Set-Point Pressure-Time Profile with the PI and PID Controllers.

increase. The profile of Figure 6.11 shows a ramp to a plateau followed by a sudden decrease just prior to the packing phase. The PID controller again performs better than the PI controller, particularly for the sudden changes. Both controllers were not capable of regulating the pressure during the packing stage. This is seen from the large error during this stage. Also it should be noted that the servovalve opening during packing approaches 100% open. Such behavior is not due to a controller defect but rather is symptomatic of demanding a performance of the hydraulic system of the injection molding machine that it is incapable of providing. Obviously, this is a situation to be avoided, but, unless the machine is correctly instrumented, it cannot be detected.

Dahlin's method was applied to the direct control of nozzle pressure. The pulse transfer functions for the nozzle pressure response obtained by Equations 6.18 and 6.22 were substituted in the Dahlin controller given by Equation 6.10 to give the following control laws:

$$(i) \ D(Z) = \frac{M(Z)}{E(Z)} = \frac{b_0 - b_1 Z^{-1}}{1 - a_1 Z^{-1} - a_2 Z^{-2}} \quad (6.44)$$

$$(ii) \ D(Z) = \frac{M(Z)}{E(Z)} = \frac{f_1 Z^{-1} - f_2 Z^{-2} + f_3 Z^{-3}}{h_0 - h_1 Z^{-1} - h_2 Z^{-2} + h_3 Z^{-3}} \quad (6.45)$$

where a_i , b_i , h_i and f_i are the controller parameters in terms of the process model parameters, controller tuning parameter, Λ (L), and the sampling time (T) as given in Table 6.6. The control equations 6.44 and 6.45 were written for different values of Λ and sampling times. The resulting control equations are given in Tables 6.7 and 6.8. The controller was made free of excessive oscillation of the manipulated variable (ringing) by removing poles of magnitude -0.6 or greater [131]. The controller gain was adjusted by incorporating the following compensation factor in the algorithm [131] :

$$\frac{1}{\lim_{Z \rightarrow 1} (1 + P Z^{-1})} \quad (6.46)$$

where P is a ringing pole.

The simulation of nozzle pressure with the Dahlin controller for different values of the tuning parameter (L) with a sampling interval of 5 ms is shown in Figure 6.12. A sampling interval close to the actual process dead time was chosen. The responses of curves 1, 2 and 3 exhibit overshoot because the value of L is much smaller than the process time constant (0.05 s). Curve 1 shows the largest peak overshoot and the lowest damping, and curve 3 shows the smallest peak overshoot and the greatest damping.

TABLE 6.6

Parameters of the Dahlin Controller for
Nozzle Pressure (Equations 6.44 & 6.45)

Parameter	Expression
b_0	$(1 - \exp(-T/L)) / K(1 - \exp(-T/\tau))$
b_1	$b_0 \exp(-T/\tau)$
a_1	$\exp(-T/L)$
a_2	$1 - \exp(-T/L)$
f_1	$1 - a_1$
f_2	$c_1 (1 - a_1)$
f_3	$c_2 (1 - a_1)$
h_0	d_1
h_1	$a_1 d_1 - d_2$
h_2	$d_1 (1 - a_1) - a_1 d_2$
h_3	$d_2 (1 - a_1)$
c_1	$c + d$
c_2	$c d$
d_1	$A(1-c) + B(1-d)$
d_2	$A d(1-c) + B c(1-d)$
A	$K(\tau + D_1) / (\tau - D_1)$
B	$2 K D_1 / (D_1 - \tau)$
c	$\exp(-T/\tau)$
d	$\exp(-T/D_1)$

Table 6.7

Dahlin Controller Equations for Nozzle Pressure Control Loop Using Equation 6.44 with Different Sampling Time, T, and Different Tuning Parameter, L, Used in this Study

T (sec)	L	D(Z)
0.005	0.006	$\frac{0.03 - 0.02 Z^{-1}}{1 - 0.36 Z^{-1} - 0.63 Z^{-2}}$
0.008	0.006	$\frac{0.03 - 0.02 Z^{-1}}{1 - 0.20 Z^{-1} - 0.79 Z^{-2}}$
0.010	0.006	$\frac{0.02 - 0.01 Z^{-1}}{1 - 0.13 Z^{-1} - 0.87 Z^{-2}}$
0.005	0.008	$\frac{0.02 - 0.02 Z^{-1}}{1 - 0.35 Z^{-1} - 0.46 Z^{-2}}$
0.008	0.008	$\frac{0.02 - 0.02 Z^{-1}}{1 - 0.63 Z^{-1} - 0.37 Z^{-2}}$
0.010	0.008	$\frac{0.02 - 0.02 Z^{-1}}{1 - 0.29 Z^{-1} - 0.71 Z^{-2}}$
0.005	0.010	$\frac{0.02 - 0.02 Z^{-1}}{1 - 0.61 Z^{-1} - 0.39 Z^{-2}}$
0.008	0.010	$\frac{0.02 - 0.02 Z^{-1}}{1 - 0.45 Z^{-1} - 0.55 Z^{-2}}$
0.010	0.010	$\frac{0.02 - 0.01 Z^{-1}}{1 - 0.37 Z^{-1} - 0.63 Z^{-2}}$

Table 6.8

Dahlin Controller Equations for Nozzle Pressure Control
 Loop Using Equation 6.45 with Different Sampling Time
 T, and Different Tuning Parameter L, Used in this Study

T (s)	L	D(Z)
0.005	0.006	$\frac{0.63 Z^{-1} - 0.66 Z^{-2} + 0.08 Z^{-3}}{0.09 + 14.37 Z^{-1} - 14.47 Z^{-2} - 9.11 Z^{-3}}$
0.008	0.006	$\frac{0.80 Z^{-1} - 0.71 Z^{-2} + 0.03 Z^{-3}}{12.41 + 14.28 Z^{-1} - 26.69 Z^{-2} - 13.40 Z^{-3}}$
0.010	0.006	$\frac{0.86 Z^{-1} - 0.72 Z^{-2} + 0.01 Z^{-3}}{20.22 + 14.38 Z^{-1} - 34.61 Z^{-2} - 14.80 Z^{-3}}$
0.005	0.008	$\frac{0.46 Z^{-1} - 0.483 Z^{-2} + 0.07 Z^{-3}}{0.09 + 14.36 Z^{-1} - 14.45 Z^{-2} - 6.69 Z^{-3}}$
0.008	0.008	$\frac{0.63 Z^{-1} - 0.56 Z^{-2} + 0.02 Z^{-3}}{12.41 + 12.22 Z^{-1} - 24.63 Z^{-2} - 10.61 Z^{-3}}$
0.010	0.008	$\frac{0.71 Z^{-1} - 0.59 Z^{-2} + 0.01 Z^{-3}}{20.22 + 11.32 Z^{-1} - 31.55 Z^{-2} - 12.21 Z^{-3}}$
0.005	0.010	$\frac{0.39 Z^{-1} - 0.41 Z^{-2} + 0.05 Z^{-3}}{0.09 + 14.35 Z^{-1} - 14.44 Z^{-2} - 5.67 Z^{-3}}$
0.008	0.010	$\frac{0.55 Z^{-1} - 0.492 Z^{-2} + 0.02 Z^{-3}}{12.41 + 11.21 Z^{-1} - 23.62 Z^{-2} - 9.24 Z^{-3}}$
0.010	0.010	$\frac{0.632 Z^{-1} - 0.53 Z^{-2} + 0.01 Z^{-3}}{20.22 + 9.68 Z^{-1} - 29.90 Z^{-2} - 10.82 Z^{-3}}$

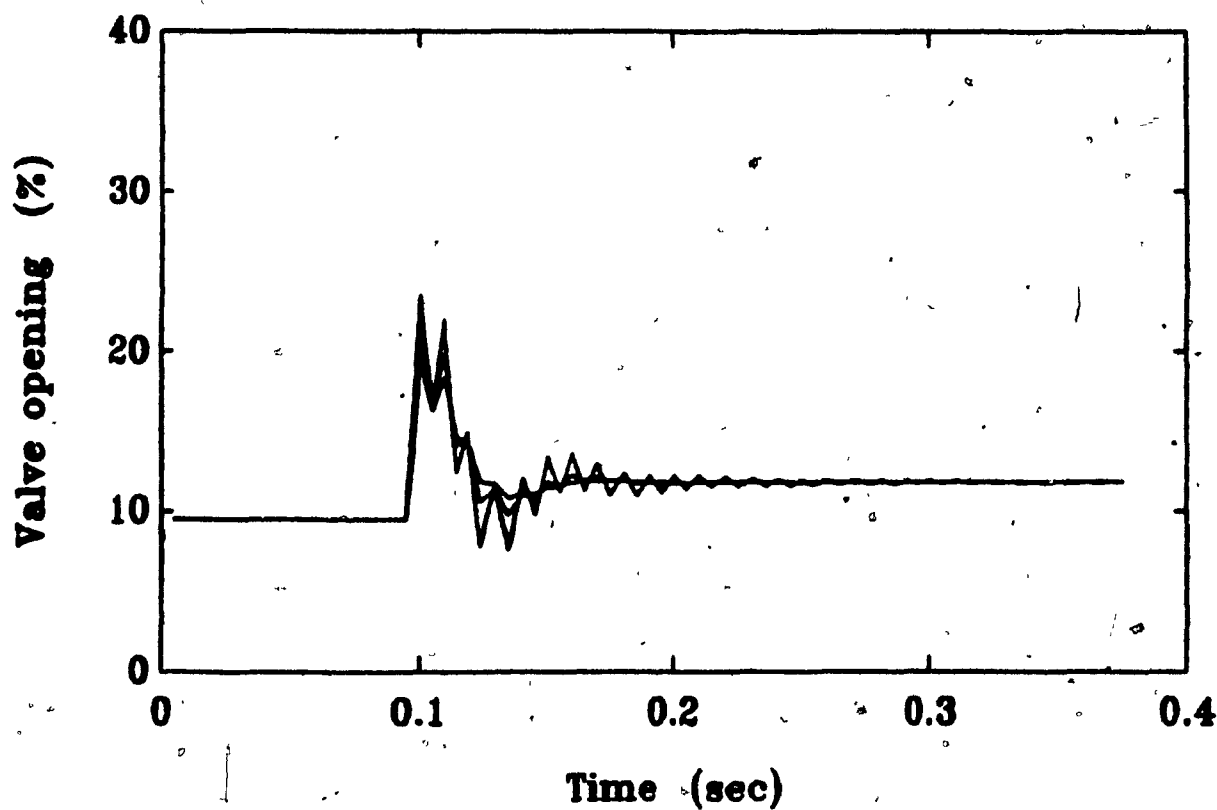
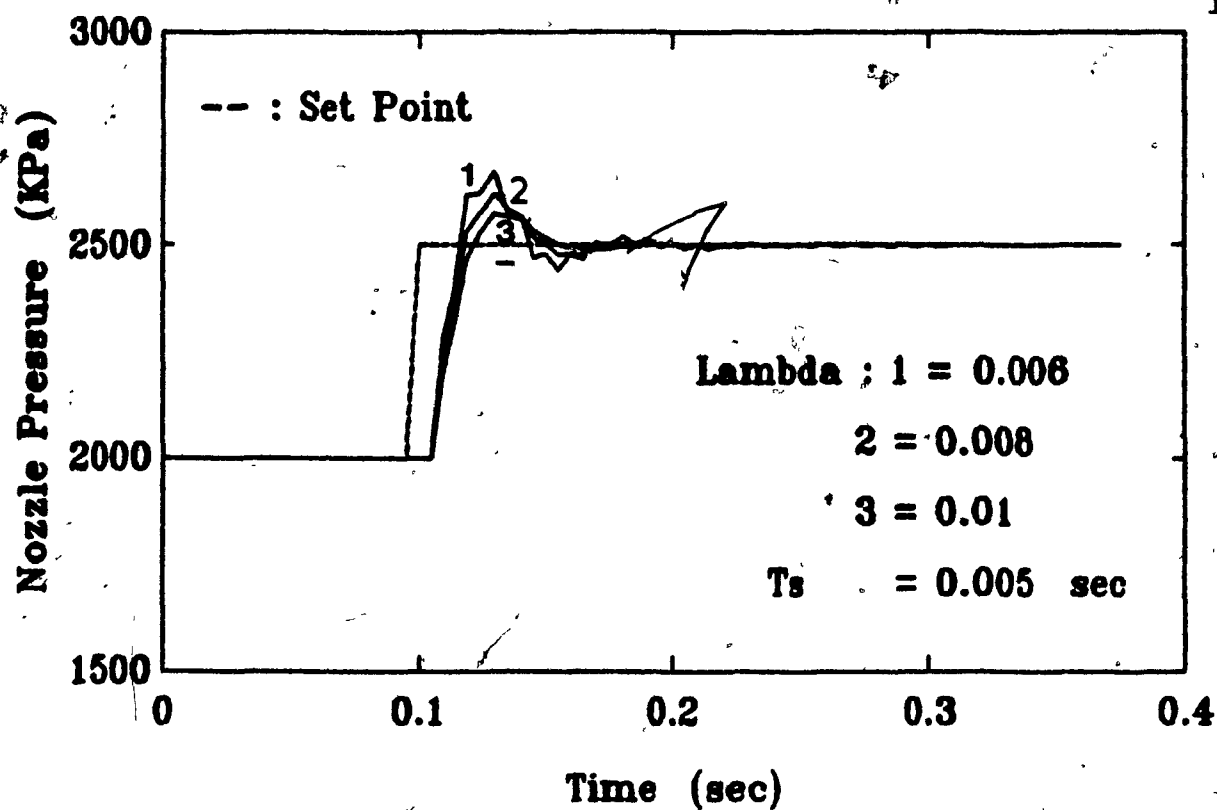


Figure 6.12 Control of Nozzle Pressure Using Dahlin Controller with Different Tuning Parameter, Λ .

The corresponding performance indices are given in Table 6.9, which shows that the ISE and IAE decrease with increasing L . The ITAE shows a minimum for $L = 0.01$. Simulation runs were then performed with $L = 0.01$, for different sampling intervals. The results are shown in Figure 6.13. Curve 3 showed the highest peak overshoot and exhibited some ringing. The ISE, IAE and ITAE, as shown in Table 6.10, increase with the increase in sampling time for the range of sampling times used. Based on these results, the values for L and T were chosen as 0.01 and 0.005 sec., respectively.

Figure 6.14 shows a comparison of the nozzle pressure responses with Dahlin and PID controllers. Both controllers give almost the same rise time, but the Dahlin controller gives a larger overshoot. The typical response of Dahlin controller as a first order plus delay response can be achieved by increasing the tuning parameter L . However, this will cause a slower response. Hence, overshoot caused by a smaller L is tolerated to achieve a fast response necessary for the control of nozzle pressure.

As a conclusion, the following controller settings were chosen for nozzle pressure control :

PID controller :

$$\begin{aligned} K_C &= 0.006 \\ \tau_I &= 0.052 \\ \tau_D &= 0.007 \\ T &= 0.005 \end{aligned}$$

Dahlin controller:

$$\begin{aligned} L &= 0.01 \\ T &= 0.005 \end{aligned}$$

TABLE 6.9

Performance Indices of Nozzle Pressure Control Simulation
Using Dahlin Controller with Different Tuning Parameter, L
and Sampling Interval, $T = 0.005$ sec

L	ISE	IAE	ITAE
0.006	4.41×10^3	13.17	0.268
0.008	4.38×10^3	12.05	0.183
0.010	4.47×10^3	11.76	0.159

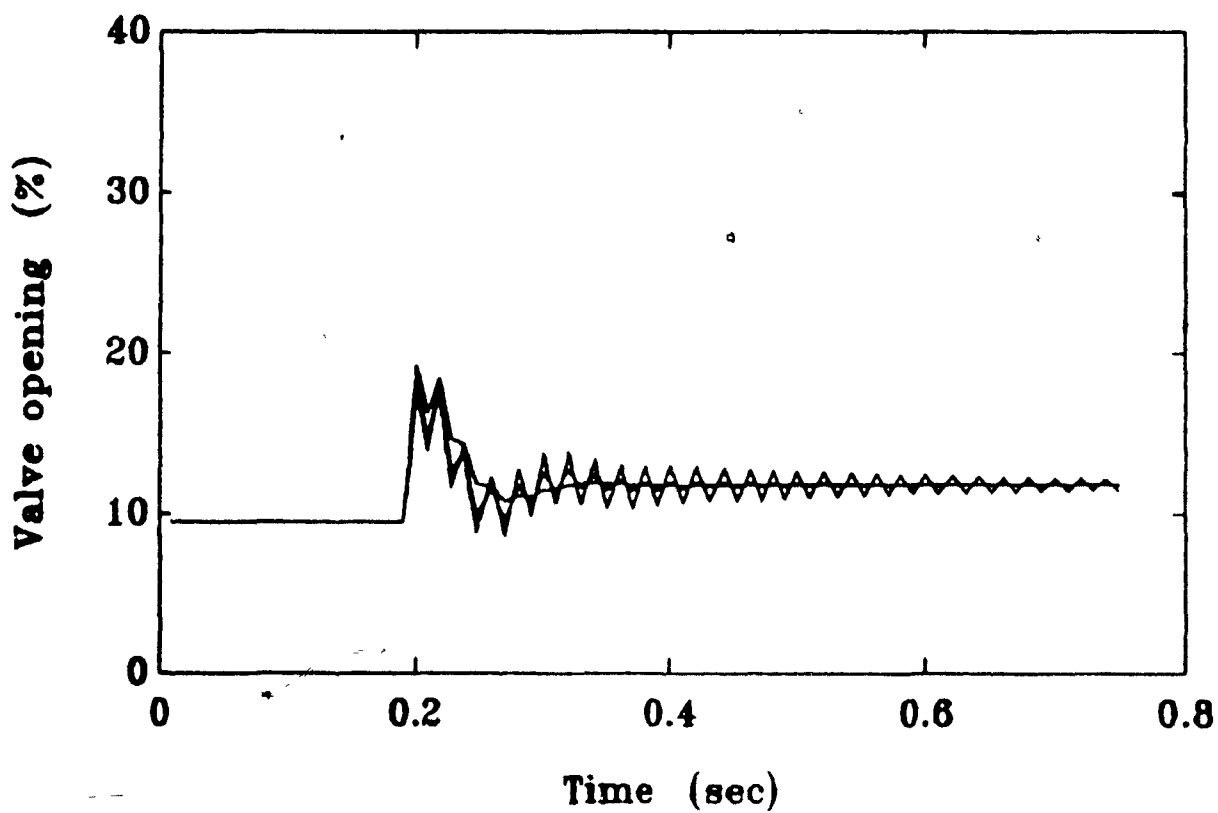
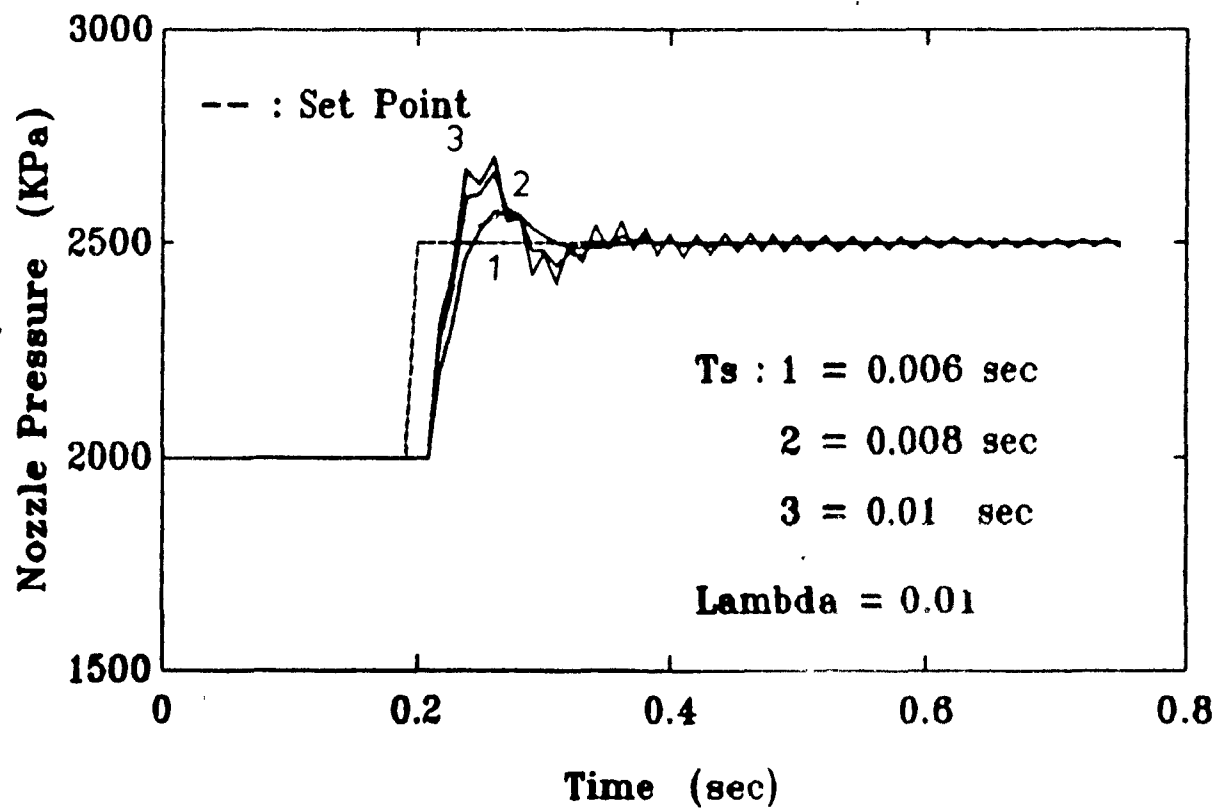


Figure 6.13 Control of Nozzle Pressure Using Dahlin Controller with Different Sampling Intervals.

TABLE 6.10

Performance Indices of Nozzle Pressure Control Simulation
Using Dahlin' Controller with Different Sampling Interval, T
and Tuning Parameter, L = 0.01

T (sec)	ISE	IAE	ITAE
0.005	4.47×10^3	11.76	0.159
0.008	7.03×10^3	20.61	0.616
0.010	9.19×10^3	33.39	3.090

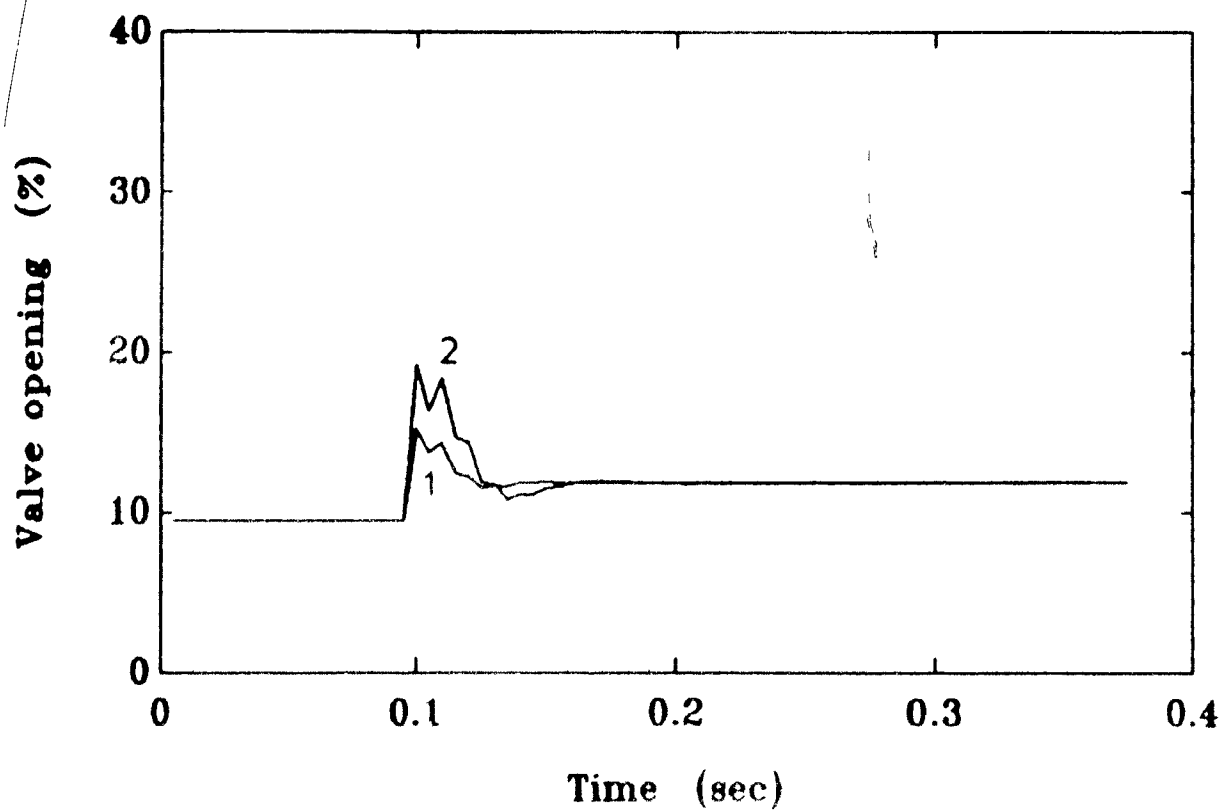
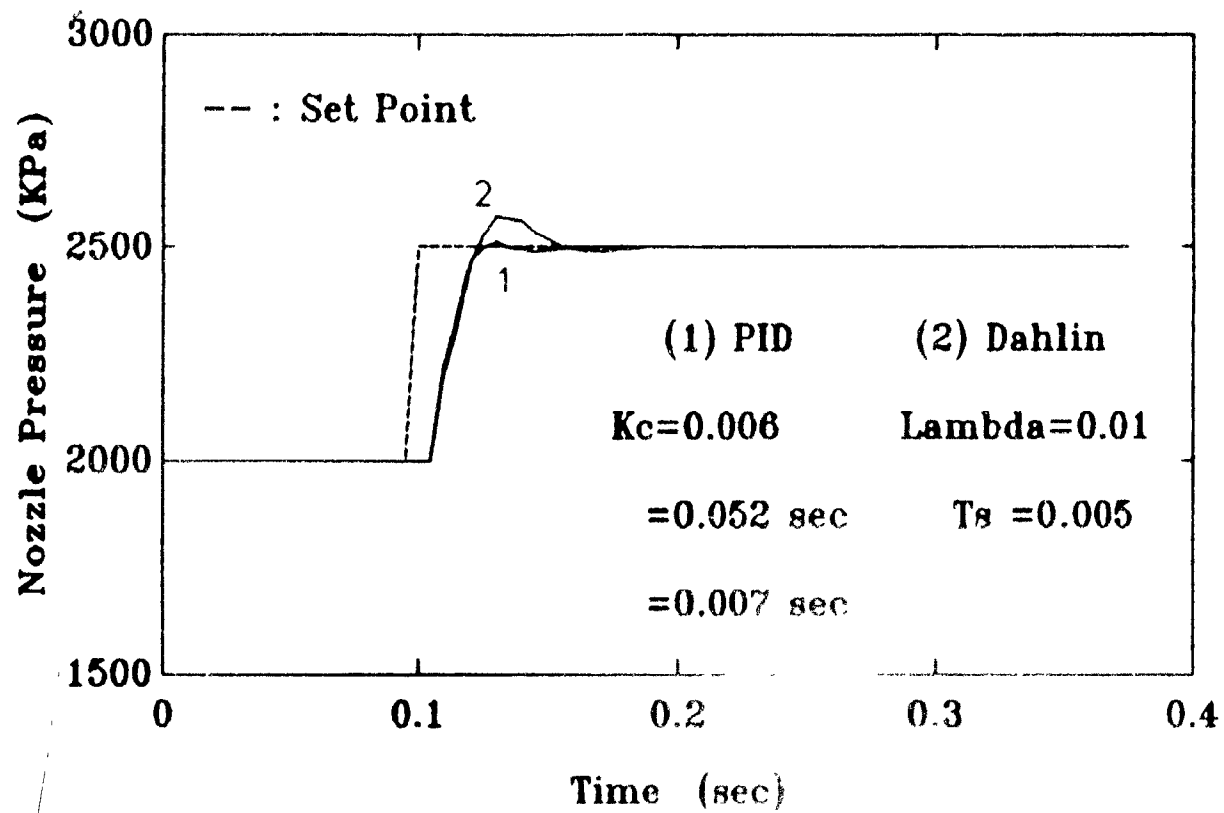


Figure 6.14 Control of Nozzle Pressure Using Dahlin and PID Controllers.

6.4.3 Cavity Pressure Control Loop Simulation

Direct cavity pressure control was simulated using the cavity gate pressure model with PI and PID controllers. The discrete models obtained earlier for cavity gate pressure, with two approximations for the dead time are rewritten below :

$$(i) \quad \frac{P_C(Z)}{M(Z)} = \frac{b_1 Z^{-1} - b_2 Z^{-2} - b_3 Z^{-3}}{1 - a_1 Z^{-1} + a_2 Z^{-2}} \quad (6.47)$$

$$(ii) \quad \frac{P_C(Z)}{M(Z)} = \frac{f_1 Z^{-1} - f_2 Z^{-2} + f_3 Z^{-3}}{1 - h_1 Z^{-1} + h_2 Z^{-2} - h_3 Z^{-3}} \quad (6.48)$$

The model parameters, a_1 , b_1 , f_i and h_1 are as defined earlier in section 6.2.3 in terms of the process gain, time constant, dead time and sampling interval. The numerical values of these parameters are calculated using the values for the process parameters given in Table 6.1 and various sampling intervals. Thus, the above models can be written as in Table 6.11. The discrete PI and PID controllers given by Equations 6.3 and 6.34 have been employed. Initial parameters for the controllers calculated by the ITAE are given in Table 6.12.

TABLE 6.11
Discrete Models for the Cavity Pressure Response
(Equations 6.47 and 6.48)

Sampling Time, sec	Discrete Model	
0.005	Model (I)	$P_C(Z) = 0.07 Z^{-1} + 0.08 Z^{-2} + 0.15 Z^{-3}$
		$M(Z) = 1 - 1.95 Z^{-1} + 0.95 Z^{-2}$
	Model (III)	$P_C(Z) = 0.03 Z^{-1} + 0.04 Z^{-2} + 0.09 Z^{-3}$
		$M(Z) = 1 - 2.93 Z^{-1} + 1.86 Z^{-2} - 0.93 Z^{-3}$
0.010	Model (I)	$P_C(Z) = 0.14 Z^{-1} + 0.14 Z^{-2} + 0.30 Z^{-3}$
		$M(Z) = 1 - 1.91 Z^{-1} + 0.91 Z^{-2}$
	Model (III)	$P_C(Z) = -0.15 Z^{-1} + 0.45 Z^{-2} + 0.18 Z^{-3}$
		$M(Z) = 1 - 2.89 Z^{-1} + 1.78 Z^{-2} - 0.29 Z^{-3}$

TABLE 6.12

Initial Controller Parameter Values Calculated by ITAE
for the Cavity Pressure Control Loop

Controller	K_C	T_I	T_D
PI	1.141	0.129	-
PID	1.653	0.167	0.006

Parameters for Discrete P, PI and PID Controllers
for the Cavity Pressure Control Loop

Controller	Sampling Time, sec	a_0	a_1	a_2
PI	0.005	1.185	-1.141	-
	0.010	1.229	-1.141	-
PID	0.005	3.587	-5.423	1.885
	0.010	2.695	-3.538	0.942

The physical nature of the cavity gate pressure during filling and its dynamic model (Equation 5.4) indicate that a realistic set point profile for cavity gate pressure should incorporate a ramping component. Figure 6.15 shows the response of cavity gate pressure under a PI controller to set point profile consisting of a step change followed by a ramp. As it can be seen, the response of the controller is well fast with short rise and settling time. The response of cavity gate pressure to the realistic set point profile under PID control is shown in Figure 6.16.

The optimum settings of the PI and PID controllers for the cavity gate pressure control loop were obtained by minimizing the ITAE criterion using the Nelder-Mead (N-M) optimization routine [149]. The cavity gate pressure model given by Equation (5.4) was used in the optimization. The optimum parameters were as follows:

PI controller: $K_p = 0.063$, $\tau_i = 0.070$

PID controller: $K_p = 0.029$, $\tau_i = 0.063$, $\tau_D = 0.009$

Figure 6.17 shows that both the N-M) optimum PI and PID controllers give equally good performance. Therefore, the simpler PI controller is the stronger candidate for cavity pressure control.

The discrete equivalent model obtained for cavity pressure based on the Padé approximation for the dead time (Equation 6.48), was employed in conjunction with the

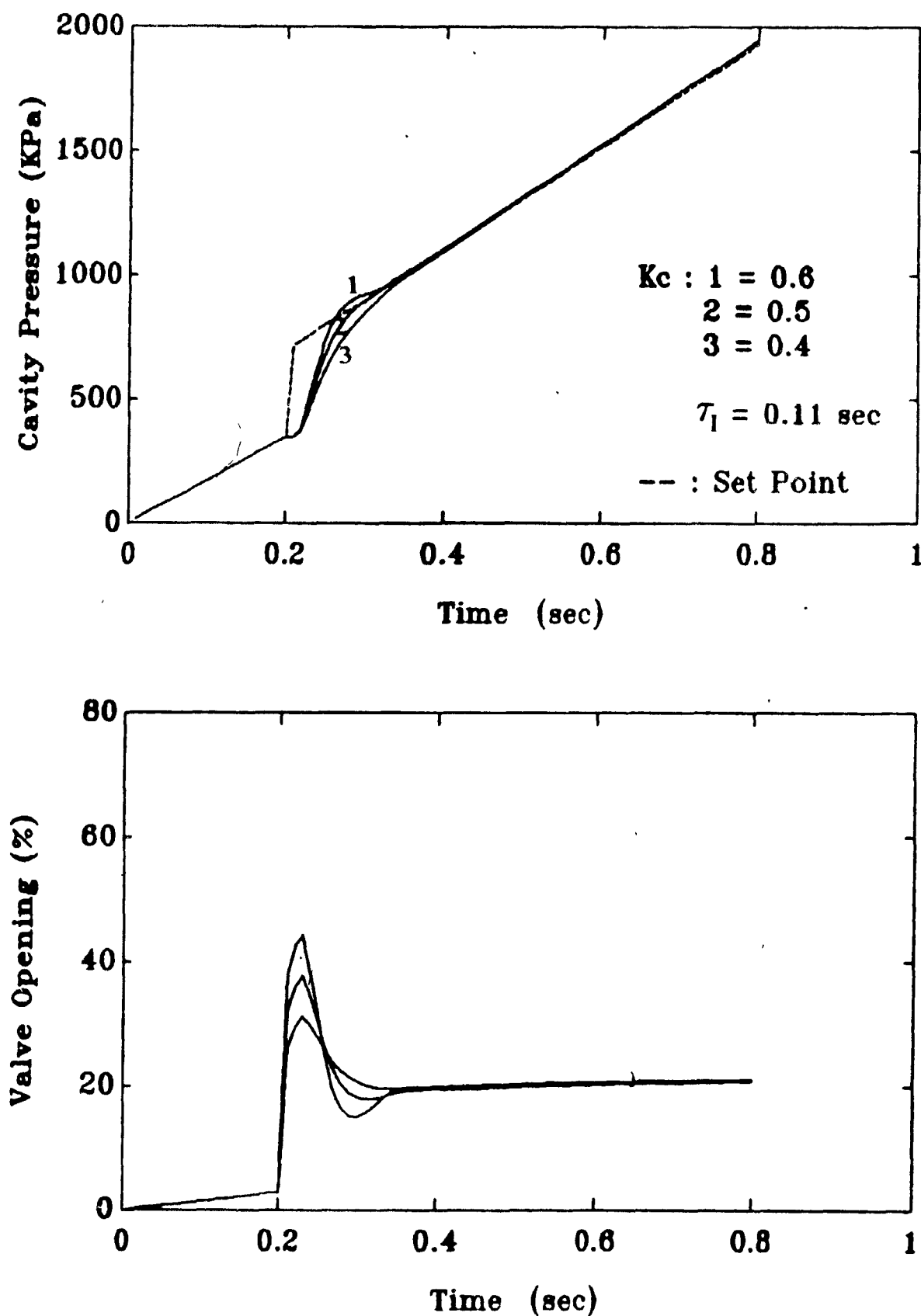


Figure 6.15 Cavity Gate Pressure Response to a Step Change Plus Ramp in the Set-Point with a PI Controller.

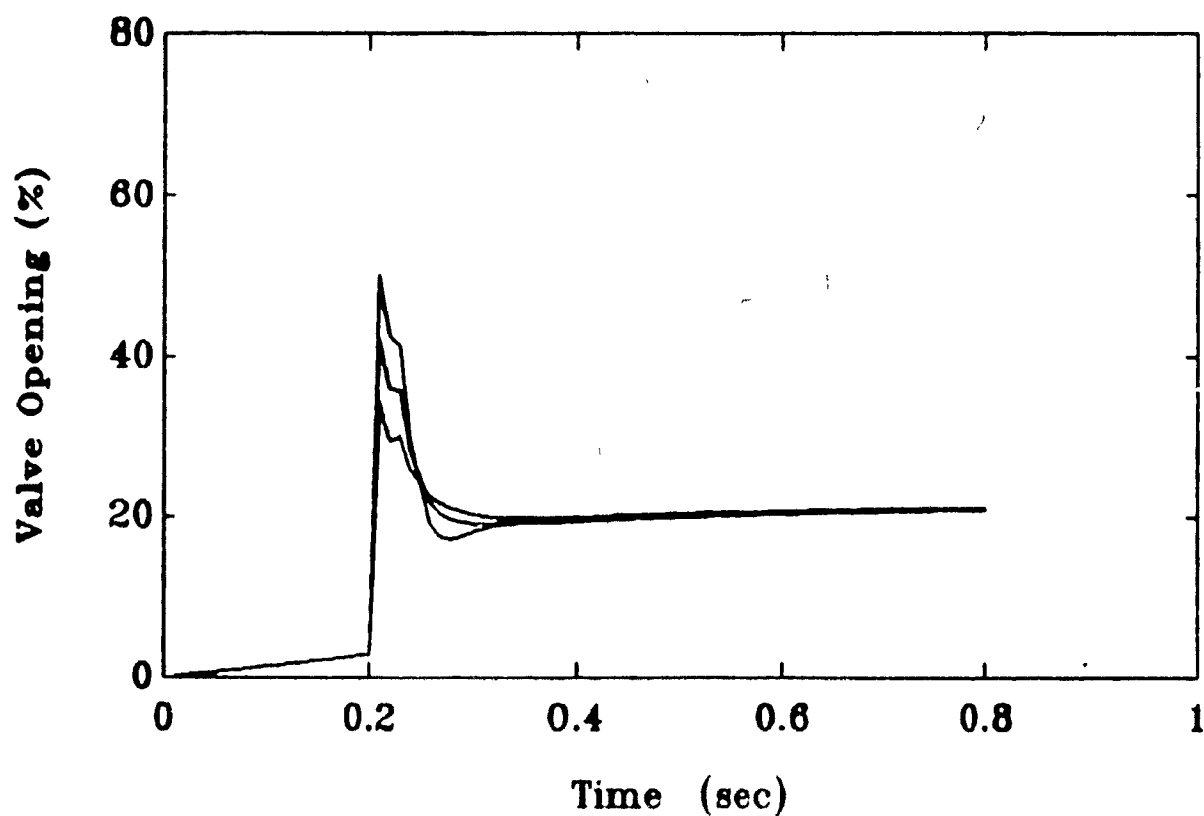
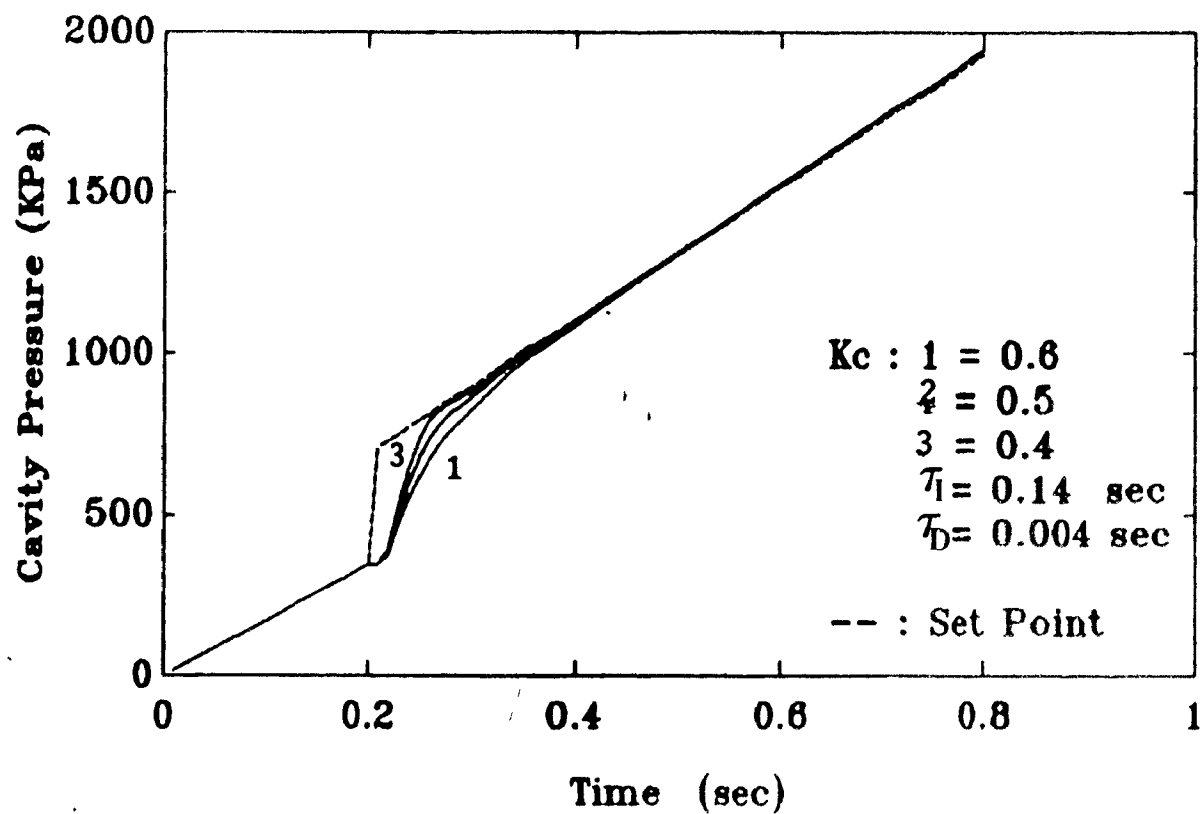


Figure 6.16 Cavity Gate Pressure Response to a Step Change Plus Ramp in the Set-Point with a PID Controller.

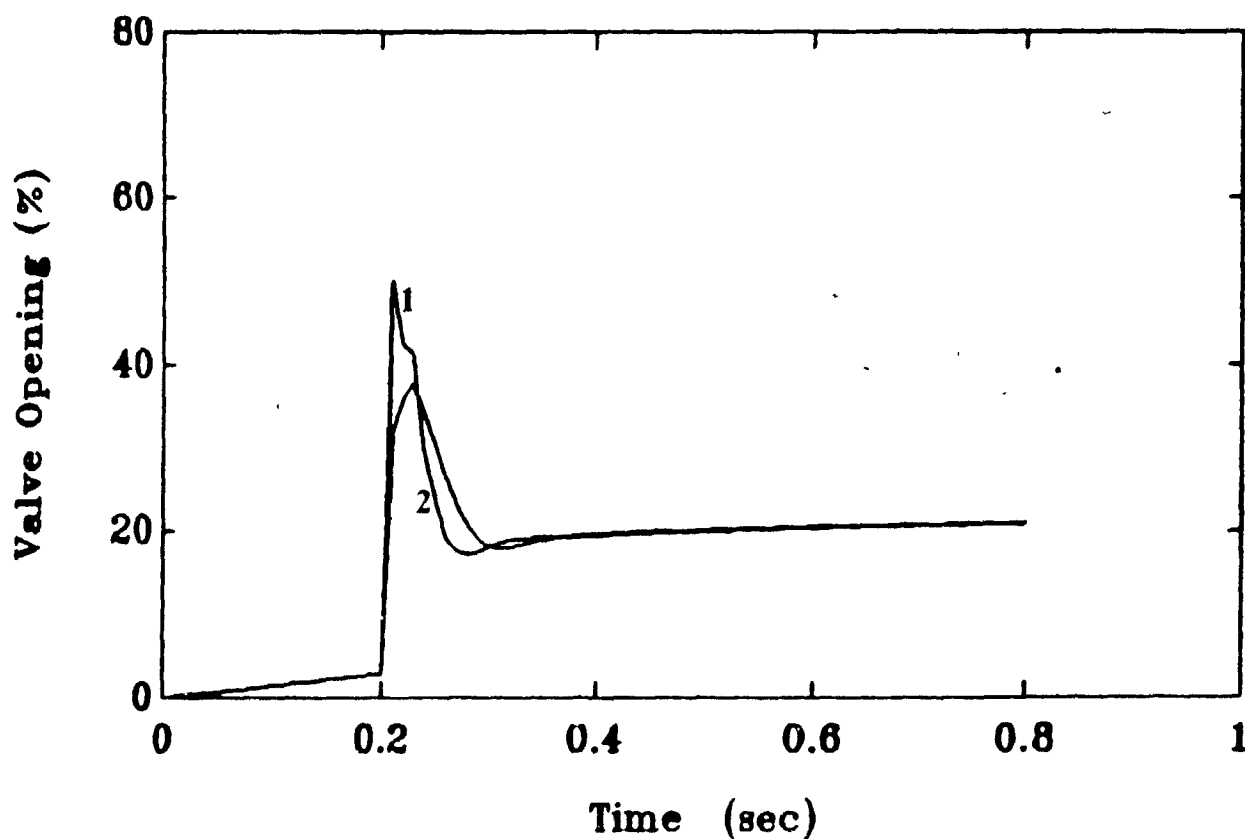
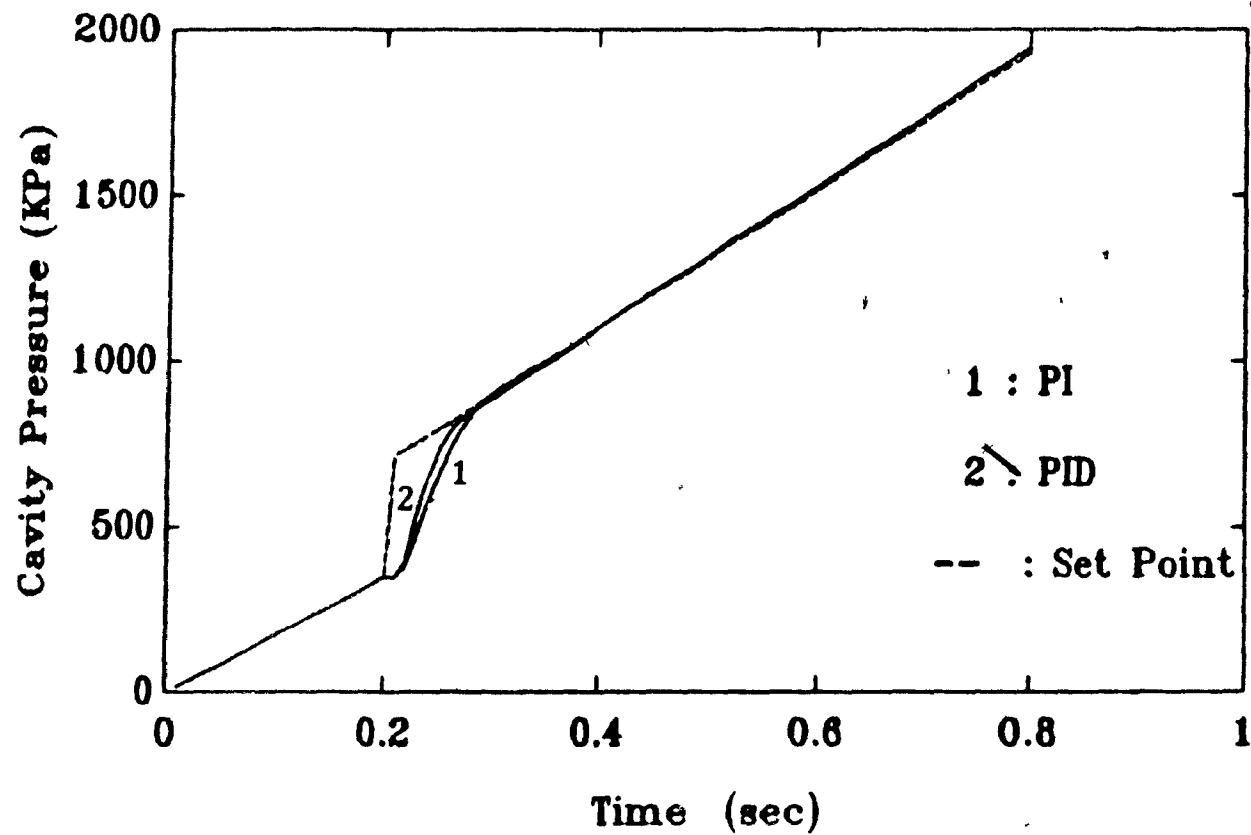


Figure 6.17 Cavity Gate Pressure Response to a Step Change Plus Ramp in the Set-Point with PI and PID Controllers.

chosen PI and PID controllers. The results, as shown in Figure 6.18, suggest that good performance is obtained by equating the dead time to one sampling interval. Thus, the use of the simpler discrete dynamic model (Equation 6.47) in the cavity pressure control loop is justified.

6.4.4 Summary

The results of control loop simulations can be summarized as follows:

- (a) Hydraulic pressure was best controlled by the PI controller. Little improvement was obtained with the PID controller, but the PID controller was sensitive to changes in the parameters.
- (b) In the nozzle pressure control loop, PID showed some advantage over the PI controller.
- (c) Cavity pressure was well controlled by PI and PID controllers. Good control performance was achieved using the discrete models obtained by the two approximations for the dead time. The simpler one, which approximates the dead time by one sampling interval, was chosen for control experiments.

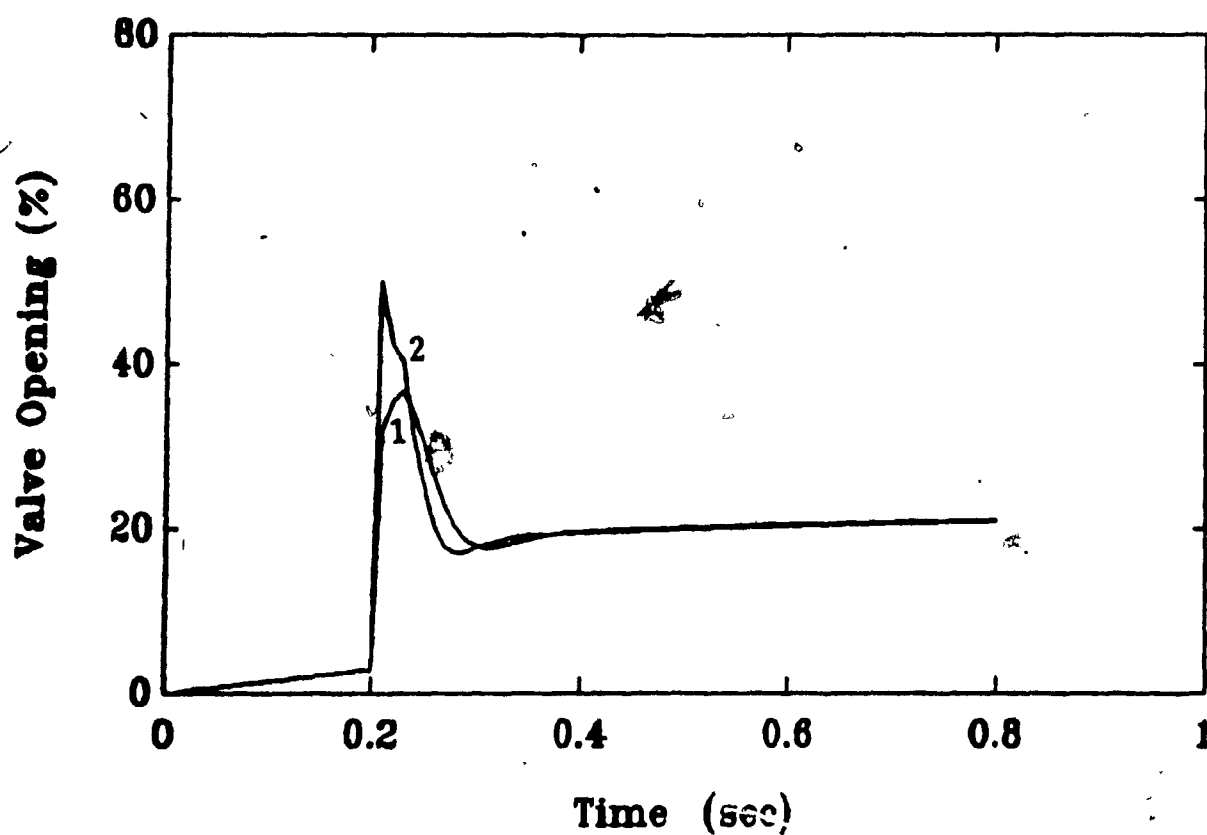
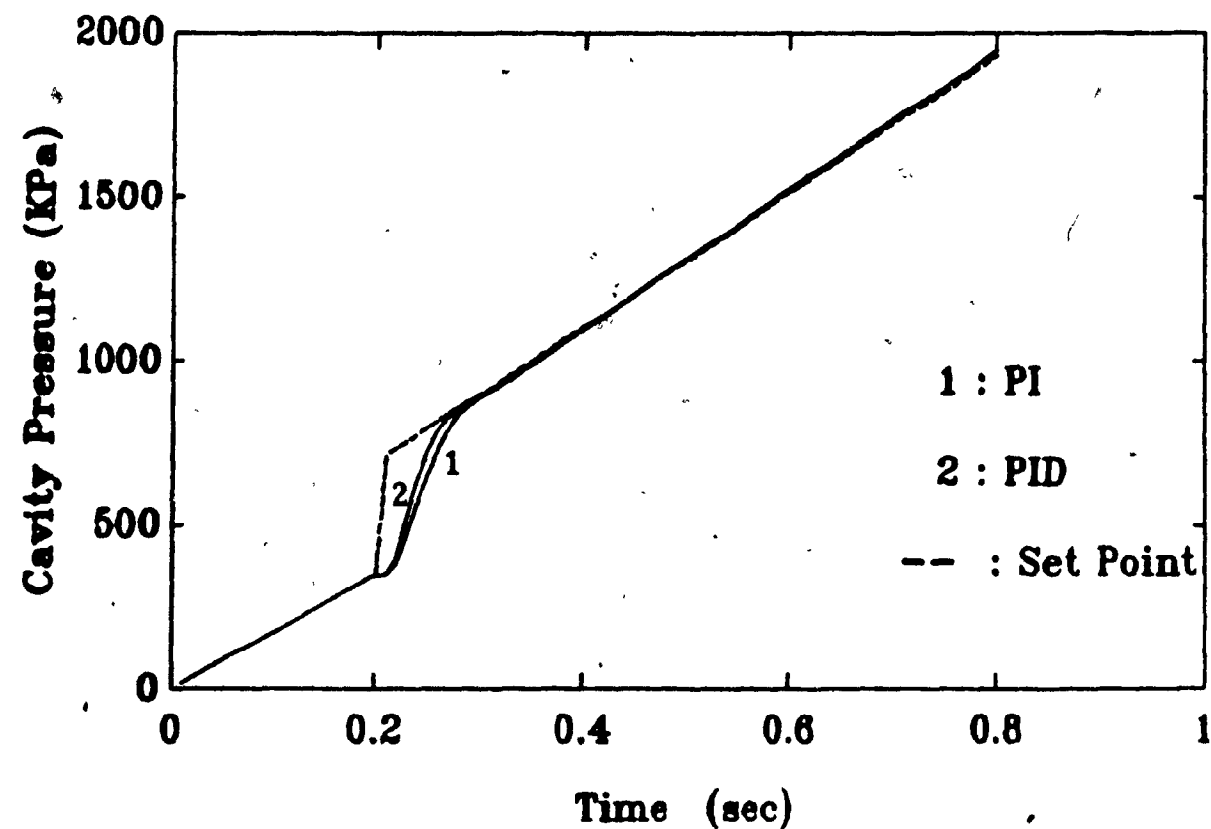


Figure 6.18 Cavity Gate Pressure Response to a Step Change Plus Ramp in the Set-Point with PI and PID Controllers Using Pade Approximation for the Dead Time.

6.5 Filling Stage Control Experiments

The results of the simulation study presented in the previous section indicated the feasibility of accurate control of the hydraulic, nozzle, and cavity gate pressures during the filling stage. The objective of the part of the study covered in this section was to perform a series of control experiments using PI, PID and Dahlin controllers to verify the simulation results and to demonstrate experimentally the feasibility of pressure control during the filling stage of the injection molding cycle. Due to the fact that hydraulic pressure is remote from the cavity, it is preferable to control the nozzle and / or cavity pressure since they have a more direct effect on the situation in the cavity. Also, both nozzle and cavity pressures relate directly to the polymer melt, which is of primary interest.

Closed loop control experiments for the nozzle and cavity gate pressures were carried out using the injection molding machine and the associated microcomputer system described in Chapter 4. The control equations for the PI, PID and Dahlin controllers with the optimum tuned parameters obtained in the simulation section were scaled for implementation on the Z-80 based microcomputer for 16-bit arithmetic. The following experiments were performed :

- (a) Control of the nozzle pressure using PI, PID and Dahlin controllers,
- (b) Control of cavity gate pressure using PI and PID controllers.

6.5.1 Experimental Control of Nozzle Pressure

Based on the results of nozzle pressure control loop simulation, the following controllers were chosen for nozzle pressure control experiments :

PI controller : $K_C = 0.005$
 $\tau_I = 0.048$

$$m(k) = m(k-1) + 0.006 e(k) - 0.005 e(k-1) \quad (6.49)$$

PID controller : $K_C = 0.006$
 $\tau_I = 0.052$
 $\tau_D = 0.007$

$$m(k) = m(k-1) + 0.084 e(k) - 0.11 e(k-1) + 0.03 e(k-2) \quad (6.50)$$

Dahlin controller

$$L = 0.01$$

$$T = 0.005$$

$$m(k) = a_1 m(k-1) + a_2 m(k-2) + b_0 e(k) - b_1 e(k-1) \quad (6.51)$$

The responses of nozzle pressure using PI, PID, and Dahlin controllers are shown in Figures 6.19 - 6.21. The set-point profile was chosen from previous open loop experiments. The three responses have a large initial overshoot. The large overshoot is attributed to leakage through the servovalve, even when it is fully closed. Monitoring the ram movement showed forward movement for a fully closed valve supporting the leakage hypothesis. Clearly, the response was very well controlled after the initial overshoot. The Dahlin controller suffers some ringing as shown by the valve opening plot of Figure 6.21.

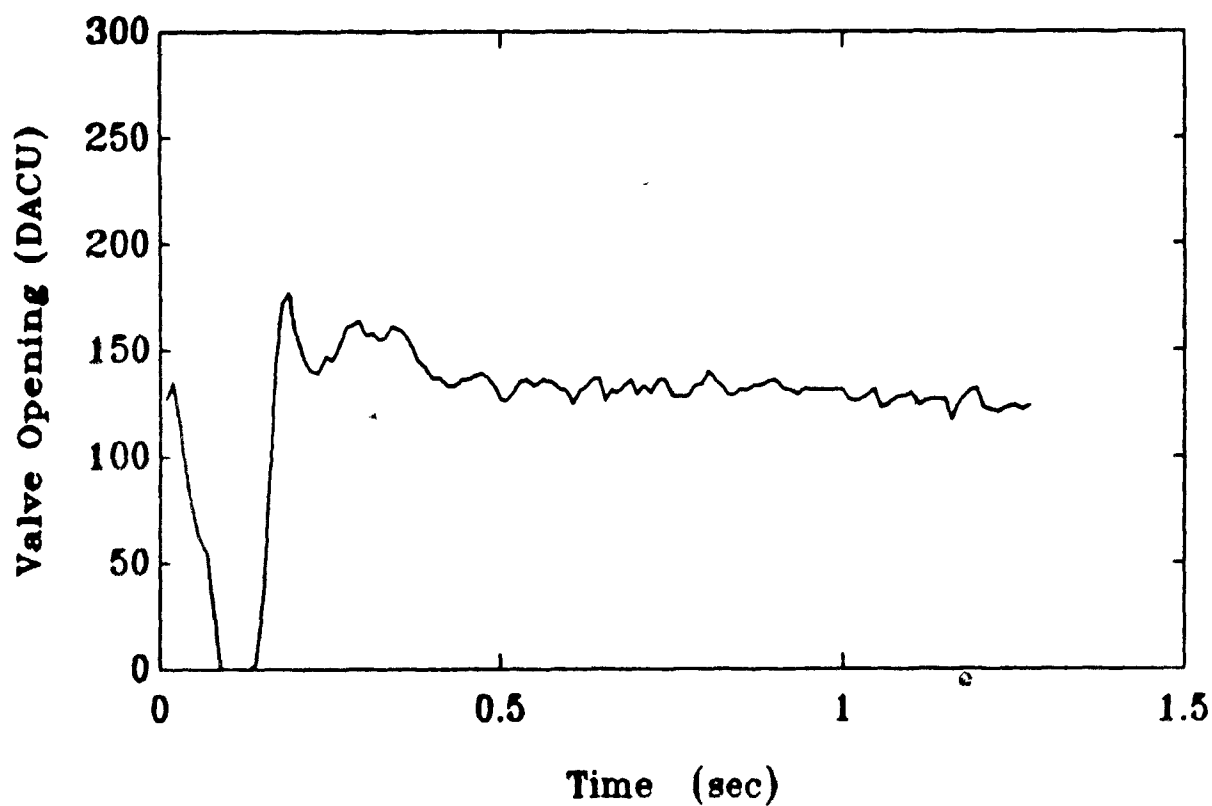
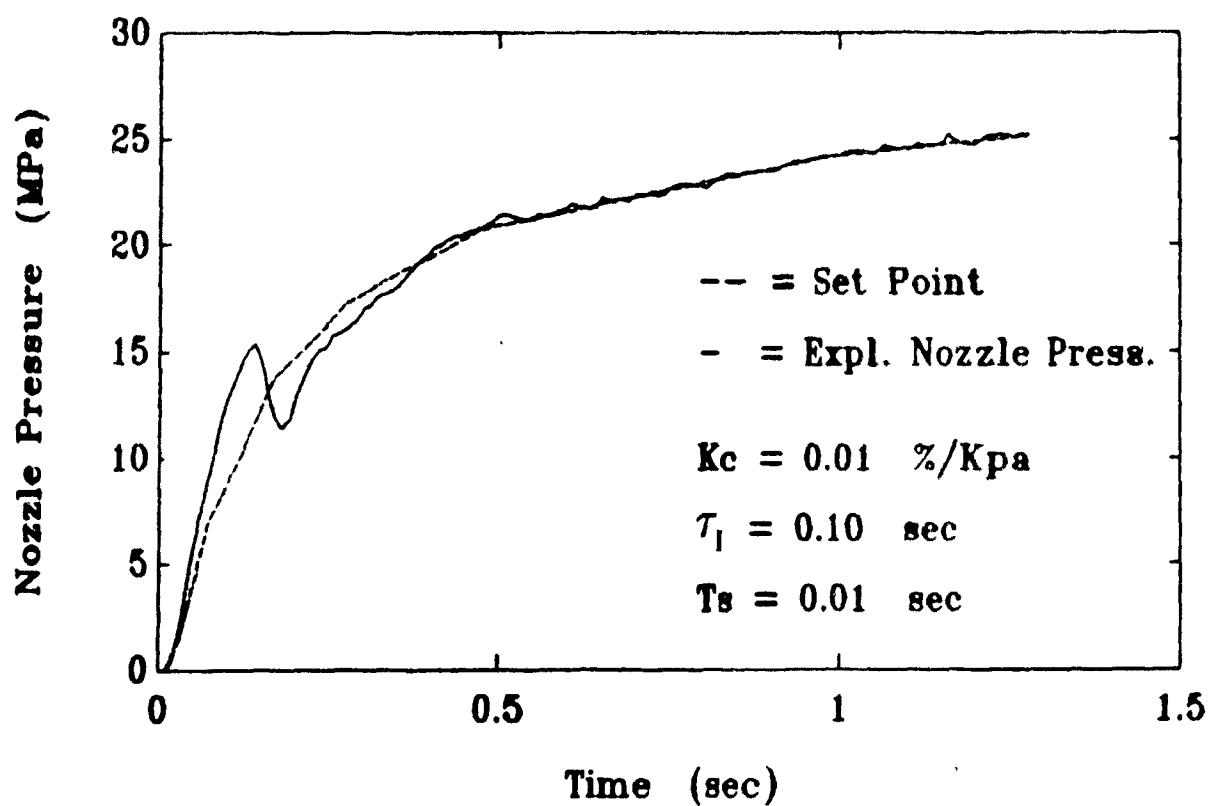


Figure 6.19 Experimental Nozzle Pressure Control Using PI Controller.

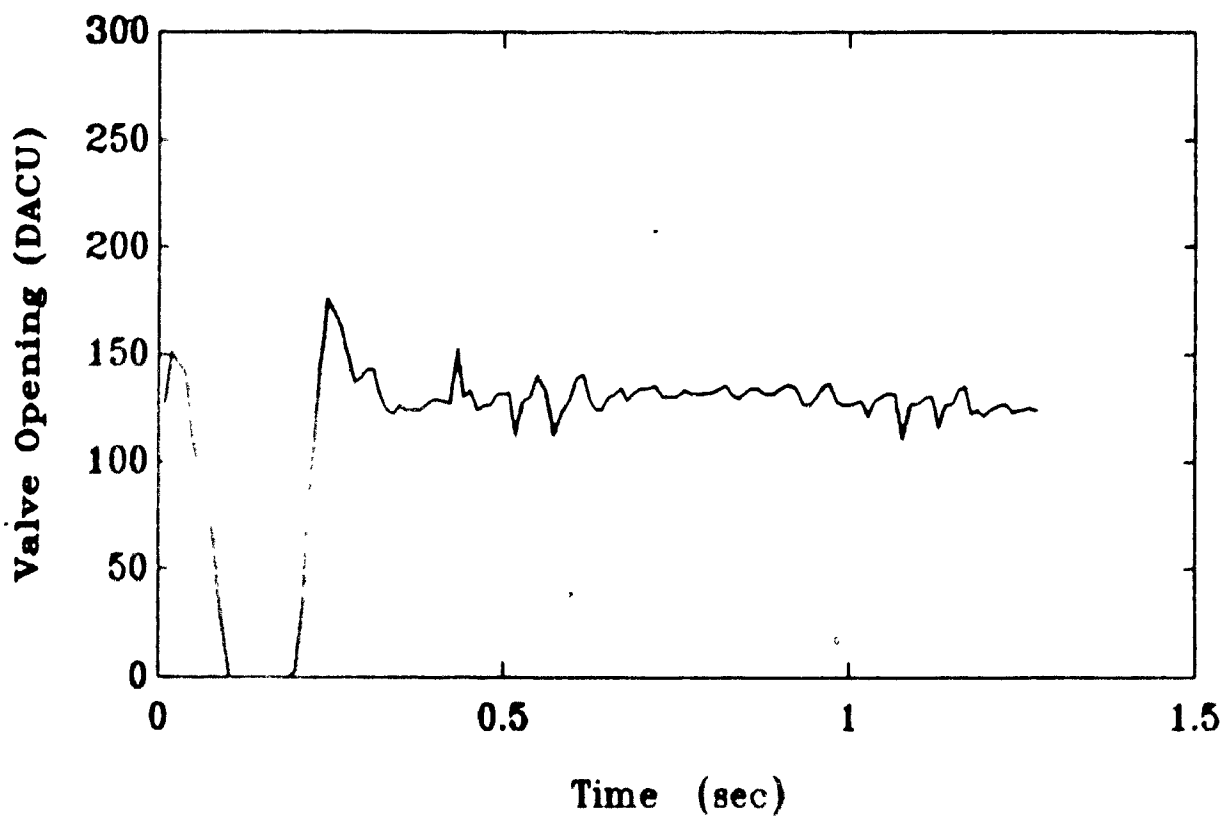
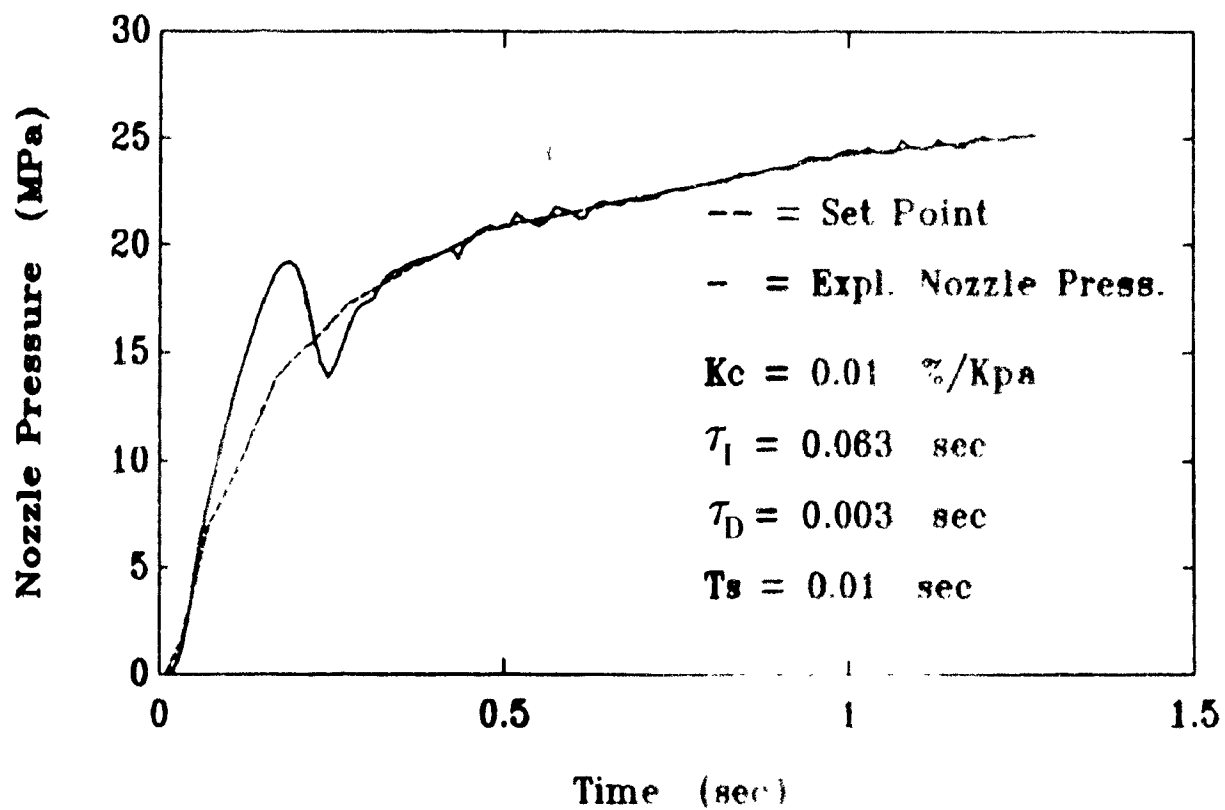


Figure 6.20 Experimental Nozzle Pressure Control Using PID Controller.

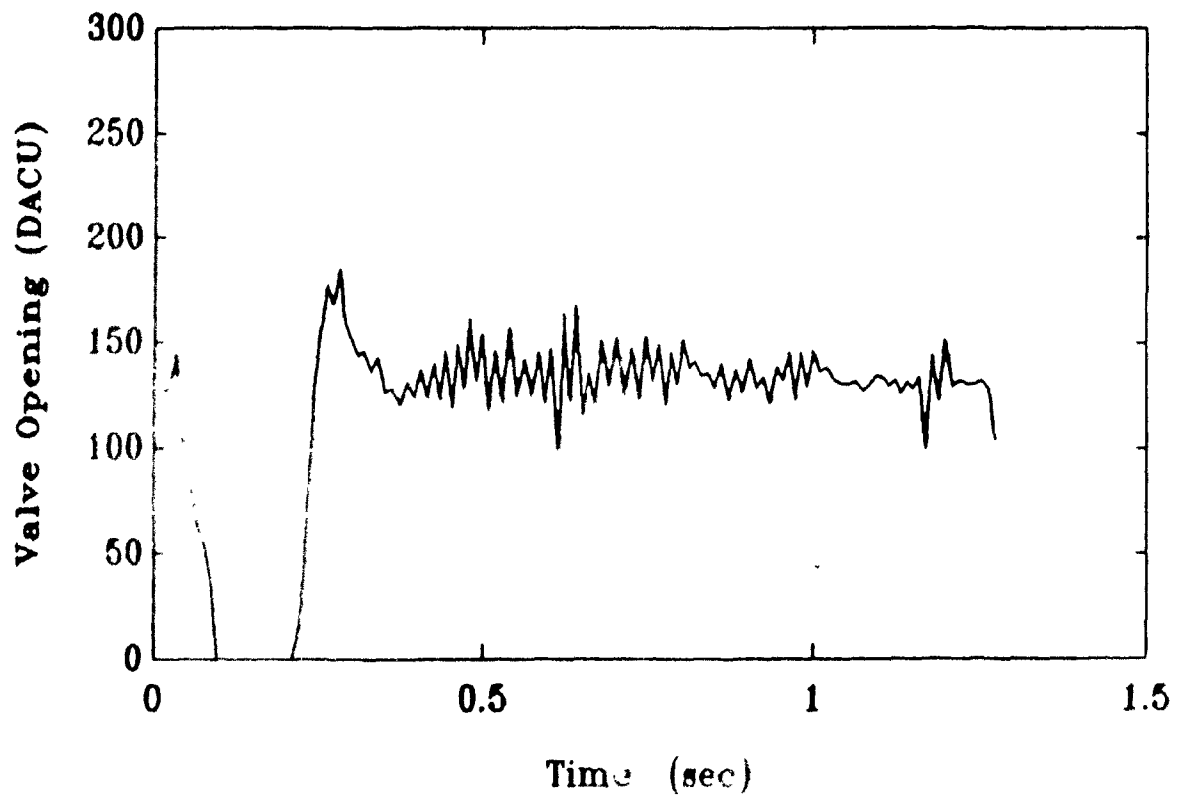
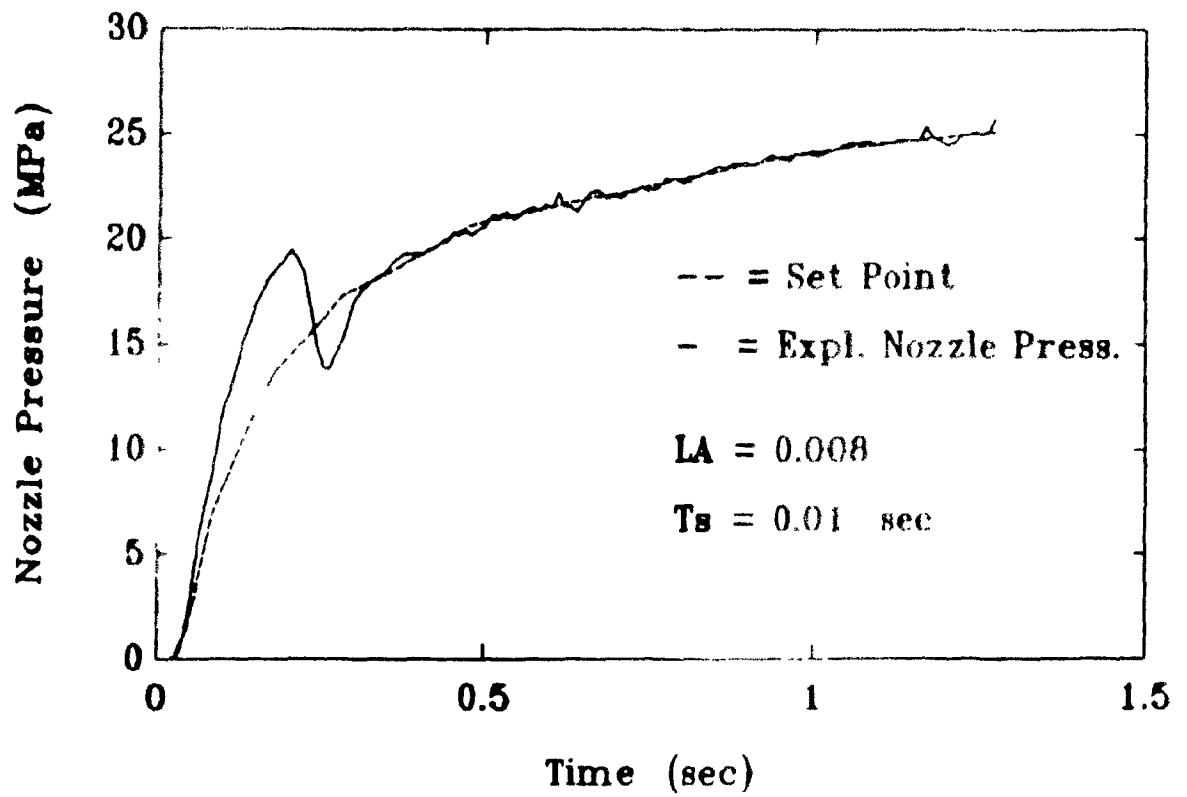


Figure 6.21 Experimental Nozzle Pressure Control Using Dahlin Controller.

6.5.2 Experimental Control of Cavity Pressure

The PI and PID algorithms were applied for direct control of the cavity pressure. The controller parameters and the equations obtained by the simulation are given below.

PI Controller

$$K_C = 0.667 \quad \% \text{ valve opening/psi}$$

$$\tau_I = 0.072 \quad \text{sec}$$

$$T = 0.01 \quad \text{sec}$$

$$m(k) = m(k-1) + 0.542 e(k) - 0.5 e(k-1) \quad (6.52)$$

PID Controller

$$K_C = 0.782 \quad \% \text{ valve opening/psi}$$

$$\tau_I = 0.062 \quad \text{sec}$$

$$\tau_D = 0.002 \quad \text{sec}$$

$$T = 0.01 \quad \text{sec}$$

$$m(k) = m(k-1) + 0.883e(k) - 1.08e(k-1) + 0.24e(k-2) \quad (6.53)$$

The experimental response of cavity gate pressure under PI control is given in Figure 6.1.1. It shows that the controlled pressure follows the set point very closely

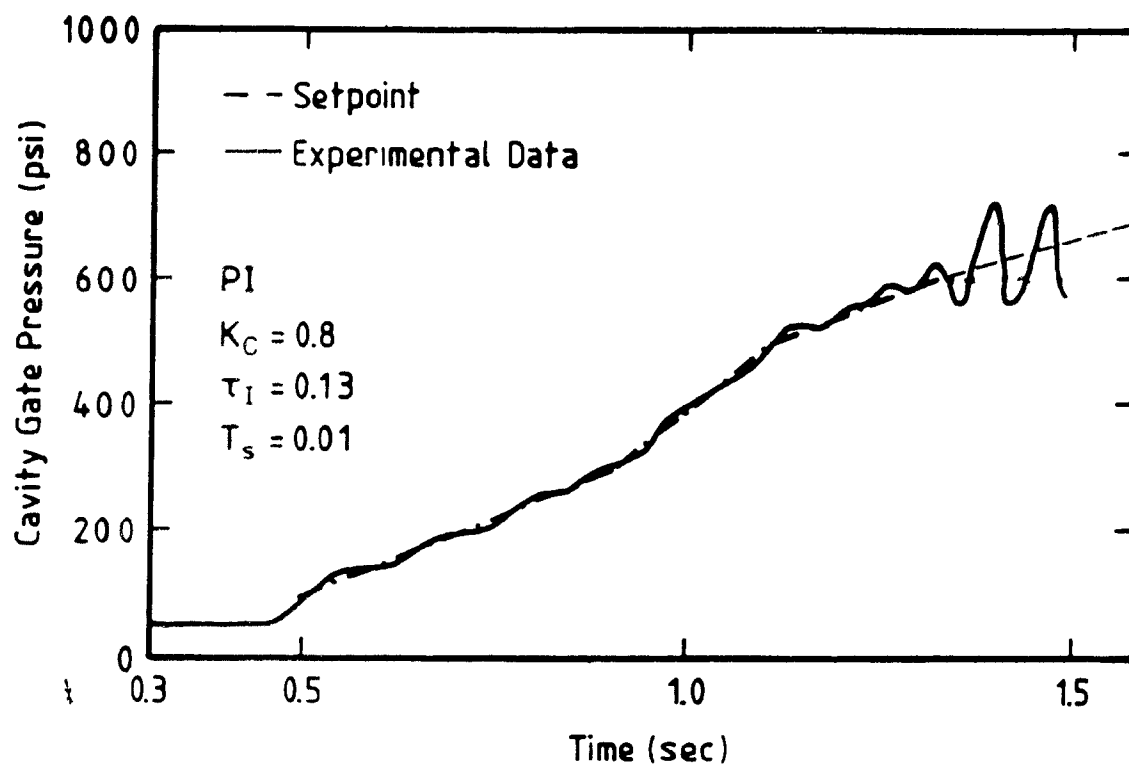


Figure 6.22 Experimental Nozzle Pressure Control Using PID Controller.



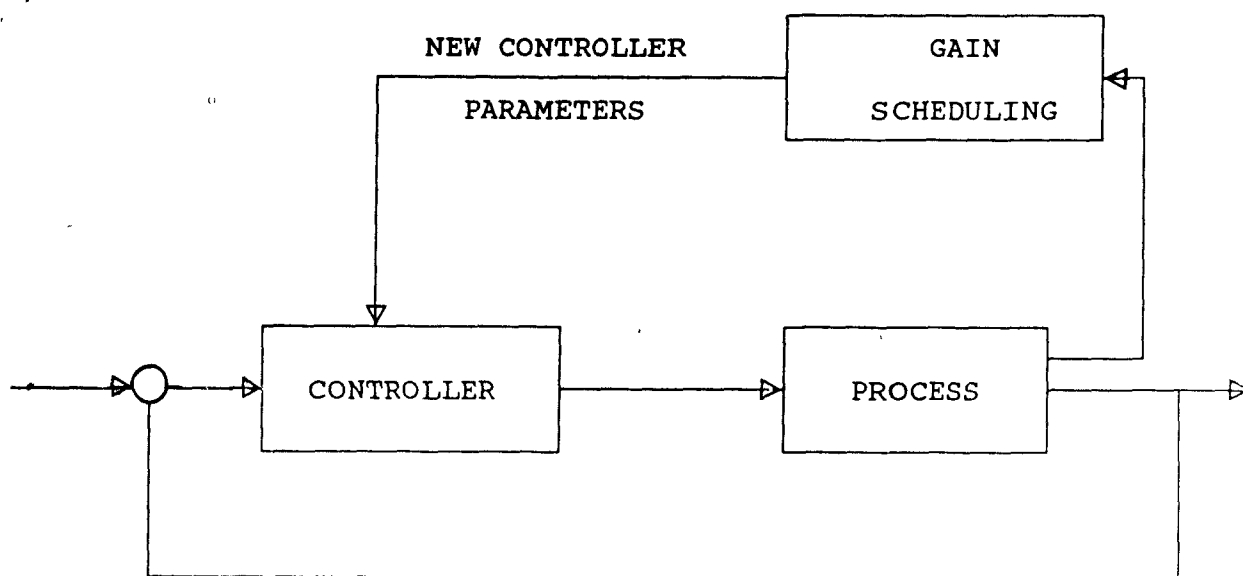


Figure 6.23 Gain Scheduling Adaptive Control

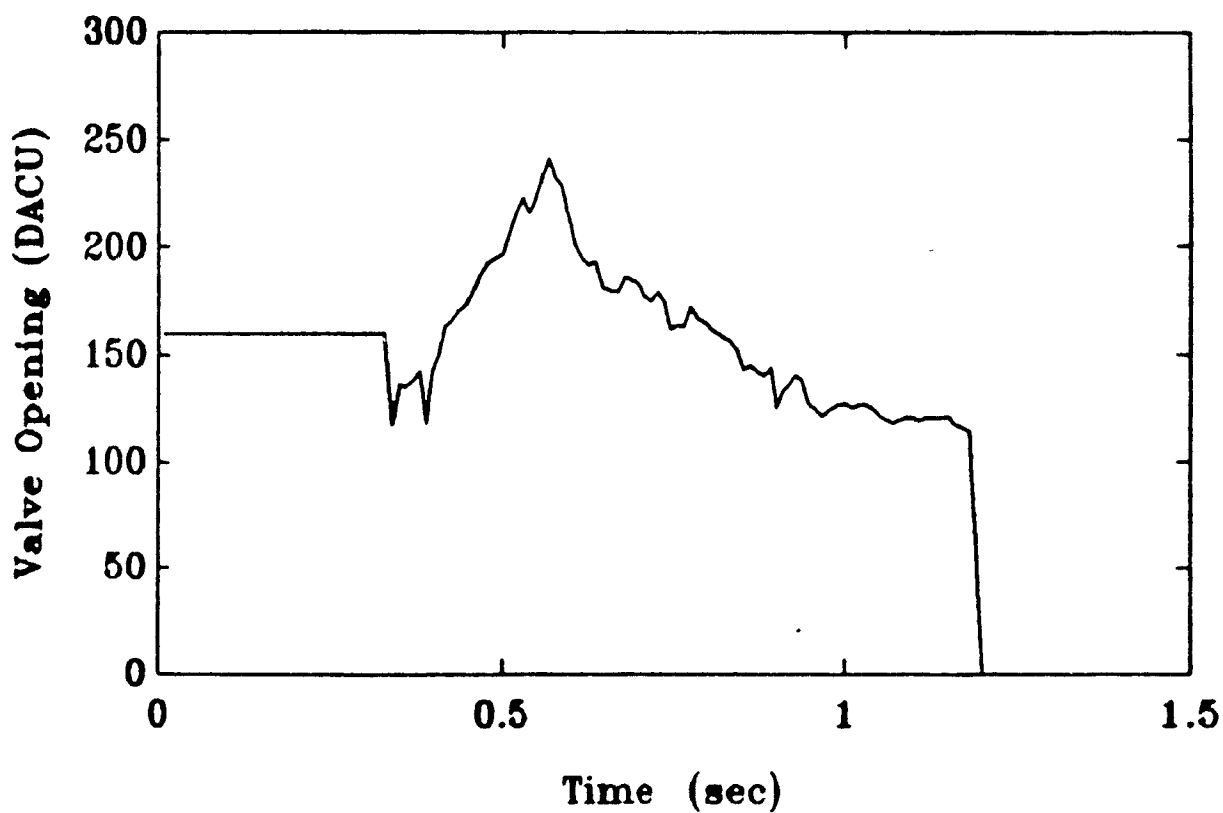
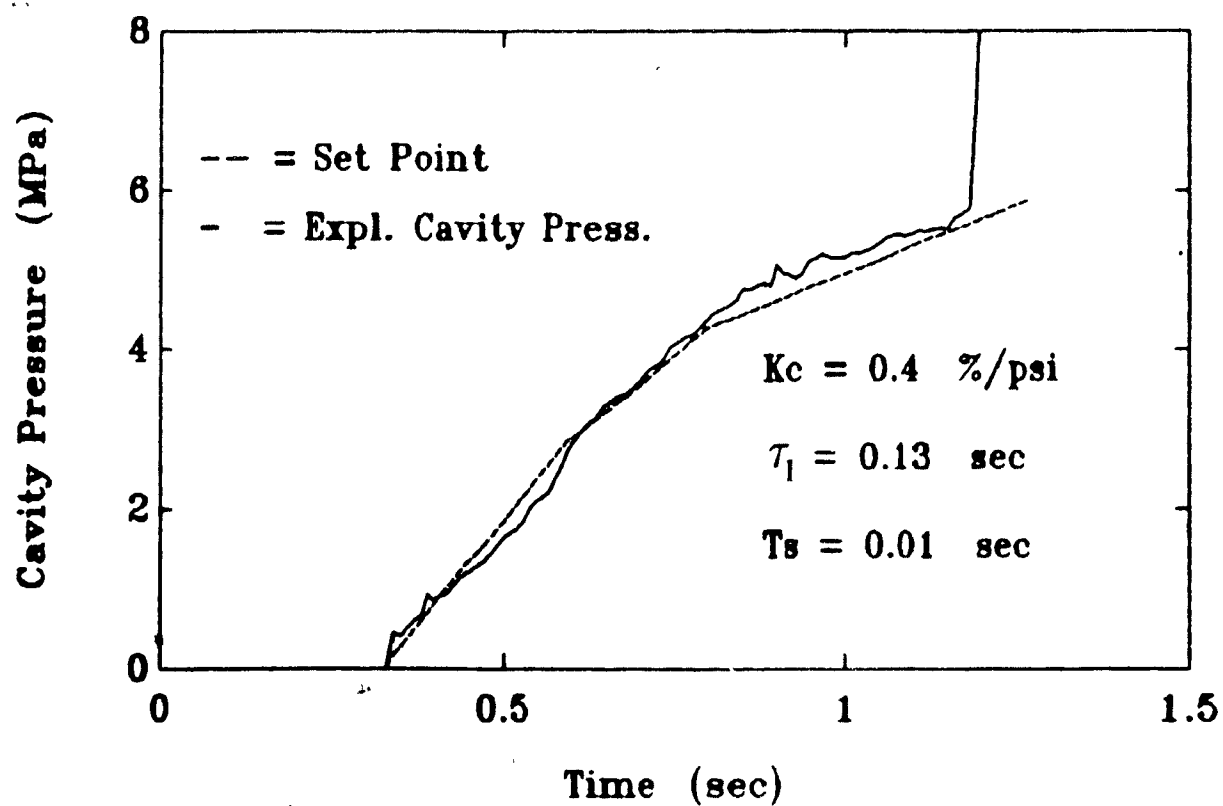


Figure 6.24 Experimental Cavity Gate Pressure Control Using PI Controller.

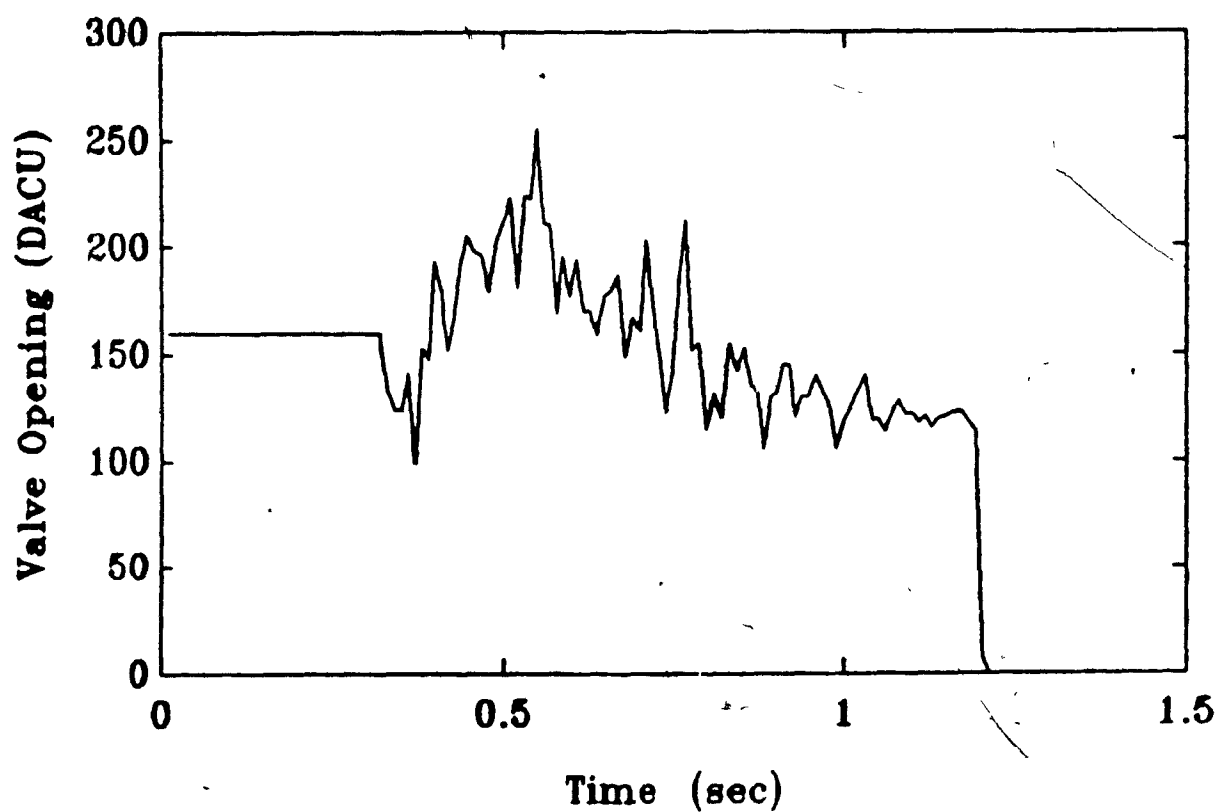
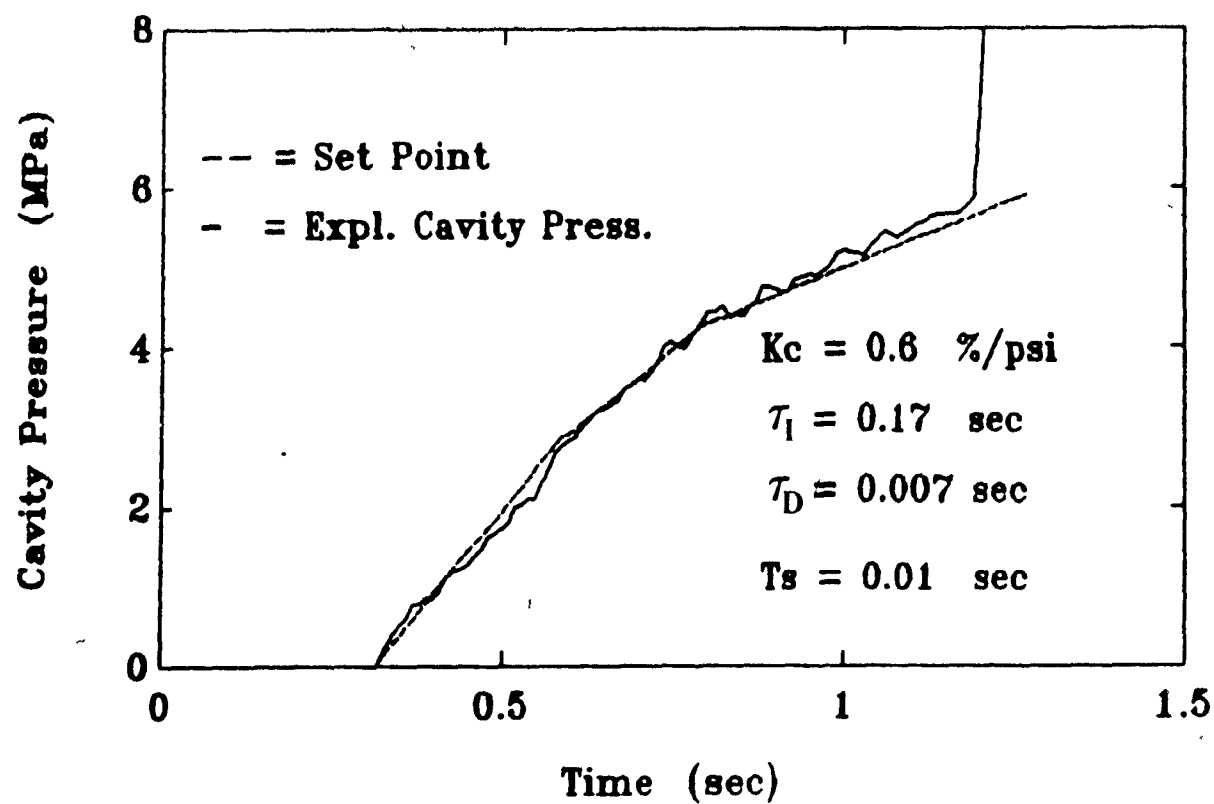


Figure 6.25 Experimental Cavity Gate Pressure Control Using PID Controller.

The above experiments were performed in the open-loop mode until a predetermined pressure (≈ 150 psi) was measured at the cavity gate. The process was then switched to closed-loop control operation. This strategy was based on the results of the dynamic studies, which showed that cavity pressure must reach a certain level before it could respond to changes in the manipulated valve opening. This suggests the desirability of controlling nozzle or hydraulic pressure at the beginning of the injection. When the gate pressure has reached a predetermined level, operation is switched to cavity pressure control. Control of the injection molding cycle using nozzle and cavity pressure is presented in Chapter 8.

6.5.3 Summary

- (1) Good control over nozzle pressure was obtained after an initial overshoot with PI, PID and Dahlin controllers.
- (2) The effect of nonlinearity in cavity gate pressure response appeared in an increasing oscillation at the end of filling.
- (3) The oscillatory behavior at the end of filling was rectified by using a simple gain scheduling control strategy.

CHAPTER 7

DYNAMIC MODELLING OF THE
PACKING STAGE

After the cavity is completely filled, the melt flow rate is substantially reduced and packing causes cavity pressure to rise rapidly to a peak value. The peak cavity pressure is an important processing variable, as it influences the molded part quality [152]. Thus, controlling the packing rate, the peak cavity pressure and holding pressure is essential. These variables are related to the amount of additional material forced into the cavity after completion of filling.

This chapter deals with the following issues :

- (a) The modifications of the experimental system.
- (b) Dynamic modelling of the packing stage.
- (c) The problems encountered in the control of packing and peak cavity pressures.

7.1 Feasibility of Packing Pressure Control

It should be noted that accurate closed-loop control of cavity pressure during the packing stage is difficult. This arises from two factors. Firstly, pressure rises very rapidly during the packing of the mold and thus, very fast responses are required from the control system and the machine hydraulics. Secondly, there is very little flow through the control valve, which, thus, must be operated close to the point of shut-off. Often, because of these difficulties, the fill to packing transition is not monitored, and, consequently, the packing stage is not controlled.

7.1.1 Modification of the Hydraulic System

Preliminary experiments to control peak cavity and holding pressures revealed that control is not achievable with the hydraulic system of the machine as described in Chapter 4. The system, as shown in Figure 7.1, contains one servovalve to control the flow of oil to the injection cylinder. The difficulties of this design are twofold. Firstly, it is difficult to control the valve near the shut-off point, a situation may arise to counteract the large overshoot caused by the rapid packing. Secondly,

- 1 Electric Motor
- 2 Pump
- 3 Safety Valve
- 4 Ball Valve
- 5 Main Pressure Distributor
- 6 Hydraulic Safety Pilot Operated Injection Relief Valve
- 7 Ramp Speed Adjusting Valve
- 8 Ramp Cylinder
- 9 Main Pressure Relief Valve with Two Pilots
- 10 Accumulator
- 11 Filter
- 12 Check Valve
- 13 Hydraulic Motor Injection Cylinder
- 14 Injection Carriage Cylinder
- 15 Injection Speed And Screw
- 16 Pressure Regulating Valve
- 17 Pressure Transducer
- 18 Check Valve
- 19 Injection Carriage Forward and Return Valve
- 20 Drive Regulating Valve
- 21 Heat Exchanger

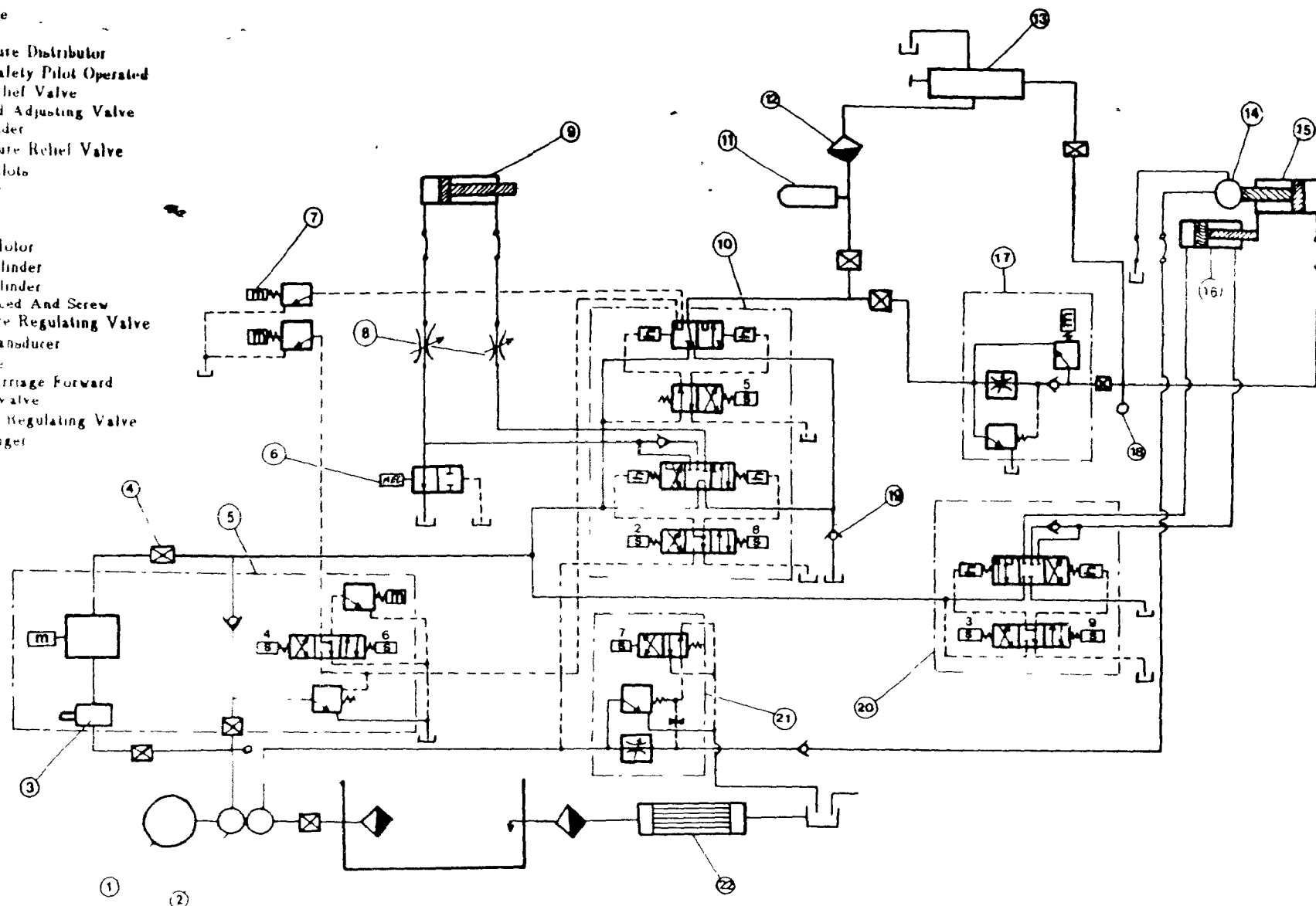


Figure 7.1 Hydraulic System of the Injection Molding Machine.

although the valve is completely closed, and there is no flow supply to the injection cylinder, the oil is still confined in the cylinder pushing the ram forward to raise pressure in the cavity. This situation has led us to the idea of modifying the hydraulic system by incorporating two servovalves : a supply and a relief servovalve. Barnaby [153] has suggested such a design, but, although simple, it has not been implemented to the author's knowledge.

The essential circuit of the modified system is shown in Figure 7.2. The complete design of the modified hydraulic system is given in Figure 7.3. The system can be operated with only one of the servovalves or with the two servovalves which are identical. Either valve can be used as a supply or a relief valve. The two valves are manipulated according to different control strategies as will be explained below. The valves will be referred to as supply servovalve (SSV) and relief servovalve (RSV).

7.2 Packing Stage Dynamics : Experiments and Models

The objective of this section is to develop dynamic models which relate the responses of cavity gate pressure, nozzle pressure, and hydraulic pressure, in the packing stage, to the changes in the manipulated servovalves.

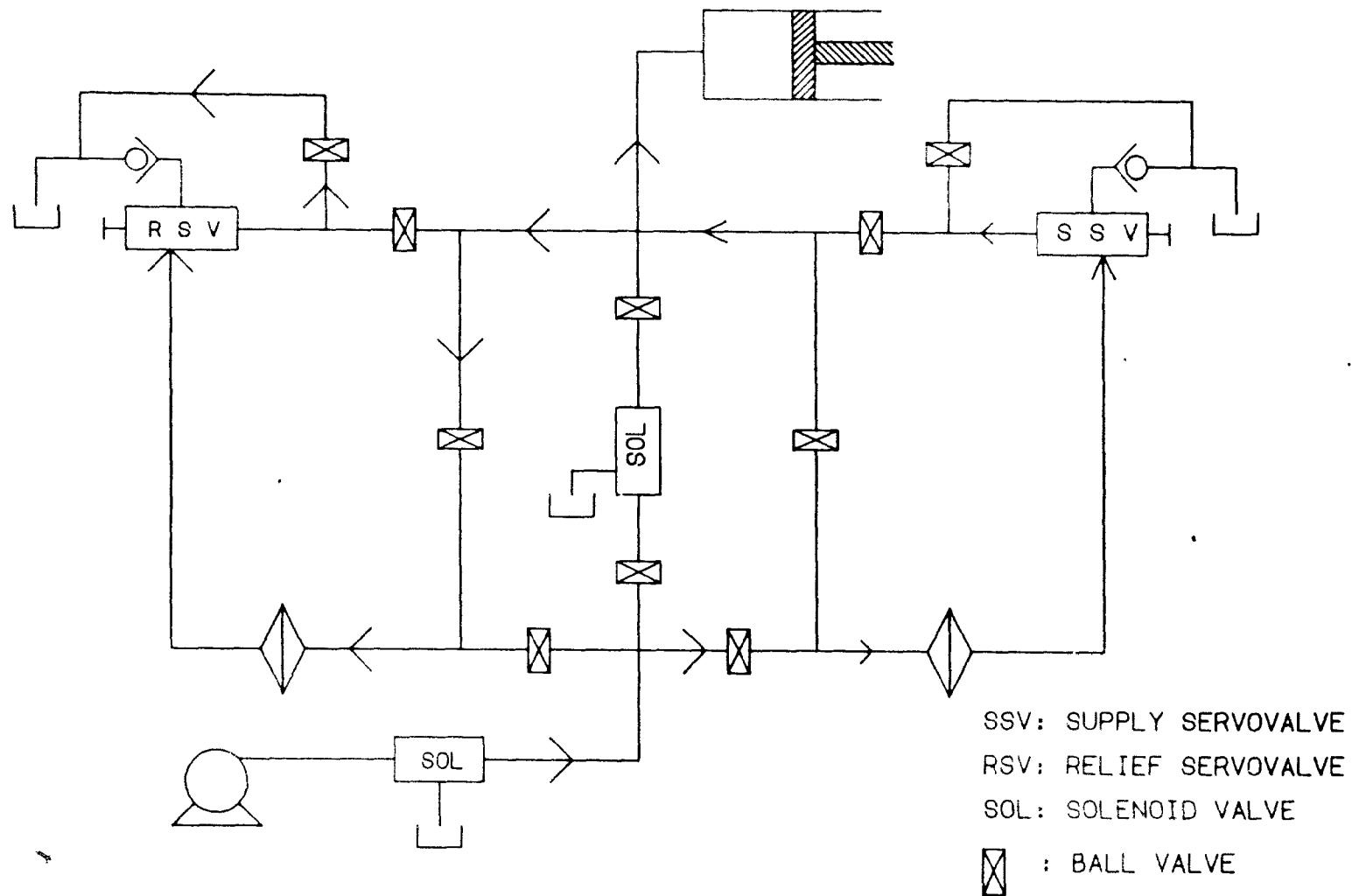
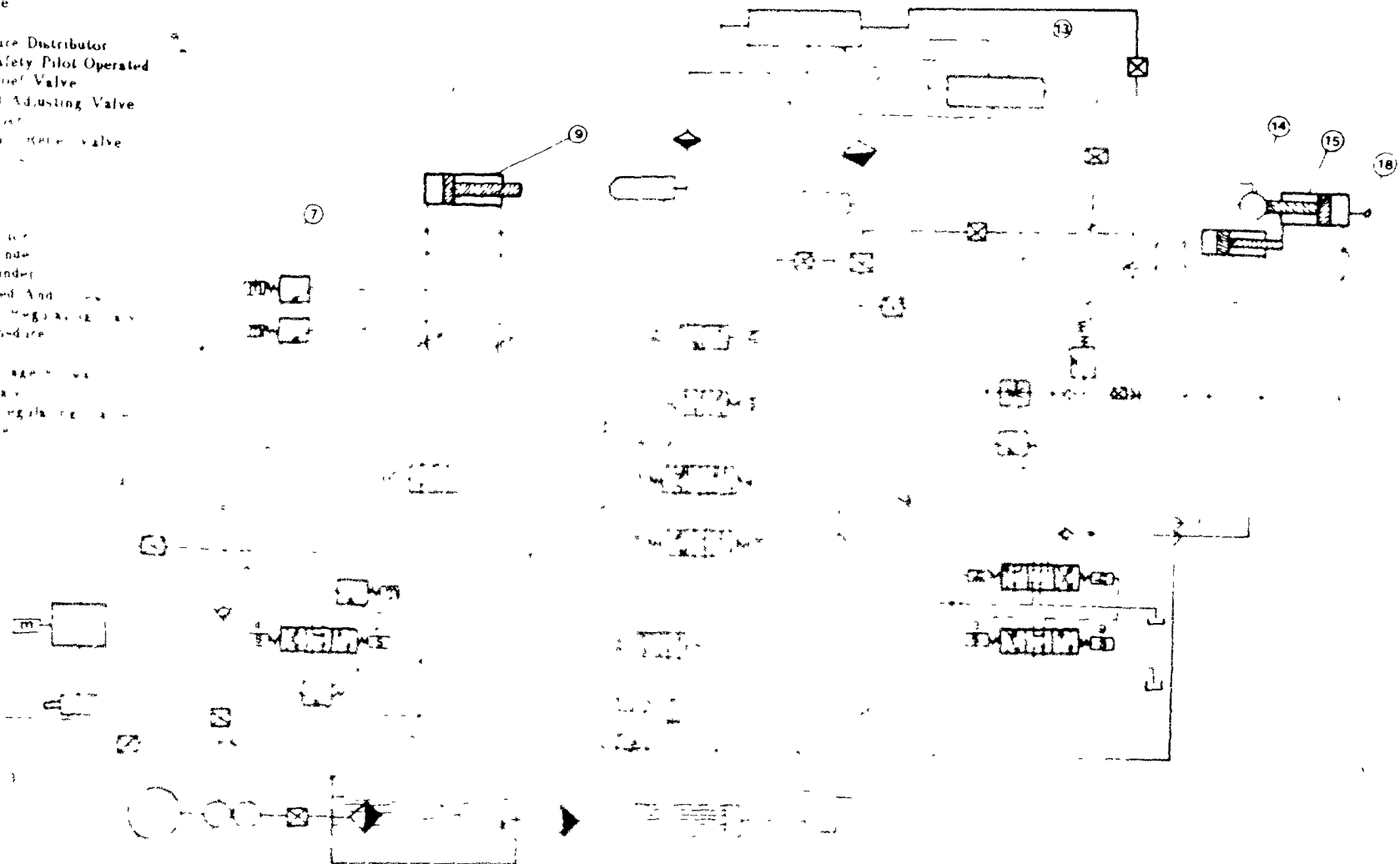


Figure 7.2: A Simplified Schematic of the Hydraulic System of The Injection Molding Machine.

[illegible]

openings. The following tests were performed :

- (a) Step test in which opening of the supply valve and the retraction of the ball in the center of both valves of the system was carried out together.
- (b) The step change was carried out at different times after the achievement of the equilibrium stage to examine the behavior of the model parameters.

The following discussion summarizes the experimental results and the fitted models.

7.2.1 Cavity Gate Pressure

The effect of the cavity gate pressure to various step changes in the supply and the valve opening is shown in Figure 7.2.1. The figure shows that the cavity gate pressure increases with the opening of the valve and the retraction of the ball. The result of the step change in the cavity gate pressure is either a first order or a second order model. The second order model is the best fit to the experimental data and the first order model is the best fit to the experimental data. The figure shows that the cavity gate pressure increases with the opening of the valve and the retraction of the ball. The result of the step change in the cavity gate pressure is either a first order or a second order model. The second order model is the best fit to the experimental data and the first order model is the best fit to the experimental data. The figure shows that the cavity gate pressure increases with the opening of the valve and the retraction of the ball. The result of the step change in the cavity gate pressure is either a first order or a second order model. The second order model is the best fit to the experimental data and the first order model is the best fit to the experimental data.

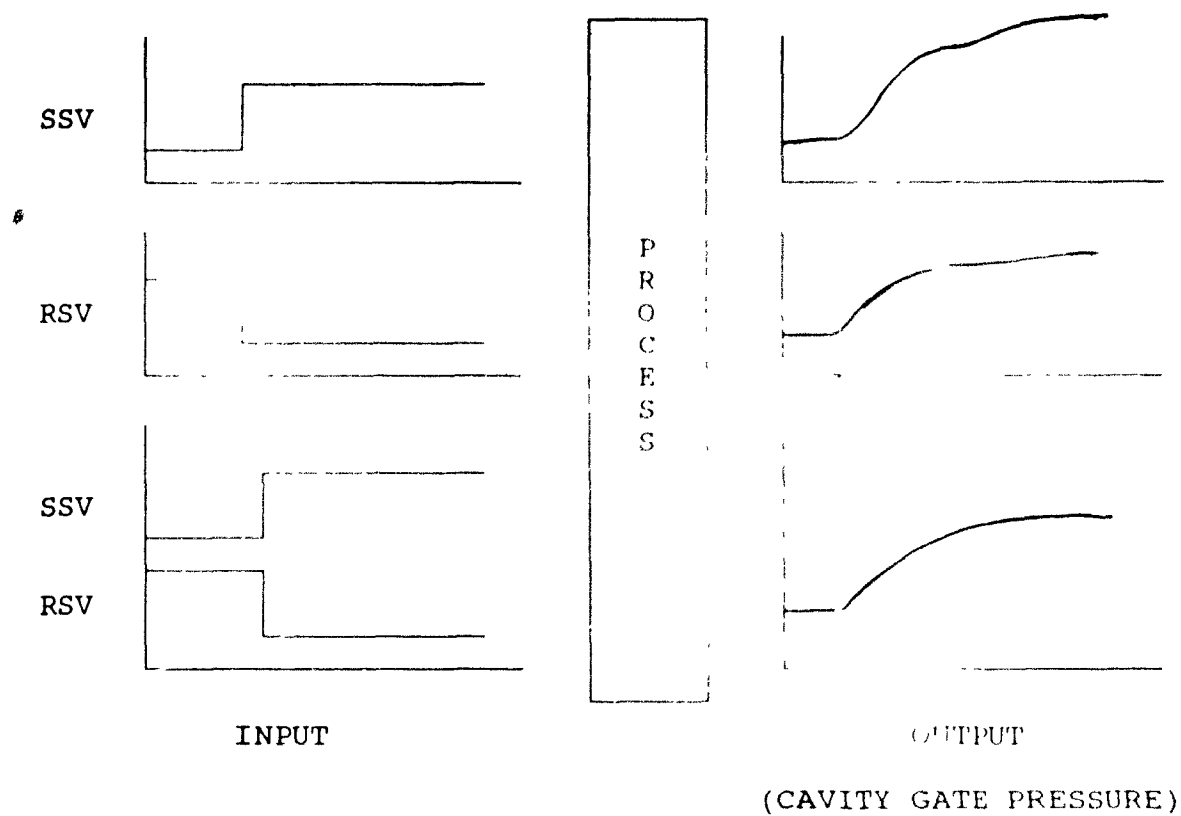


Figure 7.4: Step Changes in the Supply and Relief Valve Openings in the Packing Stage

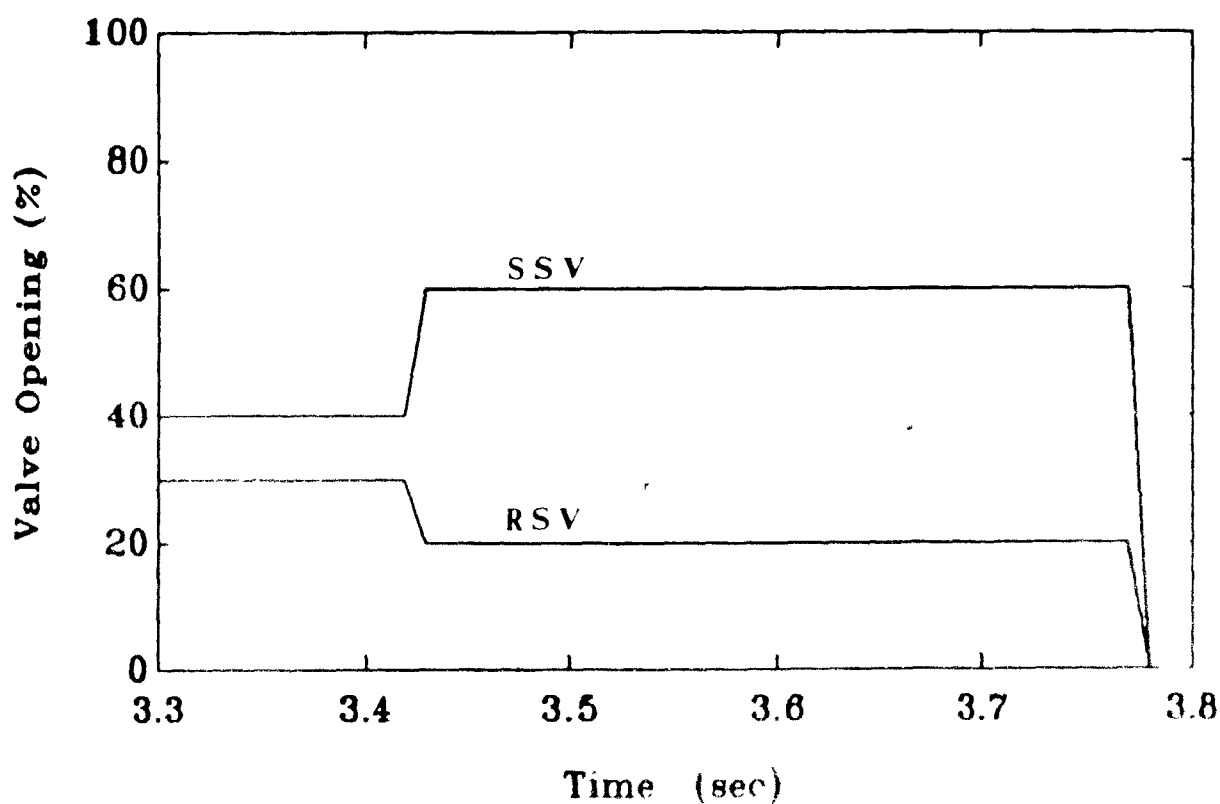
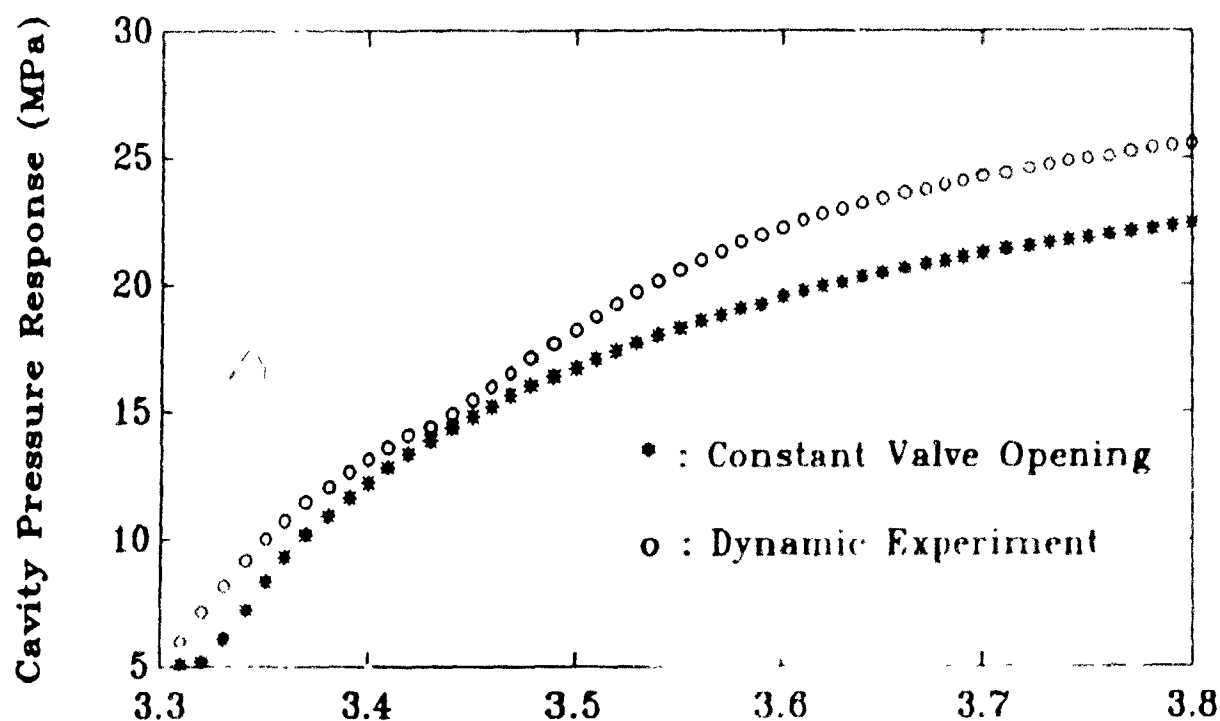


Figure 7.5 Response of Cavity Gate Pressure in the Packing Stage to Step Change of 40-60% in the SSV and 30-20% in the RSV Opening.

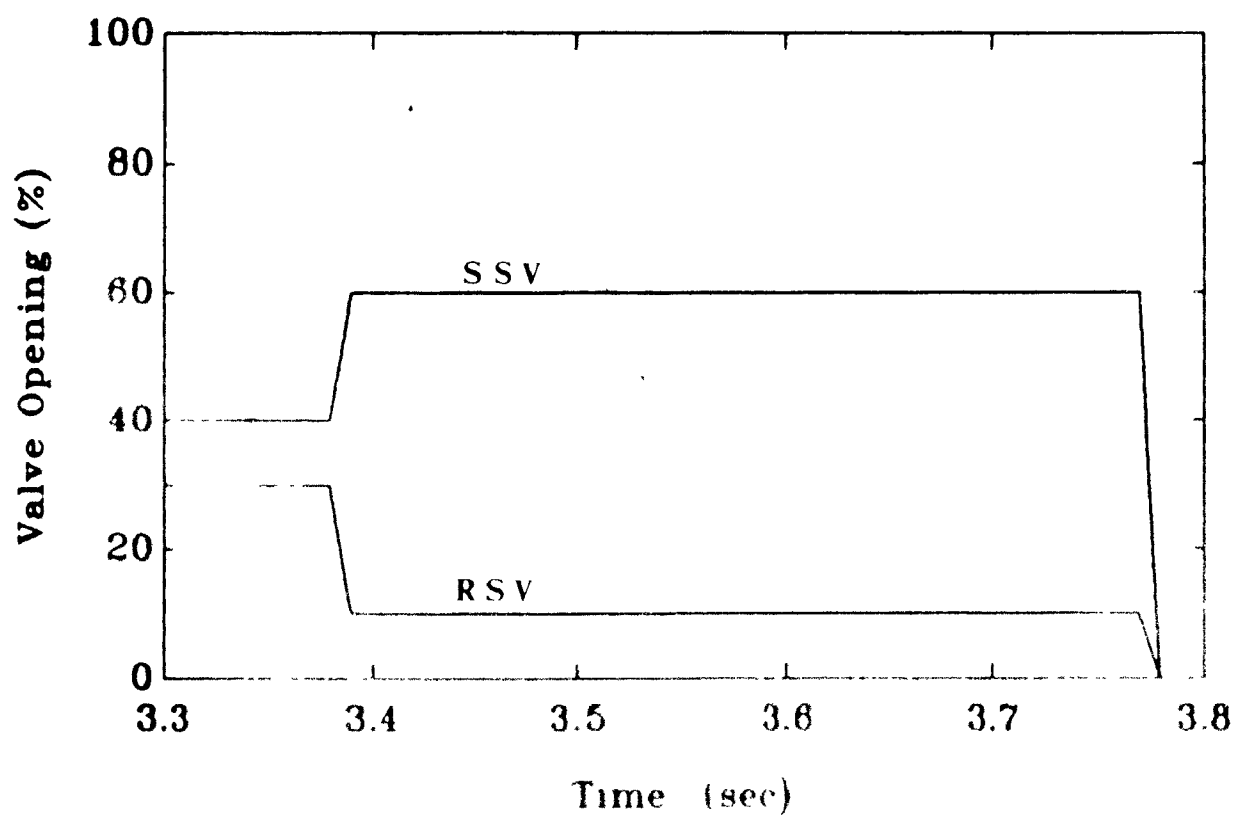
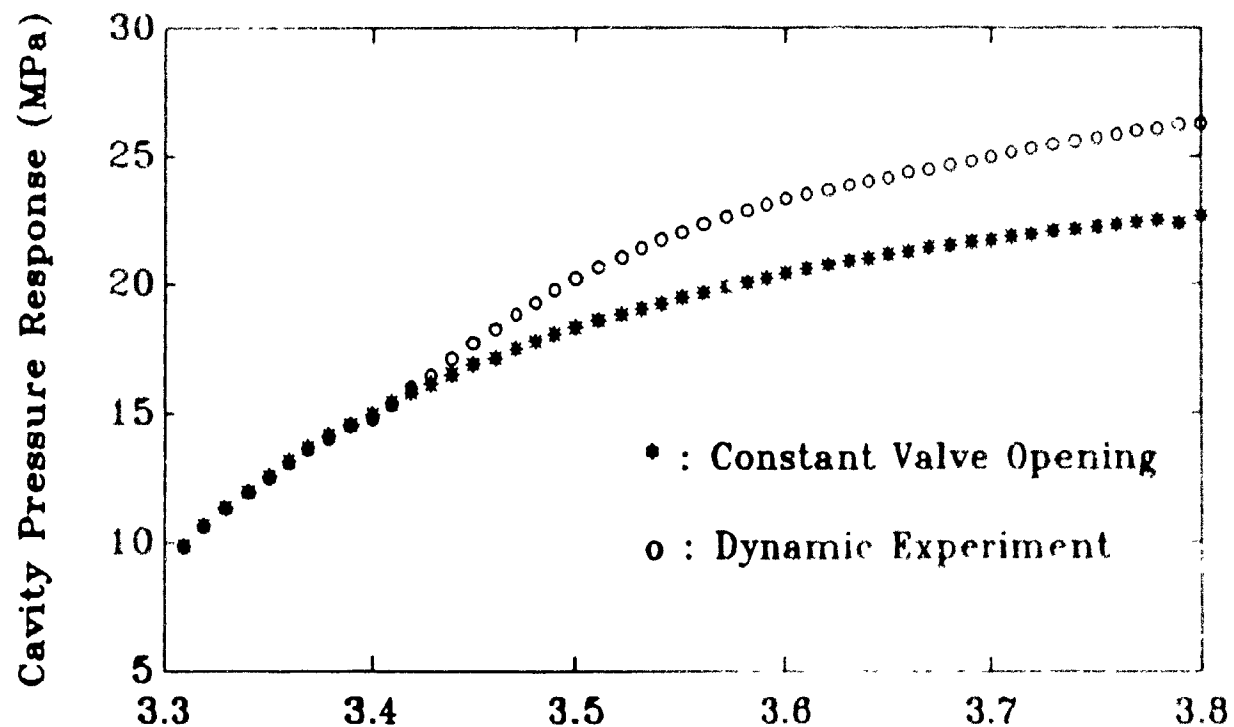


Figure 7.6 Response of Cavity Gate Pressure in the Packing Stage to step of 40-60% in the SSV and 30-10% in the RSV opening.

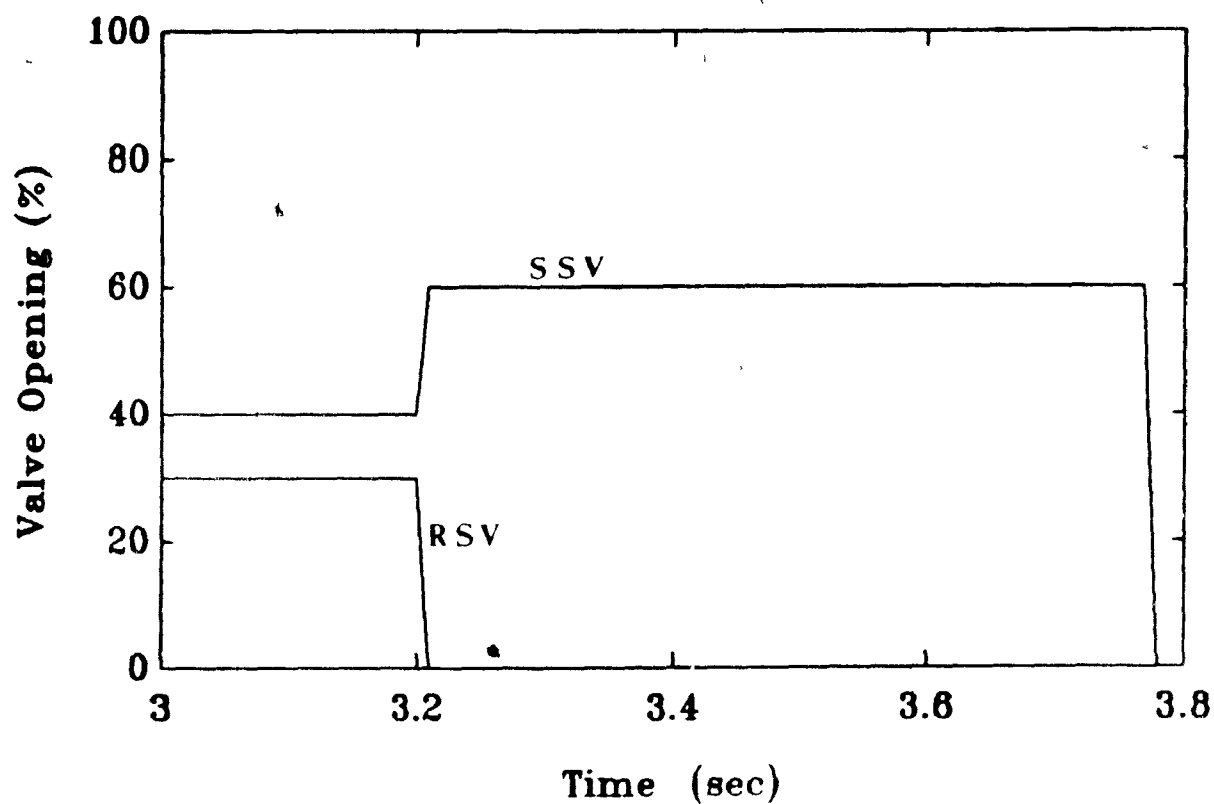
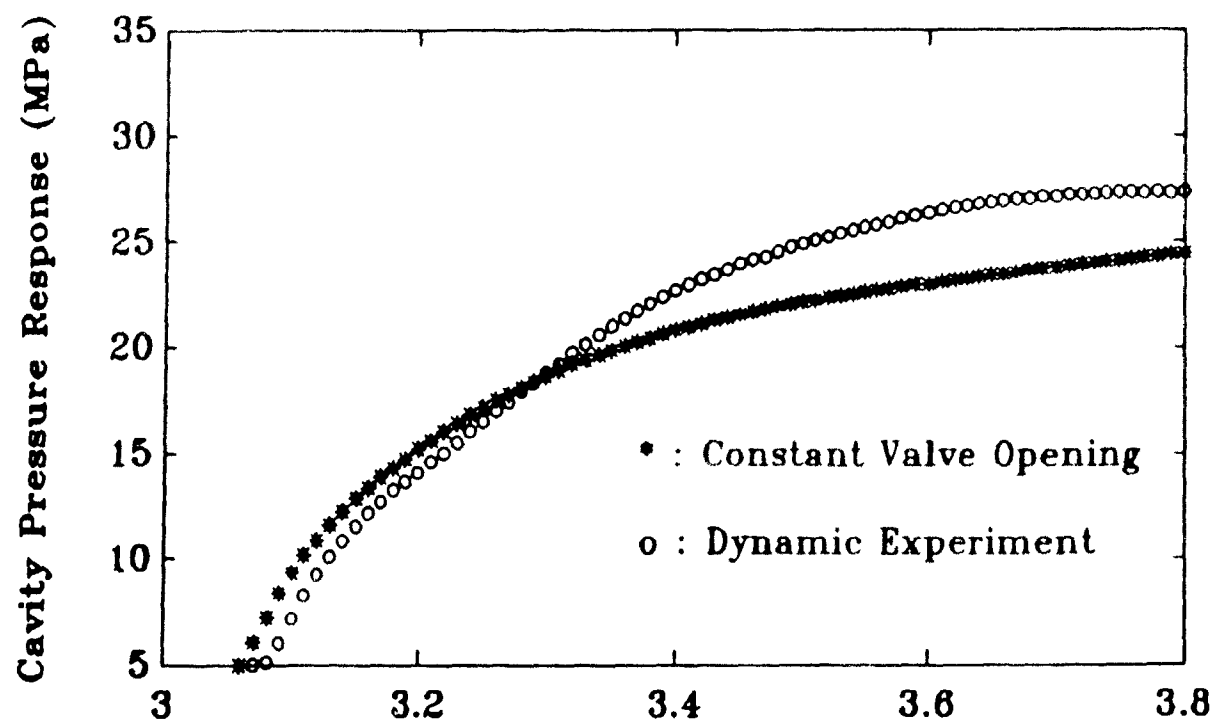


Figure 7.7 Response of Cavity Gate Pressure in the Packing Stage to Step of 40-60% in the SSV and 30-0% in the RSV Opening.

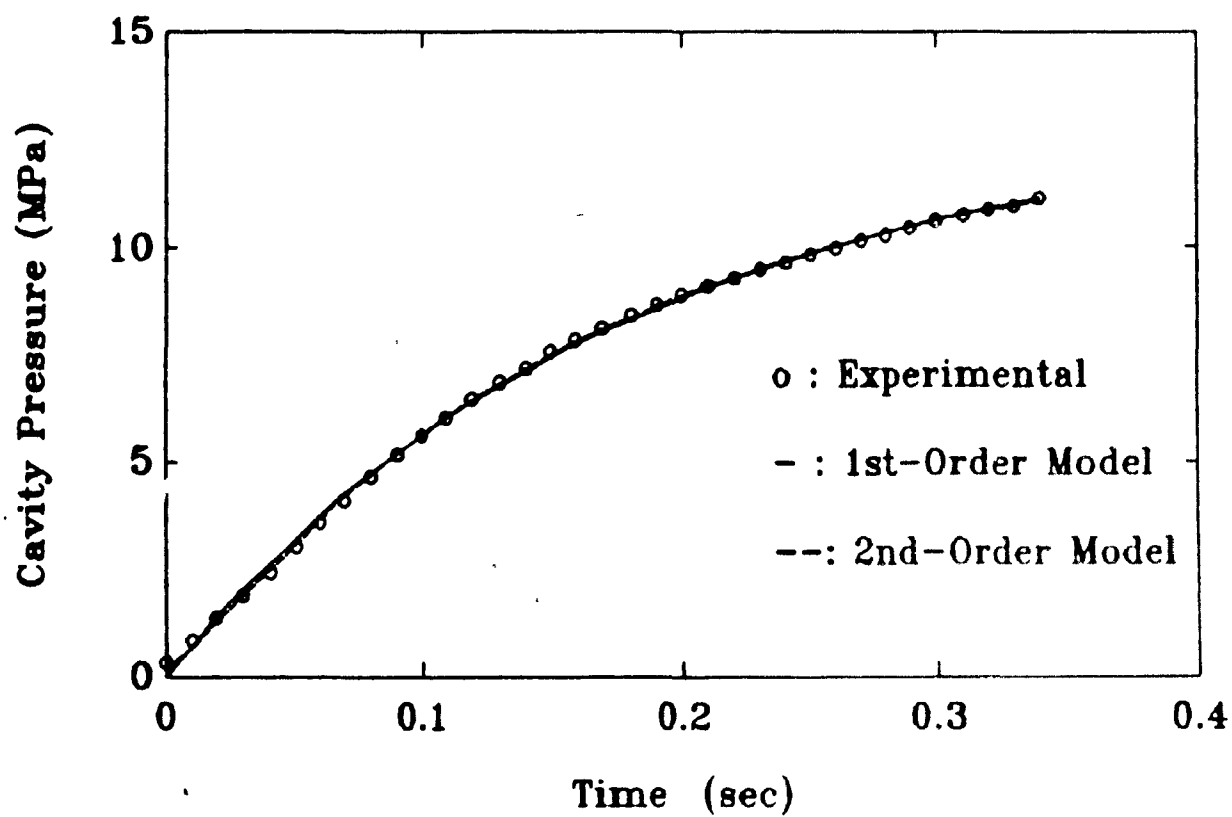


Figure 7.8 Comparison Between Experimental Cavity Gate Pressure and Fitted First and Second-Order Models.

The fits for both the first and second order models are about equally good, thus, the cavity gate pressure response in the packing stage will be represented by the simpler first order model of the form :

$$P_C(t) = K [1 - e^{-(t-D)/\tau}] \quad (7.1)$$

Where : P_C = cavity gate pressure, Pa

K = process gain, Pa/% change in valve opening

τ = process time constant, sec

D = time delay, sec

The average values of the parameters for Equation (7.1) are given in Table 7.1. The results show that the process parameters change with the magnitude of the step change. This can be attributed to the different degree of packing obtained by different step magnitudes.

To examine the behavior of the parameters of the cavity gate pressure model, step tests were performed at different times after the commencement of the packing stage. The time of the step was determined when the cavity gate pressure reached a preset value. To cover the whole packing stage, step tests were performed at cavity gate pressure values of 1000, 2000, and 3000 psi ($1 \text{ Pa} = 1.45 \times 10^{-4} \text{ psi}$). The response of cavity pressure to 40% change in the valves opening introduced at 2000 and 3000 psi at the gate is shown in Figure 7.9. The parameter values for the first

TABLE 7.1

Values of the Parameters for the Cavity Gate Pressure

Model : First Order, Equation 7.1

Change in Valve Opening %		Process Gain K, MPa/%	Time Constant τ , sec	Time Delay D, sec
SSV 40 - 60 RSV 30 - 20	30	0.439	0.179	0.010
SSV 40 - 60 RSV 30 - 10	40	0.341	0.187	0.007
SSV 40 - 60 RSV 30 - 0	50	0.290	0.209	0.011

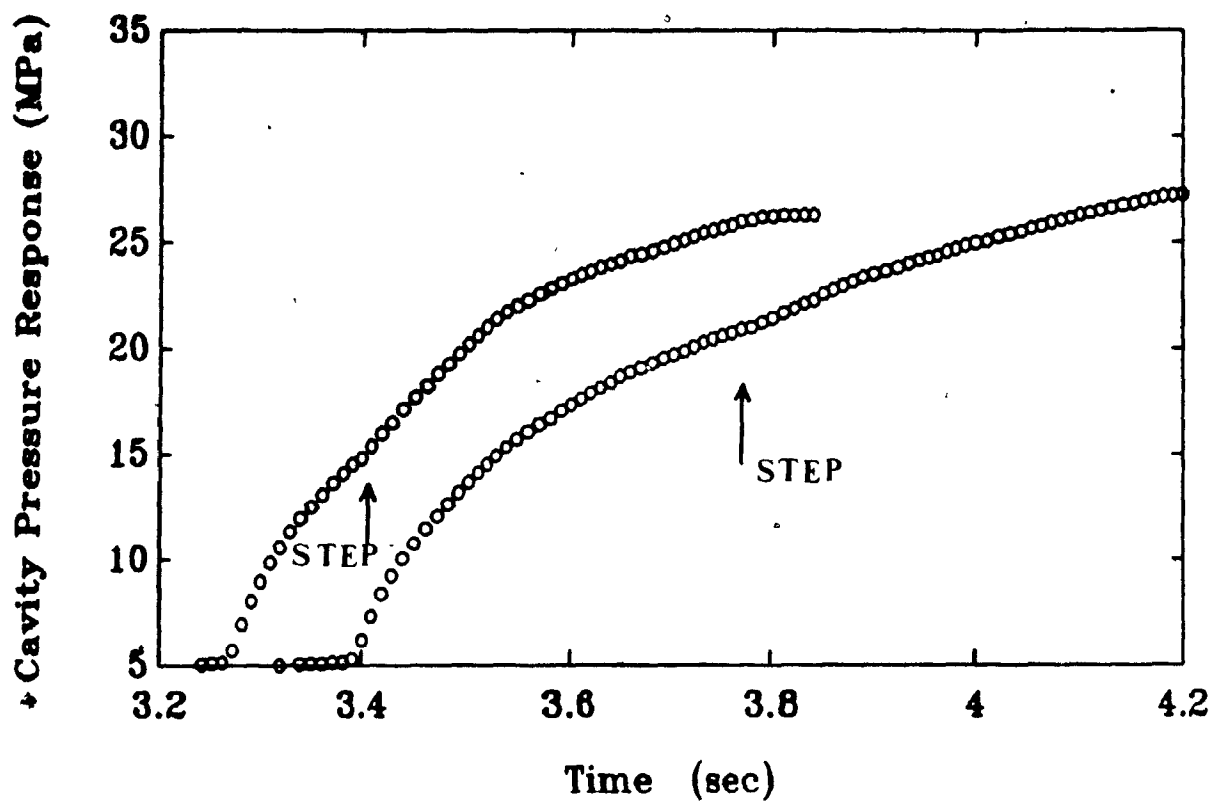


Figure 7.9 Cavity Gate Pressure Response to Step Change Introduced at Different Times.

order model fitted to the data of these two tests are given in Table 7.2. It can be seen from Tables 7.1 and 7.2 that the model parameters depend on the step magnitude and the degree of packing. The degree of packing is represented by the value of the cavity gate pressure at the time that the step was introduced. This nonlinear behavior should be taken into consideration in the design of the control loop for the packing stage, and it will be discussed in a later section.

7.2.2 Nozzle Pressure Model

The response of nozzle pressure to the step tests described in the above section was also recorded and modeled. A typical nozzle pressure response to a 40% step change in the openings of the supply and relief valves is shown in Figure 7.10. Again, the data from the various experiments were fitted with first order plus time delay and overdamped second order models. Figure 7.11 shows a comparison between the experimental nozzle pressure response and the predicted values using the first and second order models. Both models gave a good representation of the experimental response but the simpler first order model was chosen :

TABLE 7.2

Values of the Parameters for the Cavity Gate Pressure
Model (Equation 7.1) at Different Values of
Cavity Pressure

Change in Valve Opening %		Process Gain K, MPa/%	Time Constant τ , sec	Time Delay D, sec
SSV 40 - 60 RSV 30 - 10 @ 2000 psi	40	0.341	0.187	0.007
SSV 40 - 60 RSV 30 - 10 @ 3000 psi	40	0.275	0.451	0.005

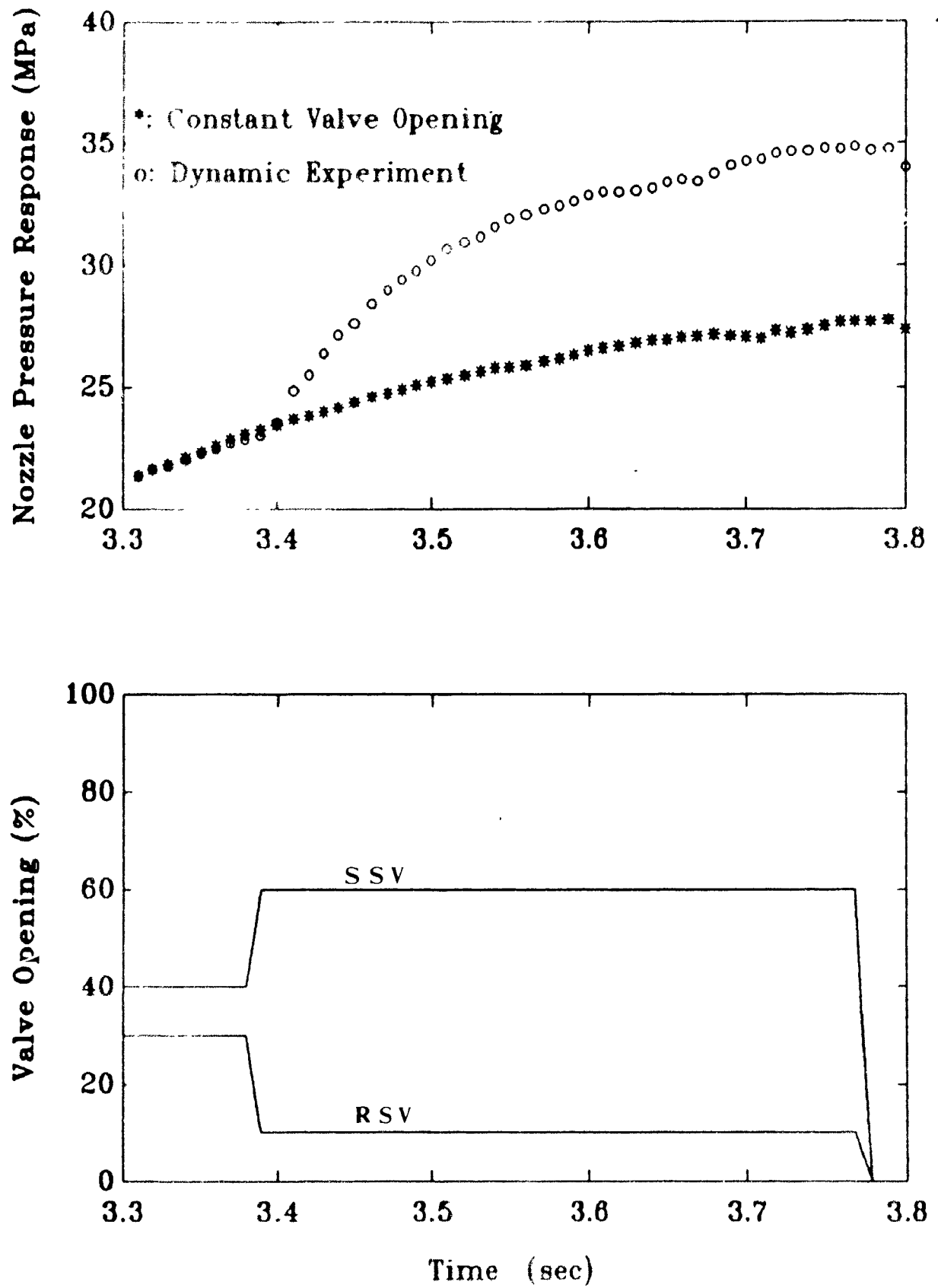


Figure 7.10 Nozzle Pressure Response to Step Change in the Valves Openings During Packing Stage.

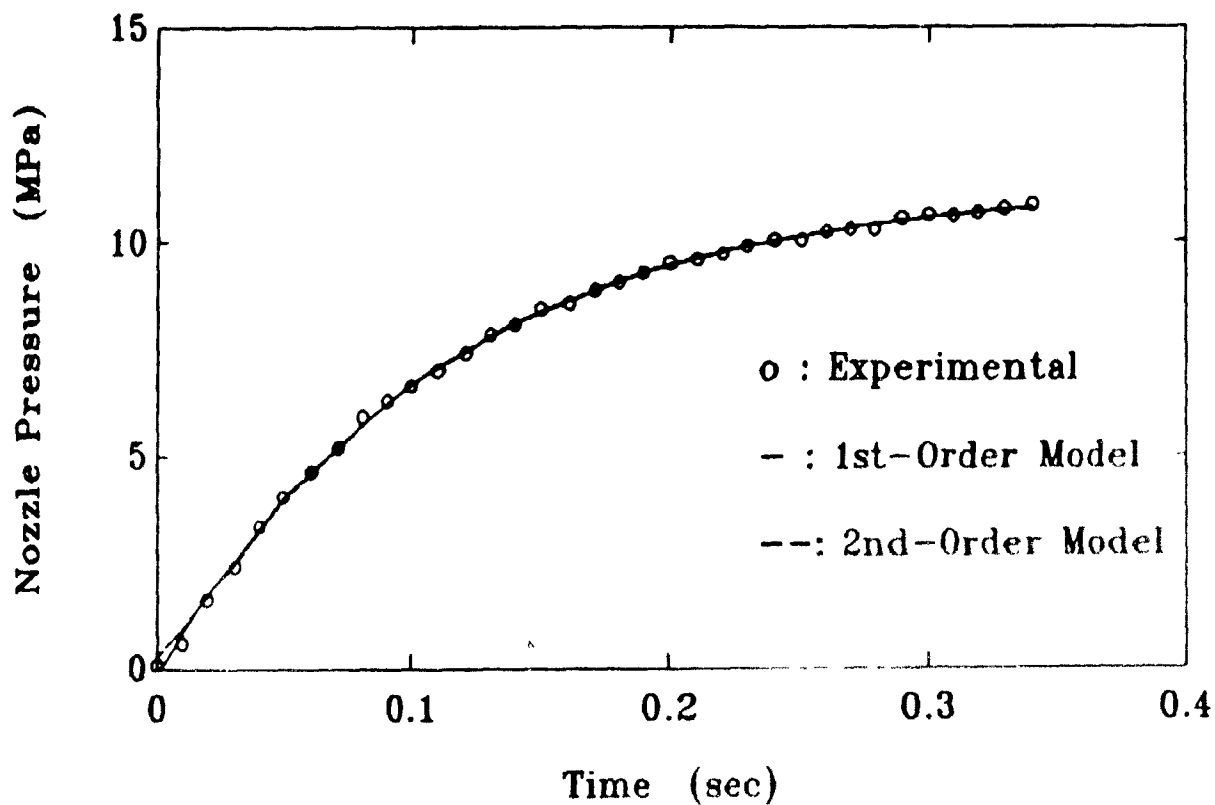


Figure 7.11 Comparison Between Experimental Nozzle Pressure and Fitted First and Second-Order Models.

$$P_N(t) = K [1 - \exp(-(t-D)/\tau)] \quad (7.2)$$

Where: P_N = nozzle pressure, psi
 K = process gain = pressure change in valve opening
 τ = process time constant, sec
 D = time delay, sec

The average values of the model parameters K , τ , and D are given in Table 7.2. The results indicate that the model parameters depend on the step magnitude and the degree of packing, suggesting a nonlinear nozzle pressure response.

7.2.3 Hydraulic Pressure Model

Figure 7.12 shows the response of hydraulic pressure to step changes in the valve opening. The modeling procedure used for cavity and nozzle pressure was repeated for hydraulic pressure response. The data were best fitted by a first order plus time delay model of the form:

$$P_H(t) = K [1 - \exp(-(t-D)/\tau)] \quad (7.3)$$

TABLE 2.3

Values of the Parameters for the Nozzle Pressure

Mode 1: 1000

Change of Valve Opening	Pressure at Nozzle	Time of onset	Time Delay
10	0	0	0
20	0	0	0
30	0	0	0
40	0	0	0
50	0	0	0
60	0	0	0
70	0	0	0
80	0	0	0
90	0	0	0
100	0.210	0.063	0.005
110			
120			
130			
140			
150			
160			
170			
180			
190			
200			
210			
220			
230			
240			
250			
260			
270			
280			
290			
300			
310			
320			
330			
340			
350			
360			
370			
380			
390			
400			
410			
420			
430			
440			
450			
460			
470			
480			
490			
500			
510			
520			
530			
540			
550			
560			
570			
580			
590			
600			
610			
620			
630			
640			
650			
660			
670			
680			
690			
700			
710			
720			
730			
740			
750			
760			
770			
780			
790			
800			
810			
820			
830			
840			
850			
860			
870			
880			
890			
900			
910			
920			
930			
940			
950			
960			
970			
980			
990			
1000			

① 3000 Hz
(20.7 MHz)

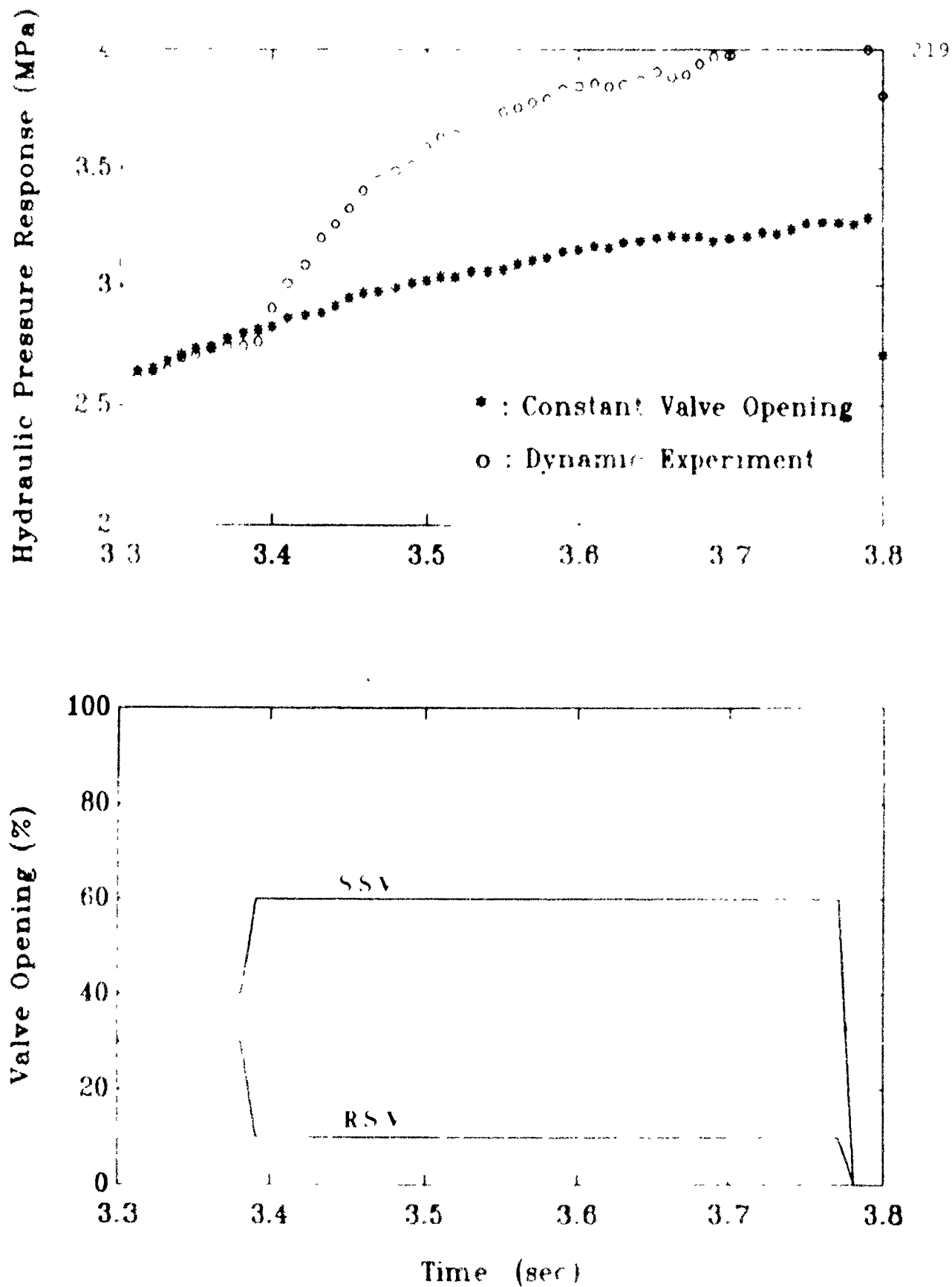


Figure 7.12 Hydraulic Pressure Response to Step Change in the Valves Openings During the Packing Stage.

The average values for the model parameters E , r , and D are given in Table 7.4. The results show that the fluidized pressure response to low flow rate changes are similar to the case of a step change in flow rate. The results in Figure 7.13 show a good agreement between the experimental data and the fitted first and second order models.

7.4 Summary

- (1) The step change responses of cavity gate pressure, nozzle pressure, and fluidized pressure in the three stage system are well modeled by first order systems with delay.
- (2) The three pressure responses exhibited nonlinear behavior with respect to the degree of packing.

TABLE 7.4

Values of the Parameters for the Hydraulic Pressure

Model - 1000 - 1000

	Charge in Valve (p.m.)	Pressure (MPa)	Time Delay (s)
SSV			
PSV			
SSV			
PSV			
SSV			
PSV			

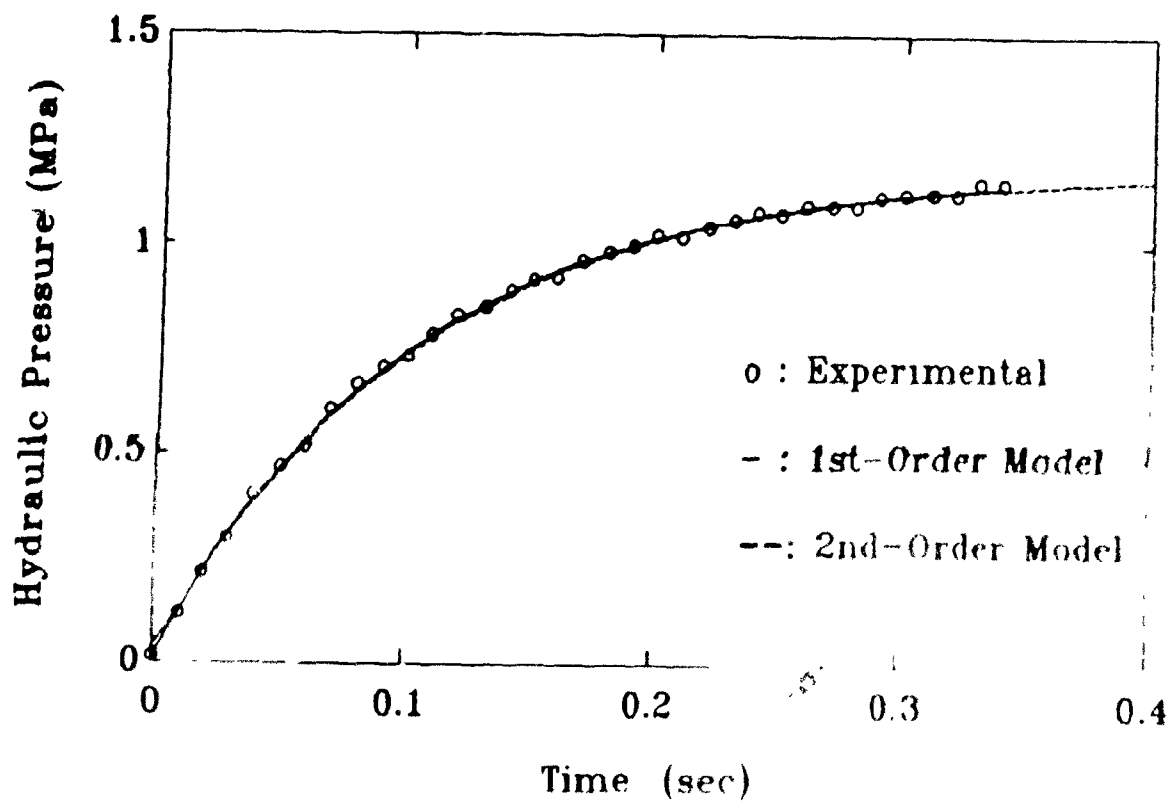


Figure 7.13 Comparison Between Experimental Hydraulic Pressure and Fitted First and Second-Order Models.

7.3 Analysis of the Dynamic Behavior of Cavity Pressure During the Packing Stage

Polymer flow into the cavity is caused by the pressure gradient between the nozzle and cavity gate :

$$Q = \frac{P_N - P_C}{R} \quad (7.4)$$

where :

Q = polymer mass flow rate into the cavity, g/sec

P_N = nozzle pressure, Pa

P_C = cavity pressure, Pa

R = resistance to flow between the nozzle and cavity gate

For a compressible flow in the cavity, the bulk modulus of compression is defined as [154,155] :

$$K_p = - \frac{dP}{dv} \quad (7.5)$$

where P is the pressure in the cavity and v is the specific volume of the polymer melt.

Let m = mass of polymer in the cavity

$$v = V/m \quad (7.6)$$

where V is the volume of the cavity, which is assumed to be constant throughout the packing stage. Thus,

$$K_p = \frac{dP}{\frac{d(V/m)}{(V/m)}} \quad (7.7)$$

$$= \frac{dP}{m \, d(1/m)} \quad (7.8)$$

$$= \frac{dP}{m(-1/m^2) \, dm} \quad (7.9)$$

therefore,

$$K_p = -m \frac{dP}{dm} \quad (7.10)$$

or

$$dm = -\frac{m}{K_p} dP \quad (7.11)$$

A simple mass balance gives :

$$dm = Q(t) \cdot dt \quad (7.12)$$

where $Q(t)$ is the mass flow rate of polymer into the cavity (g/sec). Therefore,

$$-\frac{m}{K_p} dP = Q(t) \, dt \quad (7.13)$$

or

$$-\frac{m}{K_p} \frac{dP}{dt} = Q(t) \quad (7.14)$$

where $(-m/K_p)$ is the mass capacitance of the cavity, C .

Applying Equation (7.14), the change in cavity pressure, due to the flow of the compressible polymer into the cavity, can be written as :

$$C_c \frac{dP_c}{dt} = Q(t) \quad (7.15)$$

where C_c is the total capacitance of the cavity including the polymer compressibility and the change in cavity volume due to mold separation. We simplify by assuming that mold separation is zero. From Equations (7.4) and (7.15) we have :

$$C_c \frac{dP_c}{dt} = \frac{P_N - P_c}{R} \quad (7.16)$$

or

$$R C_c \frac{dP_c}{dt} + P_c = P_N \quad (7.17)$$

Since K_p may be considered constant and considering the mass flow rate into the cavity is small during the short packing stage, it is assumed that C_c is constant as a first approximation.

If it is assumed that both R and C_C are constant, Equation (7.17) is a linear first order differential equation and cavity gate pressure has a first order response to a change in nozzle pressure [134]. The transfer function between cavity gate pressure as the output and the nozzle pressure as the input is obtained from Equation (7.17) using the Laplace transform as follows :

$$R C_C S P_C(s) + P_C(s) = P_N(s) \quad (7.18)$$

$$(R C_C S + 1) P_C(s) = P_N(s) \quad (7.19)$$

$$\frac{P_C(s)}{P_N(s)} = \frac{1}{R C_C S + 1} \quad (7.20)$$

or in a general form :

$$\frac{P_C(s)}{P_N(s)} = \frac{K}{\tau S + 1} \quad (7.21)$$

Where :

K = the process gain = 1

τ = the process time constant = $R C_C$

It is desirable to investigate the variation of the parameters R and C_C (and thus τ) with the pressure in the cavity. Assume that at any instant, the flow in the

delivery channels is incompressible with $\Delta P = P_N - P_C$.

$$R = \frac{\Delta P}{Q} \quad (7.22)$$

where Q , according to the Hagen-Poiseuille relation, is:

$$Q = \frac{\pi D^4 \Delta P}{128 \mu L} \rho \quad (7.23)$$

therefore,

$$R = \frac{128 L}{\pi D^4} \frac{\mu}{\rho} \quad (7.24)$$

Thus, $R(t) \propto \frac{\mu}{\rho} \quad (7.25)$

Variation of Viscosity with Pressure

Several studies have been reported on the effect of pressure and temperature on the viscosity of polymer melts [156-159]. The variation of polymer melt viscosity with temperature has been shown by Williams, Landell and Ferry [156] to follow the equation (WLF) :

$$\log \frac{\mu}{\mu_g} = \frac{-C_1 (T - T_g)}{C_2 + T - T_g} \quad (7.26)$$

where C_1 and C_2 are empirical constants for a given material, T_g is the glass transition temperature, μ and μ_g are the viscosities at the temperatures T and T_g respectively.

A relation for the variation of the shear viscosity of polymer melts with pressure has been derived by Penwell, Porter, and Middelman [157]. They utilized the WLF equation and a linear relationship between the pressure and the glass transition temperature obtained by Gee [158] as:

$$T_g = T_{g0} + A_1 P \quad (7.27)$$

where T_{g0} is the glass transition at atmospheric pressure, $A_1 = dT_g/dP$, and P is the pressure. Inserting Equation (7.27) into Equation (7.26) gives :

$$\log \frac{\mu}{\mu_g} = \frac{-C_1 (T - T_{g0} - A_1 P)}{C_2 + T - T_{g0} - A_1 P} \quad (7.28)$$

$$\log \frac{\mu}{\mu_g} = \frac{A_2 + A_3 P}{A_4 - A_1 P} \quad (7.29)$$

where : $A_2 = -C_1(T-T_{g0})$, $A_3 = C_1A_1$, $A_4 = C_2 + T - T_{g0}$

$$\mu = \mu_g \exp \left[2.303 \frac{A_2 + A_3 P}{A_4 - A_1 P} \right] \quad (7.30)$$

At low pressure ($P < 25$ MPa), $A_1 P$ is a small percentage of A_4 , and to a first approximation can be ignored. Therefore, Equation (7.30) simplifies to :

$$\mu = \mu_g \exp \left[2.303 \frac{A_2 + A_3 P}{A_4} \right] \quad (7.31)$$

$$\mu = \mu_g \exp \left[\frac{2.303 A_2}{A_4} + \frac{2.303 A_3 P}{A_4} \right] \quad (7.32)$$

$$\mu = \mu_0 e^{\alpha P} \quad (7.33)$$

Where : $\mu_0 = \mu_g \exp(2.303 A_2/A_4)$

$$\alpha = 2.303 A_3/A_4$$

Equation (7.33) states that the viscosity of polymer melts increases exponentially with increasing pressure, and this was confirmed experimentally by Nyun [159] for polyethylene.

Variation of the Density of Polymer Melts with Pressure

Kalyon [160] studied the variation of density with temperature and pressure for three high density polyethylene resins, designated as EX1, EX2, and EX3. His results showed that the density of the three resins increases linearly with increasing pressure as shown in Figure 7.14. The data were fitted by linear regression and the equation obtained for resin Ex2, used in this study, was :

$$\rho = c P + d \quad (7.34)$$

where: ρ is the density in gr/cc

P is the pressure in Pa

$c = 8.01 \times 10^{-10}$, g/cc.Pa

$d = 0.757$, g/cc

Utilizing Equations (7.33) and (7.34) we write :

$$\frac{\mu}{\rho} = \frac{\mu_0 e^{\alpha P}}{c P + d} \quad (7.35)$$

$$\frac{d(\mu/\rho)}{dP} = \mu_0 e^{\alpha P} \left[\frac{\alpha}{(c P + d)} - \frac{c}{(c P + d)^2} \right] \quad (7.36)$$

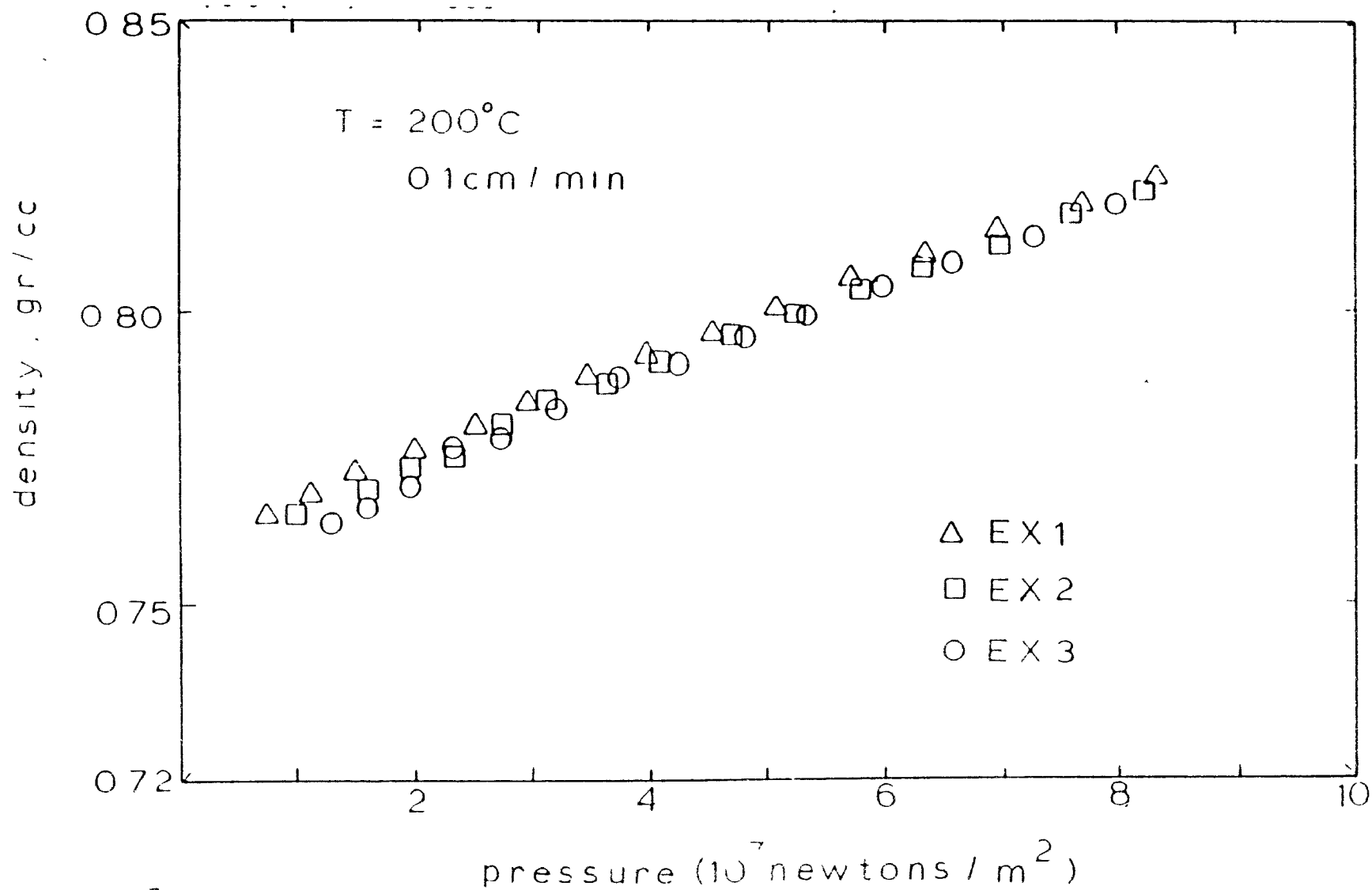


Figure 7.14 Variation of the Density of Polyethylene Resins with Pressure [160].

At high pressures, the term $[c/(c+P+d)^2]$ becomes very small and it can be neglected. Therefore, Equation (7.36) reduces to:

$$\frac{d(\mu/\rho)}{dP} = \mu_0 e^{\alpha P} \left[\frac{\alpha}{(c+P+d)} \right] \quad (7.37)$$

During the packing stage, the pressure, P , increases and the term $[\alpha/(c+P+d)]$ decreases. But on the other hand, the exponential part $e^{\alpha P}$ dominates. Therefore, the value of μ/ρ generally increases with increasing the pressure during the packing stage. The variation of $d(\mu/\rho)$ as a function of pressure is shown in Figure 7.1 where the effect of neglecting the term $[\alpha/(c+P+d)]$ is also shown. Thus,

$$\frac{d(\mu/\rho)}{dP} > 0 \quad (7.38)$$

In the case of C_C ,

$$C_C = \frac{m}{K_P} \quad (7.39)$$

where K_P may be considered constant. The mass of melt in

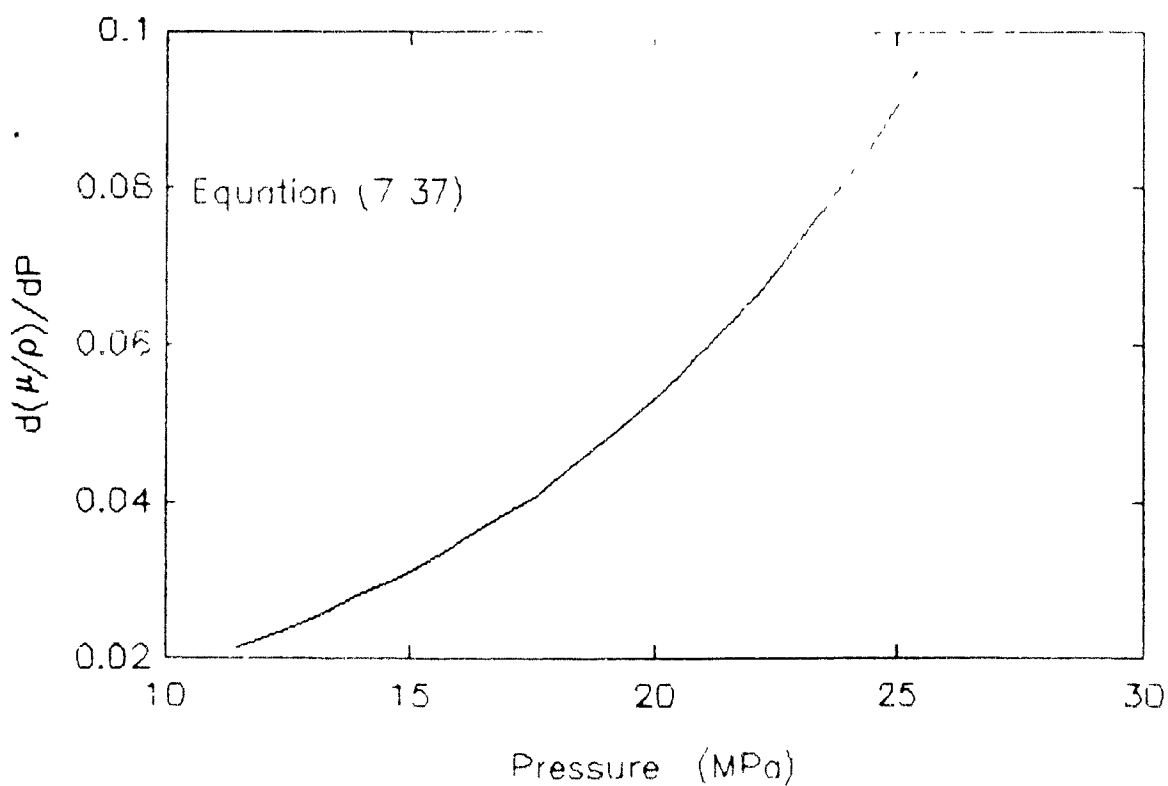
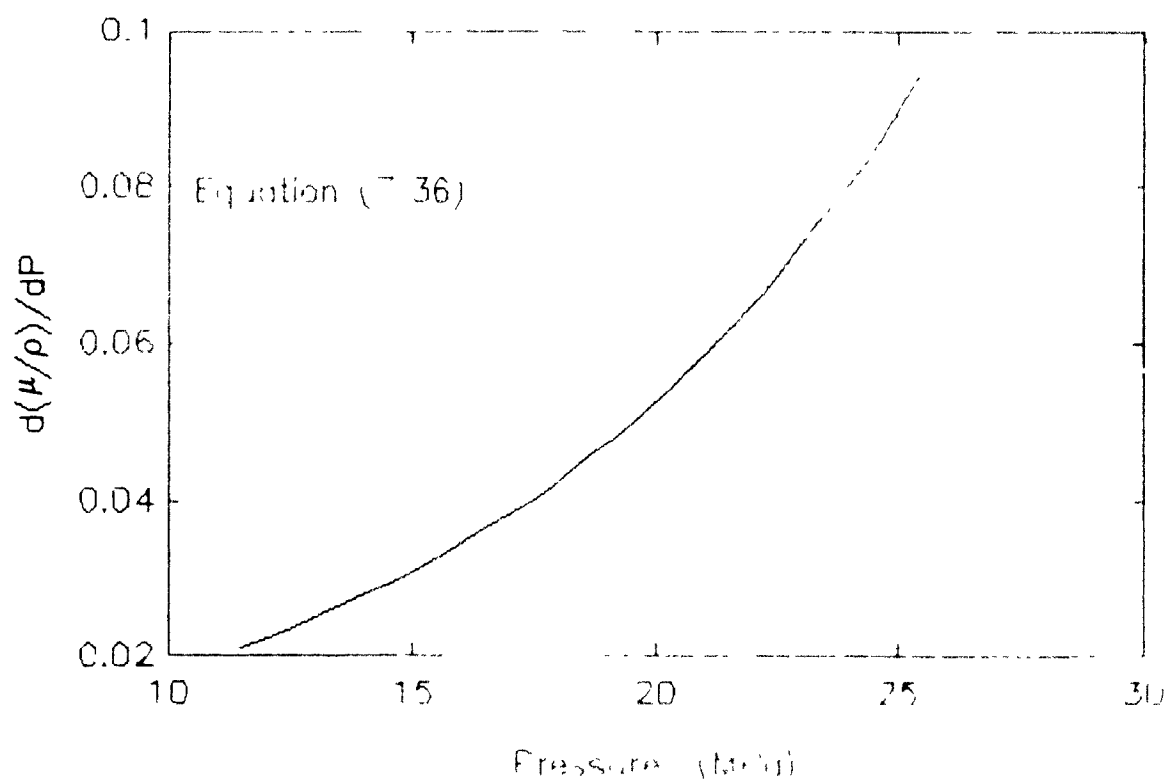


Figure 7.15: Variation of $d(\mu/\rho)/dP$ as a Function of Pressure for Polyethylene Resin.

the cavity, m , is increasing slowly. Therefore, C_c increases slowly with packing pressure, i.e.

$$\frac{dC_c}{dp} > 0 \quad (7.41)$$

As a result, the process time constant, τ , of the cavity pressure response ($\tau = RC_c$) increases with packing pressure. This agrees with the experimental results shown in Table 7.2.

CHAPTER 10

CONTROL OF THE PACKING AND HOLDING STAGES,
AND PEAK CAVITY FRESHENUP

In the present section, the control of the packing and holding stages, and the peak cavity freshenup, are discussed. The packing stage is the most important stage in the casting process, and the holding stage is the next most important. The peak cavity freshenup is a stage that is often overlooked, but it is very important for the quality of the casting. The control of these stages is discussed in the following sections.

- (1) De-
 - (a) ...
 - (b) ...
 - (c) ...
- (2) Con-
 - (a) ...
 - (b) ...

- (c) Control of pressure during the complete injection molding cycle, including filling, packing, peak cavity and holding pressures.

8.1 Design of the Control Loop for Packing Stage

8.1.1 Cavity Pressure Discrete Model

Cavity pressure response in the packing stage was modelled in section 7.4.1, with a first order plus delay model equation. In this model, the transfer function form, for a step change in the manipulated supply and relief servovalves is:

$$\frac{P_C(S)}{M(S)} = \frac{K e^{-\Theta S}}{\tau S + 1} \quad (8.1)$$

Where :

P_C = cavity gate pressure during packing

M = the sum of the change in the SSV and RSV
openings

K = process gain

τ = process time constant

Θ = time delay

The simulation results of cavity pressure control during the filling stage (section 6.4.3) showed that, for the purpose of Z-transform, the time delay can be approximated by nT , where n is an integer and T is the sampling interval. Thus, the discrete transfer function of Equation (8.1), in conjunction with a zero order hold, is :

$$\frac{P_C(Z)}{M(Z)} = \frac{K (1 - e^{-T/\tau}) a^2}{1 - (1 - e^{-T/\tau}) Z^{-1}} \quad (8.2)$$

Accordingly, the discrete response of cavity gate pressure response in the time domain is :

$$P_C(k) = (1-a) P_C(k-1) + K (1-a) M(k-2) \quad (8.3)$$

where :

- $P_C(k)$ = Cavity pressure at the sampling instant, k
- $P_C(k-1)$ = Cavity pressure at the sampling instant, $k-1$
- $M(k)$ = Sum of the change in the SSV and RSV openings at the sampling instant, k
- a = $\exp(-T/\tau)$

8.1.2 Combinations of the Supply and Relief Valve Openings

Various combinations of the supply and relief servovalve openings were investigated to gain more understanding of the dynamic behavior of the new hydraulic system. The following strategies were used to manipulate the two valves :

- (1) The supply and relief servovalves were manipulated with two separate controllers, as shown in Figure 8.1. The operating range for each of the two valves was set to 0.0 - 100% opening.
- (2) The supply and relief servovalves were manipulated according to one control law. The controller output was calculated according to the signal going to the supply valve (M_S) and the relief valve signal (M_R) was calculated by the following relationship :

$$M_R = M_{R_{MAX}} - \left(\frac{1 - Y}{Y} \right) M_S \quad (8.1)$$

where :

- M_R = opening of the relief servovalve
- $M_{R_{MAX}}$ = maximum opening for the relief servovalve
- M_S = opening of the supply servovalve
- Y = ratio between M_R and M_S

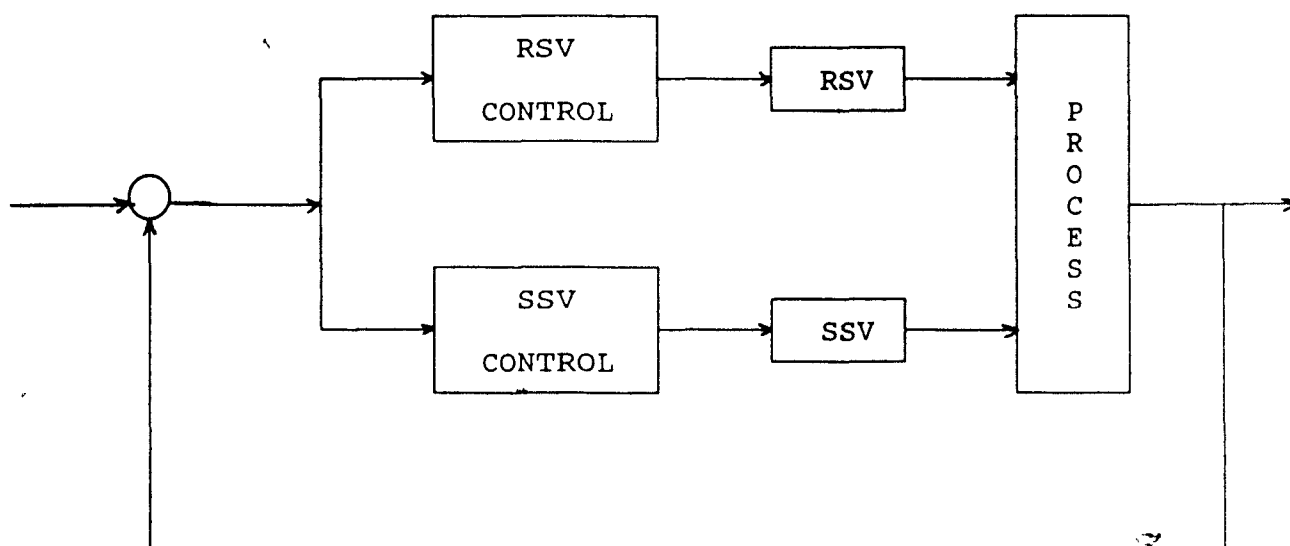


Figure 8.1: Control Scheme for the Supply and Relief Valves Using Two PI Controllers.

The control scheme, is shown in Figure 8.2. The operation range for the supply servovalve was set to 0.0 - 100%, while the relief servovalve was operated with different ranges to investigate its effect. The operation ranges of the valves are indicated with the specific experiments.

8.1.3 Simulation of the Control Loop

The results of the control simulation and experiments in the filling stage showed that both the PI and PID controllers gave satisfactory results. It was expected that both controllers will also perform well in the packing stage. Thus, the simpler PI controller was selected for cavity pressure control during the packing and holding stages.

The results of cavity gate pressure dynamic studies for the packing stage, presented in the previous chapter, indicated the nonlinear character of the process gain and time constant. Thus, the effective design of the control loop for packing cavity pressure should compensate for this nonlinearity. The gain scheduling control strategy, presented in section 6.5.2, was employed. The dynamic study of the cavity gate pressure during the packing stage showed that the process parameters were related to the

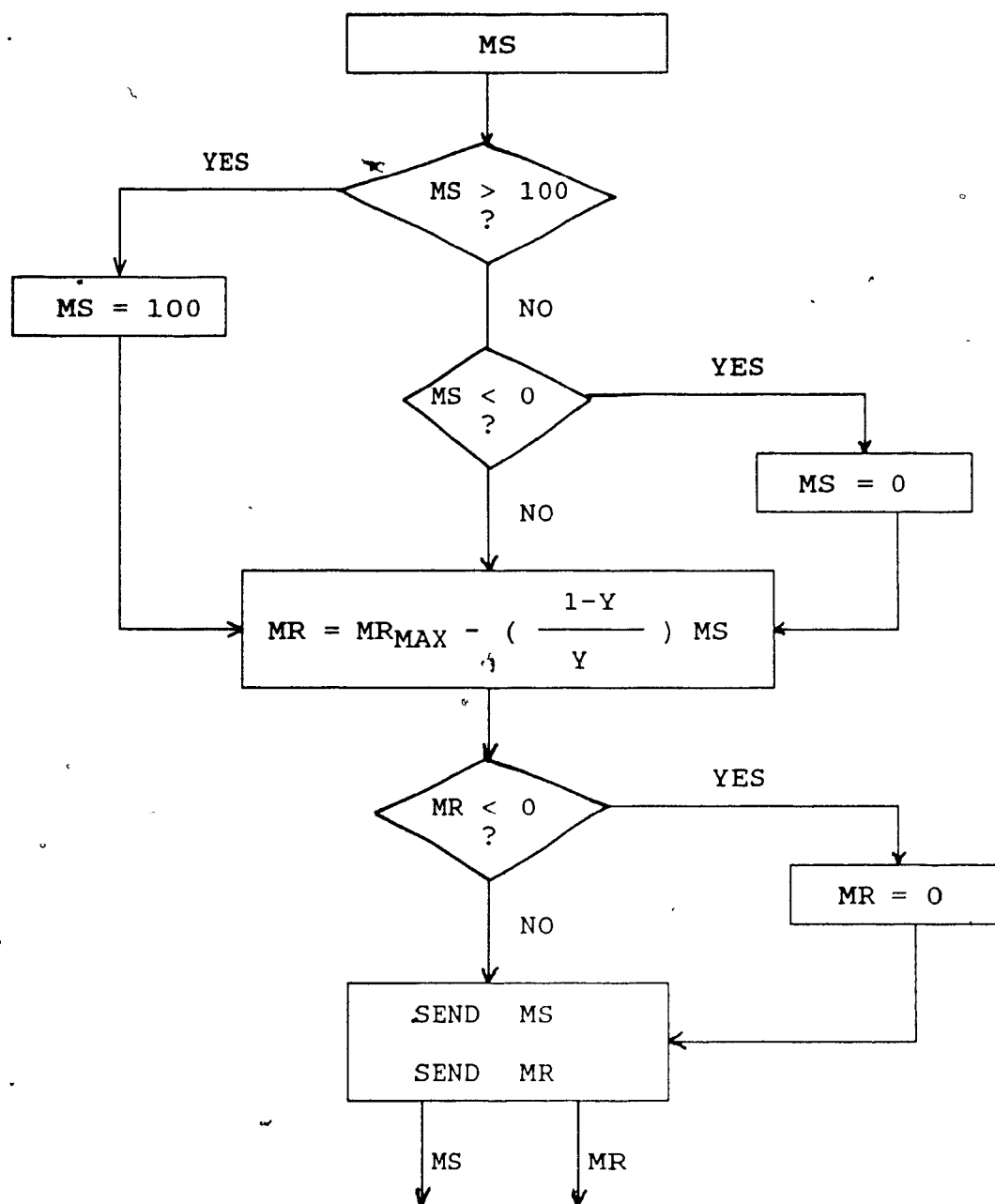


Figure 8.2 Control Scheme with One Controller for Both Servovalves

value of cavity gate pressure at the time of the step change. In view of the short duration of the packing stage, it was divided, as a first approximation, into two intervals with different process parameters. A controller was tuned for each interval and operation was switched from one zone to the next based on the value of the cavity gate pressure.

The initial controller parameters for the PI controller calculated by the ITAF criterion using the model parameters in Table 7.2 are given in Table 8.1. The simulation of the cavity gate pressure control during the packing and holding stages using a PI controller is shown in Figure 8.3. The results show that the above proposed control strategy provides a reasonable approach.

8.2 Control Experiments

8.2.1 Sequential Control

Strategies for sequential transfer from one stage to the next throughout the injection molding cycle were discussed in section 3.4. It was concluded that strategies based on cavity pressure are the most effective. Two strategies are used and evaluated in the following control

TABLE 8.1

Initial Controller Parameter Values Calculated by the
ITAE for Cavity Gate Pressure During the Packing Stage

Process Parameters (from Table 7.1)	PI Controller Parameters	
	K_C	τ_I
$K = 0.341 \text{ MPa/\%}$ $\tau = 0.107 \text{ sec}$ $\theta = 0.007 \text{ sec}$ $T = 0.01 \text{ sec}$	21.252	0.183
$K = 0.275 \text{ MPa/\%}$ $\tau = 0.451 \text{ sec}$ $\theta = 0.005 \text{ sec}$ $T = 0.01 \text{ sec}$	73.368	0.439

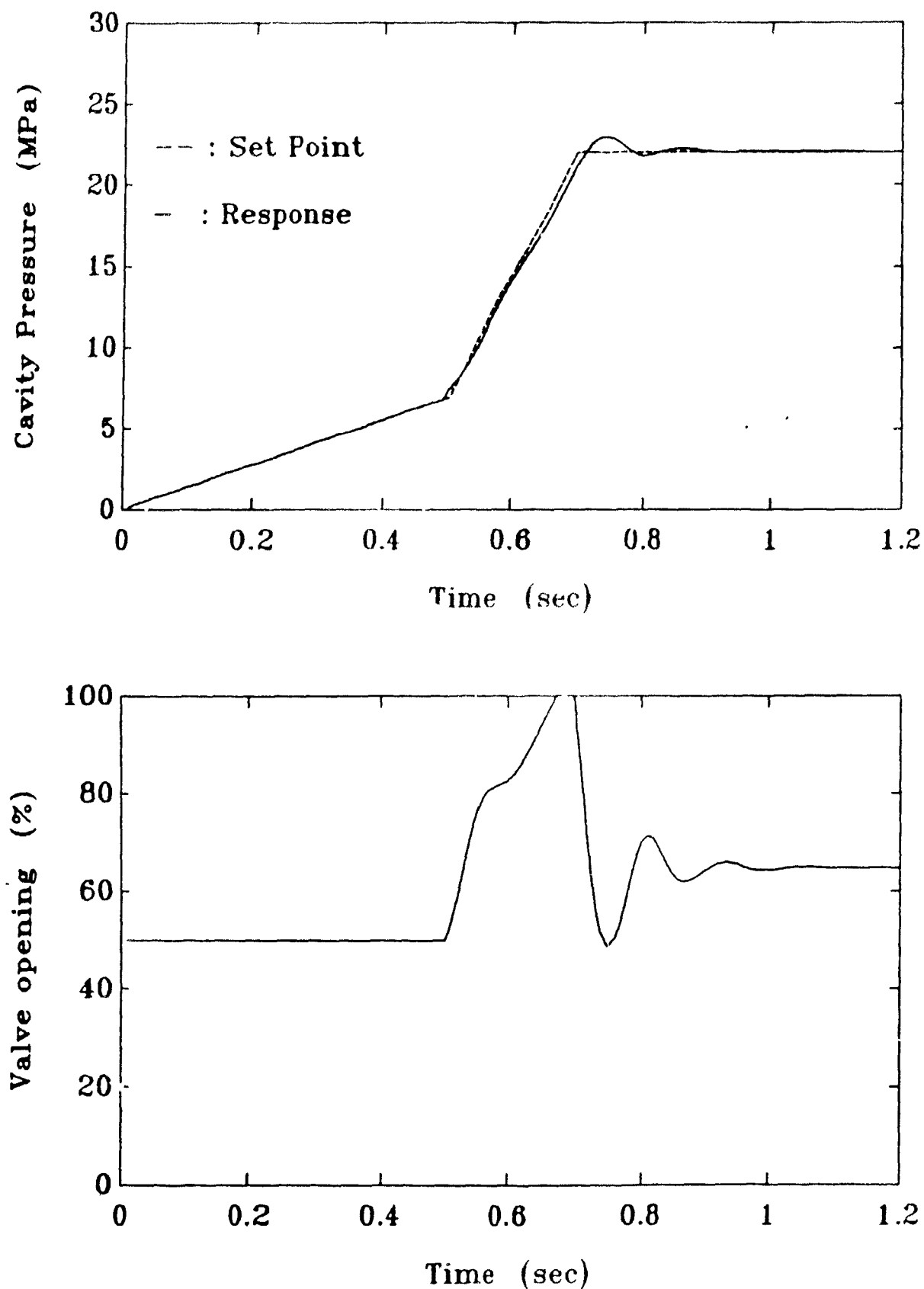


Figure 8.3 Control Simulation of Cavity Gate Pressure During Packing and Holding Stages Using a PI Controller.

experiments for the injection molding cycle :

- (a) Transfer based on the value of cavity gate pressure.
- (b) Transfer based on the change in the slope of cavity gate pressure - time profile.

8.2.2 Control of Peak Cavity and Hold Pressures

The objective of the first experiment was to test the capability of the new hydraulic system, presented in section 7.4.1, to control both the peak cavity and hold pressures at a constant level. The mold cavity was filled under open loop operation until the cavity gate pressure reached a preset value which assured complete filling of the cavity (EOF). Then, the operation was switched to closed loop control. The set point profile was chosen to be a step change from the EOF point to the peak cavity value at which the pressure was held constant for the specified holding time. The supply and relief servovalves were controlled by two separate PI controllers. The control scheme is shown in Figure 8.4. Both valves were operated with a full range of 0.0 - 100% opening.

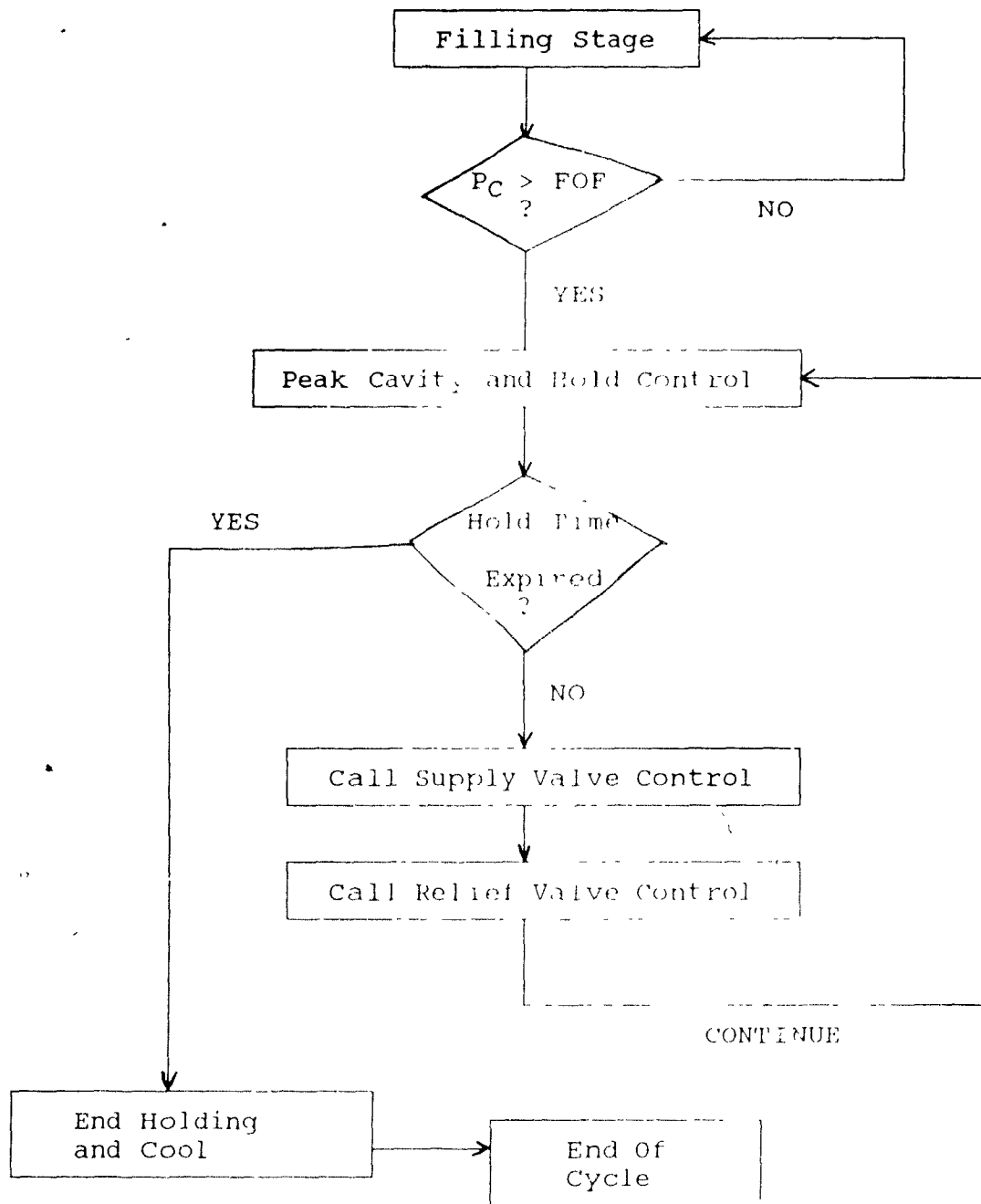


Figure 8.4 Peak Cavity and Hold Pressure Control Scheme Using Two Separate PI Controllers

The results shown in Figure 8.5 demonstrate the ability of the proposed control scheme to achieve peak cavity and hold pressure control. The initial large overshoot is caused by the initial large error due to the direct transfer from the end of filling to the peak pressure set point. The hold pressure response to set point pressure time profile is also investigated. Figure 8.6 demonstrates the possibility of controlling cavity hold pressure according to a pressure time profile set point control. Over hold pressure can be implemented with selection of control parameters in the controller (eq. 8.2).

8.2.3 Control of the Overall Injection Molding Cycle

The results of the previous section demonstrated the feasibility of peak cavity and hold pressure control using the new hydraulic system. The initial large overshoot is believed to be caused by the direct transfer from the end of filling point to the peak value without controlling the rapid pressure rise during the packing stage. Thus, it would be of more interest to control pressure during the very short packing stage. This section deals with the control of the injection molding cycle including the

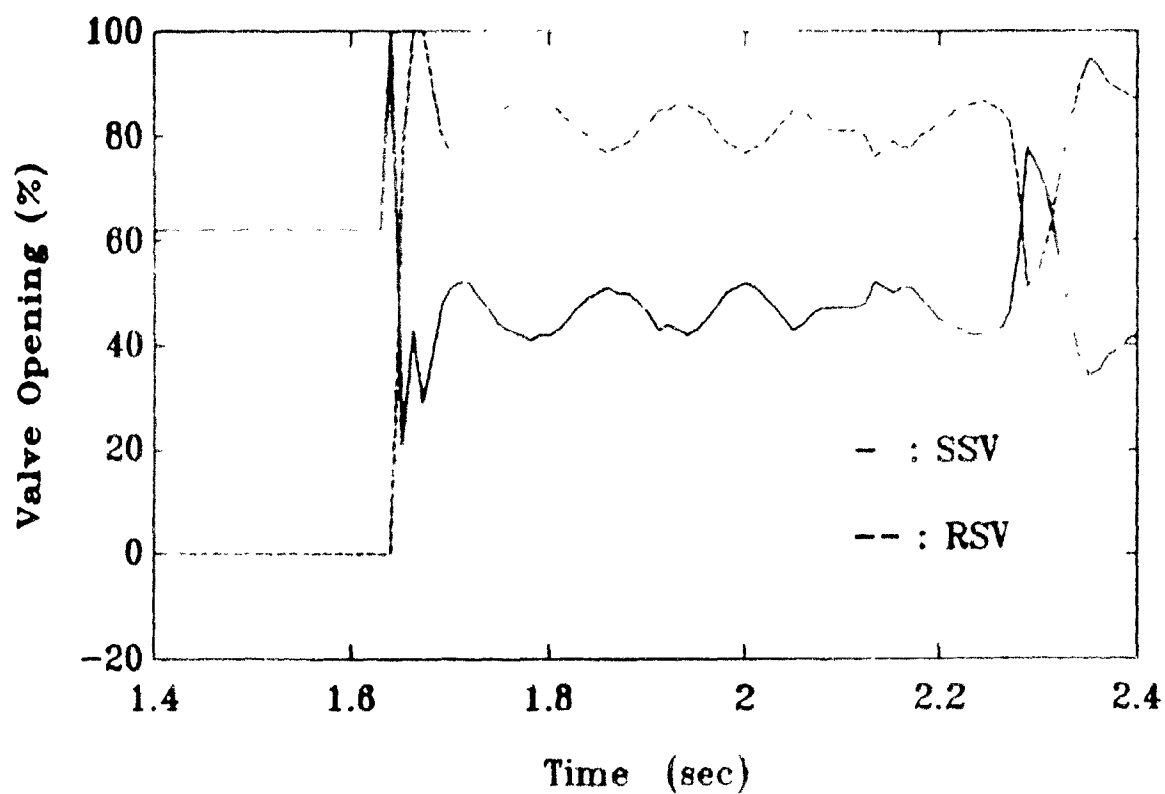
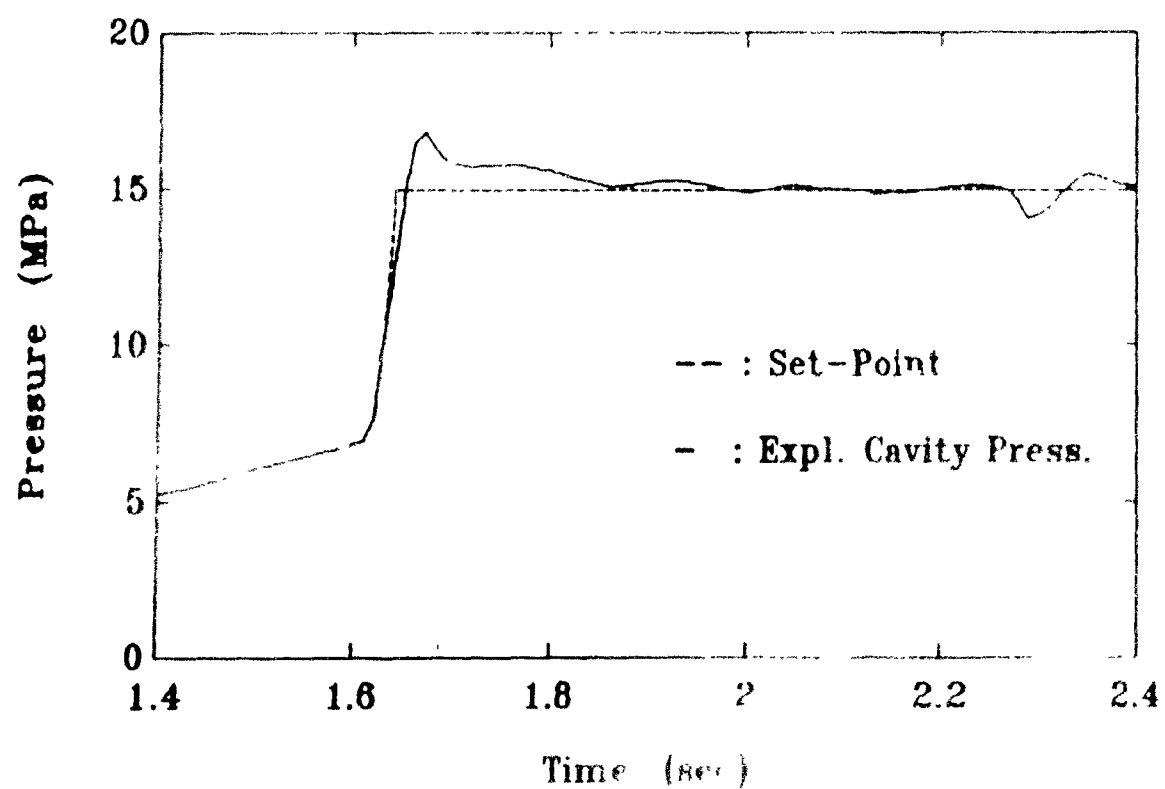


Figure 8.5 Control of Peak Cavity and Hold Pressure Using a PI Controller.

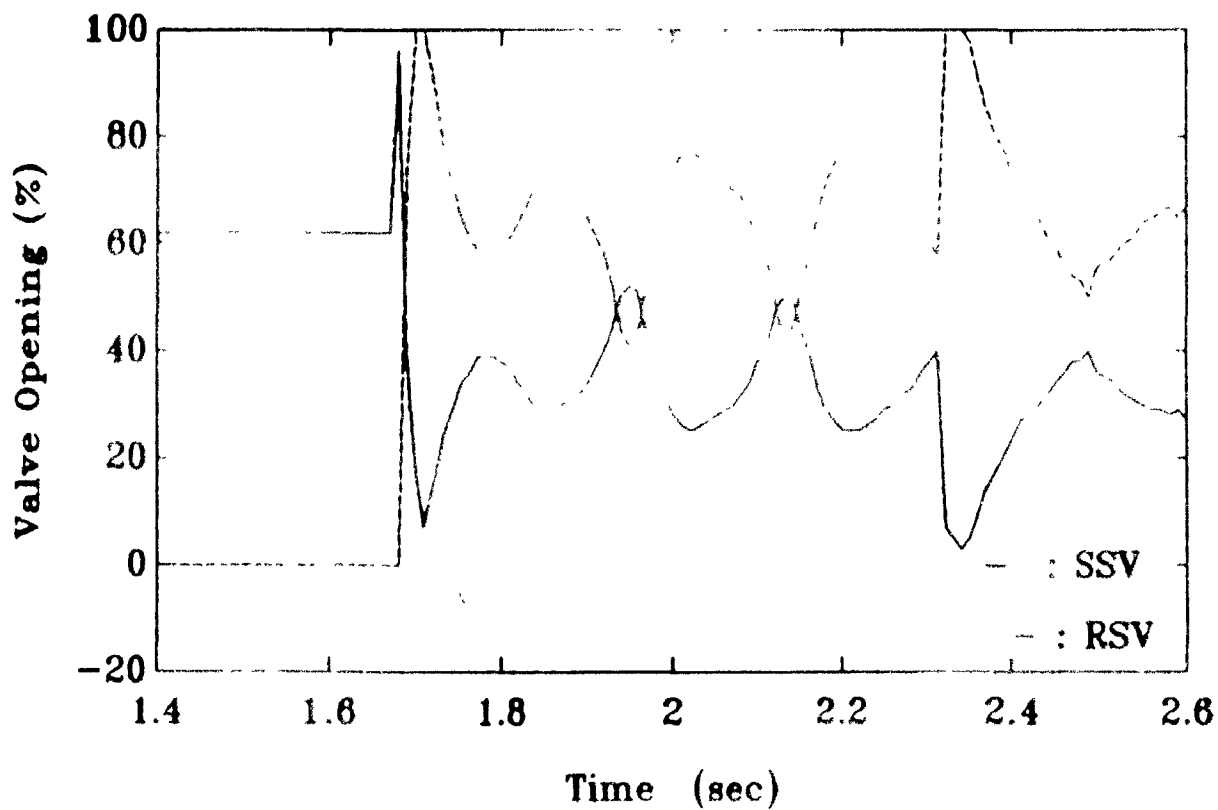
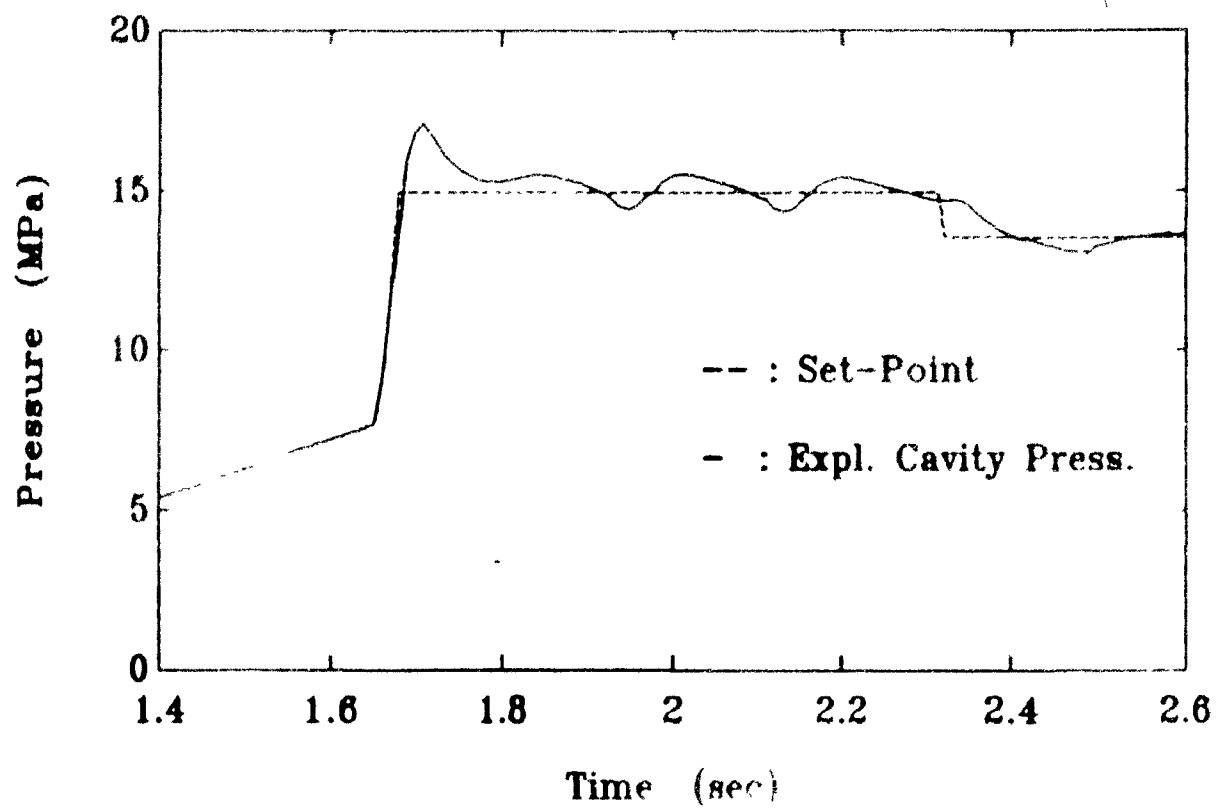


Figure 8.6 Control of Peak Cavity Pressure and a Variable Hold Pressure Using a PI Controller.

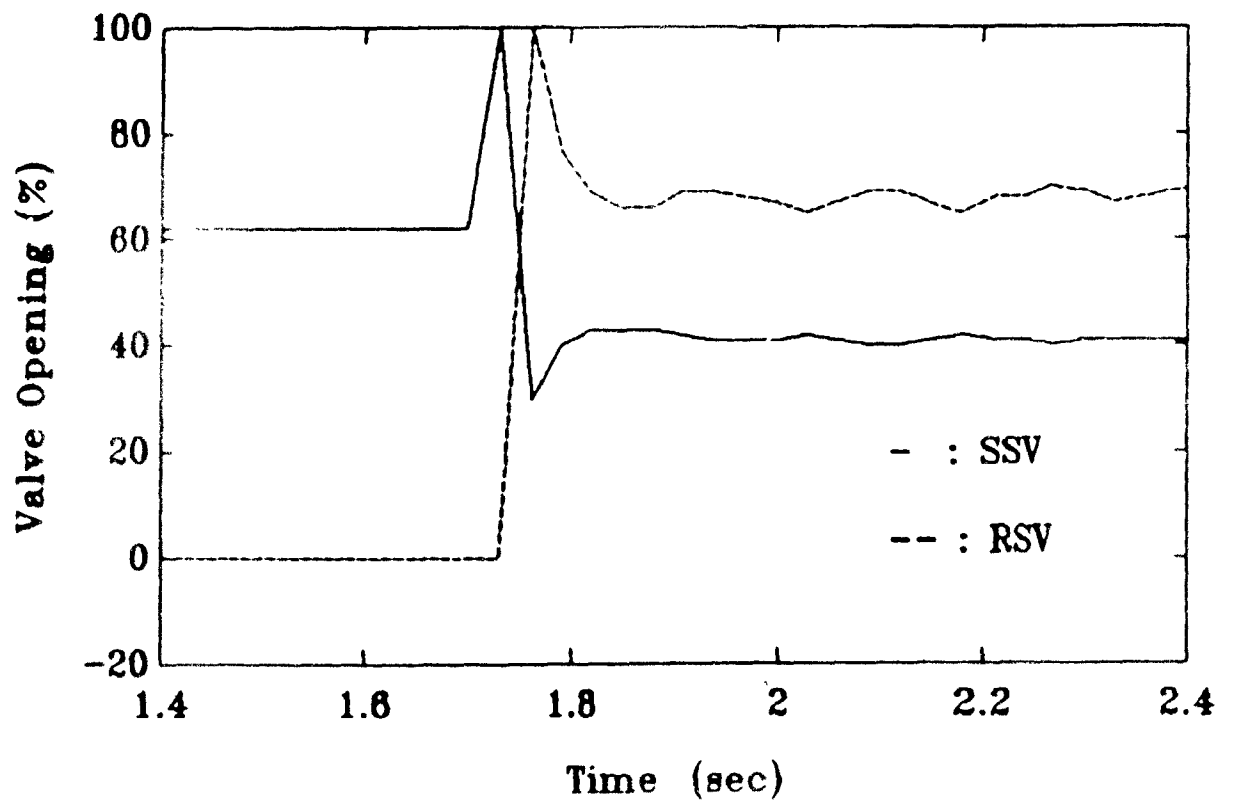
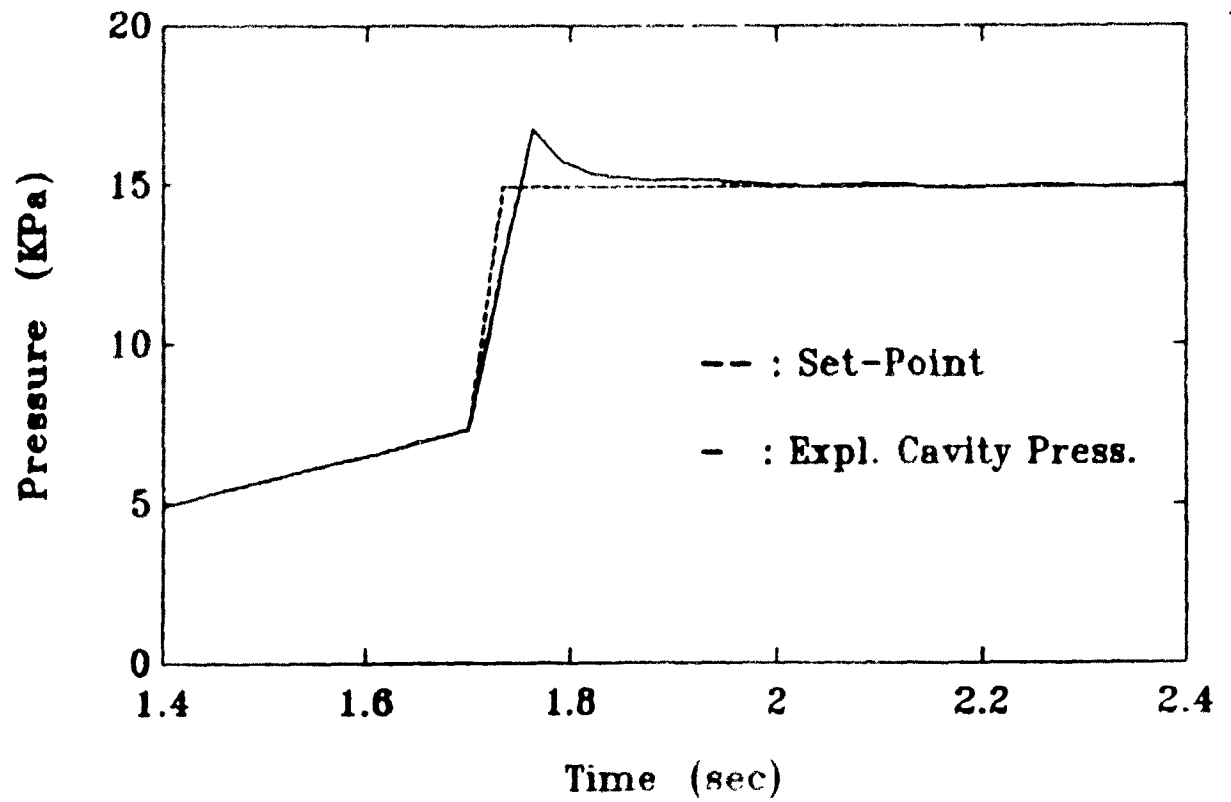


Figure 8.7 Improved Control of Peak Cavity and Hold Pressure Using a PI Controller.

control of filling, packing, peak cavity and hold pressures.

It was concluded in Chapter 5 that, in order to control cavity gate pressure during the filling stage, another process variable, preferably nozzle pressure, should be used at the beginning of the filling. In the following experiments control of filling was performed by controlling nozzle pressure until the cavity gate pressure reached a preset value. When a rapid drop in response of cavity gate pressure (20 psi or 1.3 MPa) subsequently, control was switched to the cavity pressure control loop. The end of filling was determined when a preset cavity gate pressure was reached, control was then switched to regulate the packing stage, and peak cavity and hold pressures. The control scheme is depicted in Figure 8.1. The supply and relief valves were manipulated according to one control law, a strategy discussed in Section 8.1.1 (Figure 8.2). The set point profile was chosen according to open loop experimental data and was composed of four parts. The first part is a rapidly increasing nozzle pressure at the start of filling. The second part is cavity gate pressure throughout the filling stage. The packing cavity gate pressure was set as a rapid ramp from the EOF to the peak cavity pressure value at which the pressure was held constant for the holding stage.

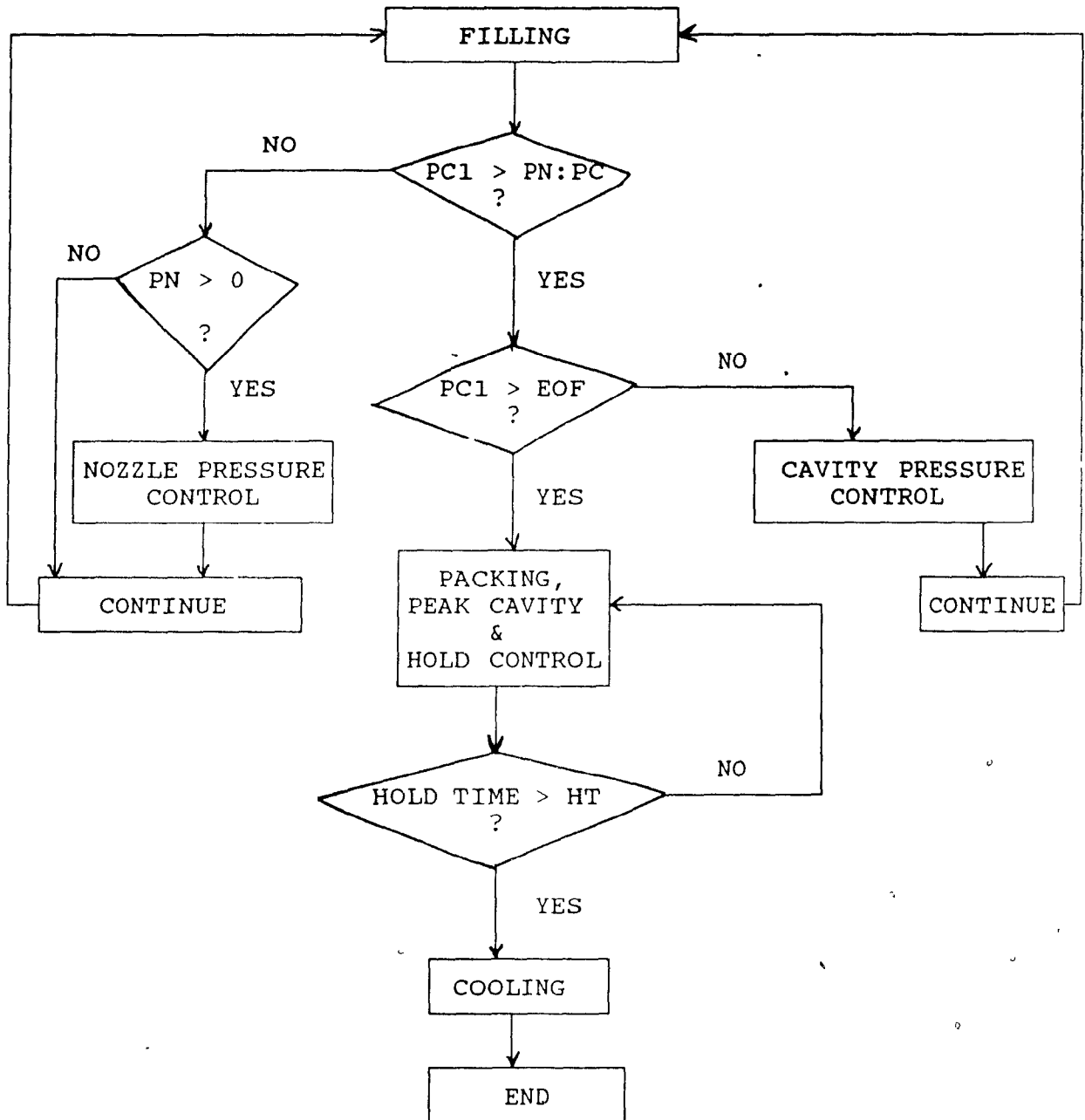


Figure 8.8: Control Scheme for Nozzle Pressure, Cavity Pressure, and Peak Cavity and Hold Pressure (See Nomenclature, Figure 8.13).

Several control experiments were performed with different combinations of the supply and relief valve openings. The supply valve was always operated with the full range of 0 - 100% opening and the opening of the relief valve was calculated according to Equation (8.1). The first set of experiments was performed with the maximum opening of the relief valve (MR_{MAX}) restricted to 50% and the ratio between the relief and supply valve openings (Y) set at 0.5. End of filling was determined as a cavity gate pressure of 1400 psi (9.6 MPa) which was chosen according to results from open loop experiments. The hold pressure control was run for a specified holding time. Figure 8.9 shows that satisfactory control was achieved for nozzle pressure even, in the presence of disturbances at the start of the injection. Good control was achieved over cavity pressure throughout the filling stage.

Three problems were encountered in the performance of peak cavity and hold pressure control: overshoot, long settling time and the oscillation of nozzle pressure (to the extent of dropping below the cavity gate pressure which causes back flow, a situation which is to be avoided). Possible causes for these problems are poor tuning of the controller in this stage, an ineffective combination of the supply and relief valves, or an unsuitable hold set point profile.

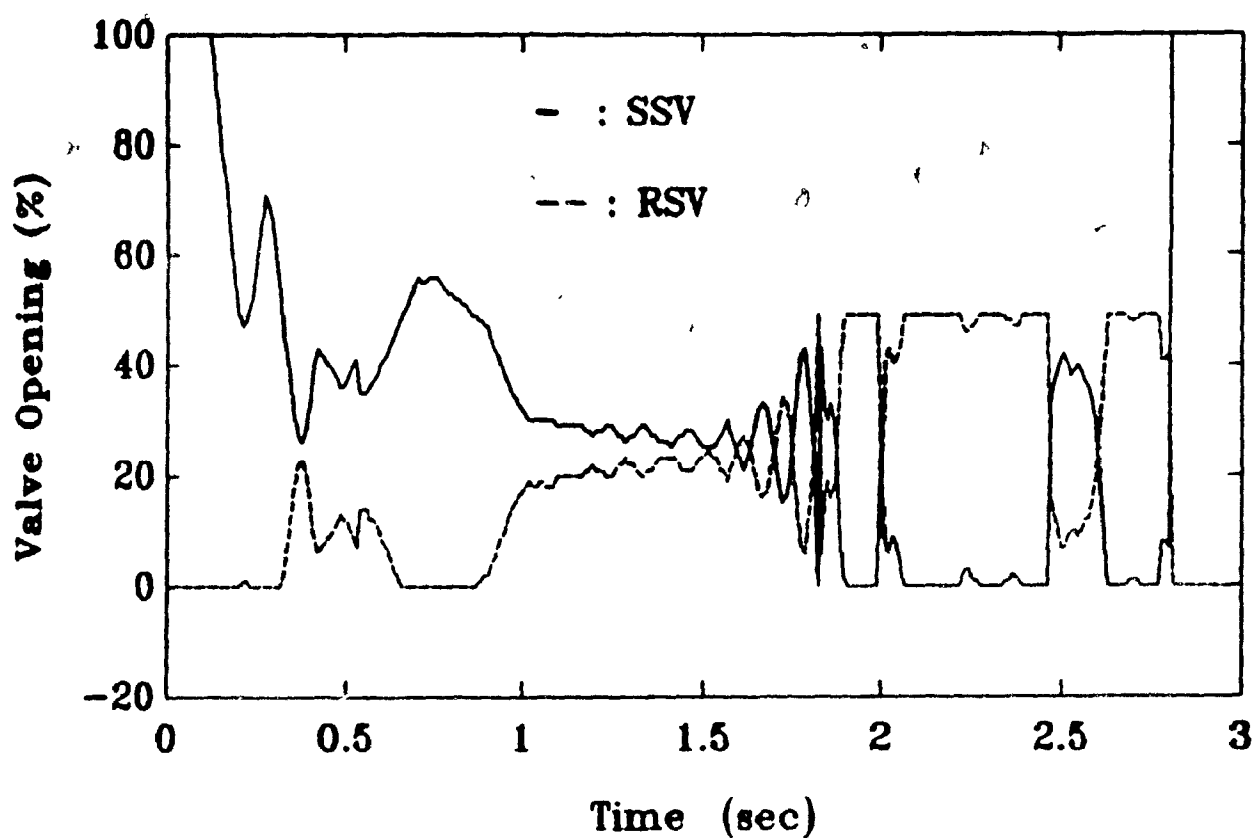
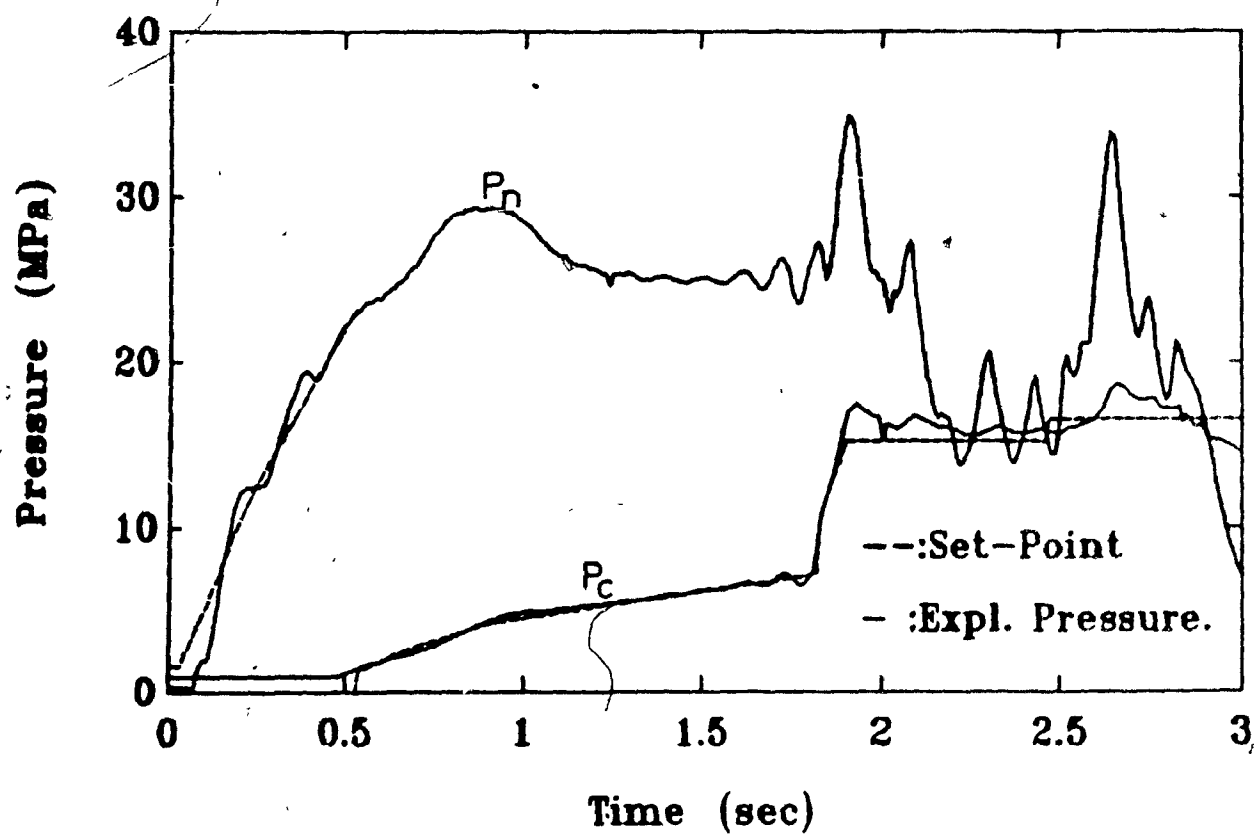


Figure 8.9 Control of Injection Molding Cycle Using a PI Controller.

The hold pressure controller was manually adjusted in the experiments represented by Figure 8.10. Improved results in terms of overshoot and settling time were obtained, but there was still excessive oscillation of nozzle pressure during the holding period. Figure 8.10 also shows that an increase in cavity pressure occurred during the holding but the controller did not respond with appropriate speed to correct the situation. These problems are believed to be due to the small role played by the relief valve which was operated only in the range of 0.0-50 % opening. Thus, the combination of supply and relief valve operated over the full range of 0 - 100% was evaluated. Experiments were performed with the same conditions as in Figure 8.10 with the new valve opening combinations. Much improved peak cavity and hold pressure control was obtained as shown in Figure 8.11.

A large number of experiments were carried out under the same processing conditions to test the reliability of the above control strategy. Very good reproducibility was obtained as shown in Figure 8.12. The results exhibited a drop in the nozzle pressure at the start of packing and a relatively large deviation between packing cavity pressure and its set point profile. This is due to the following reasons :

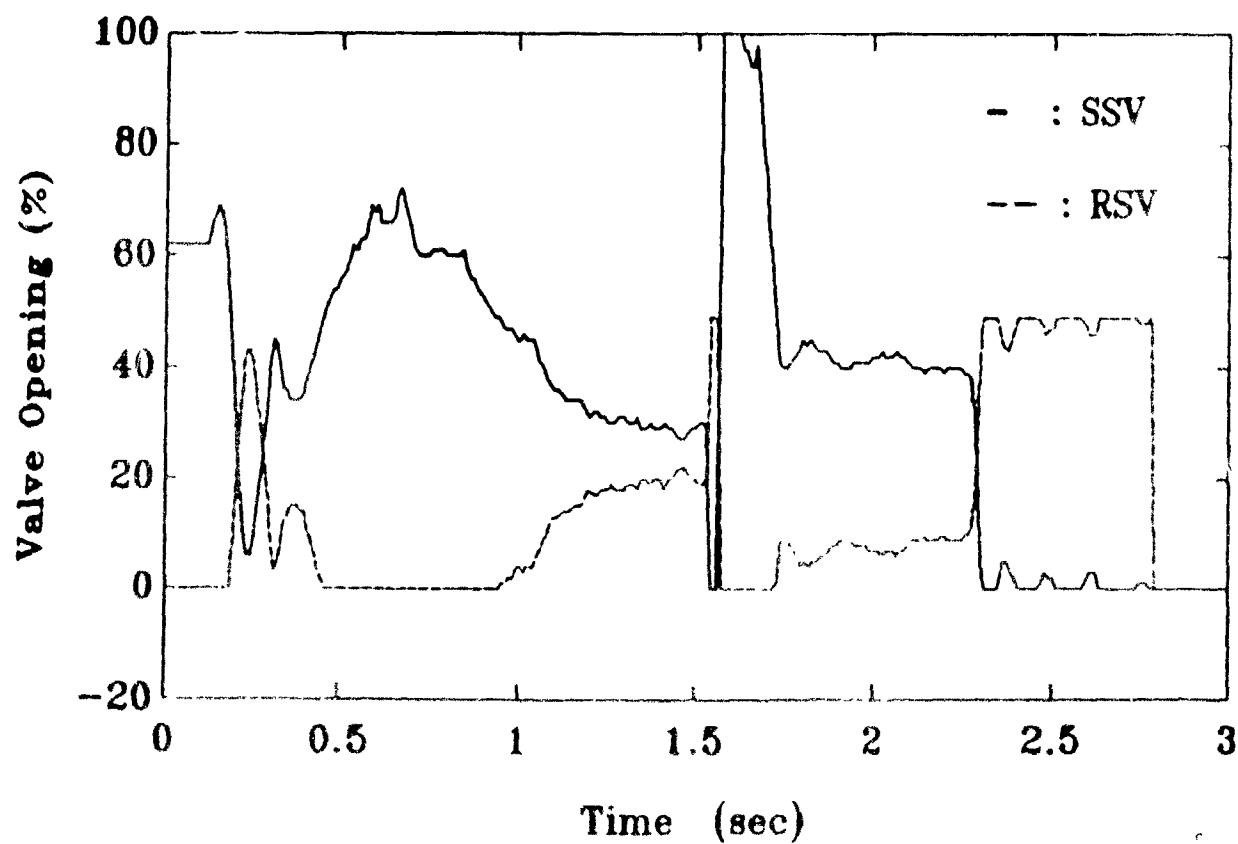
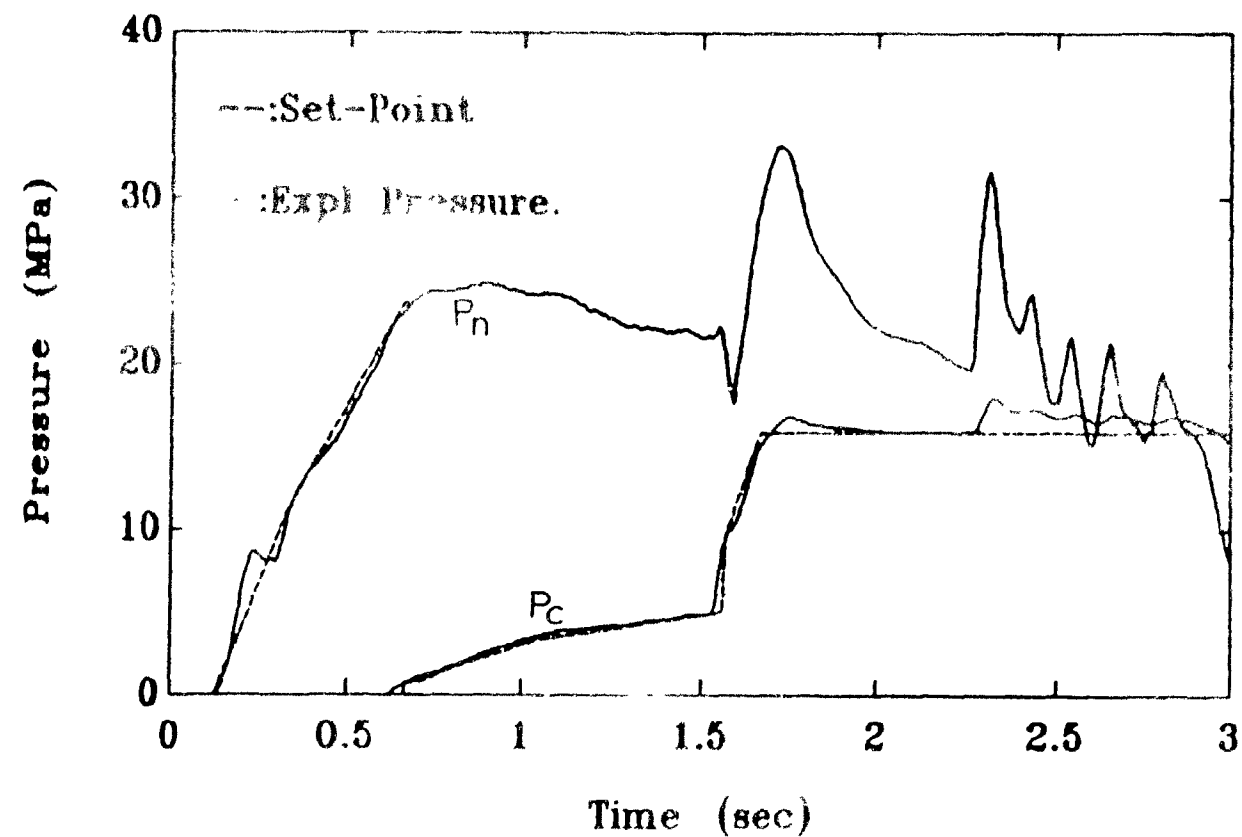


Figure 8.10 Control of Injection Molding Cycle with Retuned Hold Pressure Controller.

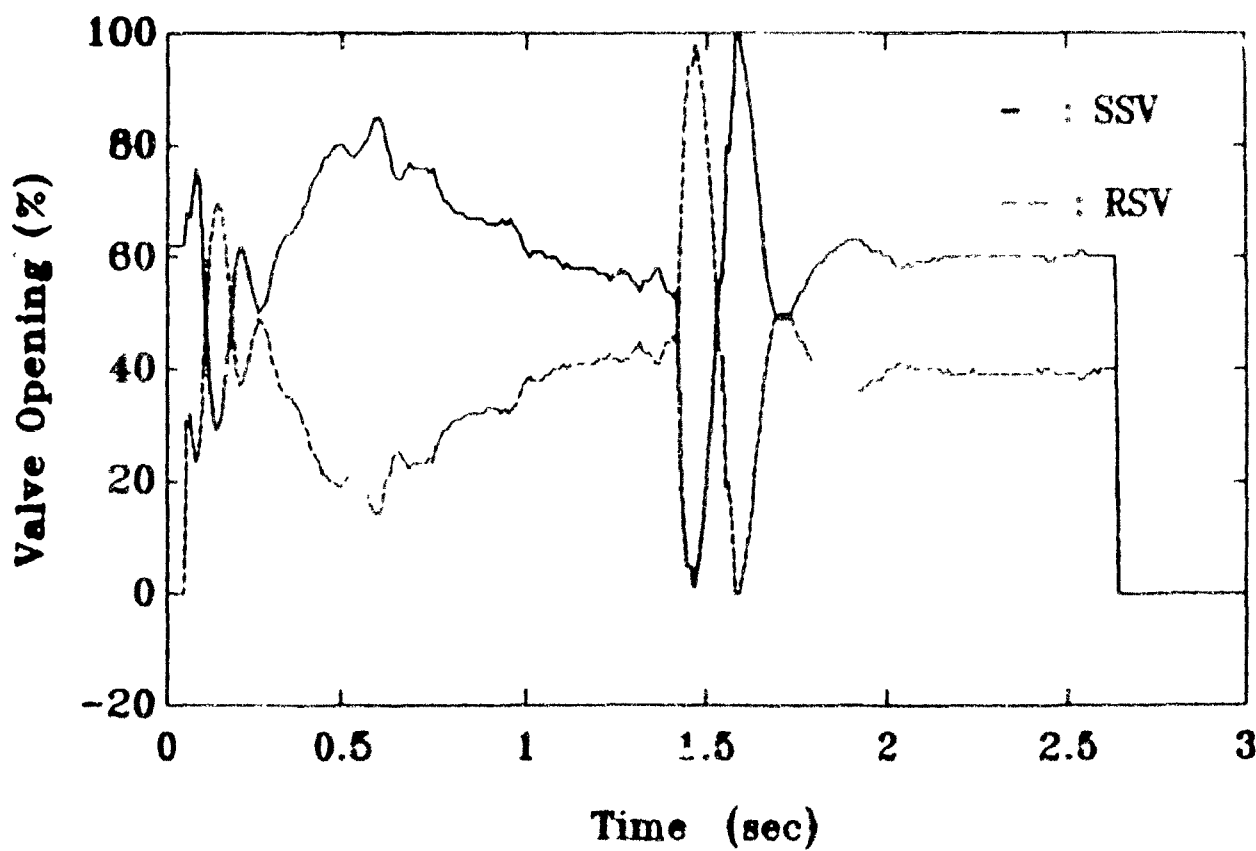
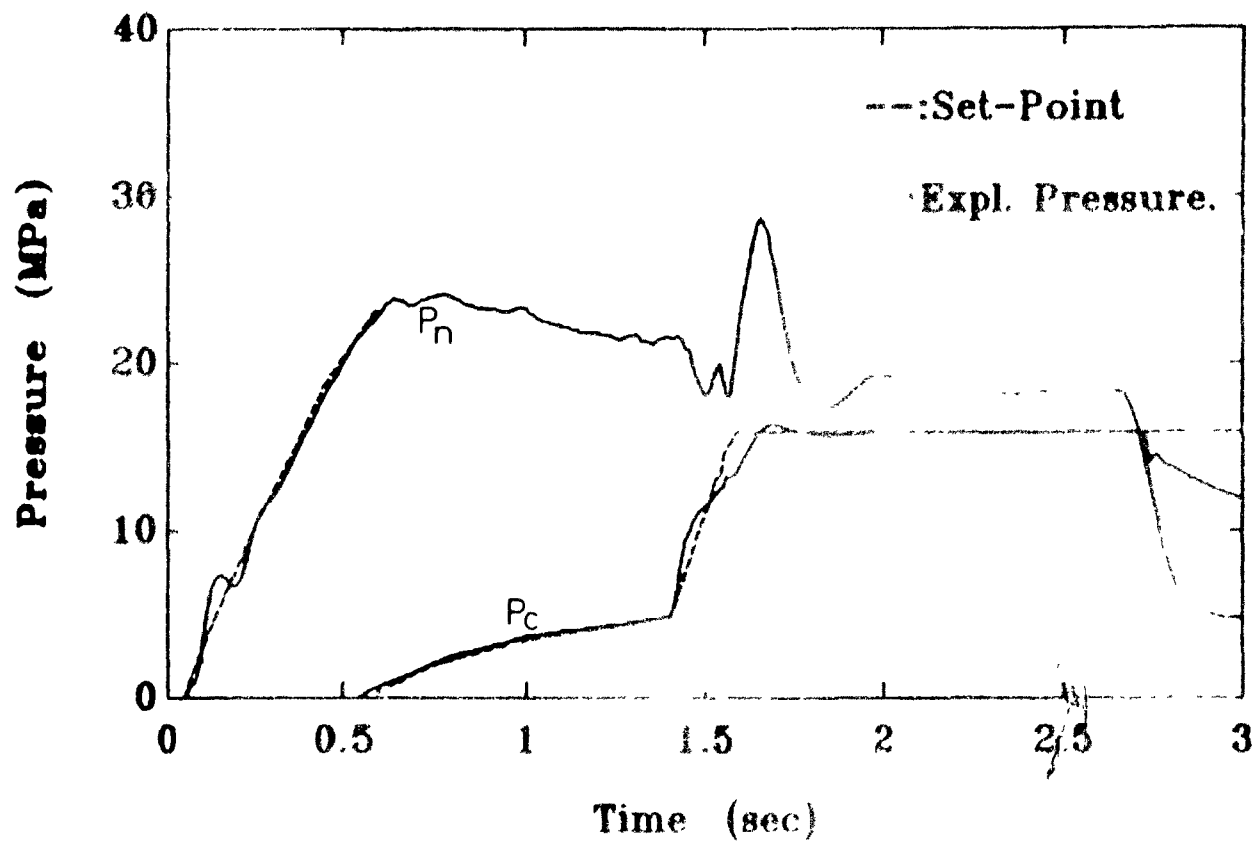


Figure 8.11 Control of Injection Molding Cycle Using a PI Controller with Full Scale Operation of Supply and Relief Valves.

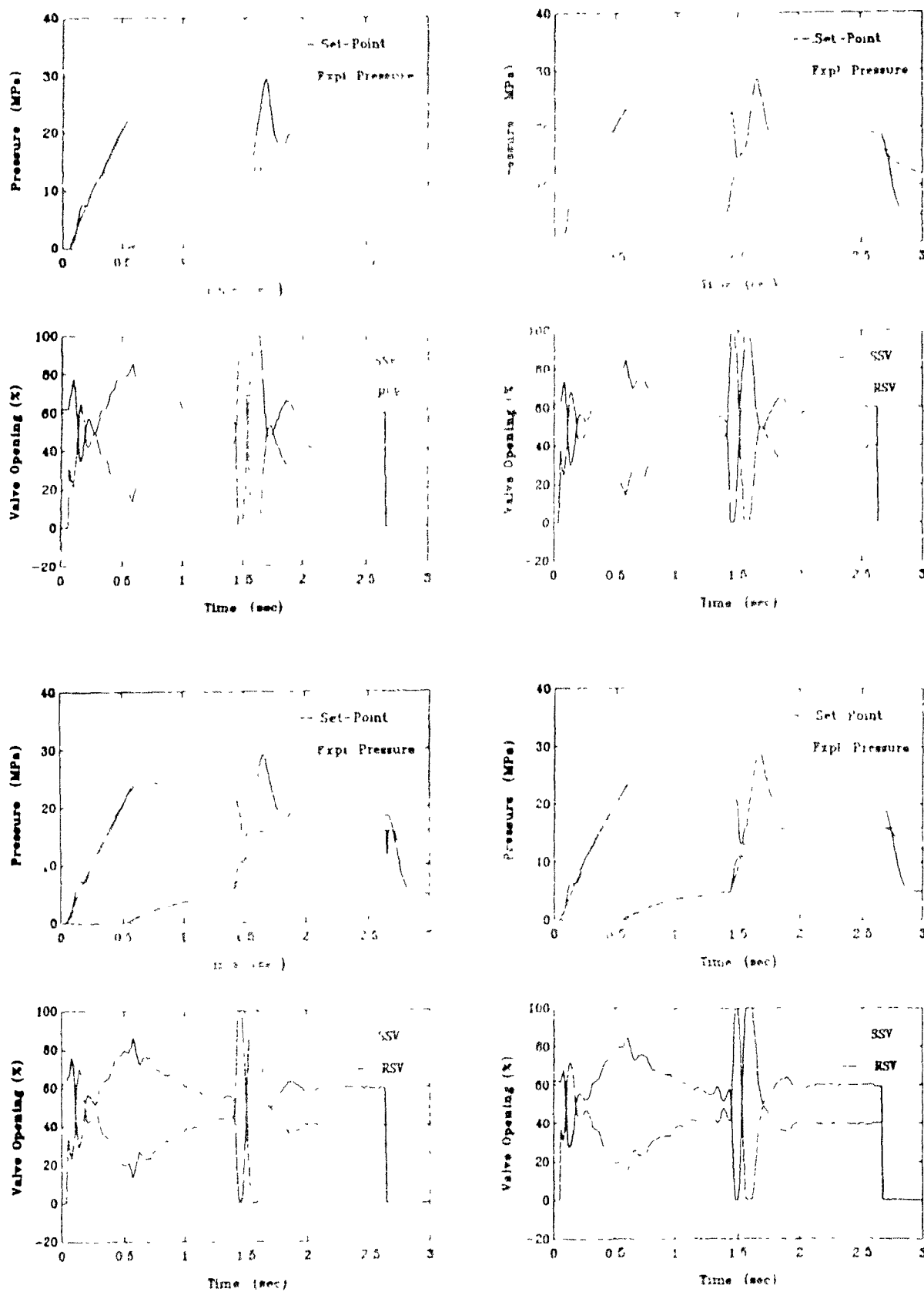


Figure 8.12 Reproducibility of the Control of Injection Molding Cycle.

- (a) uncertain detection of the end of filling and the consequent mismatching between the filling and the start of the packing set point profiles.
- (b) The choice of the packing pressure set point profile.

A new method was employed to detect the end of filling, based on the change in the slope of the cavity gate pressure time profile. Figure 8.13 presents the general control scheme where control is transferred the control from one variable to another during the injection molding cycle. A listing of the control program is given in Appendix I.

The packing stage for a large number of open loop experiments was examined and found to be well fit by a fourth order polynomial. Therefore, the set point profile for cavity gate pressure during the packing stage was chosen to be a fourth order polynomial projected from the detected end of filling point.

A typical result of injection molding cycle control using the above control strategy is given in Figure 8.14. The results demonstrate the complete control over the cavity pressure during the integrated filling and packing stages of the injection molding cycle. It is emphasized that the proposed strategy is independent of mold geometry and operating conditions.

Figure 8.13 - Nomenclature

PC1	:	Cavity gate pressure
PN	:	Nozzle Pressure
PN/PC	:	Cavity gate pressure value at which the control is switched from nozzle pressure control to cavity pressure control.
PN Control:		Control algorithm using nozzle pressure
S(t)	:	Slope of cavity gate pressure - time profile at time t
S(t-1)	:	Slope of cavity gate pressure - time profile at time t-1.
PC2	:	Cavity pressure at the second transducer position in the mold cavity (Figure 4.3).
PG	:	Cavity pressure gradient.
PC/PG	:	Value of PC2 at which the control is switched from cavity pressure control to cavity pressure gradient control.
PG Control:		Control algorithm which uses cavity pressure gradient.
PC Control:		Control algorithm for cavity gate pressure.
Packing Control	:	Packing stage control algorithm.

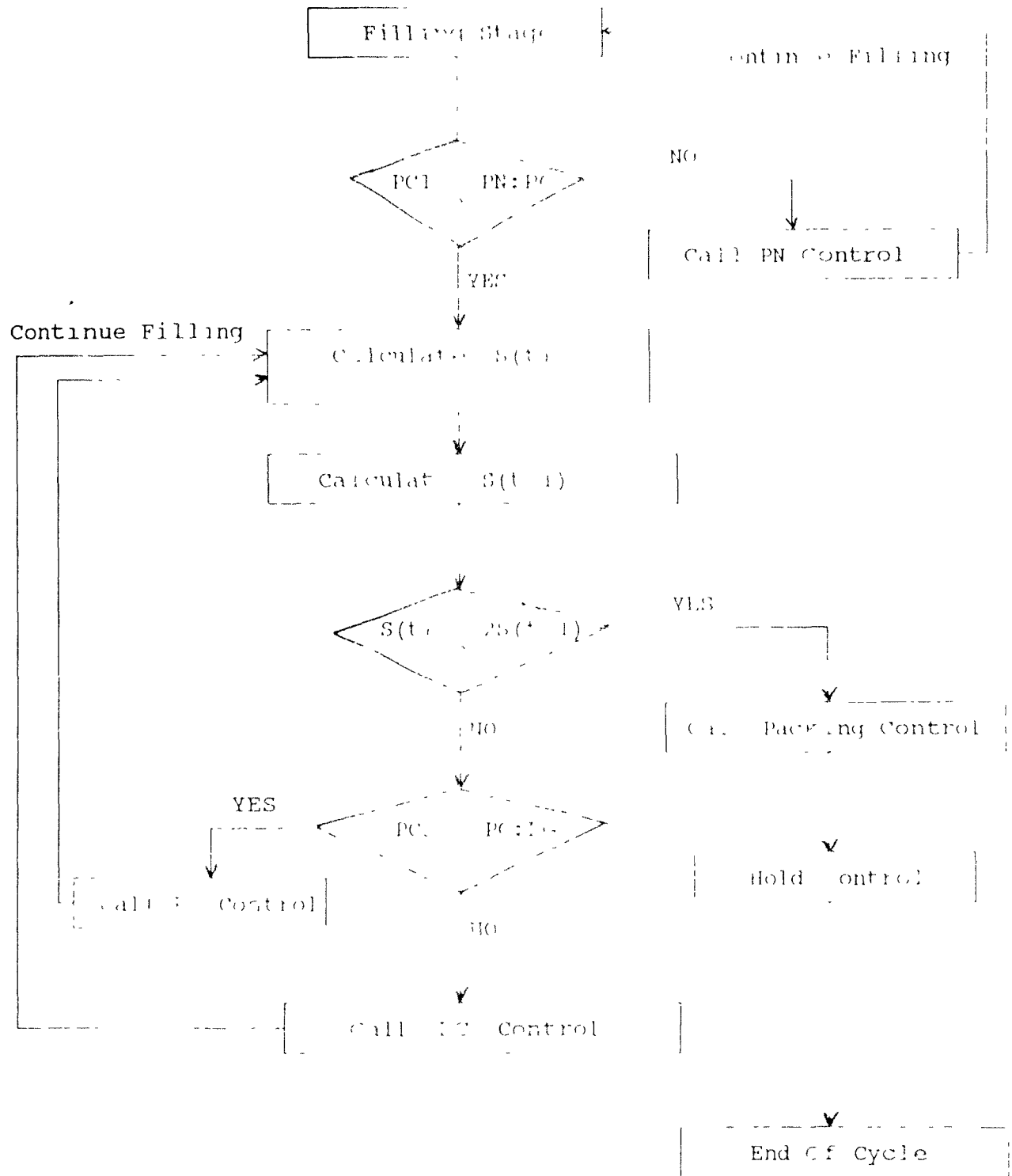


Figure 8.11 Overall Control Strategy for the Injection Molding Cycle

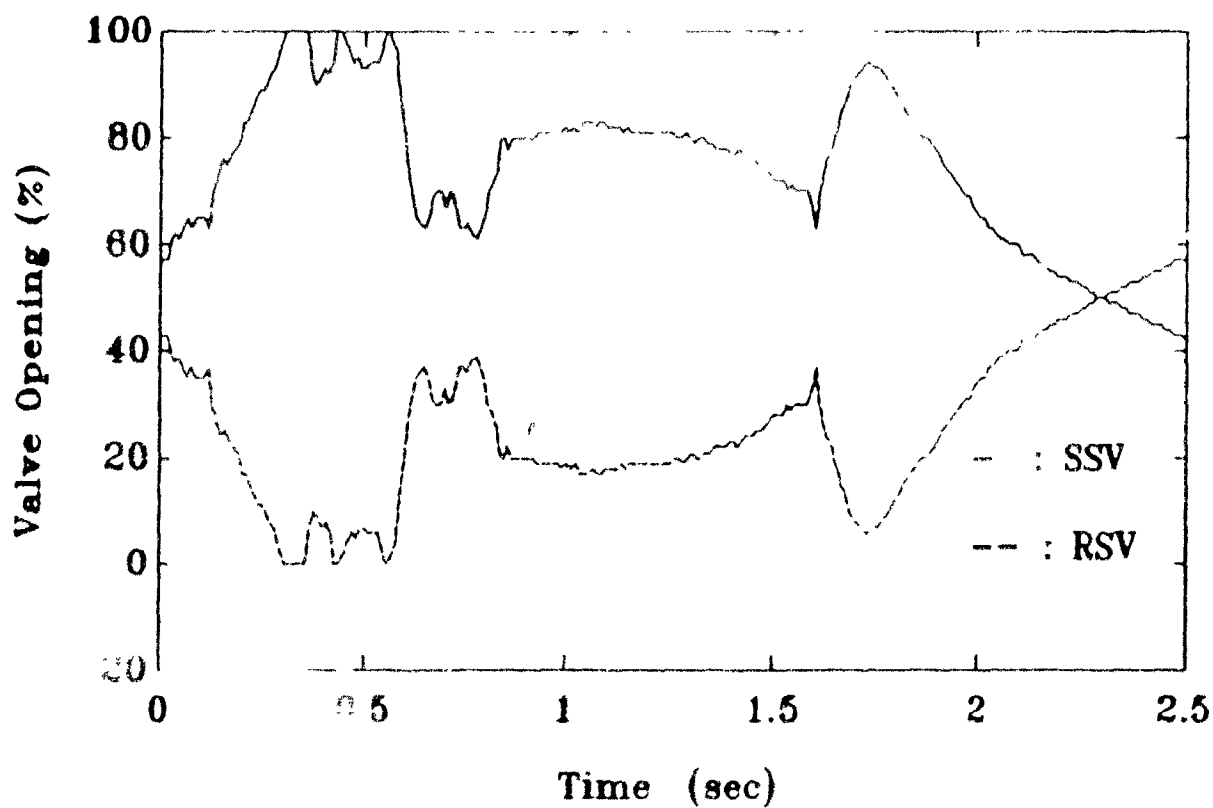
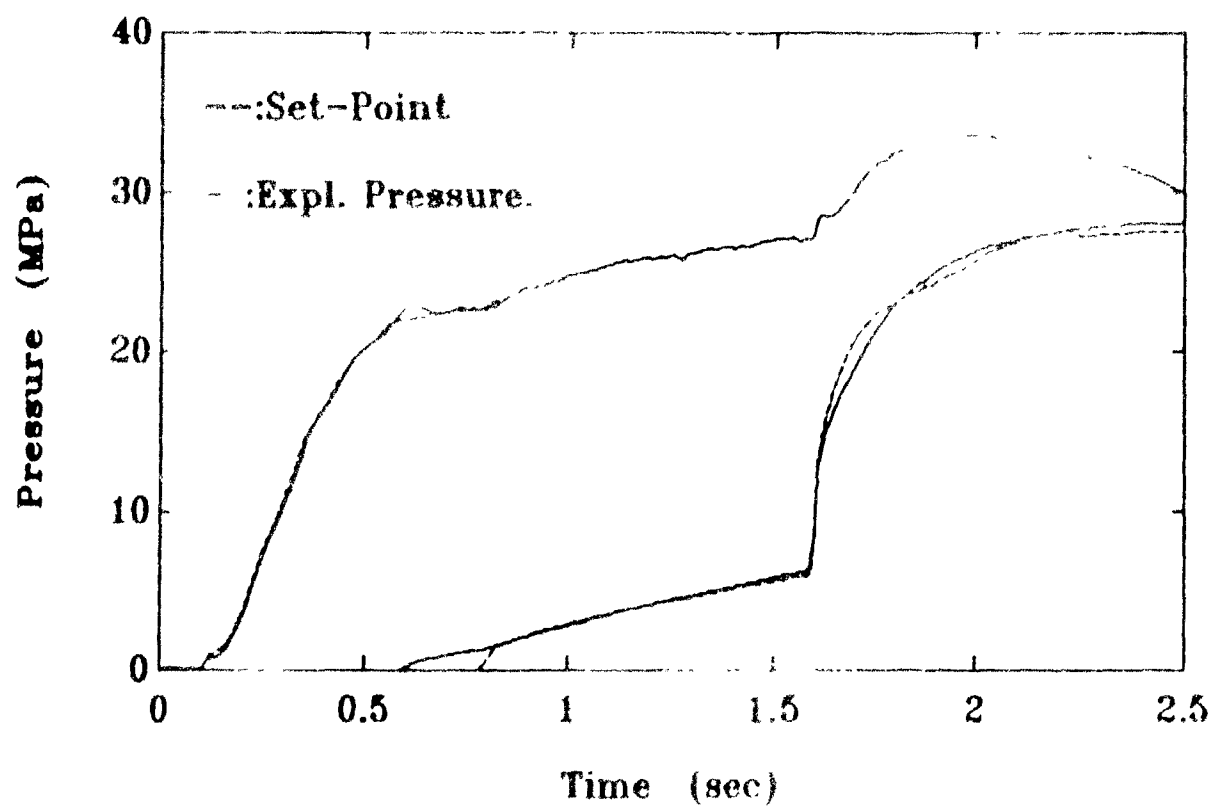


Figure 8.14 Control of Injection Molding Cycle Using an Overall Control Strategy.

8.3 Summary

The conclusions of this chapter are summarized as follows:

- (a) Good control of pressure, cavity profile, peak cavity and hold pressures was achieved using new hardware and software schemes. The best control results were obtained by using a combination of supply and retract servovalves, both operating over the full range (0-100% opening).
- (b) Injection and retraction controlled pressure profiles were the same for both the supply and retraction phases, avoiding pressure spikes.
- (c) End of fill can be detected by monitoring the change in the slope of the cavity rate pressure-time profile.
- (d) The overshoot of the cavity pressure, which can be prevented by accurate determination of the end of the filling stage and the use of proper parking of pump control. The best rate of profile to cavity rate pressure during the retraction stage was found to be fit by a fourth order polynomial of pressure with time.
- (e) Good and reliable integrated control over the filling, packing and holding stages of the injection molding cycle was achieved by a general control scheme which allows the transfer of control from one variable to another during the various stages of the process.

CHAPTER 9

CONCLUSIONS AND RECOMMENDATIONS9.1 Conclusions

The objectives of this research were to study the process dynamics of pressure variability in various parts and stages of the injection molding process and to achieve microcomputer control of pressure throughout the filling, packing and holding stages. These objectives were realized successfully.

9.1.1 Dynamic Studies

- (a) Cavity gate pressure response in the filling stage was best modeled by a first-order plus time delay superimposed on a constant (pressure) component. Good agreement was obtained between the experimental data and the fitted model.
- (b) The pressure variability in the filling stage of the process during the injection molding process was percent of the gate pressure at the start of the filling stage.
- (c) The top chamber pressure, the cavity pressure, nozzle pressure, and the mold pressure in the packing

stage were best modelled by a first-order plus time delay model.

- (d) The three pressure response (hydraulic, nozzle, and cavity) exhibited nonlinear behavior with respect to the degree of packing.

9.1.2 Control Studies

The dynamic models were employed to design and evaluate control schemes for the injection molding cycle. Nozzle and cavity pressures were used in conjunction with PI, PID and Dahlin controllers. The hydraulic system of the injection molding cycle was redesigned to incorporate two servovalves in order to achieve control over the cavity pressure-time profile during the packing stage as well as over peak cavity and hold pressure. The control loops were designed through a simulation study which also gave good indications of system limitations.

CONTROL SIMULATIONS

- (a) Hydraulic pressure was best controlled by a PI controller. Little improvement was obtained with a PID controller but the PI controller was very sensitive to changes in the parameters.

- (b) In the nozzle pressure control loop, PID has advantage over the PI controller. Both PID and Dahlin controllers gave satisfactory results.
- (c) Cavity pressure was well controlled by PI and PID controllers. Good control performance was achieved using the discrete models obtained by the two approximations for the dead time. The simpler model approximating the dead time by one sampling interval was chosen for control experiments.

CONTROL EXPERIMENTS

- (a) Good control over nozzle pressure during filling was obtained after an initial overshoot with PI, PID and Dahlin controllers.
- (b) The effect of nonlinearity in cavity gate pressure response appeared as an increasing oscillation at the end of filling.
- (c) The oscillatory behavior at the end of filling was rectified by using a sample gain scheduling control strategy.
- (d) Good control of peak cavity and mold pressures was achieved using new hardware and software schemes. The best control results were obtained by using a combina-

tion of supply and relief servovalves, both operating over the full range (0 - 100% opening).

- (e) Injection start up was controlled using nozzle pressure while the rest of the cycle was controlled using cavity gate pressure.
- (f) End of filling was best detected by monitoring the change in the slope of the cavity gate pressure-time profile.
- (g) Good and reliable integrated control over the filling, packing, and holding stages was achieved by a general control scheme which allows the transfer of control from one variable to another during the various stages of the process.

9.2 Recommendations

Detailed stochastic identification and application of modern control theory to the injection molding process would be desirable. Multivariable schemes have to be considered for control of the injection molding process.

The rapidly growing availability of powerful and inexpensive computer hardware and software capabilities provide opportunities for achieving on-line process identification and adaptive control techniques.

9.3 Claims For Original Work

- (1) The present study is the first attempt to obtain a detailed dynamic model useful for control of cavity pressure during the filling stage.
- (2) This study provides the first dynamic models for cavity gate pressure, nozzle pressure, and hydraulic pressure during the packing stage.
- (3) The present study is the first to achieve integrated cavity pressure control during the filling, packing, and holding stages, as well as control of peak cavity pressure.
- (4) The present study proposes a novel and dependable strategy to transfer control from the filling to the packing stages. The transfer strategy is based on the change in the slope of the cavity gate pressure-time profile.
- (5) A control strategy, introducing novel hardware and software schemes, was employed to achieve pressure control during the filling, packing and holding stages of the injection molding cycle.

REFERENCES

- 1 Andres, P, "Process Control and the Hydraulic Circuit", SPE Technical Papers, 29, 652 (1983)
- 2 Shaffer, R.R., "Digital Hydraulics for Injection Molding in the Computer Age", SPE Technical Papers, 31, 800 (1985)
- 3 Harris, H.E., "Computer Control of Large Numbers of Plastics Machines", SPE Technical Papers, 16, 430 (1970)
- 4 Hold, P., "Trends in Processing Equipment Advances During the 1970's", SPE Technical Papers, 16, 343 (1970)
- 5 Heldrich, G.C., "Computerization of Operations is a Challenge to Research Engineers", SPE Technical Papers, 16, 341 (1970)
- 6 Menges, G., S. Stitz and J. Vargel, "What Must be Known About Injection Molding for Computer Control", SPE Technical Papers, 18, 843 (1972)
- 7 Menges, G. and J. Vargel, "Injection Molding Process - Computer Controlled", SPE Technical Papers, 19, 516 (1973)
- 8 Hubbauer, P., "Controlling Injection Molding Parameters for Optimum Part Properties", SPE Technical Papers, 19, 523 (1973)
- 9 Inslee, T., "The Use of Computer in Injection Molding", SPE Technical Papers, 20, 260 (1974)
- 10 Hunkar, D.B., "On Line Process Diagnostics - A Tool for Technical Management of an Injection Molding Plant", SPE Technical Papers, 29, 655 (1983)
- 11 Forrester, J., "An Approach to Computerized Injection Molding Operations", SPE Technical Papers, 29, 666 (1983)

- 12 Hellmeyer, H.O. and G. Menges, "Applications of Process Computers for the Control and Optimization of the Injection Molding Process", SPE Technical Papers, 22, 386, (1976)
- 13 Medley, J., "The Opportunities & Challenges of Using Process Control Devices for Injection Molding Machines", SPE Technical Papers, 29, 650 (1983)
- 14 Halsall, K., "A Rational Route to Unattended Molding", Plast. Eng., January, 69 (1985)
- 15 Golden, N.H., "An Experimental Evaluation of a Peak Cavity Pressure Controller in Injection Molding", SPE Technical Papers, 21, 158 (1975)
- 16 Paulson, D.C., "Closed Loop Control Brings Ten-Fold Gain in Molded Part Accuracy", Modern Plastics, 56, August (1979) P. 60
- 17 Recker, H. and G. Menges, "Methods for Indirect Measurement of Internal Mold Pressure", SPE Technical Papers, 28, 327, (1982)
- 18 Stitze, S., SPE Technical Papers, 27, 775 (1981)
- 19 Johannaber, F., SPE Technical Papers, 26, 146 (1980)
- 20 Hieber, C., G. Vandengel and H. Chiang, "Cavity Pressure Variations During the Post-Filling Stage of Injection Molding", SPE Tech. Papers, 32, 181 (1986)
- 21 Fasol, K.H. and H.P. Jorgl, "Principles of Model Building and Identification", Automatica, 16, 505 (1980).
- 22 Isermann, R., "Practical Aspects of Process Identification", Automatica, 16, 575 (1980).
- 23 Astrom, K.J. and P. Eykhoff, "System Identification - A Survey", Automatica, 7, 123 (1971).
- 24 Nieman, Fisher and Seborg, Int. J. Control, 13, 209 (1971).
- 25 Gustavsson, I., L. Ljung and T. Soderstrom, "Survey Paper: Identification of Processes in Closed Loop - Identifiability and Accuracy Aspects", Automatica, 13, 59 (1977).

- 26 Franklin, G.F. and J.D. Iowell, "Digital Control of Dynamic Systems", Addison Wesley, Reading MA (1980).
- 27 Smith, C.L., "Digital Computer Process Control", Intext Educational Publisher, N.Y (1972).
- 28 Deshpande, P.B. and R.H. Ash, "Elements of Computer Process Control", ISA, Research Triangle Park (1981).
- 29 Isermann, R., "Digital Control Systems", Springer-Verlag, NY (1981)
- 30 Box, G.E.P. and G.M. Jenkins, "Time Series Analysis: Forecasting and Control", Holden-Day, San Francisco (1976).
- 31 Saridis, G.N., "Comparison of Six On-Line Identification Algorithms", Automatica, 10, 69 (1974).
- 32 Isermann, R., U. Baur, W. Bamberger, P. Kneppo and H. Siebert, "Comparison of Six On-Line Identification and Parameter Estimation Methods", Automatica, 10, 81 (1974).
- 33 Baur, U. and R. Isermann, "On-Line Identification of a Heat Exchanger with a Process computer - A Case Study", Automatica, 13, 487 (1977).
- 34 Sinha, N.K. and A. Sen, "Comparison of Some On-Line Identification Methods for a Simulated First Order Process", Aut. Cont. Theory and Applications, 2, 37 (1974).
- 35 Sinha, N.K. and A. Sen, "Comparison of Six Different Methods for On-Line Estimation of the Parameters of a Daul-Input Heat Exchanger", Aut. Cont. Theory and Applications, 3, 62 (1975).
- 36 Donovan, R.C., D.E. Thomas and D. Leversen, "An experimental Study of plasticating in a Reciprocating Screw Injection Molding Machine", Polym. Eng. Sci., 11, 353 (1971)
- 37 Donovan, R.C., "A theoretical Melting Model for plasticating Extruders", Polym. Eng. Sci., 11, 247 (1971)
- 38 Donovan, R.C., "A theoretical Model for a Reciprocating-Screw Injection Molding Machine", Polym. Eng. Sci., 11, 361 (1971)

- 39 Hillier, M.J., "Analysis of the In-Line Screw Injection Machine", Polym. Eng. Sci., 7, 175 (1967)
- 40 Chung, C.I., R.J. Nichols and G.A. Kruder, "Screw Horsepower Dependence on Screw Speed and Size-Theory and Experiment", Polym. Eng. Sci., 14, 28 (1974).
- 41 Donovan, R., "The Plasticating Process in Injection Molding", Polym. Eng. Sci., 14, 101 (1974).
- 42 Gissing, K. and W. Knappe, "Analysis of Plastizising Time During Injection Molding", Kunststoffe, 72 (2), 78 (1982).
- 43 Lipshitz, S.D., R. Lavie and Z. Tadmor, "A Melting Model for Reciprocating Screw Injection Molding Machines", Polym. Eng. Sci., 14, 553 (1974)
- 44 Tadmor, Z., S.D. Lipshitz and R. Lavie, "Dynamic Model of a plasticating Extruder", Polym. Eng. Sci., 14, 112 (1974)
- 45 M.R. Kamal, W.I. Patterson, and V. Gomes, "An Injection Molding Study: Melt and Barrel Temperature Dynamics Part I", Polym. Eng. Sci., 26, 854 (1986).
- 46 Ballman, R.L., T. Shusman, and J.L. Toor, "Injection Molding - Flow of a Molten Polymer in a Cold Cavity", Ind. Eng. and Chemistry, July, 847 (1959)
- 47 Barrie, I.T., "Understanding How an Injection Mold Fills", SPE Journal, 27, 64 (1971)
- 48 Harry, D.H. and R.G. Parrott, "Numerical Simulation of Injection Molding", Polym. Eng. Sci., 10, 209 (1970)
- 49 Berger, J.L. and C.G. Gogos, "A Numerical Simulation of the Cavity Filling Process", Polym. Eng. Sci., 13, 102 (1973)
- 50 Wu, P.C., C.F. Huang and C.G. Gogos, "Simulation of the Mold Filling Process", Polym. Eng. Sci., 14, 223 (1974)
- 51 Kamal, M.R. and S. Kenig, "The Injection Molding of Thermoplastics Part I: Theoretical Model", Polym. Eng. Sci., 12, 294 (1972)

- 52 Kamal, M.R. and S. Kenig, "The Injection Molding of Thermoplastics Part II: Experimental Test of the Model", Polym. Eng. Sci., 12, 302 (1972)
- 53 Kamal, M.R., Y. Kuo and P.H. Doan, "The Injection Molding Behaviour of Thermoplastics in Thin Rectangular Cavities", Polym. Eng. Sci., 15, 863 (1975)
- 54 Chung, T.S. and M.E. Ryan, "Analysis of the Packing Stage in Injection Molding", Polym. Eng. Sci., 21, 271 (1981)
- 55 Borger, E., C. Gutfinger and Z. Tadmor, "A Theoretical Model for the Cavity Filling Process in Injection Molding", Trans. Soc. Rheol., 19, 423 (1975)
- 56 White, J.L., "Fluid Mechanical Analysis of Injection Mold Filling", Polym. Eng. Sci., 15, 44 (1975)
- 57 Williams, G. and H.A. Lord, "Mold-Filling Studies for the Injection Molding of Thermoplastic Materials. Part I: The Flow of Plastic Materials in Hot-and Cold-walled Circular Channels", Polym. Eng. Sci., 15, 553 (1975)
- 58 Lord, H.A. and G. Williams, "Mold-Filling Studies for Injection Molding of Thermoplastic Materials. Part II: The Transient Flow of Plastic Materials in the Cavities of Injection Molding Dies", Polym. Eng. Sci., 15, 569 (1975)
- 59 Barrie, I., "Understanding How an Injection Mold Fills", SPE Journal, 27, 64 (1971)
- 60 Kuo, Y. and M.R. Kamal, "The Fluid Mechanics and Heat Transfer of Injection Mold Filling of Thermoplastic Materials", A.I.Ch.E. Journal, 22, 661 (1976)
- 61 Ryan, M.E. and T.S. Chung, "Conformal Mapping Analysis of Injection Mold Filling", Polym. Eng. Sci., 20, 642 (1980)
- 62 Wang, K.K. et.al., Injection Molding Project, College of Engineering, Cornell University, Progress Report # 6, September (1979)
- 63 Lafleur, P.G. and M.R. Kamal, "Computer Simulation of Thermoplastic Injection Molding", Adv. Polym. Tech., 1 (4), 8 (1981)

- 64 Kamal, M.R., E. Chu, P.G. Lafleur and M.E. Rayan, "Computer Simulation of Injection Mold Filing for Vescoelastic Melts with Fountain Flow", SPE Technical Papers, 29, 818 (1983)
- 65 Clark, E.S., "Morphology and Properties of Injection Molded Crystalline Polymers", Polymer Preprints, 14 (1), 268 (1973)
- 66 Boehme, E., Kunststoffe, 60, 273 (1970)
- 67 Kantz, M.R., H.D. Newman and F.H. Stigale, "The Skin-Core Morphology and Structure-Property Relationships in Injection Molded Polypropylene", J. Appl. Polym. Sci., 16, 1249 (1972)
- 68 Fitchmun, D.R. and Z. Mencik, "Morphology in Injection - Molded polypropylene", J. Polym. Sci.: Polym. Phys. Ed., 11, 951 (1973)
- 69 Hobbs, S.Y. and C.F. Pratt, "The Effect of Skin - Core morphology on the Impact Fracture of Poly-(Butylene Terephthalate)", J. Appl. Polym. Sci., 19, 1701 (1975)
- 70 Henke, S.J., C.E. Smith and R.F. Abbott, "Effect of Mold Temperature on the Morphology and Properties of polypropylene : I. A Propylene-Ethylene Copolymer", Polym. Eng. Sci., 15, 79 (1975)
- 71 Tan, V. and M.R. Kamal, "Morphological Zones and Orientation in Injection - Molded Polyethylene", J. Appl. Polym. Sci., 22, 2341 (1978)
- 72 Tan, V. and M.R. Kamal, "The Effect of Processing Variables on the Distribution of Morphological Zones and Orientation in Injection - Molded Polyethylene", Science and Technology of Polymer Processing, Suh and Sung (eds.), 1979
- 73 Kamal, M.R., D.M. Kalyon and J.M. Dealy, "An Integrated Experimental Study of the Injection Molding Behavior of Some Polyethylene Resins", Polym. Eng. Sci., 20, 1117 (1980)
- 74 Moy, H.F. and M.R. Kamal, "Crystalline and Amorphous Orientation in Injection Molded Polyethylene", Polym. Eng. Sci., 20, 975 (1980)
- 75 Seferis, J.C. and R.J. Samuels, "Coupling of Optical and Mechanical Properties in Crystalline Polymers", Polym. Eng. Sci., 19, 975 (1979)

- 76 Spencer, R.S. and G.D. Gilmore, J. Colloid Sci., 6, 118 (1958)
- 77 Menges, G. and G. Wubken, "Influence of Processing Conditions on Molecular Orientation in Injection Moldings", Technical Papers, 31st ANTEC, 19, 519 (1973)
- 78 Bakerdjian, Z. and M.R. Kamal, "Distribution of Some Physical Properties in Injection-Molded Thermoplastic Parts", Polym. Eng. Sci., 17, 96 (1977)
- 79 Fleissner, M. and E. Paschke, "Orientation Conditions and Mechanical Properties of Thin-Wall Injection Moldings HD Polyethylene", Kunststoffe, 61, 195 (1971)
- 80 Paschke, E., Kunststoffe, 60, 187 (1970)
- 81 Tadmor, Z., "Molecular Orientation in Injection Molding", J. Appl. Polym. Sci., 18, 1753 (1974)
- 82 Menges, G. and G. Wubken, "Influence of Processing Conditions on Molecular Orientation in Injection Moldings", Technical Papers, 31st ANTEC, 19, 519 (1973)
- 83 Oda, K., J.L. White and E.S. Clark, "Influence of Melt Deformation History on Orientation in Vitrified Polymers", Polym. Eng. Sci., 18, 53 (1978)
- 84 Dietz, W., J.M. White and E.S. Clark, "Orientation Development and Relaxation in Injection Molding of Amorphous Polymers", Polym. Eng. Sci., 18, 273 (1978)
- 85 Matsui, M. and D.C. Bogue, "Studies in Non-Isothermal Rheology", Trans. Soc. Rheo., 21, 133 (1977)
- 86 Kamal, M.R. and V. Tan, "Orientation in Injection Molded Polystyrene", Polym. Eng. Sci., 19, 558 (1979)
- 87 Wales, J.L.S., "Apparatus for the Measurement of Flow birefringence of Polymer Melts at High Shear Stresses", Rheol. Acta, 8, 38 (1969)
- 88 Wales, J.L.S., J. Van Leeuwen and R. Van Der Vijgh, "Some Aspects of Orientation in Injection Molded Objects", Polym. Eng. Sci., 12, 358 (1972)

- 89 Paulson, D.C., "Guide to Injection Machine Control", SPE Journal, 27, 37 (1971)
- 90 Peter, J.W., "Injection Molding Process Investigation for Automatic Control", SPE Technical Papers, 18, 847 (1972)
- 91 Jordan, T.J., F.L. Laczko, R.T. Maher and H.T. Plant, "Understanding and Controlling the Injection Molding Process", Mod. Plast., September, 96 (1972).
- 92 Mann, J.W., "Multi Parameter Process Control for Injection Molding Machines", SPE Technical Papers, 19, 513, (1973).
- 93 Ma, C.Y., "A Design Approach to a Computer-Controlled Injection Molding Machine", Polym. Eng. Sci., 14, 768 (1974)
- 94 Keyes, D.L., "State of the Art Injection Molding Process Control", SPE Technical Papers, 20, 50 (1974).
- 95 Allen, O.E. and D.A. VanPutte, "Know All Your Molding Variables", Plast. Eng., July, 37 (1974).
- 96 Mahoney, F.E., "Taking a Direct Route to Process Control", Mod. Plast., October, 74 (1974).
- 97 Plant, H.T. and R.T. Maher, "A Preliminary Analysis of the Injection Molding Process and Factors Affecting Part Size Control", SPE Technical Papers, 21, 74 (1975).
- 98 Hunkar, D.B., "The Interdependence of Part Parameters on Process Control Adjustable Functions in Injection Molding of Thermoplastics", SPE Technical Papers, 21, 161, (1975)
- 99 Catic, J., "Controlled Injection Molding System-One Way for Better Injection Molding of Thermoplastics", SPE Technical Papers, 22, 391 (1976).
- 100 Hunkar, D.B. and J.P. DeJean, "A Process and Production Controller for Injection Molding", SPE Technical Papers, 24, 130 (1978).
- 101 Bongardt, W. and G. Menges, "An Injection Molding Machine, Which Automatically Finds its Optimum Working Point", SPE Technical Papers, 26, 141 (1980).

- 102 Border, J. and N.P. Suh, "Intellegent Injection Molding", SPE Technical Papers, 28, 40 (1982)
- 103 Kamal, M.R., W.I. Patterson and D. Abu Fara, "Simple Models of Hydraulic and Nozzle Pressure Responses in Injection Molding", SPE RETEC, NJ (1983)
- 104 Abu Fara, D., "The Dynamics of Injection Hydraulics in Thermoplastics Injection Molding", M.Eng. Thesis, McGill University, Montreal (1983)
- 105 Davis, M.A., "Servocontrolled Injection Molding", SPE Technical Papers, 22, 618 (1976)
- 106 Thayer, W.J., "Transfer Functions for Moog Servovalves", Moog Technical Bulletin # 103 (1965)
- 107 Wang, K.K., et.al., "Injection Molding Project", College of Engineering, Cornell University, Progress Report #10, January (1984)
- 108 Pandelidis, I.O. and A.R. Agrawal, "Self-Tuning Control of Ram Velocity in Injection Molding", SPE Technical Papers, 33, 235 (1987).
- 109 Kamal, M.R., W.I. Patterson, D. Abu Fara and A. Haber, "A Study in Injection Molding Dynamics", Polym. Eng. Sci., 24, 686 (1984)
- 110 Conley, M., M.Eng. Thesis, McGill University, Montreal, (1985)
- 111 Sanschagrin, B., "Process Control of Injection Molding", Polym. Eng. Sci., 23, 431 (1983).
- 112 Haber, A. and M.R. Kamal, "The Dynamics of Peak Cavity Pressure in Injection Molding", Polym. Eng. Sci., 27, 1411 (1987).
- 113 Shankar, A. and F.W. Paul, "A Mathematical Model for Evaluation of Injection Molding Machine Control", ASME Trans., J. Dyn. Syst. Measurement and Control, 104, 86 (1982)
- 114 Wang et.al., "Injection Molding Project", College of Engineering, Cornell University, Progress Report # 11 April (1985)
- 115 Aguinat, T., M.Eng. Thesis, McGill University, Montreal, In Preparation.

- 116 Agrawal, A.R., I.O. Pandelidis and M. Pecht, "Injection Molding Process Control - A Review", Polym. Eng. Sci., 27, 1345 (1987).
- 117 Thayer, W.J., "Is There an Optimum Control for Injection Molding ?", Plastics World, March, 45 (1975)
- 118 Thayer, W.J. and M.A. Davis, "Controls for Injection Molding of Thermoplastics", Advances in Plast. Tech., July, 28, (1981)
- 119 Johannaber, F., "Injection Molding Machines, A Users Guide", Hansen and Macmillan Publishing Co. Inc., NY (1983)
- 120 Emmerich, A., "Injection Process Controls: Which Way to Go ?", Plastics Technology, April, 91 (1979)
- 121 Cole, N.V., "Optimization of Injection Molding Using A Data Acquisition System", SPE Tech. Papers, 30, 795 (1984)
- 122 Malloy, R.A., S.J. Chen and S.A. Orroth, "A Study of Injection to Holding Pressure Switch-Over Techniques Based on Time, Position or Pressure", SPE Technical Papers, 33, 225 (1987).
- 123 Haber, A., "Microprocessor Control System for the Injection Molding Process", M.Eng. Thesis, McGill University, Montreal (1982).
- 124 Gomes, V., "The Dynamics and Control of Melt Temperature in Thermoplastics Injection Molding", M.Eng. Thesis, McGill University, Montreal (1985)
- 125 Moy, F., "Microstructure and the Distribution of Tensile Properties in Injection Molded Polyethylene" Ph.D. Thesis, McGill University, Montreal (1980).
- 126 Kalyon, D., "An Integrated Experimental Study of the Injection Molding behavior of Polyethylene Resins", M.Eng. Thesis, McGill University, Montreal (1977).
- 127 Middelmann, S., "Fundamentals of Polymer Processing", McGraw-Hill Book Company, NY (1977).
- 128 Daniel, C. and F. Wood, "Fitting Equations to Data", John Wiley, N.Y. (1980).
- 129 Ljung, L., "System Identification: Theory for the User", Prentice-Hall, Englewood Cliffs, NJ (1987).

- 130 PC-MATLAB User's Guide, The MathWorks, Inc., MA (1987).
- 131 Smith, C.L., "Digital Computer Process Control", Intext Education Publisher, NY (1972).
- 132 Isermann, R., "Digital Control Systems", Springer-Verlag, NY (1981).
- 133 Dahlin, E.B., "Designing and Tuning Digital Controllers", Instruments and Control Systems, 41, 77 (1968).
- 134 Stephanopoulos, G., "Chemical Process Control: An Introduction to theory and Practice", Prentice-Hall, Englewood Cliffs, N.J. (1984).
- 135 Kamal, M.R., W.I. Patterson, D. Abu Fara, and A. Haber, "A Study in Injection Molding Dynamics", Polym. Eng. Sci., 24, 686 (1984).
- 136 Ziegler, J.G. and N.B. Nicols, "Optimum Setting for Automatic Controllers", Trans. ASME, 64, 759 (1942).
- 137 Cohen, G.H. and G.A. Coon, "Theoretical Investigations of Retarded Control", Trans. ASME, 75, 827 (1953).
- 138 Lopez, A.M., J.A. Miller, C.L. Smith, and P.W. Murrill, "Tuning Controllers with Error Integral Criteria", Instrumentation Technology, 14 (11), 57 (1967)
- 139 Lopez, A.M., P.W. Murrill and C.L. Smith, "Optimal Tuning of Digital Controllers", Instruments & Control Systems, 41 (10), 97 (1968).
- 140 Rovira, A.A., P.W. Murrill and C.L. Smith, "Tuning Controllers for Setpoint Changes", Instruments & Control Systems, 42 (12), 67 (1969).
- 141 Lopez, A.M., C.L. Smith and P.W. Murrill, "An Advanced Tuning Method", British Chem. Eng., 14 (11), 1553 (1969).
- 142 Moore, C.F., C.L. Smith and P.W. Murril, "Simplifying Digital Control Dynamics for Controller Tuning and Hardware Lag Effects", Instrument Practice, 23 (1) (1969) p. 45.

- 143 Rovira, A.A., P.W. Murril and C.L. Smith, "Modified PI Algorithm for Digital Control", Instruments & Control Systems, 43 (8), 101 (1970).
- 144 Chiu, K. and C.L. Smith, "Digital Control Algorithms Part III Tuning PI and PID Controllers", Instruments & Control Systems, 46 (12), 41 (1973).
- 145 Martin, J., A.B. Corripio and C.L. Smith, "How to Select Controller Modes and Tuning Parameters from Simple Process Models", ISA Transactions, 15 (4), 314 (1976)
- 146 Yuwana, M. and D.E. Seborg, "A New Method for On-Line Controller Tuning", AIChE Journal, 28, 434 (1982).
- 147 Smith, C.A. and A.B. Corripio, "Principles and Practice of Process Control", John Wiley & Sons, NY (1985)
- 148 Astrom K.J. and B. Wittenmark, "Computer Controlled Systems: Theory and Design", Prentice-Hall, Inc., Englewood, N.J. (1984).
- 149 Woods, D.J., "The Nelder-Mead Simplex Algorithm for Minimizing a Non-Linear Function of Several Variables", Report 85-5, Dept. Math. Sciences, Rice University, May, 1985.; PC-MATLAB Users' Guide, The MathWorks, Inc, MA (1987).
- 150 Shinskey, F.G., "Process Control Systems: Application, Design, Adjustment", McGraw-Hill Book Company, NY, (1979).
- 151 Belanger, P.R., "A Review of Some Adaptive Control Schemes for Process Control", in "Chemical Process Control 2", Seborg, D.E. and B. Egardt (eds), AIChE Publications (1982).
- 152 Crawford, R., V. Klewpatinond and P.P. Benham, "A Study of Injection Molding Parameters and their Influence on Mechanical Properties", Plastics and Rubber: Processing, Dec., p. 133 (1978).
- 153 Parnaby, J., P.G. Battye and G.A. Hassan, "Computer-Controlled injection Molding and Extrusion", Plastics and Rubber: Processing, Sept. (1978) P. 89
- 154 Saad, M.A., "Compressible Fluid Flow", Prentice-Hall, Inc., Englewood Cliffs, NJ (1985).

- 155 Campbell, D.P., "Process Dynamics", John Wiley & Sons, Inc., NY (1958).
- 156 Williams, M.L., R.F. Landell and J.D. Ferry, J. Am. Chem. Soc., 77, 370 (1955).
- 157 Penwell, R.C., R.S. Porter and S. Middleman, "Determination of the Pressure Coefficient and Pressure Effects in Capillary Flow", J. polym. Sci., A-2, 9, 273 (1971).
- 158 Gee, G., Polymer, 7, 177 (1966).
- 159 Nyun, H., "The Effect of Pressure on the Viscosity of Polymer Melts", Ph.D Thesis, McGill University, Montreal, Canada (1973).
- 160 Kalyon, D., "An Integrated Experimental Study of the Injection Molding Behavior of Polyethylene Resins", M.Eng. Thesis, McGill University, Montreal, Canada (1977).
- 161 Dynisco, "Plastic Melt Pressure Transducers", Dynisco Bulletin 100/R80 (1980).
- 162 Chander Engineering Co., Manufacturers of Physical Property Testing Instruments, Tulsa, Oklahoma, CAT. 23-1.
- 163 TRANS-TEK Inc. Bulletin # 100 LGI.
- 164 MOOG Bulletin, Catalog 762 578.

APPENDIX A

MODELLING OF THE INJECTION MOLDING PROCESS

A.1 Plastication Stage

The majority of the studies regarding plastication phase have far been performed for conventional plasticating extrusion. The models for plastication in injection molding are extensions of these. A brief discussion of the models derived for extruders is presented by Gomes [45]. The models derived for plastication in injection molding are based on the two major stages of operation during the injection molding cycle [38] [44] :

- (1) Screw rotation period
- (2) Screw stationary, conduction melting period

Hillier [39] has developed a simple equation relating flow rate, screw rpm, and pressure for the plasticating stage of injection molding. Calculated flow rate could then be used to estimate the time for run-back. A number of simplifying assumptions were made; the screw is untapered and of uniform cross section, and the flow of the polymer can be treated as a liquid regardless of its actual state.

Donovan et.al. [36] conducted studies to examine the

plasticating process in a reciprocating screw injection molding machine. They concluded that plastication in injection molding behaves as a transient plasticating extrusion process. When screw rotation time is a large fraction of the total cycle time, the plasticating behavior is very similar to steady-state extrusion behavior. Better plastication is achieved by combining low screw RPM with long rotation time than by combining high screw RPM and short rotation time. Based on the previous observations and a steady-state extrusion model [37], Donovan [38] proposes a heuristic model with empirical coefficients for the transient melting behavior in the reciprocating-screw injection molding machine. He assumes that the solid bed profile decays exponentially with the screw rotation. Good agreement between model predictions and experimental data is reported for three different polymers.

Lipshitz et.al. [43] have proposed a theoretical model for melting in reciprocating injection molding machines. It consists of a combination of the pseudo-dynamic extrusion melting model developed by Tadmor et.al. [44] for the screw rotation period and Donovan's model [38] for the screw rest period. The model predicts the relative positions of the solid bed profile. It is in qualitative agreement with the experimental data presented by Donovan [38]. The lack of adequate experimental data has restricted the quantitative verification of the model.

A.2 Filling and Packing Stages

Harry and Parrott [48] coupled the analysis of one-dimensional quasi steady-state flow of a power-law fluid with a heat balance equation to study the filling of a rectangular cavity. Viscous heat generation was considered. The most serious limitation was related to the assumption of a constant pressure gradient in the direction of flow. For non-isothermal flow, the model would yield a conservative estimate of the pressure. In consequence, their simulation results were successful in predicting short shots and successful fill, but there was considerable error in the predicted lengths of short shots and the fill time for the full shot condition.

Berger and Gogos [49] and later Wu, Huang and Gogos [50] treated the radial flow filling of a disk cavity. The transport equations for one-dimensional flow of a power-law fluid were solved. They considered two cases: the non-isothermal and the isothermal problems. They demonstrated that, for the prediction of filling times, the isothermal solution could be used under high pressures and corresponding short filling times. The same would apply for relatively thick cavities. If the cavity has extensive thin sections, the full non-isothermal flow problem should be considered.

The model proposed by Kamal and Kenig [51,52] presented an integrated mathematical treatment of the filling, packing and cooling stages of the injection molding cycle. For the analysis of the filling stage, equations of continuity, motion and energy were simplified for a one-dimensional creeping flow of a power-law fluid. Viscous heating, latent heat effects, viscosity dependence on temperature, and the variation of polymer density with temperature and pressure were considered. For the packing and cooling stages, the heat conduction equation was applied to the solid and melt phases, assuming constant (but different) values of the thermal properties. Numerical solutions were obtained, using a finite-difference method, and compared with experimental results for the case of spreading radial flow in a semi-circular cavity. Their model yielded predictions in good agreement with experimental data for the progression of the melt front during the filling and the pressure distribution during all stages of the injection molding cycle.

Kamal et. al. [53] extended the above model to the treatment of the injection molding behavior of thermoplastics in rectangular cavities. Their model included a complex analytical expression for the pressure distribution in the mold cavity, obtained by linearizing the governing non-linear partial differential equations. Calculated results based on the analytical treatment of the compres-

sible flow into the cavity were compared to experimental pressure distributions. Both experimental and calculated pressure profiles showed change towards a flat pressure profile during the packing. Chung and Ryan [54] presented a numerical solution for the same non-linear partial differential equation but with different boundary conditions from those suggested by Kamal [53]. Because of the short duration of the packing stage, temperature changes within the molten polymer were neglected. Their calculated pressure distributions during packing showed a higher pressure gradient near the gate which became essentially uniform at a short distance from the gate. The pressure gradient decreased with time and the pressure distribution in the mold cavity tended to become more uniform. The above analyses show the importance of the fluid motion and deformations which occur during the packing stage of the injection molding cycle, influencing the morphology and microstructure of the molded part.

Broyer, Gutfinger and Tadmor [55] considered two dimensional, fully developed, isothermal, creeping flow in each of the directions (Hele-Shaw type flow). The filling stage was solved isothermally for a non-Newtonian melt, using the finite-element method. In studying the filling of a rectangular cavity with a high aspect ratio cross section, White [56] developed a model based on a one-dimensional Hele-Shaw flow. The model was divided into three

regions: region 1, near the gate, radial flow; region 2, which comprises the area stretching from region 1 to vicinity of the front, where a fully developed flow prevails; region 3, which consists of the moving front and the fluid immediately behind it. Their model cannot be applied with success to region 3, where the velocity field in the gapwise direction has to be considered.

Williams and Lord [57,58] analyzed the mold filling portion of the injection molding cycle in two parts: firstly, the flow of the melt in the delivery system (sprue, runner and gate) and, secondly, the flow in the mold cavity itself. The analysis of the flow in the delivery system is important, because the behavior of the plastic in the mold cavity is affected by what occurs in the upstream channels. Also, an analysis starting at the nozzle will remove the need of inserting measuring devices in the cavity. This can be very important for industrial and control applications. Model predictions for the pressure drop in the cavity were compared to the experimental results obtained with an instrumented plaque mold. The model was found to correctly describe trends, such as the increase in the pressure required to fill molds as injection rate, melt temperature, and mold temperature decreased, but agreement between predictions and measurements was not particularly good. Barrie [59] studied the filling of a canter-gated disk cavity of uniform thickness. Experimental

data of pressure losses in the cavity and the delivery channels for varying flow rates at three different temperatures were obtained. Pressure losses in the delivery system were estimated by using the Hagen-Poiseuille equation modified for non-Newtonian fluids by using the apparent viscosity at different shear rates. The effects of pressure dependence of viscosity and viscous heating were ignored as they act in opposition to each other and were assumed to cancel the effects of each other. In order to simplify the flow equations in the cavity, two empirical assumptions were made: (i) at the instant the melt reaches cavity extremities, the layer of frozen material is of constant thickness; and (ii) the thickness of frozen layer is proportional to the cube-root of time. Reasonable agreement between experimental and calculated values was obtained for pressure losses in the nozzle and delivery channel and for cavities with thickness of 0.067 inches and more.

An analytical- numerical method based on the thin cavity approximations and the two dimensional flow and energy equations was developed by Kuo and Kamal [60] for predicting flow quantities and temperature distributions in complex cavities. The shear rate and temperature dependence of viscosity were considered. Ryan and Chung [61] presented a detailed analytical solution of the analysis of the filling stage in thin rectangular mold cavities based upon the Helé-Shaw flow theory combined with a conformal mapping

technique. They claimed that the model gave a simpler and more direct determination of the pressure distribution, temperature distribution and filling time. Model predictions were compared with the experimental data of Kuo and Kamal [53] and showed good agreement.

Wang et.al. [62] modeled the filling and cooling stages employing a viscoelastic constitutive equation. The model involved one-dimensional, unsteady, non-isothermal pressure flow of polymer between two parallel plates. The model gives good predictions for the birefringence as a function of melt temperature, wall temperature, gap thickness and fill time. Recently, Lafleur and Kamal [63] and Kamal et.al. [64] proposed a computer simulation of the injection molding process which permits the prediction of some microstructural parameters in the molded articles, such as the distributions of crystallinity and frozen stresses.

A.3 Product Quality Studies

An important objective of injection molding modelling must be the prediction of the ultimate properties of the molded articles. For this purpose, it would be necessary to develop product quality models that relate the thermo-mechanical history of the polymer to the development of

microstructure, mainly morphology, orientation and crystallinity in the molded part, and ultimately to relate the final properties of the molded articles to the distribution of microstructure.

A variety of experimental studies regarding microstructure distribution and its influence on the ultimate properties of molded parts have been reported in the literature. Clark [65] studied the structure development of injection molded acetal polymers under different molding conditions, and the influence on the mechanical properties of the molded parts. He observed, by optical microscopy, that injection moldings consist of a composite of different morphologies forming a laminated structure. Three types of morphology occur: a skin of high molecular orientation, a less highly oriented intermediate "transcrystalline layer", and a spherulitic core. Clark [65] pointed out that the skin represents that portion of the melt crystallizing during the filling period. The transcrystalline and spherulitic regions result from crystallization under low melt stress. Furthermore, the variation in skin thickness in a molding is due to the expected decrease of melt velocity with distance from the gate and its corresponding influence on the creation of fibril nuclei. Further, the relative volumes of the transcrystalline and spherulitic regions are determined by the rate of heat transfer to the mold wall. Boehme [66] observed that the thicknesses of the

three developing zones are influenced both by the molding procedure and the mold temperature, which in turn, modified the mechanical properties and the dimensional stability of the molded part.

Kantz, Newman and Stigale [67] studied the skin-core morphology and microstructure property relationships in injection molded tensile bars of polypropylene. They employed optical microscopy and X-ray diffraction to study the effects of melt temperature and injection pressure on the morphology and crystalline orientation and their influence on the mechanical properties of the molded parts. Their studies revealed the presence of three distinct crystalline zones, namely, a highly oriented non-spherulitic skin, a shear-nucleated spherulitic intermediate layer, and a typically spherulitic core. Ultimate properties were related to the thicknesses of the different morphological zones. The thickness of the oriented skin layer varied inversely with polymer melt temperature, and it was slightly affected by injection pressure. The sum of the area fractions of the skin and intermediate shear zones, which reflects the oriented portion of the specimen, varied linearly with temperature. Injection pressure had a noticeable effect on the area fraction of the shear zone. The results suggested that operating at, or close, to the melting point would produce a highly oriented structure. The preferred crystallite

orientation in the skin and intermediate layer had a profound effect on mechanical properties. The tensile yield strength, impact strength and shrinkage increased with increasing combined thickness of the two oriented outer layers (see Figure 3.A.3-a,b,c).

Fitchmun and Mencik [68] and later Hobbs and Pratt [69] made observations concerning the composite structure or skin - core morphology of injection molded crystalline polymers. The former workers used optical and scanning electron microscopy to characterize the morphology in injection molded polypropylene, while the latter employed optical microscopy, X-ray diffraction and density measurements to characterize the skin - core morphology in injection molded poly (butylene terephthalate). Henke, et.al. [70] studied the effect of mold temperature on the morphological structure and physical properties of propylene-ethylene copolymer injection molded tensile bars. They showed that izod and tensile impact strengths decreased with increasing mold temperature. They attributed this effect to the increase in the spherulite size in the shear and core regions, by increasing mold temperature.

Tan and Kamal [71,72] studied the effect of melt and mold temperatures on the development of the various morphological zones and the orientation distribution in injection molded polyethylene. Four different textures of microstructure were observed. The distribution and thick-

nesses of the morphological zones varied with distance from the gate. They were also strongly affected by processing variables such as melt and mold temperatures. The thicknesses of the skin and shear zones decreased with increasing melt temperature. Increasing the mold temperature caused a decrease the thickness of the shear zone.

Polarized light microscopy and differential scanning calorimetry were used by Kamal, Kalyon and Dealy [73] to determine the morphology and orientation of two different injection molded polyethylene resins. Shrinkage and tensile properties of the moldings were determined experimentally. Measurements of the distributions of density, birefringence, sonic modulus, tensile modulus and wide angle X-ray diffraction were employed by Moy and Kamal [74] to characterize the microstructure (crystallinity and orientation distributions) of injection molded polyethylene parts. Particularly, they attempted to separate and estimate the contributions of the crystalline and amorphous components to the overall orientation in such products. Experimental results were employed in conjunction with an existing mechanical model developed by Seferis and Samuels [75] to calculate the distribution of sonic and tensile moduli in the moldings. The calculations were in good agreement with experimental measurements.

A number of studies in the area of injection molding have concentrated on the study of orientation in the

injection molded parts. Pioneering work conducted by Spencer and Gilmore [76] has shown that increasing packing time increases the frozen orientation in injection molded polystyrene boxes. Menges and Wubken [77] have studied orientation in polystyrene moldings by means of heat shrinkage measurements. They have concluded that the flow direction is the main direction of orientation in planar moldings and that maximum orientation is observed at the surface, while minimum orientation is observed at the centre of the moldings. Their results show that the degree of orientation decreases with increasing melt temperature. Raising cavity wall temperature caused a similar effect, but increasing the melt temperature is more effective. Increasing the injection rate tends to marginally increase the orientation at the surface while it significantly reduces the internal orientation. Similar results have been reported by Bakerdjian and Kamal [78] from birefringence measurements in polystyrene moldings. More complex behavior of the orientation distribution is observed in conjunction with polyethylene moldings. This complex behavior is attributed to the interaction between the orientation and crystallization phenomena.

Fleissner and Paschke [79] and Paschke [80] have studied the influence of melt temperature on the development of orientation as measured by birefringence and heat shrinkage measurements, and by its effect on the mechanical

properties of thin-wall (1 mm) injection moldings of high density polyethylene. They have found that for high-flow materials, increasing the melt temperature in the range of 140 C to 340 C tends to decrease the notched impact strength, while for low-flow materials, the notched impact strength tends to increase as the melt temperature is increased. Furthermore, the tensile yield stress is observed to decrease as the melt temperature is increased, due to the lower orientation. The elongation at yield tends to increase for high-flow materials, but decreases for low-flow materials. Fleissner and Paschke attributed the differences in mechanical properties to the lower orientation at higher melt temperature, and to the molecular weight differences between high-flow and low-flow materials. On the basis of their findings, they suggested that the optimum temperature range for injection molding of high density polyethylene is between 280-310 C.

Tadmor [81] developed a model incorporating flow and heat transfer coupled with molecular theories in an attempt to predict orientation in terms of shrinkage of injection molded parts. The model showed that orientation increased with increasing injection speed and decreased with an increase in temperature and cavity thickness. Orientation in the surface layer (skin) was considered to be induced by steady elongational flow in the advancing front. However, the proposed theory could only qualitatively describe

the data points reported by Menges and Wubken [82], because of the crude form of the model and the insufficient information on experimental conditions.

Oda, White and Clark [83] reported in an experimental study on polystyrene melts, that orientation development during non-isothermal polymer processing operations involving vitrification could be predicted by a knowledge of the stress field prior to solidification and by the application of stress-optical laws where the birefringence could be related to the stress field through the stress-optical coefficient. Dietz, White and Clark [84] applied this idea to orientation distribution in injection molded parts. The stress distribution during mold filling was obtained using isothermal steady state shear flow. Relaxation during the subsequent cooling and solidification was followed by the using Matsui-Bogue [85] formulation for non-isothermal relaxation. They assumed that the melt relaxed in a Maxwellian manner. Based on this simplified flow model, the calculated birefringence was lower than the measured levels by about 15%. Similar work was reported by Kamal and Tan [86] for the injection molding of polystyrene using a relation proposed by Wales [87] for the dependence of birefringence on shear stress at the wall $[n = A(T)]$. Fairly good agreement between the experimental and calculated values for birefringence was obtained.

Wales, et.al. [88] have shown that the relationship

between birefringence and shear stress at the wall is independent of temperature as shown in Figure 3.A.7. This suggests that for the non-isothermal cavity filling process, the shear stress might be an appropriate variable to estimate the orientation.

The above studies suggest that although the physical properties of injection molded thermoplastics are affected by orientation, they do not all react to it in the same way. Therefore, in order to achieve certain properties in a formed article, orientation effects on the properties must be understood and considered in the design and manufacture of the article. Controlled molecular orientation can be a valuable aid in achieving optimum properties and performance.

APPENDIX B

TRANSDUCER SPECIFICATIONS AND CALIBRATION

B.1 Pressure Transducers

The pressure transducers used in this study were Dynisco models PT435A and TPT432A. Specifications of the transducers are given in reference [161].

Calibration of the pressure transducers was performed using a high pressure dead-weight tester [162]. It represents a source of accurate pressure. The calibration procedure of the manufacturer was followed [162]. The calibration was performed in psi as working units ($1 \text{ Pa} = 1.45 \times 10^{-4} \text{ psi}$). The calibration data were fitted by linear regression and shown in Figures B.1 - B.4.

B.2 Linear Velocity Transducer

The ram velocity was measured using a linear velocity transducer, TRANS-TEK (Model 112-001) [163]. The calibration of the transducer was performed using the Instron Universal Testing Machine in conjunction with known velocities. The output of the transducer was traced on a chart recorder. The calibration curve obtained by linear regression of the calibration data is given in Figure B.5.

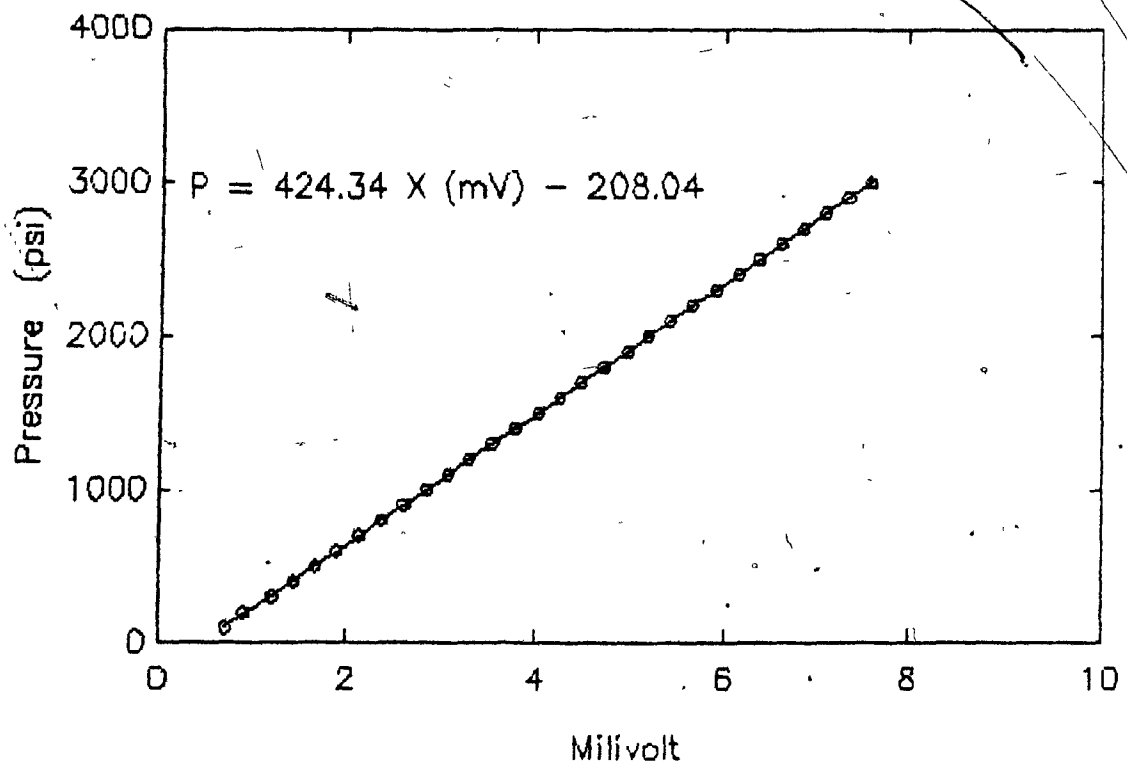
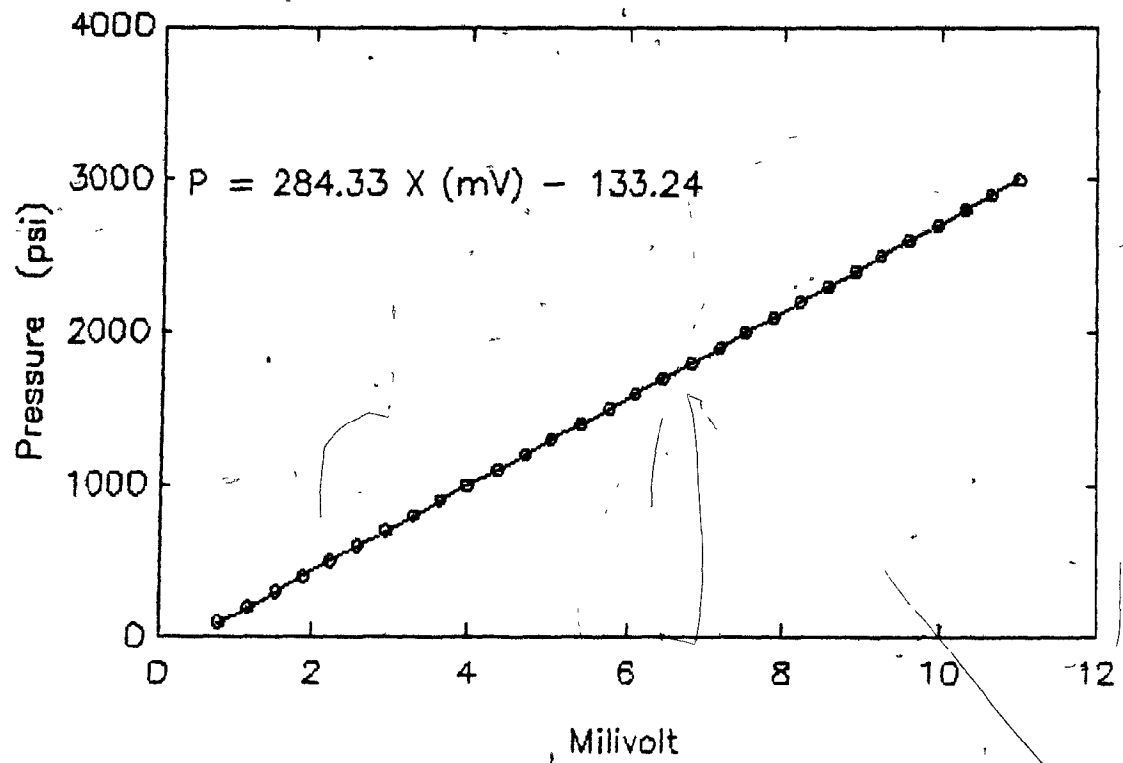


Figure B.1: Calibration Curves for Cavity Pressure Transducers.

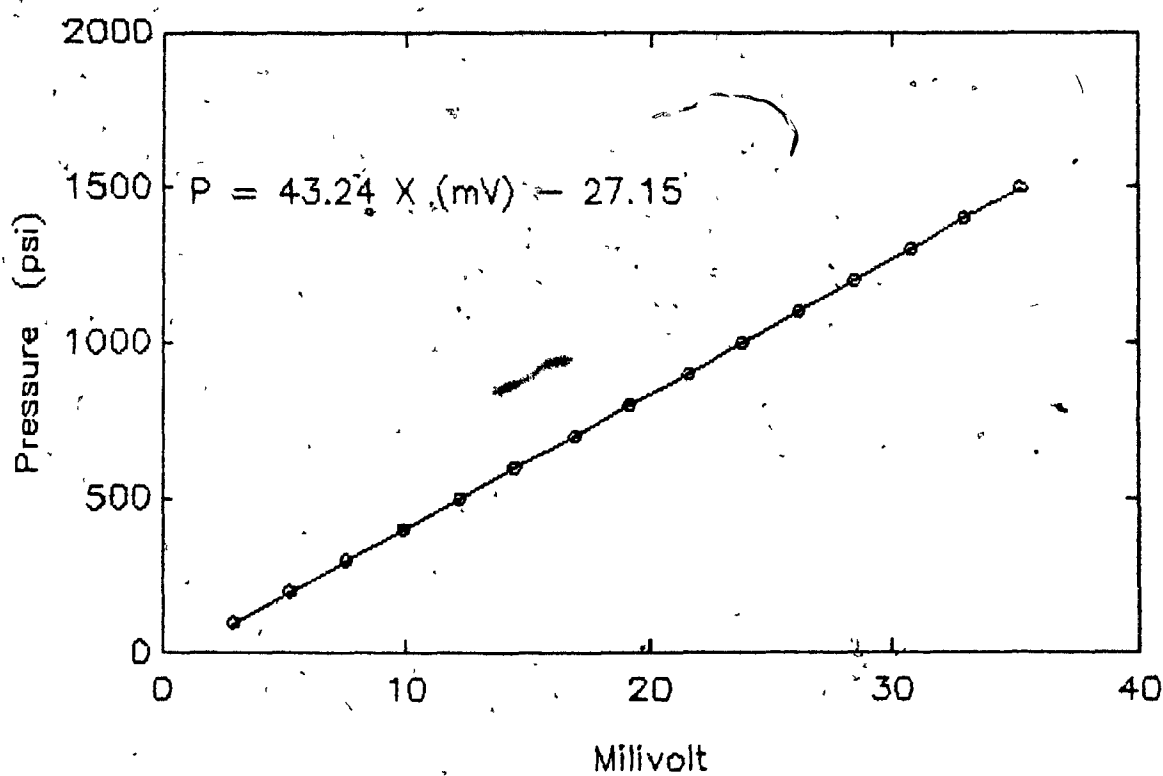
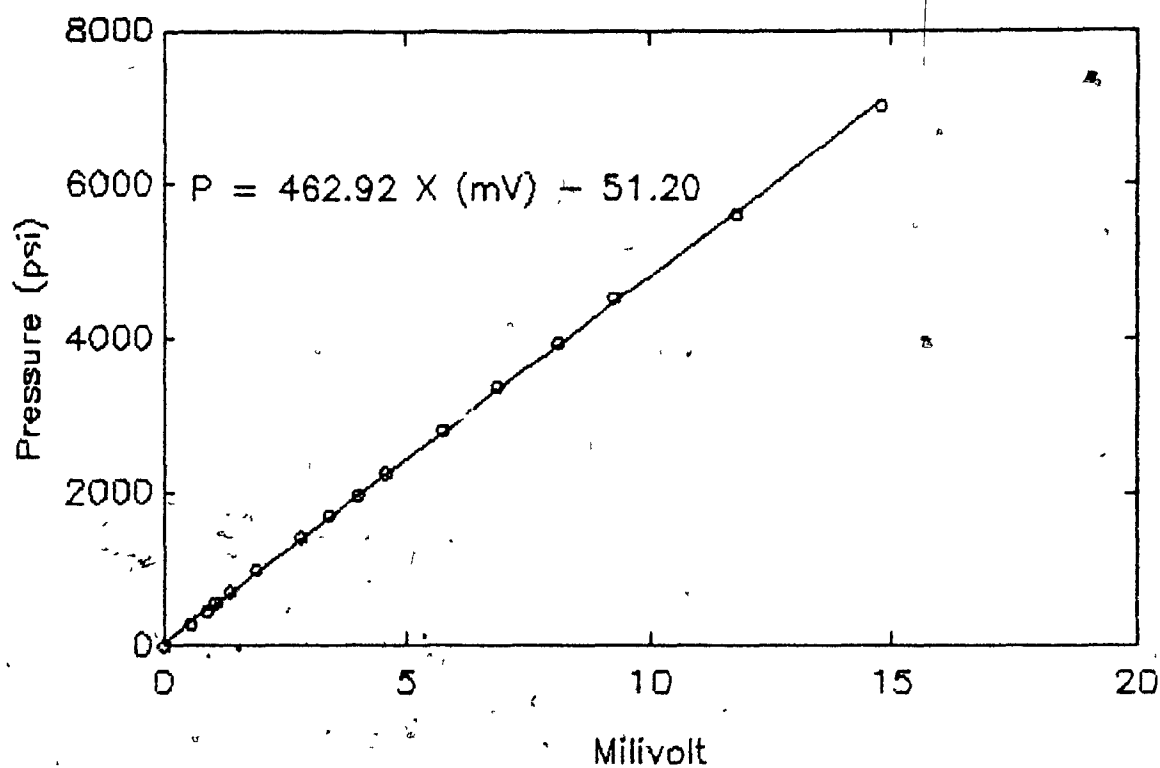


Figure B.2: Calibration Curves for Nozzle and Hydraulic Pressure Transducers.

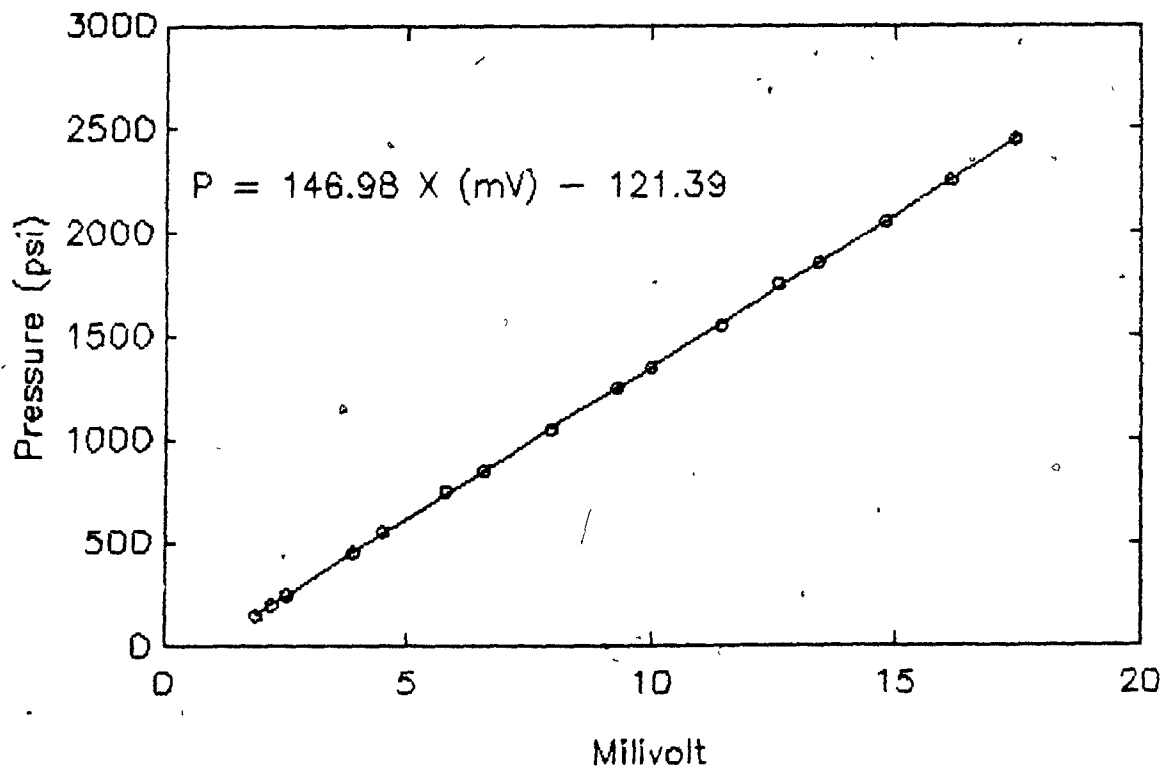
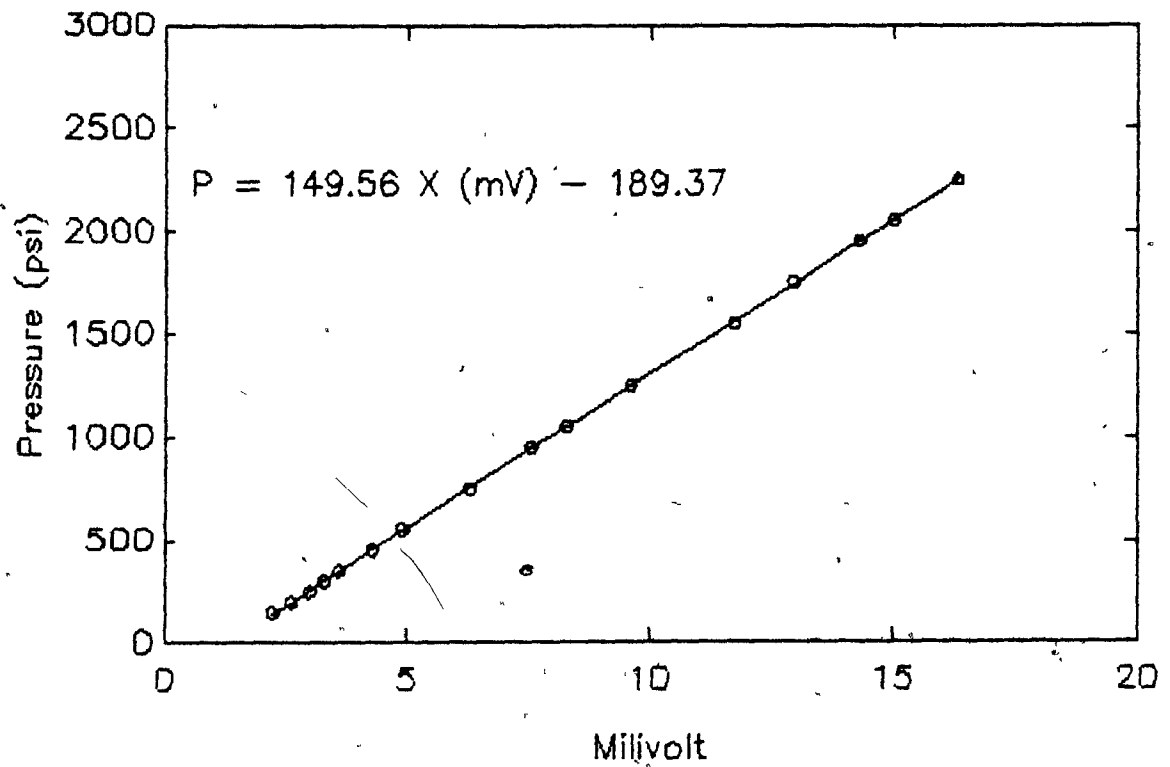


Figure B.3: Calibration Curves for System Pressure Transducers.

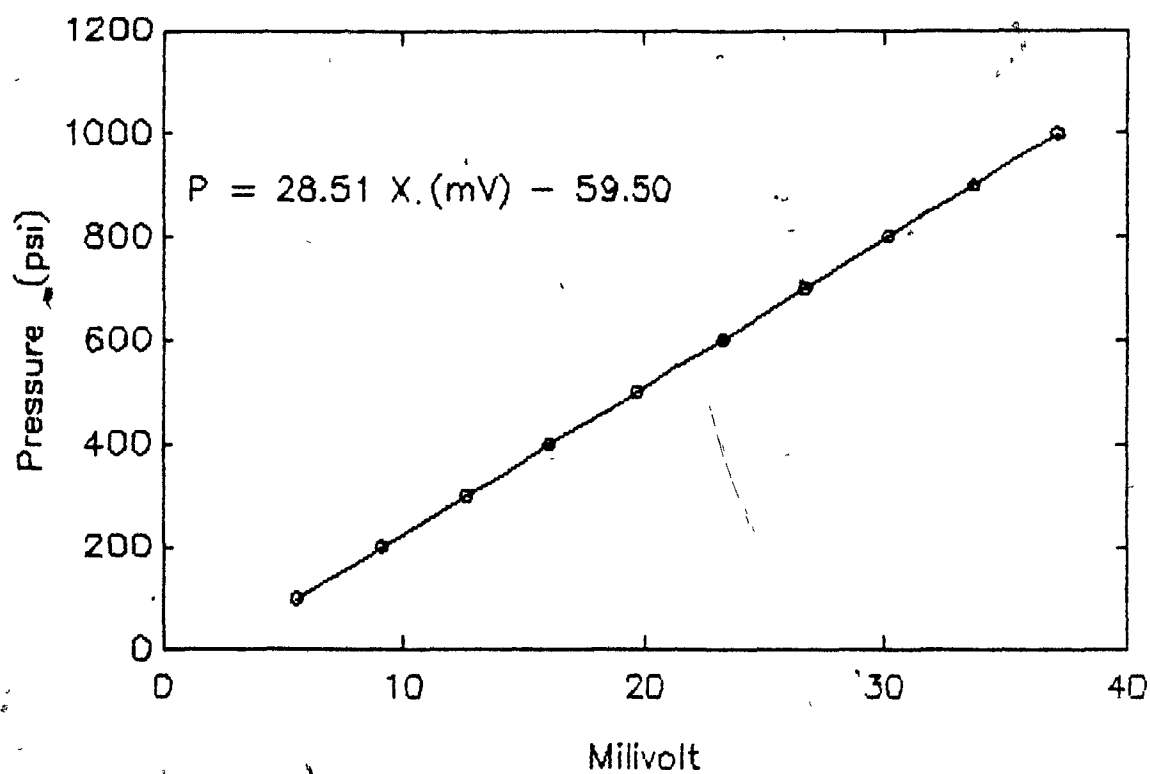


Figure B.4: Calibration Curves for Clamping Pressure Transducer.

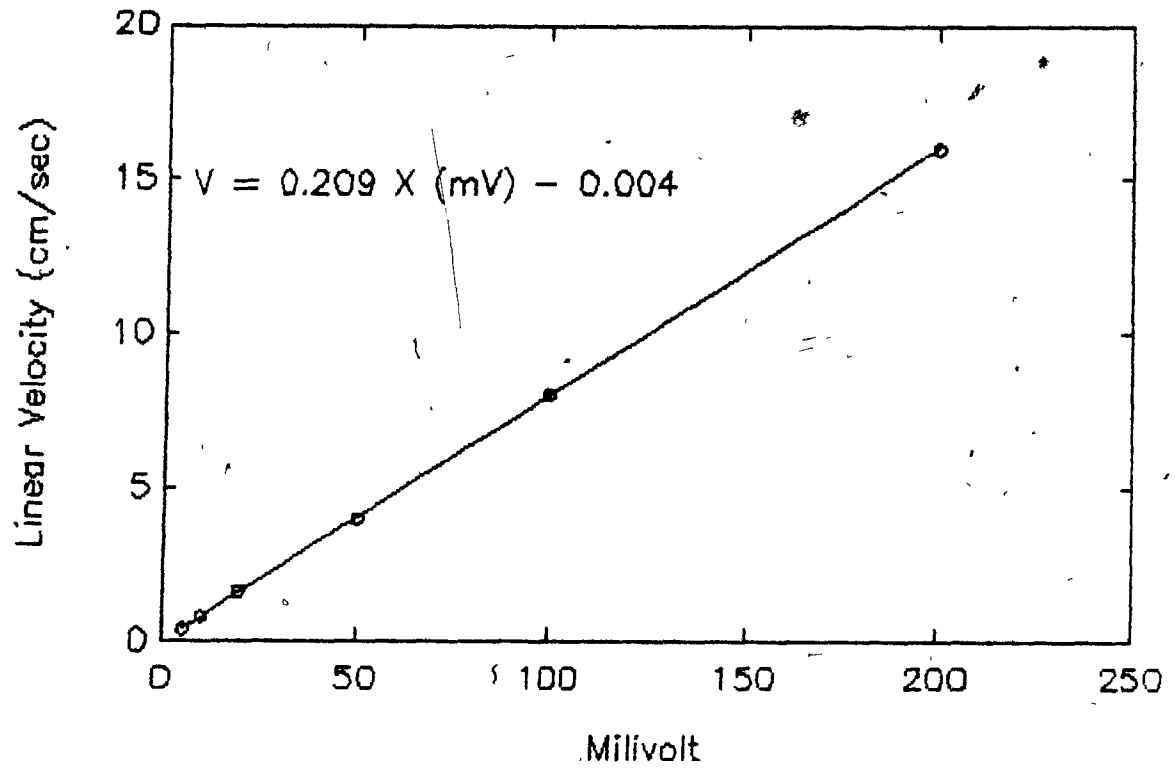


Figure B.5: Calibration Curve for Linear Velocity Transducer.

B.3 Linear Displacement Transducer

The linear displacement transducer was calibrated by applying a known displacement and determining the corresponding output in millivolts. The calibration curve is shown in Figure B.6.

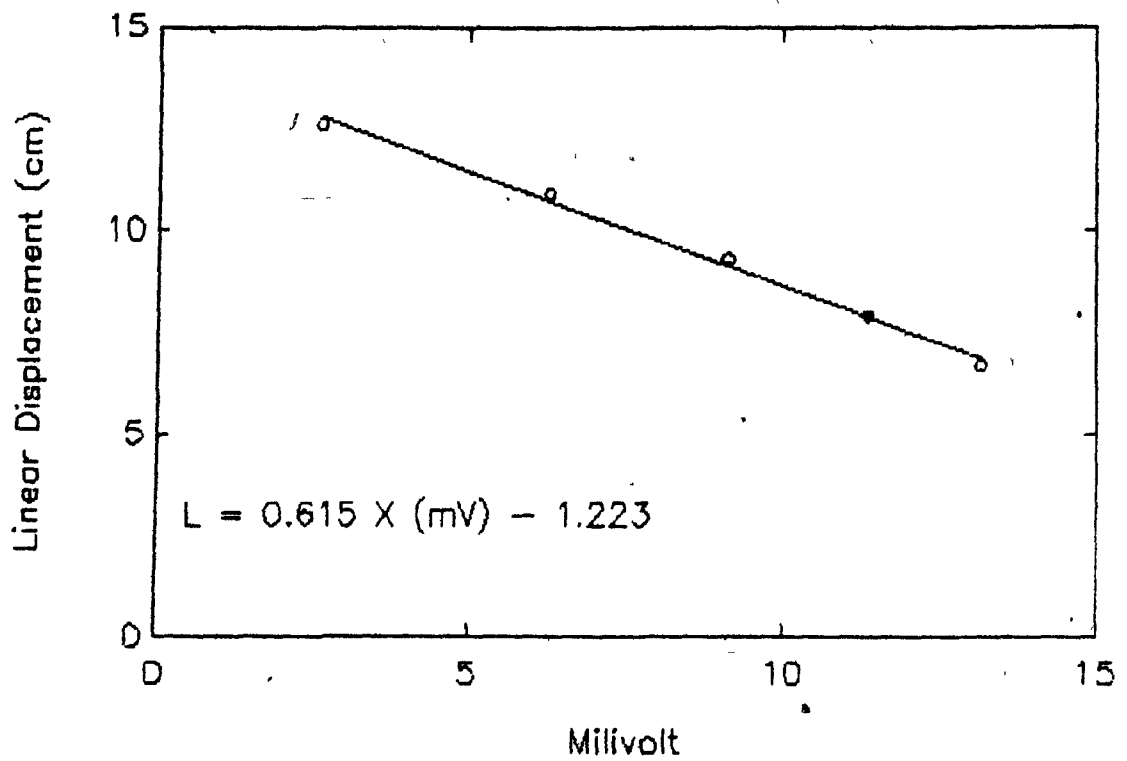


Figure B.6: Calibration Curve for Linear Displacement Transducer

APPENDIX C**SERVOVALVE CHARACTERISTICS**

The servovalves used in the system are two stage valves, Moog A0-76-103 model. The valve has a rated flow of 10 gpm (U.S.) at 1000 psi valve pressure drop. The hydraulic and performance characteristics are given in the attached sheets reproduced from the manufacturer's documentation [164].

HYDRAULIC CHARACTERISTICS

Unless specified otherwise, all performance parameters are given for valve operation on Mobil DTE-24 fluid at 100°F (38°C).

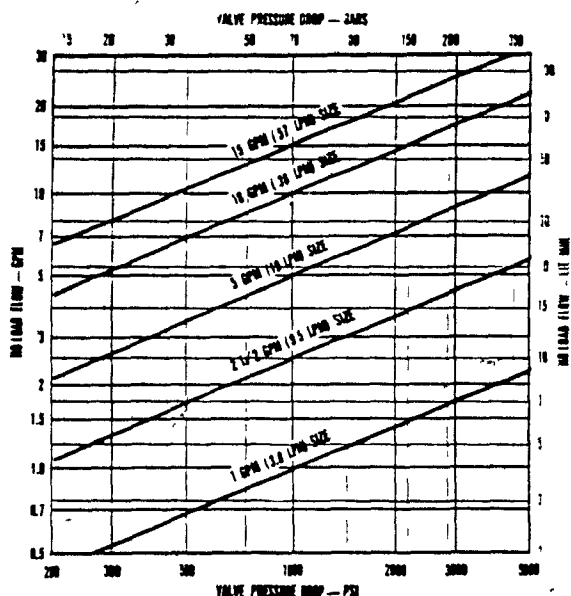


FIGURE 1 CHANGE IN RATED FLOW WITH PRESSURE

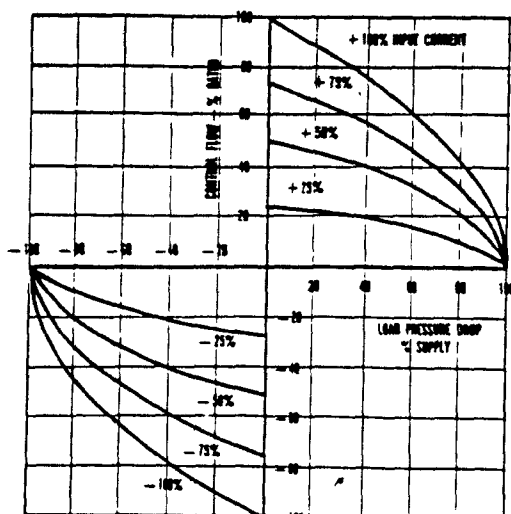


FIGURE 2—CHANGE IN CONTROL FLOW WITH CURRENT AND LOAD PRESSURE

FLUID SUPPLY A076 Servovalves are intended to operate with constant supply pressure.

Supply Pressure
 minimum 200 psi (14 bars)
 maximum standard 3000 psi (210 bars)
 maximum special order 5000 psi (350 bars)

Proof Pressure
 at pressure port 150% supply
 at return port 100% supply

NFPA static pressure rating* 6900 psi
 (test pressure 10,700 psi)

NFPA cyclic pressure rating 3000 psi
 (pressure port)*
 (cyclic test pressure
 4350 psi for > 10⁶ cycles)

Fluid† petroleum base hydraulic fluids 60-450 SUS @ 100° F (10-97 cST @ 38° C)

Supply filtration required 10µm nominal (25µm absolute) or finer recommended

Operating temperature
 minimum - 40° F (- 40° C)
 maximum + 275° F (+ 135° C)
 (unless limited by fluid)

*Method of verifying static and fatigue pressure ratings per NFPA/T2.6.1-1974, category 3/90

†Buna N seals are standard, Viton A and EPR available on special order

RATED FLOW Five standard sizes are available having rated flows of 1, 2½, 5, 10, and 15 gpm at 1000 psi valve drop (3.8, 9.5, 19, 38, and 57 lit/min at 70 bars). See plot at left for corresponding rated flows at other supply pressures.

Flow with various combinations of supply pressure and load pressure drop can be determined by calculating the valve pressure drop.

$$P_v = (P_s - P_R) - P_L$$

P_v = valve pressure drop
 P_s = supply pressure
 P_R = return pressure
 P_L = load pressure drop

FLOW-LOAD CHARACTERISTICS Control flow to the load will change with load pressure drop and electrical input as shown in Figure 2. These characteristics follow closely the theoretical square-root relationship for sharp-edged orifices, which is

$$Q_L = K i \sqrt{P_v}$$

Q_L = control flow
 K = valve sizing constant
 i = input current
 P_v = valve pressure drop

INTERNAL LEAKAGE Maximum internal leakage for each size servovalve is:

Flow with 1000 psi (70 bars) Supply		
	Rated Flow	Internal Leakage
1	gpm (3.8 lit/min)	< 0.17 gpm (0.66 lit/min)
2½	gpm (9.5 lit/min)	< 0.22 gpm (0.83 lit/min)
5	gpm (19 lit/min)	< 0.35 gpm (1.32 lit/min)
10	gpm (38 lit/min)	< 0.35 gpm (1.32 lit/min)
15	gpm (57 lit/min)	< 0.35 gpm (1.32 lit/min)

PERFORMANCE CHARACTERISTICS

Unless specified otherwise, all performance parameters are given for valve operation on Mobil DTE-24 fluid at 100°F (38°C).

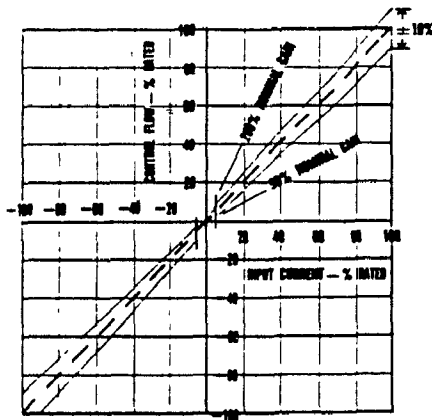


FIGURE 3
NO-LOAD FLOW
GAIN TOLERANCES

FLOW GAIN The no-load flow characteristics of AO76 Servovalves can be plotted to show flow gain, symmetry, and linearity. Typical limits (excluding hysteresis effects) are shown in Figure 3.

LINEARITY The nonlinearity of control flow to input current will be most severe in the null region due to variations in the spool null cut. With standard production tolerances valve flow gain about null (within $\pm 5\%$ of rated current input) may range from 50 to 200% of the normal flow gain.

RATED FLOW TOLERANCE $\pm 10\%$
SYMMETRY $< 10\%$
HYSTERESIS $< 3\%$
THRESHOLD $< \frac{1}{2}\%$

SPOOL DRIVING FORCES

The maximum hydraulic force available to drive the second-stage spool will depend upon the supply pressure, and the hydraulic amplifier pressure gradient. The normal first-stage configuration for AO76 Servovalves will produce a spool driving force gradient which exceeds 1 lb/% (0.4 daN/%) input current with a 3000 psi (210 bars) supply. This gradient will be reduced about 30% when operating on a 1000 psi (70 bars) supply. The maximum spool driving force with 3000 psi (210 bars) supply is 150 pounds (67 daN).

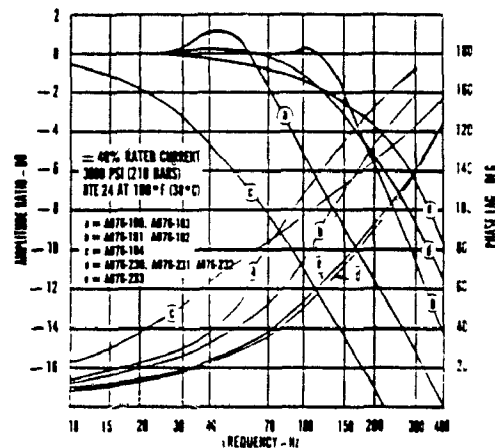


FIGURE 4 REDUCED AMPLITUDE FREQUENCY RESPONSE

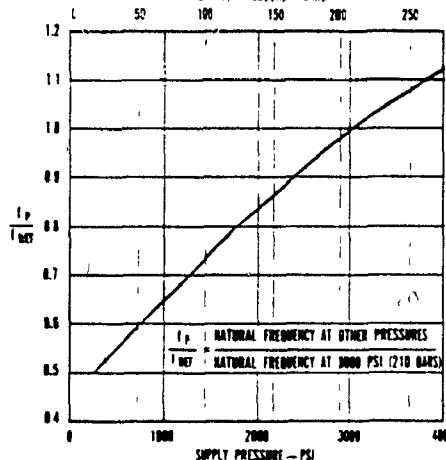


FIGURE 6 FREQUENCY RESPONSE CHANGE WITH PRESSURE

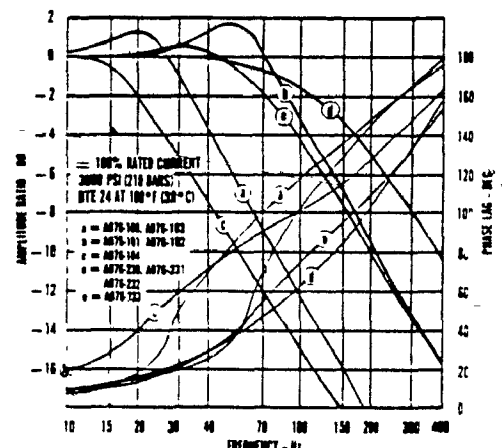


FIGURE 5 FULL AMPLITUDE FREQUENCY RESPONSE

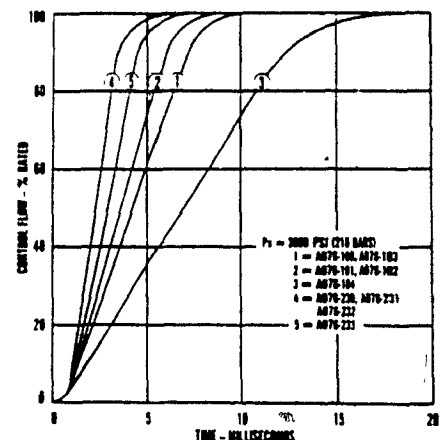


FIGURE 7 STEP RESPONSE

PRESSURE GAIN The blocked load differential pressure will change rapidly from one limit to the other as input current causes the valve spool to traverse the null region. Normally the pressure gain at null for AO76 Servovalves exceeds 30% of supply pressure for 1% of rated current and can be as high as 80%.

NULL

externally adjustable

NULL SHIFT

With Temperature	100°F variation (56°C)	$< \pm 2\%$
With Acceleration	to 10 g	$< \pm 2\%$
With Supply Pressure	80% to 110% nominal	$< \pm 2\%$
With Quiescent Current	50% to 100% rated current	$< \pm 2\%$
With Back Pressure	0% to 20% of supply	$< \pm 2\%$

FREQUENCY RESPONSE Typical response characteristics for AO76 Servovalves are shown in Figures 4 and 5. Servovalve frequency response will vary with signal amplitude, supply pressure, temperature, and internal valve design parameters. The variation in response with supply pressure, as expressed by the change in frequency of the 90° phase point, is given in Figure 6.

STEP RESPONSE Typical transient response of AO76 Servovalves is given in Figure 7. The straight-line portion of the response represents saturation flow from the pilot stage which will increase with higher supply pressures.

Appendix D

Discrete Model for Hydraulic Pressure:

The hydraulic pressure response (P_H) to a change in the valve opening (M) is modelled by a first order model plus a damping oscillatory component. The model, written in the time domain, is:

$$P_H(t) = K \left(1 - e^{-(t-D)/\tau} \right) + K_1 \left[\frac{1}{(1 - \zeta^2)^{1/2} \tau_1} e^{-\zeta t/\tau_1} \sin \left\{ (1 - \zeta^2)^{1/2} \frac{t}{\tau_1} \right\} \right] \quad (\text{D.1})$$

let

$$\begin{aligned} \frac{1}{(1 - \zeta^2)^{1/2} \tau_1} &= c \\ \zeta/\tau_1 &= a \\ \frac{(1 - \zeta^2)^{1/2}}{\tau_1} &= \omega \end{aligned}$$

Equation (D.1) becomes:

$$P_H(t) = K \left(1 - e^{-(t-D)/\tau} \right) + K_1 \left[c e^{-at} \sin(\omega t) \right] \quad (\text{D.2})$$

In the Laplace domain, Equation (D.2) becomes:

$$P_H(S) = \frac{K e^{-DS}}{S(\tau S + 1)} + \frac{K_1 c \omega}{(S + a)^2 + \omega^2} \quad (\text{D.3})$$

for a step change in the valve opening, $M(S) = \frac{1}{S}$

Therefore, Equation (D.3) can be written in the transfer function form as:

$$G(S) = \frac{P_H(S)}{M(S)} = \frac{K e^{-DS}}{(\tau S + 1)} + \frac{K_1 c \omega S}{(S + a)^2 + \omega^2} \quad (\text{D.4})$$

Using a zero order hold, $HG(S)$ can be written as:

$$HG(S) = \left(\frac{1 - e^{-TS}}{S} \right) \left[\frac{K e^{-DS}}{(\tau S + 1)} + \frac{K_1 c \omega S}{(S + a)^2 + \omega^2} \right] \quad (D.5)$$

let $D = nT$ where T = Sampling time

n = Integer

$$HG(S) = \left(\frac{1 - e^{-TS}}{S} \right) \left[\frac{K e^{-nTS}}{(\tau S + 1)} + \frac{K_1 c \omega S}{(S + a)^2 + \omega^2} \right] \quad (D.6)$$

$$HG(S) = \left(\frac{1 - e^{-TS}}{S} \right) \left(\frac{K e^{-nTS}}{(\tau S + 1)} \right) + \left(\frac{1 - e^{-TS}}{S} \right) \left(\frac{K_1 c \omega}{(S + a)^2 + \omega^2} \right) \quad (D.7)$$

Z-transform of Equation (D.7) gives the pulse transfer function as follows:

$$\begin{aligned} HG(Z) &= K(1 - Z^{-1}) Z^{-n} Z \left\{ \frac{1}{S(\tau S + 1)} \right\} \\ &\quad + (1 - Z^{-1}) Z \left[\frac{K_1 c \omega}{(S + a)^2 + \omega^2} \right] \end{aligned} \quad (D.8)$$

$$\begin{aligned} HG(Z) &= K(1 - Z^{-1}) Z^{-n} Z \left[\frac{1}{S} - \frac{1}{S + 1/\tau} \right] \\ &\quad + K_1 c (1 - Z^{-1}) Z \left[\frac{\omega}{(S + a)^2 + \omega^2} \right] \end{aligned} \quad (D.9)$$

$$\begin{aligned}
 HG(Z) = & K(1 - Z^{-1}) Z^{-n} \left[\frac{1}{1 - Z^{-1}} - \frac{1}{1 - e^{-T/\tau} Z^{-1}} \right] \\
 & + K_1 c (1 - Z^{-1}) \frac{Z^{-1} e^{-aT} \sin \omega T}{1 - 2 Z^{-1} e^{-aT} \cos \omega T + e^{-2aT} Z^{-2}}
 \end{aligned}
 \tag{D.10}$$

Let

$$\begin{aligned}
 b &= e^{-T/\tau} \\
 d &= e^{-aT} \\
 f &= 2 e^{-aT} \cos \omega T \\
 g &= e^{-2aT} \\
 h &= K(1 - b)
 \end{aligned}$$

Equation (D.10) can be written as:

$$\begin{aligned}
 HG(Z) = & K Z^{-n} (1 - Z^{-1}) \left[\frac{1 - b Z^{-1} - 1 + Z^{-1}}{(1 - Z^{-1})(1 - b Z^{-1})} \right] \\
 & + K_1 c (1 - Z^{-1}) \frac{d Z^{-1}}{1 - f Z^{-1} + g Z^{-2}}
 \end{aligned}
 \tag{D.11}$$

For $n = 1$

$$HG(Z) = \frac{K(1 - b) Z^{-2}}{1 - b Z^{-1}} + \frac{K_1 c d Z^{-1} - K_1 c d Z^{-2}}{1 - f Z^{-1} + g Z^{-2}}
 \tag{D.12}$$

$$\begin{aligned}
 & (K(1-b)Z^{-2})(1-fZ^{-1}+g^2Z^{-3}) \\
 & + (1-bZ^{-1})(K_1cdZ^{-1}-K_1cdZ^{-2}) \\
 H_6(z) = & \frac{\quad}{(1-bZ^{-1})(1-fZ^{-1}+gZ^{-2})} \quad (D.13)
 \end{aligned}$$

$$\begin{aligned}
 & hZ^{-2} - hfZ^{-3} + hgZ^{-4} + K_1cdZ^{-1} \\
 & - K_1cdZ^{-2} - K_1cdbZ^{-2} + K_1cdbZ^{-3} \\
 = & \frac{\quad}{1-fZ^{-1}+gZ^{-2}-bZ^{-1}+bfZ^{-2}-bgZ^{-3}} \quad (D.14)
 \end{aligned}$$

$$\begin{aligned}
 & K_1cdZ^{-1} + (h - K_1cd - K_1cdb)Z^{-2} \\
 & - (hf - K_1cdbZ^{-3}) + hgZ^{-4} \\
 = & \frac{\quad}{1 - (f+b)Z^{-1} + (bf+g)Z^{-2} - bgZ^{-3}} \quad (D.15)
 \end{aligned}$$

Let

$$\begin{aligned}
 b_1 &= K_1cd \\
 b_2 &= (h - K_1cd - K_1cdb) \\
 b_3 &= (hf - K_1cdb) \\
 b_4 &= hg \\
 a_0 &= 1 \\
 a_1 &= (f+b) \\
 a_2 &= (bf+g) \\
 a_3 &= bg
 \end{aligned}$$

Equation (D.15) can be written as follows:

$$HG(Z) = \frac{P_H(Z)}{M(Z)} = \frac{b_1 Z^{-1} + b_2 Z^{-2} - b_3 Z^{-3} + b_4 Z^{-4}}{1 - a_1 Z^{-1} + a_2 Z^{-2} - a_3 Z^{-3}} \quad (D.16)$$

Or in the time domain:

$$\begin{aligned} P_H(k) = & a_1 P_H(k-1) - a_2 P_H(k-2) + a_3 P_H(k-3) + b_1 M(k-1) \\ & + b_2 M(k-2) - b_3 M(k-3) + b_4 M(k-4) \end{aligned} \quad (D.17)$$

where k is the sampling instant.

Appendix E

Discrete Model for Nozzle Pressure:

Nozzle pressure (P_N) was modelled by a first order response of the form:

$$P_N(t) = K(1 - e^{-(t-D)/\tau}) \quad (\text{E.1})$$

where:

P_N	=	Nozzle pressure at sampling instant, t
K	=	Process gain
τ	=	Process time constant
D	=	Time delay

Laplace transform of Equation (E.1) gives:

$$P_N(S) = \frac{K e^{-DS}}{(\tau S + 1)} \cdot \frac{1}{S}$$

For a step change in the valve opening, $M(S) = \frac{1}{S}$,

$$G(S) = \frac{P_N(S)}{M(S)} = \frac{K e^{-DS}}{(\tau S + 1)} \quad (\text{E.2})$$

Using a zero order hold, Equation (E.2) becomes:

$$HG(S) = \left(\frac{1 - e^{-TS}}{S} \right) \left(\frac{K e^{-DS}}{\tau S + 1} \right) \quad (\text{E.3})$$

The pulse transfer function of Equation (E.3) is:

$$HG(Z) = Z \left[\frac{1 - e^{-TS}}{S} \cdot \frac{K e^{-DS}}{\tau S + 1} \right] \quad (\text{E.4})$$

Two approximations for the dead time are used to derive the discrete model:

(i) $D = nT$ where $n = \text{integer}$ and $T = \text{the sampling time}$.

$$HG(Z) = Z \left[\frac{1 - e^{-TS}}{S} \cdot \frac{Ke^{-nTS}}{\tau S + 1} \right] \quad (\text{E.5})$$

$$HG(Z) = K(1 - Z^{-1})Z^{-n} Z \left[\frac{1}{S(\tau S + 1)} \right] \quad (\text{E.6})$$

$$HG(Z) = K(1 - Z^{-1}) Z^{-n} Z \left[\frac{1}{S} - \frac{1}{S + 1/\tau} \right] \quad (\text{E.7})$$

$$HG(Z) = K(1 - Z^{-1}) Z^{-n} \left[\frac{1}{1 - Z^{-1}} - \frac{1}{1 - e^{-T/\tau} Z^{-1}} \right] \quad (\text{E.8})$$

$$HG(Z) = KZ^{-n} \left[\frac{-e^{-T/\tau} + Z^{-1}}{(1 - e^{-T/\tau} Z^{-1})} \right] \quad (\text{E.9})$$

$$HG(Z) = \frac{K(Z^{-1} - e^{-T/\tau} Z^{-1})Z^{-n}}{1 - e^{-T/\tau} Z^{-1}} \quad (\text{E.10})$$

for $n = 1$

$$HG(Z) = \frac{K(1 - a)Z^{-2}}{1 - aZ^{-1}} \quad (\text{E.11})$$

where $a = e^{-T/\tau}$

$$HG(Z) = \frac{P_N(Z)}{M(Z)} = \frac{K(1 - a)Z^{-2}}{1 - aZ^{-1}} \quad (\text{E.12})$$

Therefore the discrete response of nozzle pressure in the time domain is:

$$P_N(k) = a P_N(k-1) + K(1-a) M(k-2) \quad (\text{E.13})$$

where:

$$\begin{aligned} P_N(k) &= \text{Nozzle pressure at sampling instant, } k \\ P_N(k-1) &= \text{Nozzle pressure at sampling instant, } k-1 \\ M(k) &= \text{Valve opening at sampling instant, } k \end{aligned}$$

(ii) Padé Approximation for the Dead Time:

The exponential term in Equation (E.2) can be approximated by a first order Padé approximation of the form:

$$e^{-DS} = \frac{1 - \frac{D}{2}S}{1 + \frac{D}{2}S} \quad (\text{E.14})$$

let $D1 = D/2$

$$G(S) = \frac{K(1 - D1S)}{(\tau S + 1)(D1S + 1)} \quad (\text{E.15})$$

Using partial fraction technique:

$$G(S) = \frac{A}{\tau S + 1} + \frac{B}{D1S + 1} \quad (\text{E.16})$$

where

$$A = \frac{K(\tau + D1)}{\tau - D1}$$

$$B = \frac{2KD1}{D1 - \tau}$$

$$G(S) = \frac{A/\tau}{S + \frac{1}{\tau}} + \frac{B/D1}{S + \frac{1}{D1}} \quad (\text{E.17})$$

$$HG(S) = \left(\frac{1 - e^{-TS}}{S} \right) \left[\frac{A/\tau}{S + 1/\tau} + \frac{B/D1}{S + 1/D1} \right] \quad (\text{E.18})$$

Z-Transform of Equation (6.B.18) gives:

$$HG(Z) = (1 - Z^{-1}) Z \left[\frac{A/\tau}{S(S + 1/\tau)} + \frac{B/D1}{S(S + 1/D1)} \right] \quad (\text{E.19})$$

$$HG(Z) = \left[\frac{A(1 - e^{-T/\tau})Z^{-1}}{(1 - e^{-T/\tau}Z^{-1})} + \frac{B(1 - e^{-T/D1})Z^{-1}}{(1 - e^{-T/D1}Z^{-1})} \right] \quad (\text{E.20})$$

Let

$$c = e^{-T/\tau}$$

$$d = e^{-T/D1}$$

$$HG(Z) = \frac{A(1 - c)Z^{-1}}{1 - cZ^{-1}} + \frac{B(1 - d)Z^{-1}}{1 - dZ^{-1}} \quad (\text{E.21})$$

$$HG(Z) = \frac{A(1 - c)Z^{-1}(1 - dZ^{-1}) + B(1 - d)Z^{-1}(1 - cZ^{-1})}{(1 - cZ^{-1})(1 - dZ^{-1})} \quad (\text{E.22})$$

$$HG(Z) = \frac{A(1 - c)Z^{-1} - A(1 - c)dZ^{-2} + B(1 - d)Z^{-1} - B(1 - d)cZ^{-2}}{1 - dZ^{-1} - cZ^{-1} + cdZ^{-2}} \quad (\text{E.23})$$

$$HG(Z) = \frac{[A(1-c) + B(1-d)]Z^{-1} - [A(1-c)d + B(1-d)c]Z^{-2}}{1 - (c+d)Z^{-1} + cdZ^{-2}} \quad (\text{E.24})$$

$$HG(Z) = \frac{P_N(Z)}{M(Z)} = \frac{b_1Z^{-1} - b_2Z^{-2}}{1 - a_1Z^{-1} + a_2Z^{-2}} \quad (\text{E.25})$$

Equation (E.25) can be written in the time domain as:

$$P_N(k) = a_1P_N(k-1) - a_2P_N(k-2) + b_1M(k-1) - b_2M(k-2) \quad (\text{E.26})$$

Where:

$$a_1 = c + d$$

$$a_2 = c d$$

$$b_1 = A(1-c) + B(1-d)$$

$$b_2 = Ad(1-c) + Bc(1-d)$$

$$c = e^{-T/\tau}$$

$$d = e^{-T/D1}$$

$$A = \frac{K(\tau + D1)}{\tau - D1}$$

$$B = \frac{2KD1}{D1 - \tau}$$

Appendix F

Cavity pressure Discrete Model:

The model for cavity pressure was obtained as a first order model superimposed on a ramp component of the form:

$$P_c(t) = K_1 t + K_2 [1 - \exp(-(t - \theta)/\tau)] \quad (\text{F.1})$$

taking Laplace transfer of Equation (F.1)

$$P_c(S) = \frac{K_1}{S^2} + \frac{K_2 e^{-\theta S}}{S(\tau S + 1)} \quad (\text{F.2})$$

For a step change in the input variable (valve opening) $M = \frac{1}{S}$, we have:

$$\frac{P_c(S)}{M(S)} = G(S) = \frac{K_1}{S} + \frac{K_2 e^{-\theta S}}{(\tau S + 1)} \quad (\text{F.3})$$

Using a zero order hold, with T = Sampling time:

$$HG(S) = \left\{ \frac{1 - e^{-TS}}{S} \right\} \left[\frac{K_1}{S} \right] + \left\{ \frac{1 - e^{-TS}}{S} \right\} \left[\frac{K_2 e^{-\theta S}}{(\tau S + 1)} \right] \quad (\text{F.4})$$

The Z -transform of Equation (F.4) gives:

$$HG(Z) = (1 - Z^{-1})Z \left[\frac{K_1}{S^2} \right] + (1 - Z^{-1})Z \left[\frac{K_2 e^{-\theta S}}{S(\tau S + 1)} \right] \quad (\text{F.5})$$

To perform the Z -transform, the following two approximations for the dead time were used:

(i) $\theta = nT$ where $n = \text{integer}$

$$HG(Z) = (1 - Z^{-1}) Z \left[\frac{K_1}{S^2} \right] + (1 - Z^{-1}) Z^{-n} Z \left[\frac{K_2}{S(\tau S + 1)} \right] \quad (\text{F.6})$$

for $n = 1$, from the Z - transform tables

$$HG(Z) = \left[\frac{K_1 T Z^{-1}}{(1 - Z^{-1})} \right] + Z^{-1} \left[\frac{K_2 (1 - e^{-T/\tau}) Z^{-1}}{(1 - e^{-T/\tau} Z^{-1})} \right] \quad (\text{F.7})$$

$$HG(Z) = \frac{K_1 T Z^{-1}}{(1 - Z^{-1})} + \frac{K_2 (1 - e^{-T/\tau}) Z^{-2}}{1 - e^{-T/\tau} Z^{-1}} \quad (\text{F.8})$$

$$HG(Z) = \frac{K_1 T Z^{-1} (1 - e^{-T/\tau} Z^{-1}) + K_2 (1 - e^{-T/\tau}) Z^{-2} (1 - Z^{-1})}{(1 - Z^{-1}) (1 - e^{-T/\tau} Z^{-1})} \quad (\text{F.9})$$

$$HG(Z) = \frac{K_1 T Z^{-1} - K_1 T e^{-T/\tau} Z^{-2} + K_2 (1 - e^{-T/\tau}) Z^{-2} - K_2 (1 - e^{-T/\tau}) Z^{-3}}{1 - e^{-T/\tau} Z^{-1} - Z^{-1} + e^{-T/\tau} Z^{-2}} \quad (\text{F.10})$$

$$HG(Z) = \frac{K_1 T Z^{-1} - [K_1 T e^{-T/\tau} - K_2 (1 - e^{-T/\tau})] Z^{-2} - K_2 (1 - e^{-T/\tau}) Z^{-3}}{1 - (1 + e^{-T/\tau}) Z^{-1} + e^{-T/\tau} Z^{-2}} \quad (\text{F.11})$$

Therefore:

$$HG(Z) = \frac{P_c(Z)}{M(Z)} = \frac{b_1 Z^{-1} - b_2 Z^{-2} - b_3 Z^{-3}}{1 - a_1 Z^{-1} + a_2 Z^{-2}} \quad (\text{F.12})$$

Where:

$$a_1 = 1 + e^{-T/\tau}$$

$$a_2 = e^{-T/\tau}$$

$$b_1 = K_1 T$$

$$b_2 = K_1 T e^{-T/\tau} - K_2 (1 - e^{-T/\tau})$$

$$b_3 = K_2 (1 - e^{-T/\tau})$$

Equation (F.12) can be written in the time domain as follows:

$$\begin{aligned} P_c(k) = & a_1 P_c(k-1) - a_2 P_c(k-2) + b_1 M(k-1) \\ & - b_2 M(k-2) - b_3 M(k-3). \end{aligned} \quad (\text{F.13})$$

(ii) Padé Approximation for the Dead Time:

$$e^{-\theta S} = \frac{1 - \frac{\theta}{2} S}{1 + \frac{\theta}{2} S} \quad (\text{F.14})$$

let $D = \theta/2$.

Equation (F.3) becomes:

$$\frac{P_c(S)}{M(S)} = G(S) = \frac{K_1}{S} + \frac{K_2(1 - DS)}{(\tau S + 1)(1 + DS)} \quad (\text{F.15})$$

$$G(S) = \frac{K_1}{S} + \frac{A}{(\tau S + 1)} + \frac{B}{(DS + 1)} \quad (\text{F.16})$$

where:

$$A = \frac{K_2(\tau + D)}{(\tau - D)},$$

$$B = \frac{2K_2D}{D - \tau}.$$

$$HG(S) = \left(\frac{1 - e^{-Ts}}{S} \right) \left[\frac{K_1}{S} + \frac{A}{\tau S + 1} + \frac{B}{DS + 1} \right] \quad (\text{F.17})$$

$$HG(Z) = (1 - Z^{-1})Z \left[\frac{K_1}{S_2} + \frac{A/\tau}{S(S + \frac{1}{\tau})} + \frac{B/D}{S(S + \frac{1}{D})} \right] \quad (\text{F.18})$$

$$HG(Z) = \left[\frac{K_1 T Z^{-1}}{(1 - Z^{-1})} + \frac{A(1 - e^{T/\tau}) Z^{-1}}{(1 - e^{-T/\tau} Z^{-1})} + \frac{B(1 - e^{-TD}) Z^{-1}}{(1 - e^{-T/D} Z^{-1})} \right] \quad (\text{F.19})$$

let

$$c = e^{-T/\tau},$$

$$d = e^{-T/D}$$

$$HG(Z) = \frac{K_1 T Z^{-1}}{(1 - Z^{-1})} + \frac{A(1 - c)Z^{-1}}{1 - c Z^{-1}} + \frac{B(1 - d)Z^{-1}}{1 - d Z^{-1}} \quad (\text{F.20})$$

$$HG(Z) = \frac{K_1 Z^{-1} (1 - c Z^{-1})(1 - d Z^{-1}) + A(1 - c) Z^{-1} (1 - Z^{-1})(1 - d Z^{-1}) + B(1 - d) Z^{-1} (1 - Z^{-1})(1 - c Z^{-1})}{(1 - Z^{-1})(1 - c Z^{-1})(1 - d Z^{-1})} \quad (\text{F.21})$$

$$\begin{aligned}
 & [K_1 T Z^{-1} (1 - d Z^{-1} - c Z^{-1} + cd Z^{-2}) \\
 & + A(1 - c) Z^{-1} (1 - d Z^{-1} - Z^{-1} + d Z^{-2}) \\
 & + B(1 - d) Z^{-1} (1 - c Z^{-1} - Z^{-1} + c Z^{-2})] \\
 H(z) = & \frac{\quad}{(1 - Z^{-1})(1 - d Z^{-1} - c Z^{-1} + cd Z^{-2})} \quad (F.22)
 \end{aligned}$$

$$\begin{aligned}
 & [K_1 T Z^{-1} \{1 - (c + d) Z^{-1} + cd Z^{-2}\} \\
 & + A(1 - c) Z^{-1} \{1 - (1 + d) Z^{-1} + d Z^{-2}\} \\
 & + B(1 - d) Z^{-1} \{1 - (1 + c) Z^{-1} + c Z^{-2}\}] \\
 = & \frac{\quad}{(1 - Z^{-1})[1 - (c + d) Z^{-1} + cd Z^{-2}]} \quad (F.23)
 \end{aligned}$$

$$\begin{aligned}
 & [K_1 T Z^{-1} - K_1 T (c + d) Z^{-2} + K_1 T cd Z^{-3} \\
 & + A(1 - c) Z^{-1} - A(1 - c) (1 + d) Z^{-2} + A(1 - c) d Z^{-3} \\
 & + B(1 - d) Z^{-1} - B(1 - d) (1 + c) Z^{-2} + B(1 - d) c Z^{-3}] \\
 = & \frac{\quad}{1 - (1 + c + d) Z^{-1} + (c + d + cd) Z^{-2} - cd Z^{-3}} \quad (F.24)
 \end{aligned}$$

$$HG(Z) = \frac{P_c(Z)}{M(Z)} = \frac{f_1 Z^{-1} - f_2 Z^{-2} + f_3 Z^{-3}}{1 - h_1 Z^{-1} + h_2 Z^{-2} - h_3 Z^{-3}} \quad (\text{F.25})$$

and the response of cavity gate pressure in the time domain becomes:

$$\begin{aligned} P_c(k) = & h_1 P_c(k-1) - h_2 P_c(k-2) + h_3 P_c(k-3) \\ & + f_1 M(k-1) - f_2 M(k-2) + f_3 M(k-3) \end{aligned} \quad (\text{F.26})$$

Where:

$$h_1 = 1 + c + d$$

$$h_2 = c + d + c d$$

$$h_3 = c d$$

$$f_1 = K_1 T + A(1 - c) + B(1 - d)$$

$$f_2 = K_1 T + A(1 - c)(1 + d) + B(1 - d)(1 + c)$$

$$f_3 = K_1 T c d + A d(1 - c) + B c(1 - d)$$

$$A = K_2(+D_1)/(-D_1)$$

$$B = 2 K_2 D_1/(D_1 -)$$

$$c = \exp(-T/)$$

$$d = \exp(-T/D_1)$$

Appendix G

Derivation of Dahlin Controller for Nozzle Pressure

Dahlin Controller is give by equation (6.10) as:

$$D(Z) = \frac{M(Z)}{E(Z)} = \frac{(1 - e^{-T/\lambda}) Z^{-n-1}}{1 - e^{-T/\lambda} Z^{-1} - (1 - e^{-T/\lambda}) Z^{-n-1}} \cdot \frac{1}{HG(Z)} \quad (G.1)$$

Substituting for $HG(Z)$ from Equations (E.12) and (E.25) for the two cases of dead-time approximation:

(i) $D = nT, n = 1.$

$$HG(Z) = \frac{K(1-a)Z^{-2}}{1-aZ^{-1}} = \frac{K(1-e^{-T/\tau})Z^{-2}}{1-e^{-T/\tau}Z^{-1}} \quad (G.2)$$

$$D(Z) = \frac{M(Z)}{E(Z)} = \frac{(1 - e^{-T/\lambda})}{1 - e^{-T/\lambda} Z^{-1} - (1 - e^{-T/\lambda}) Z^{-2}} \cdot \frac{1 - e^{-T/\tau} Z^{-1}}{K(1 - e^{-T/\tau})} \quad (G.3)$$

$$D(Z) = \frac{M(Z)}{E(Z)} = \frac{1 - e^{-T/\lambda}}{K(1 - e^{-T/\tau})} \cdot \frac{1 - e^{-T/\tau} Z^{-1}}{1 - e^{-T/\lambda} Z^{-1} - (1 - e^{-T/\lambda}) Z^{-2}} \quad (G.4)$$

Let

$$b_0 = \frac{1 - e^{-T/\lambda}}{K(1 - e^{-T/\tau})}$$

$$b_1 = b_0 e^{-T/\tau}$$

$$a_1 = e^{-T/\lambda}$$

$$a_2 = 1 - e^{-T/\lambda}$$

$$\frac{M(Z)}{E(Z)} = \frac{b_0 - b_1 Z^{-1}}{1 - a_1 Z^{-1} - a_2 Z^{-2}} \quad (\text{G.5})$$

$$M(k) = a_1 M(k-1) + a_2 M(k-2) + b_0 E(k) - b_1 E(k-1) \quad (\text{G.6})$$

(ii) Padé Approximation:

for $n = 1$

$$D(Z) = \frac{(1-b)Z^{-2}}{1-bZ^{-1}-(1-b)Z^{-2}} \cdot \frac{1-a_1Z^{-1}+a_2Z^{-2}}{b_1Z^{-1}-b_2Z^{-2}} \quad (\text{G.7})$$

where $b = e^{-T/\lambda}$

$$D(Z) = \frac{(1-b)Z^{-1}}{1-bZ^{-1}-(1-b)Z^{-2}} \cdot \frac{1-a_1Z^{-1}+a_2Z^{-2}}{(b_1-b_2Z^{-1})} \quad (\text{G.8})$$

$$D(Z) = \frac{(1-b)Z^{-1}}{1-bZ^{-1}-(1-b)Z^{-2}} \cdot \frac{1-a_1Z^{-1}+a_2Z^{-2}}{b_1-b_2Z^{-1}} \quad (\text{G.9})$$

$$D(Z) = \frac{M(Z)}{E(Z)} = \frac{(1-b)[1-a_1Z^{-1}+a_2Z^{-2}]}{[1-bZ^{-1}-(1-b)Z^{-2}][b_1-b_2Z^{-1}]} \quad (\text{G.10})$$

$$\frac{M(Z)}{E(Z)} = \frac{(1-b)Z^{-1} - a_1(1-b)Z^{-2} + a_2(1-b)Z^{-3}}{b_1 - bb_1Z^{-1} - b_1(1-b)Z^{-2} - b_2Z^{-1} + bb_2Z^{-2} + b_2(1-b)Z^{-3}} \quad (\text{G.11})$$

$$\frac{M(Z)}{E(Z)} = \frac{(1-b)Z^{-1} - a_1(1-b)Z^{-2} + a_2(1-b)Z^{-3}}{b_1 - (bb_1 - b_2)Z^{-1} - [b_1(1-b) - bb_2]Z^{-2} + b_2(1-b)Z^{-3}} \quad (\text{G.12})$$

$$\frac{M(Z)}{E(Z)} = \frac{f_1 Z^{-1} - f_2 Z^{-2} + f_3 Z^{-3}}{h_0 - h_1 Z^{-1} - h_2 Z^{-2} + h_3 Z^{-3}} \quad (\text{G.13})$$

or

$$M(k) = \frac{1}{h_0} [h_1 M(k-1) + h_2 M(k-2) - h_3 M(k-3) + f_1 E(k-1) - f_2 E(k-2) + f_3 E(k-3)]$$

where:

$$f_1 = 1 - e^{-T/\lambda}$$

$$f_2 = (1 - e^{-T/\lambda}) (e^{-T/\tau} + e^{-T/D1})$$

$$f_3 = e^{-T/\tau} e^{-T/D1} (1 - e^{-T/\lambda})$$

$$h_0 = \frac{K(\tau + D1)}{\tau - D1} (1 - e^{-T/\tau}) + \frac{ZKD1}{D1 - \tau} (1 - e^{-T/D1})$$

$$h_1 = \frac{K(\tau + D1)}{\tau - D1} (1 - e^{-T/\tau}) (e^{-T/\lambda} - e^{-T/D1}) + \frac{2KD1}{D1 - \tau} (1 - e^{-T/D1}) (e^{-T/\lambda} - e^{-T/\tau})$$

$$h_2 = \frac{K(\tau + D1)}{\tau - D1} (1 - e^{-T/\tau}) \left[1 - \frac{2KD1}{D1 - \tau} e^{-T/D1} \right] \\ + \frac{ZKD1}{D1 - \tau} (1 - e^{-T/D1}) \left[1 - \frac{ZKD1}{D1 - \tau} e^{-T/\tau} \right]$$

$$h_3 = \left[\frac{K(\tau + D1)}{\tau - D1} e^{-T/D1} (1 - e^{-T/\tau}) + \frac{2KD1}{D1 - \tau} e^{-T/\tau} (1 - e^{-T/D1}) \right] (1 - e^{-T/\lambda})$$

APPENDIX H

SIMULATION PROGRAMS

%
% HYDRAULIC PRESSURE CONTROL
% SIMULATION PROGRAM

1 % Simulation program for hydraulic pressure control using
% PID controller. Different controller parameter values are used.
% PI controller can be run by setting td=0.0.
% The program calculates the integral criteria for
% controller performance comparison.

echo on
ni=75;
nii=20;

% Controller Parameters
kc=0.01;
ti=0.045
td=0.0;

ts=0.01; % Sampling time
sp=500.0; % Set-point

% Process Model Parameters

k=30.7;
t=0.045;
ded=0.011;
k1=0.022;
t1=0.005;
z=0.168;
a=z/t1;
zz=z^2;
c=1/(((1-zz)^0.5)*t1);
w=(1-zz)^0.5/t1;
b=exp(-ts/t);
d=exp(-a*ts)*sin(w*ts);
f=2*exp(-a*ts)*cos(w*ts);
g=exp(-2*a*ts);
h=k*(1-b);
b1=k1*c*d;
b2=h-k1*c*d-k1*c*d*b;
b3=h*f-k1*c*d*b;
b4=h*g;
a0=1;
a1=f+b;
a2=b*f+g;
a3=b*g;

ac=kc1*(1+(ts/ti)+(td/ts));
bc=kc1*(1+2*(td/ts));
cc=kc1*(td/ts);

se=0.0;
ae=0.0;
ta=0.0;

% Initialization

```
e1=0.0;  
e2=0.0;  
p=400;  
m=p/k;  
m1=m;  
m2=m;  
m3=m;  
m4=m;  
p1=p;  
p2=p;  
p3=p;
```

```
for i=1:nii  
    it(i)=i*ts;  
    spi(i)=p;  
    mi(i)=m;  
    ph(i)=p;  
end
```

```
for i=nii:ni  
    it(i)=i*ts;  
    spi(i)=sp;  
    e=sp-p;  
    abse=abs(e);
```

```
    m1(i)= m1 + ac*e - bc*e1 + cc*e2;
```

```
    if mi(i) > 100  
        mi(i)=100;  
    else  
        if mi(i)<0  
            mi(i)=0;  
        end  
    end
```

```
    ph(i)=a1*p1 - a2*p2 + a3*p3 + b1*m1 + b2*m2 - b3*m3 +b4*m4;
```

```
    se= se + e*e;  
    ae= ae + abse;  
    ta= ta + (it(i)-nii*ts)*abse;
```

```
    e2=e1;  
    e1=e;  
    m4=m3;  
    m3=m2;  
    m2=m1;  
    m1=m1(i);  
    p=ph(i);  
    p3=p2;  
    p2=p1;  
    p1=p;  
end
```

```
se = (se - e*e/2)*ts ;  
ae = (ae - abse/2)*ts ;  
ta = (ta - (it(i)-nii*ts)*abse/2)*ts ;
```

```
clg
```

```
subplot(211)  
axis([0 0.8 1000 3000])  
plot(it,spi,'--',it,ph,'-')  
title('PH Control, PID & PI Controllers')  
ylabel('Hydraulic Pressure (KPa)')  
xlabel('Time (sec)')
```

```
axis([0 0.8 0 50])  
plot(it,m1,'-')  
ylabel('Valve Opening (%)')  
xlabel('Time (sec)'); pause  
meta b:phpi
```

%
% NOZZLE PRESSURE CONTROL
% SIMULATION PROGRAM

% Simulation program for nozzle pressure control using
% PID controller. Different controller parameter values are used.
% PI controller can be run by setting $td=0.0$.
% The program calculates the integral criteria for
% controller performance comparison.

echo on
ni=75;
nii=20;

% Controller Parameters
kc=0.008;
ti=0.045;
td=0.005;

ts=0.01; % Sampling time
sp=2500.0; % Set-point

% Process Model Parameters
k=211.5;
t=0.05;
ded=0.01;

a1=exp(-ts/t);
ac=kc1*(1+(ts/ti)+(td/ts));
bc=kc1*(1+2*(td/ts));
cc=kc1*(td/ts);
se=0.0;
ae=0.0;
ta=0.0;

% Initialization
e1=0.0;
e2=0.0;
p=2000;
m=p/k;
m1=m;
m2=m;
p1=p;

for i=1:nii
it(i)=i*ts;
spi(i)=p;
mi(i)=m;
pn(i)=p;
end

```

for i=nii:ni
    it(i)=i*ts;
    spi(i)=sp;
    e=sp-p;
    abse=abs(e);
    mi(i)= m1 + ac*e - bc*e1 + cc*e2;
    if mi(i) > 100
        mi(i)=100;
    else
        if mi(i)<0
            mi(i)=0;
        end
    end
    pn(i)=a1*p1 + k*(1-a1)*m2;
    se= se + e*e;
    ae= ae + abse;
    ta= ta + (it(i)-nii*ts)*abse;
    e2=e1;
    e1=e;
    m2=m1;
    m1=mi(i);
    p=pn(i);
    p1=p;
end
se = (se - e*e/2)*ts ;
ae = (ae - abse/2)*ts ;
ta = (ta - (it(i)-nii*ts)*abse/2)*ts ;

```

```

clg
subplot(211)
axis([0 0.8 1500 3000])
plot(it,spi,'--',it,pn,'-')
title('PN Control, PID & PI Controller')
ylabel('Nozzle Pressure (KPa)')
xlabel('Time (sec)')

axis([0 0.8 0 50])
plot(it,m1,'-')
ylabel('Valve opening (%)')
xlabel('Time (sec)',% pause
meta b:npnid

```

```

mi(i)=a1*m1 + a2*m2 + b0*e - b1*e1; /
if mi(i) > 100
    mi(i)=100;
else
    if mi(i)<0
        mi(i)=0;
    end
end
pn(i)=a1*p1 + k*(1-a1)*m2;
se= se + e*e;
ae= ae + abse;
ta= ta + (it(i)-nii*ts)*abse;
e1=e;
m2=m1;
m1=mi(i);
p=pn(i);
p1=p;
end
se = (se - e*e/2)*ts ;
ae = (ae - abse/2)*ts ;
ta = (ta - (it(i)-nii*ts)*abse/2)*ts ;

clg
subplot(211)
axis([0 0.8 1500 3000])
plot(it,spi,'--',it,pn,'-')
title('PN Control, Dahlin Controller')
ylabel('Nozzle Pressure (KPa)')
xlabel('Time (sec)')

axis([0 0.8 0 50])
plot(it,mi,'-')
ylabel('Valve opening (%)')
xlabel('Time (sec)'),% pause
meta b:pndah

```



```

%                               NOZZLE PRESSURE CONTROL
%                               SIMULATION PROGRAM

%   Simulation program for nozzle pressure control using
%   Dahlin controller. Different controller parameter values are used.
%   The program calculates the integral criteria for
%   controller performance comparison.

echo on
ni=75;
nii=20;

%   Controller parameters
ts=0.005;      % Sampling time
la=0.006;      % Lambda

%   Process Model Parameters
k=211.5;
t=0.05;
ded=0.01;
a=exp(-ts/t);
a1=exp(-ts/la);
a2=1-exp(-ts/la);
b0=(1-exp(-ts/la))/(k*(1-exp(-ts/t)));
b1=b0*exp(-ts/t);

%       Initialization
se=0.0;
ae=0.0;
ta=0.0;
e1=0.0;
e2=0.0;
p=2000;
m=p/k;
m1=m;
m2=m;
p1=p;

for i=1:nii
    it(i)=i*ts;
    spi(i)=p;
    mi(i)=m;
    pn(i)=p;
end
for i=nii+1:ni
    it(i)=i*ts;
    spi(i)=sp;
    e=sp-p;
    abse=abs(e);

```

%
%

CAVITY PRESSURE CONTROL SIMULATION PROGRAM

% Simulation program for cavity pressure control using
% PID controller. Different controller parameter values are used.
% PI controller can be run by setting $td=0.0$.
% The program calculates the integral criteria for
% controller performance comparison.
% Pressure-time profile setpoint is used.
% Two approximations for the process time delay are used.

echo on
ni=80;

ts=0.01;

% Process Model Parameters
k1=14.0433;
k2=3.3367;
t=0.106;
td=ts;
a1=1+exp(-ts/t);
a2=exp(-ts/t);
b1=k1*ts;
b2=k1*ts*exp(-ts/t)-k2*(1-exp(-ts/t));
b3=k2*(1-exp(-ts/t));

% Controller Parameters
kc=0.6;
ti=0.12;
td=0.004;
aa1=kc*(1+(ts/ti)+(td/ts));
bb1=kc*(1+2*(td/ts));
cc1=kc*(td/ts);

% Set-point Profile
s1=250.0;
ps=50.0;
s2=300.0;

se=0.0;
ae=0.0;
ta=0.0;

for i=1:ni
it(i)=i*ts;
tt=it(i);

```

if i <= 20
    p=s1*tt;
    pc(i)=p;
    pcd(i)=p;
    spi(i)=p;
    sp1=p;
    p1=p;
    p2=p;
    p3=p;
    m=p/(k1+k2);
    mi(i)=m;
    mdi(i)=m;
    m1=m;
    m2=m;
    m3=m;
    e1=0.0;
    e2=0.0;
else
    spi(i)=sp1 + ps + s2*(tt-20*ts);
    sp2=spi(i);
    e=sp2 - p;
    abse=abs(e);
    mi(i)=m1 + aal*e - bb1*e1 + cc1*e2;
    if mi(i) > 100
        mi(i)=100;
    else
        if mi(i)<0
            mi(i)=0;
        end
    end
    pc(i)=a1*p1 - a2*p2 + b1*m1 - b2*m2 -b3*m3;
    pcd(i)=pc(i);
    mdi(i)=mi(i);
    se = se + e*e;
    ae = ae + abse;
    ta = ta + (it(i)-20*ts)*abse;
    e2=e1;
    e1=e;
    m3=m2;
    m2=m1;
    m1=mi(i);
    p=pc(i);
    p2=p1;
    p1=p;
end
end
se = (se-e*e/2)*ts ;
ae = (ae-abse/2)*ts ;
ta = (ta-(it(i)-20*ts)*abse/2)*ts ;

```

```

axis([0 1 0 300])
plot(it,spi,'--',it,pc,'-')
title('PC PID STEP + RAMP SET POINT')

```

```

xlabel('Time (sec)')
ylabel('Cavity Pressure (psi)')
text(.70,.760,'Kc (1) = 0.6','sc')
text(.70,.735,'      (4) = 0.5','sc')
text(.70,.710,'      (5) = 0.4','sc')
text(.70,.685,'TI = 0.14 ','sc')
text(.70,.660,'TD = 0.004 ','sc')
text(.70,.610,'-- : Set Point','sc')

```

```

axis([0 1 0 100])
plot(it,mi,'-')
xlabel('Time (sec)')
ylabel('Valve Opening (%)')
meta

```

```

%                               Pade Approximation

```

```

ts=0.01;
dt=0.011;
dt2=dt/2;

```

```

%                               Process Model Parameters

```

```

c=exp(-ts/t);
d=exp(-ts/dt2);
a=k2*(t+dt2)/(t-dt2);
b=2*k2*dt2/(dt2-t);
c1= 1 + c + d;
c2= c + d + (c * d);
c3= c * d;
d1= k1 * ts + a*(1-c) + b*(1-d);
d2= k1 * ts*(c+d) + a*(1-c)*(1+d) + b*(1-d)*(1+c);
d3= k1 * ts * c * d + a*d*(1-c) + b*c*(1-d);

```

```

se=0.0;
ae=0.0;
ta=0.0;

```

```

for i=1:ni
    it(i)=i*ts;
    tt=it(i);
    if i <= 20
        p=s1*tt;
        pcpd(i)=p;
        spi(i)=p;
        spl=p;
        p1=p;
        p2=p;
        p3=p;
        m=p/(k1+k2);
        mpd(i)=m;
        m1=m;
        m2=m;
        m3=m;
    end
end

```

```

    e1=0.0;
    e2=0.0;
    else
        spi(i)=spi + ps + s2*(tt-20*ts);
        sp2=spi(i);
        e=sp2 - p;
        abse=abs(e);
        mpd(i)=m1 + aa1*e - bb1*e1 + cc1*e2;
        if mpd(i) > 100
            mpd(i)=100;
        else
            if mpd(i)<0
                mpd(i)=0;
            end
        end
        pcpcd(i)=c1*p1 - c2*p2 + c3*p3 + d1*m1 - d2*m2 + d3*m3;
        se = se + e*ts;
        ae = ae + abse;
        ta = ta + (it(i)-20*ts)*abse;
        e2=e1;
        e1=e;
        m3=m2;
        m2=m1;
        m1=mpd(i);
        p=pcpcd(i);
        p3=p2;
        p2=p1;
        p1=p;
    end
end

```

```

se = (se-e*e/2)*ts ;
ae = (ae-abse/2)*ts ;
ta = (ta-(it(i)-20*ts)*abse/2)*ts ;

```

```

axis([0 1 0 300])
plot(it,spi,'--',it,pcpi,'-',it,pcpd,'-')
title('PC PI & PID, Pade, STEP + RAMP SET POINT')
xlabel('Time (sec)')
ylabel('Cavity Pressure (psi)')
text(.70,.750,' (1) : PI ', 'sc')
text(.70,.700,' (2) : PID ', 'sc')
text(.70,.650,'-- : Set Point', 'sc')

```

```

axis([0 1 0 100])
plot(it,mpi,'-',it,mpd,'-')
xlabel('Time (sec)')
ylabel('Valve Opening (%)')
meta

```

APPENDIX I

OVERALL CONTROL PROGRAM FOR THE
INJECTION MOLDING CYCLE

```

0000:                ; MAIN CONTROL PROGRAM      (SRV)
0000:
003B:    MONITOR    EQU    003BH
2020:    RCS       EQU    2020H ; READING COUNTER SETTING
2022:    SOSA      EQU    2022H ; START OF DATA STORAGE ADD.
2024:    DF        EQU    2024H ; DISPLACEMENT FACTOR:0001=128 R.
2026:    FCN       EQU    2026H ; NO OF 1ST. CHANNEL TO BE READ
2027:    LCN       EQU    2027H ; NO OF LAST CHANNEL TO BE READ
2028:    RCCR      EQU    2028H ; READING COUNTER C.R.
202A:    TSOSA     EQU    202AH ; TEMP ST. OF START OF ST.ADD
2032:    HTCS      EQU    2032H ; HOLD TIME COUNTER SETTING
2034:    CTCs      EQU    2034H ; COOL TIME COUNTER SETTING
2036:    DTBP      EQU    2036H ; DELAY TIME BEFORE PLASTICATION
2038:    TFTC      EQU    2038H ; TEMP ADD. OF FILL TIME COUNTER
203A:    THICR     EQU    203AH ; TEMP ADD. OF HOLD TIME COUNTER
203C:    C1CR      EQU    203CH ; COOLING TIME COUNTER READING
203E:    IRC       EQU    203EH ; TIMER REPEAT COUNTER
2040:    FHTP      EQU    2040H ; FILL/HOLD TRANSITION POINT
2044:    CSCCSP    EQU    2044H ; COOL ST. CONT. CHANNEL S.P.
2046:    TRCS      EQU    2046H ; TIMER REPEAT COUNTER SETTING
2048:    TFSCCCR   EQU    2048H ; TEMP ST. OF FSCC C.R.
204A:    THSCCCR   EQU    204AH ; TEMP ST. OF HSCC C.R.
204C:    TCSCCCR   EQU    204CH ; COOL ST. CONT. CHANNEL C.R.
2050:    FSCC      EQU    2050H ; FILL STAGE CONTROL CHANNEL
2051:    HSCC      EQU    2051H ; HOLD STAGE CONTROL CHANNEL
2052:    CSCC      EQU    2052H ; COOL STAGE CONTROL CHANNEL
2053:    ISVOF     EQU    2053H ; INIT. SSV OPENING FOR FILLING
2054:    SVOH       EQU    2054H ; SSV OPENING FOR HOLDING
2055:    SVOP       EQU    2055H ; SSV OPENING FOR PLASTICATION
2056:    IRSVO     EQU    2056H ; INIT. RSV OPENING
2058:    CSC        EQU    2058H ; CONT. STAGE COUNTER
2059:    TFCC       EQU    2059H ; TEMP STORAGE OF CONTROL CHANNEL
205C:    TSVO      EQU    205CH ; TEMP STORAGE OF VALVE OPENING
205D:    RSC       EQU    205DH ; READ/STORE CONTROL :0=READ & STORE
0000:                ;                          1=READ ONLY
2060:    PNA1L      EQU    2060H ; PN CONTROLLER CONST. A1 (LSB)
2061:    PNA1M      EQU    2061H ; PN CONTROLLER CONST. A1 (MSB)
2062:    PNA2L      EQU    2062H ; PN CONTROLLER CONST. A2 (LSB)
2063:    PNA2M      EQU    2063H ; PN CONTROLLER CONST. A2 (MSB)
2064:    PNSF        EQU    2064H ; PN CONTROLLER SCALING FACTOR
2066:    PNSF2      EQU    2066H ; PN CONTROLLER SCALING FACTOR/2
0000:                ;
2070:    PNCRAD     EQU    2070H ; PN CURRENT READING (C.R.) ADDR
2072:    PNSPP      EQU    2072H ; PN SET POINT PROFILE ADDR.
2074:    PNSPSA     EQU    2074H ; PN SET POINT STORAGE ADDR.
2076:    PNEGA      EQU    2076H ; PN ERROR STORAGE ADDR.
2078:    PNESSA     EQU    2078H ; PN ERROR SIGN STORAGE ADDR.
207A:    PNA1ESA   EQU    207AH ; PN A1*E1 STORAGE ADDR.
207C:    PNA2ESA   EQU    207CH ; PN A2*E1-1 STORAGE ADDR.
207E:    PNR1SA    EQU    207EH ; PN R1 (A1*E1-A2*E1-1) ST. ADDR.
2080:    PNR1SA    EQU    2080H ; PN R1 SIGN STORAGE ADDR.

```

2082:	PNDRSA	EQU	2082H	; PN DR (R1/SF) STORAGE ADDR.
2084:	SSVOSA	EQU	2084H	; SUBLY SEVOVALVE OPENING ST.ADR.
2086:	RSVOSA	EQU	2086H	; RELIEF SERVOVALVE OPENING ST. ADDR.
2088:	PNETS	EQU	2088H	; TEMP ST. OF PN ERROR
208A:	PNETS	EQU	208AH	; TEMP ST. OF PN ERROR SIGN
208C:	PNAIETS	EQU	208CH	; TEMP ST. OF PN A1*E1
208E:	PNAZETS	EQU	208EH	; TEMP ST. OF PN A2*E1-1
2090:	PNRITS	EQU	2090H	; TEMP ST. OF PN R1
2092:	PNRISTS	EQU	2092H	; TEMP ST. OF PN R1 SIGN
2094:	PNDRTS	EQU	2094H	; TEMP ST. OF PN DR
2096:	PNCRTS	EQU	2096H	; TEMP ST. OF PN CR
2098:	PNPCTP	EQU	2098H	; PN/PC CONTROL TRANSITION
209A:	PCPGTP	EQU	209AH	; PC/PG CONTROL TRANSITION
209C:	PC1CRTS	EQU	209CH	; TEMP ST. OF PC1 CR
209E:	PC2CRTS	EQU	209EH	; TEMP ST. OF PC2 CR
0000:				
20A0:	PCA1L	EQU	20A0H	; PC CONTROLLER CONST. A1 (LSB)
20A1:	PCA1M	EQU	20A1H	; PC CONTROLLER CONST. A1 (MSB)
20A2:	PCA2L	EQU	20A2H	; PC CONTROLLER CONST. A2 (LSB)
20A3:	PCA2M	EQU	20A3H	; PC CONTROLLER CONST. A2 (MSB)
20A4:	PCSF	EQU	20A4H	; PC CONTROLLER SCALING FACTOR
20A6:	PCSF2	EQU	20A6H	; PC CONTROLLER SCALING FACTOR/2
0000:				
20B0:	PCCRAD	EQU	20B0H	; PC CURRENT READING (C.R.), ADDR
20B2:	PCSPPP	EQU	20B2H	; PC SET POINT PROFILE ADDR.
20B4:	PCSPSA	EQU	20B4H	; PC SET POINT STORAGE ADDR.
20B6:	PCESA	EQU	20B6H	; PC ERROR STORAGE ADDR.
20B8:	PCESSA	EQU	20B8H	; PC ERROR SIGN STORAGE ADDR
20BA:	PCAIESA	EQU	20BAH	; PC A1*E1 STORAGE ADDR
20BC:	PCAZESA	EQU	20BCH	; PC A2*E1-1 STORAGE ADDR.
20BE:	PCRISA	EQU	20BEH	; PC R1 (A1*E1-A2*E1-1) ST. ADDR.
20C0:	PCR1SSA	EQU	20C0H	; PC R1 SIGN STORAGE ADDR.
20C2:	PCDRSA	EQU	20C2H	; PC DR (R1/SF) STORAGE ADDR.
20C4:	PC1CRAD	EQU	20C4H	; PC1 CR. ST. ADR.
20C6:	PC2CRAD	EQU	20C6H	; PC2 CR. ST. ADR.
0000:				
20C8:	PCETS	EQU	20C8H	; TEMP ST. OF PC ERROR
20CA:	PCESTS	EQU	20CAH	; TEMP ST. OF PC ERROR SIGN
20CC:	PCA1ETS	EQU	20CCH	; TEMP ST. OF PC A1*E1
20CE:	PCAZETS	EQU	20CEH	; TEMP ST. OF PC A2*E1-1
20D0:	PCRITS	EQU	20D0H	; TEMP ST. OF PC R1
20D2:	PCRISTS	EQU	20D2H	; TEMP ST. OF PC R1 SIGN
20D4:	PCDRTS	EQU	20D4H	; TEMP ST. OF PC DR
20D6:	DP1TS	EQU	20D6H	; TEMP ST. OF DP(t)
20D8:	DP2TS	EQU	20D8H	; TEMP ST. OF DP(t-1)
20DA:	DPSL	EQU	20DAH	; LSB OF SLOPE FACTOR
20DB:	DPSM	EQU	20DBH	; MSB OF SLOPE FACTOR
20DC:	DPSTS	EQU	20DCH	; TEMP ST OF SF*DP(t-1)
20E0:	HA1L	EQU	20E0H	; H CONTROLLER CONST. A1 (LSB)
20E1:	HA1M	EQU	20E1H	; H CONTROLLER CONST. A1 (MSB)

20E2:	HA2L	EQU	20E2H	; H CONTROLLER CONST. A2 (LSB)
20E3:	HA2M	EQU	20E3H	; H CONTROLLER CONST. A2 (MSB)
20E4:	HSF	EQU	20E4H	; H CONTROLLER SCALING FACTOR
20E6:	HSF2	EQU	20E6H	; H CONTROLLER SCALING FACTOR/2
0000:				;
20F0:	HCRAD	EQU	20F0H	; H CURRENT READING (C.R.) ADDR
20F2:	HSPP	EQU	20F2H	; H SET POINT PROFILE ADDR.
20F4:	HSPSA	EQU	20F4H	; H SET POINT STORAGE ADDR.
20F6:	HESA	EQU	20F6H	; H ERROR STORAGE ADDR.
20F8:	HESSA	EQU	20F8H	; H ERROR SIGN STORAGE ADDR.
20FA:	HA1ESA	EQU	20FAH	; H A1*E1 STORAGE ADDR.
20FC:	HA2ESA	EQU	20FCH	; H A2*E1-1 STORAGE ADDR.
20FE:	HR1SA	EQU	20FEH	; H R1 (A1*E1-A2*E1-1) ST. ADDR.
2100:	HR1SSA	EQU	2100H	; H R1 SIGN STORAGE ADDR.
2102:	HDRSA	EQU	2102H	; H DR (R1/SF) STORAGE ADDR.
0000:				;
2108:	HETS	EQU	2108H	; TEMP ST. OF H ERROR
210A:	HESTS	EQU	210AH	; TEMP ST. OF H ERROR SIGN
210C:	HA1ETS	EQU	210CH	; TEMP ST. OF H A1*E1
210E:	HA2ETS	EQU	210EH	; TEMP ST. OF H A2*E1-1
2110:	HR1TS	EQU	2110H	; TEMP ST. OF H R1
2112:	HR1STS	EQU	2112H	; TEMP ST. OF H R1 SIGN
2114:	HDRTS	EQU	2114H	; TEMP ST. OF H DR
0000:				;
2120:	PGA1L	EQU	2120H	; PG CONTROLLER CONST. A1 (LSB)
2121:	PGA1M	EQU	2121H	; PG CONTROLLER CONST. A1 (MSB)
2122:	PGA2L	EQU	2122H	; PG CONTROLLER CONST. A2 (LSB)
2123:	PGA2M	EQU	2123H	; PG CONTROLLER CONST. A2 (MSB)
2124:	PGSF	EQU	2124H	; PG CONTROLLER SCALING FACTOR
2126:	PGSF2	EQU	2126H	; PG CONTROLLER SCALING FACTOR/2
0000:				;
2130:	PGCRAD	EQU	2130H	; PG CURRENT READING (C.P.) ADDR
2132:	PGSPP	EQU	2132H	; PG SET POINT PROFILE ADDR.
2134:	PGSPSA	EQU	2134H	; PG SET POINT STORAGE ADDR..
2136:	PGESA	EQU	2136H	; PG ERROR STORAGE ADDR.
2138:	PGESSA	EQU	2138H	; PG ERROR SIGN STORAGE ADDR.
213A:	PGA1ESA	EQU	213AH	; PG A1*E1 STORAGE ADDR.
213C:	PGA2ESA	EQU	213CH	; PG A2*E1-1 STORAGE ADDR.
213E:	PGR1SA	EQU	213EH	; PG R1 (A1*E1-A2*E1-1) ST. ADDR.
2140:	PGR1SSA	EQU	2140H	; PG R1 SIGN STORAGE ADDR.
2142:	PGDRSA	EQU	2142H	; PG DR (R1/SF) STORAGE ADDR.
2144:	PGTS	EQU	2144H	; TEMP ST. OF PG
2146:	PGSTS	EQU	2146H	; TEMP ST. OF PG SIGN
2148:	PGETS	EQU	2148H	; TEMP ST. OF PG ERROR
214A:	PGESTS	EQU	214AH	; TEMP ST. OF PG ERROR SIGN
214C:	PGA1ETS	EQU	214CH	; TEMP ST. OF PG A1*E1
214E:	PGA2ETS	EQU	214EH	; TEMP ST. OF PG A2*E1-1
2150:	PGR1TS	EQU	2150H	; TEMP ST. OF PG R1
2152:	PGR1STS	EQU	2152H	; TEMP ST. OF PG R1 SIGN
2154:	PGDRTS	EQU	2154H	; TEMP ST. OF PG DR
2156:	PGSSA	EQU	2156H	; PG SIGN STORAGE ADD.

2400:		ORG 2400H	
2400:	CD 2D 24	CALL INIT	
2403:	CD 64 24	CALL CLEAR	
2406:	CD 6E 24	CALL CLOSE	
2409:	CD 9A 24	CALL SETUP	
240C:	CD 0C 25	CALL FILLS	
240F:	CD 1D 25	CALL HOLDS	
2412:	CD 2E 25	CALL COOLS	
2415:	CD 77 25	CALL OPEN	
2418:	CD 64 24	CALL CLEAR	
241B:	CD A3 25	CALL END	
241E:	3E FF	LD A,FFH	
2420:	D3 04	OUT(04H),A	; CLOSE THE SUPPLY SERVOVALVE
2422:	3E 00	LD A,00	
2424:	D3 0A	OUT(0AH),A	
2426:	3E 00	LD A,00	
2428:	D3 0B	OUT(0BH),A	; CLOSE THE RELIEF SERVOVALVE
242A:	C3 3B 00	JP MONITOR	

242D:	DD 21 28 20	INIT	LD IX,RCCR	; INITIALIZES ALL TEMP. ADDRESSES
2431:	0E 00		LD C,00	
2433:	06 00		LD B,00	
2435:	3E 00	IN1	LD A,00	
2437:	DD 71 00	IN2	LD (IX+00),C	
243A:	DD 23		INC IX	
243C:	3C		INC A	
243D:	FE 08		CP 08H	
243F:	20 F6		JR NZ,IN2	
2441:	11 08 00		LD DE,0008H	
2444:	DD 19		ADD IX,DE	
2446:	04		INC B	
2447:	78		LD A,B	
2448:	FE 04		CP 04	
244A:	20 E9		JR NZ,IN1	
244C:	DD 2A 22 20		LD IX,(SOSA)	
2450:	DD 22 2A 20		LD (TSOSA),IX	
2454:	21 00 00		LD HL,0000	
2457:	01 00 00		LD BC,0000	
245A:	11 00 00		LD DE,0000	
245D:	3E 00		LD A,00	
245F:	D3 F0		OUT(F0H),A	; HEATERS CONTROL
2461:	D3 F1		OUT(F1H),A	; HEATERS CONTROL
2463:	C9		RET	
2464:	F3	CLEAR	DI	; CLEARS INTERRUPT
2465:	3E 00		LD A,00	
2467:	D3 03		OUT(03H),A	
2469:	3E 01		LD A,01	
246B:	D3 02		OUT(02H),A	
246D:	C9		RET	

246E: 3E FF	CLOSE	LD A,FFH	; CLOSES THE MOLD AND CARRAGE
2470: D3 17		OUT(17H),A	; DEACTIVATE ALL SOLENOID VALVES
2472: 3E 7F		LD A,7FH	
2474: D3 17		OUT(17H),A	; ACTIVATES SOL. 2 TO CLOSE MOLD
2476: CD B9 24	CL1	CALL DELAY	
2479: DB 14		IN A,(14H)	; CHECK LIMIT SWITCH NO-- FOR
247B: FE 82		CP 82H	; COMPLETION OF MOLD CLOSE
247D: 20 F7		JR NZ,CL1	
247F: CD B9 24	CL2	CALL DELAY	
2482: DB 14		IN A,(14H)	
2484: FE 82		CP 82H	
2486: 28 F7		JR Z,CL2	
2488: 1E 00		LD E,00	
248A: CD B9 24	CL3	CALL DELAY	
248D: DB 14		IN A,(14H)	
248F: FE A2		CP A2H	
2491: 20 F7		JR NZ,CL3	
2493: 1C		INC E	
2494: 3E 20		LD A,20H	
2496: BB		CP E	
2497: 20 F1		JR NZ,CL3	
2499: C9		RET	
249A: 3E FB	SETUP	LD A,FBH	; SET UP SSV AND THE TIMER
249C: D3 17		OUT(17H),A	; ACTIVATE SOL. 5 FOR INJECTION
249E: 1E 00		LD E,00	
24A0: CD B9 24	S1	CALL DELAY	
24A3: 1C		INC E	
24A4: 3E 10		LD A,10H	
24A6: BB		CP E	
24A7: 20 F7		JR NZ,S1	
24A9: CD D2 24		CALL SERVOP	; SEND INIT. SSV0 FOR FILLING
24AC: CD B9 24		CALL DELAY	
24AF: CD B9 24		CALL DELAY	
24B2: CD B9 24		CALL DELAY	
24B5: CD E8 24		CALL TIMER	
24B8: C9		RET	
24B9: 2E 00	DELAY	LD L,00	
24BB: 3E 0F	D1	LD A,0FH	; LENGTH OF THE DELAY UNIT
24BD: D9		EXX	
24BE: 0E 00		LD C,00	
24C0: 06 00	D2	LD B,00	
24C2: 04	D3	INC B	
24C3: B8		CP B	
24C4: 20 FC		JR NZ,D3	
24C6: 0C		INC C	
24C7: B9		CP C	
24C8: 20 F6		JR NZ,D2	
24CA: D9		EXX	
24CB: 2C		INC L	
24CC: 3E 01		LD A,01H	
24CE: BD		CP L	
24CF: 20 EA		JR NZ,D1	
24D1: C9		RET	

24D2: 3E 00	SERVOP	LD A,00	
24D4: 03 04		OUT(04H),A	; SEND (+) SIGNAL TO SSV
24D6: 21 00 01		LD HL,0100H	
24D9: 3A 53 20		LD A,(ISVOF)	; INIT. V.O. FOR FILLING STAGE
24DC: 32 5C 20		LD (TSVO),A	; TEMP STORAGE OF V.O.
24DF: 16 00		LD D,00	
24E1: 5F		LD E,A	
24E2: ED 52		SBC HL,DE	
24E4: 7D		LD A,L	
24E5: 03 0A		OUT(0AH),A	
24E7: C9		RET	
24E8: 3E 08	TIMER	LD A,08	
24EA: 03 02		OUT(02),A	
24EC: 3E 02		LD A,02	
24EE: 03 03		OUT(03),A	
24F0: 3E 86		LD A,86H	
24F2: 03 06		OUT(06),A	
24F4: FB		EI	
24F5: C9		RET	
24F6: DB 00	KEYB	IN A,(00)	
24F8: E6 80		AND 80H	
24FA: C8		RET Z	
24FB: DB 01		IN A,(01)	
24FD: E6 7F		AND 7FH	
24FF: FE 1B		CP 1BH	
2501: CA 05 25		JP Z,EXIT	
2504: C9		RET	
2505: 3E FF	EXIT	LD A,FFH	; TO EXIT IF 'ESC' IS HIT
2507: 03 17		OUT(17H),A	
2509: C3 3B 00		JP MONITOR	
250C: 3A 50 20	FILLS	LD A,(FSCC)	; LOAD FILL STAGE CONTROL CHANNEL
250F: 32 59 20		LD (TFCC),A	; TEMP STORAGE OF THE CONT. CHANNEL
2512: 0D F6 24	FSI	CALL KEYB	
2515: 3A 58 20		LD A,(CSC)	; CONT. STAGE COUNTER: 0=F,1=H,2=C
2518: FE 00		CP 00	
251A: 28 F6		JR Z,FSI	
251C: C9		RET	
251D: 3A 51 20	HOLDS	LD A,(HSCC)	; LOAD HOLD STAGE CONT. CHANNEL
2520: 32 59 20		LD (TFCC),A	; TEMP STORAGE OF THE CONT. CHAN.
2523: 0D F6 24	HSI	CALL KEYB	
2526: 3A 58 20		LD A,(CSC)	; CONT. STAGE: 0=F, H=01, 2=C
2529: FE 01		CP 01	
252B: 28 F6		JR Z,HSI	
252D: C9		RET	

252E: 3A 52 20	COOLS	LD A,(CSCC)	; LOAD COOL STAGE CONT. CHANNEL
2531: 32 59 20		LD (TFCC),A	; TEMP ST. OF STAGE CONT. CHANNEL
2534: 3E 00		LD A,00	
2536: 03 08		OUT(0BH),A	; CLOSE THE R.S.V
2538: 0D F6 24	CSI	CALL KEYB	
253B: 2A 36 20		LD HL,(DTBP)	; DELAY TIME BEFORE PLASTICATION
253E: ED 5B 3C 20		LD DE,(CTCR)	; COOLING TIME COUNTER
2542: 37		SCF	
2543: 3F		CCF	
2544: ED 52		SBC HL,DE	
2546: CC 51 25		CALL Z,PLAST	
2549: 3A 58 20		LD A,(CSC)	; CONT. STAGE : COOL = 2
254C: FE 02		CP 02	
254E: 28 E8		JR Z,CSI	
2550: C9		RET	
2551: 3E AF	PLAST	LD A,AFH	
2553: 03 17		OUT(17H),A	; ACTIVATE THE PLAST. SOL. (#7)
2555: CD 6A 25		CALL SERVON	; TO SEND -VE SIGNAL TO SSV
2558: 2A 4C 20	PSI	LD HL,(TCSCCR)	; PLAST. ST. CONT CHANNEL C.R.
255B: ED 5B 44 20		LD DE,(CSCCSP)	; PLAST. ST. CONT CHANNEL SETPOINT
255F: 37		SCF	
2560: 3F		CCF	
2561: ED 52		SBC HL,DE	
2563: 30 F3		JR NC,PSI	
2565: 3E FF		LD A,FFH	
2567: 03 17		OUT(17H),A	; DEACTIVATE ALL THE SOLENOIDS
2569: C9		RET	
256A: 3E FF	SERVON	LD A,FFH	; -VE SIGNAL TO SSV
256C: 03 04		OUT(04H),A	
256E: 3A 55 20		LD A,(SVOP)	; V.O. FOR PLASTICATION
2571: 03 0A		OUT(0AH),A	
2573: 32 SC 20		LD (TSVO),A	
2576: C9		RET	
2577: 3E 7F	OPEN	LD A,7FH	
2579: 03 17		OUT(17H),A	; ACTIVATE THE SOL. WHICH OPENS
257B:			; THE MOLD AND THE CARRAGE
257B: CD 89 24	OP1	CALL DELAY	
257E: DB 14		IN A,(14H)	; CHECK LIMIT SWITCH NO ---
2580: FE 32		CP 32H	
2582: 20 F7		JR NZ,OP1	
2584: CD 89 24	OP2	CALL DELAY	
2587: DB 14		IN A,(14H)	
2589: FE 32		CP 32H	
258B: 28 F7		JR Z,OP2	
258D: 1E 00		LD E,00	
258F: CD 89 24	OP3	CALL DELAY	
2592: DB 14		IN A,(14H)	
2594: FE B2		CP B2H	
2596: 20 F7		JR NZ,OP3	
2598: 1C		INC E	

2599: 3E 10		LD A,10H	
259B: 8B		CP E	
259C: 20 F1		JR NZ,OP3	
259E: 3E FF		LD A,FFH	
25A0: D3 17		OUT(17H),A	; STOP THE MACHINE
25A2: C9		RET	
25A3: 21 85 25	END	LD HL,EMESS	; END CYCLE MESSAGE
25A6: DB 00	E1	IN A,(00)	
25A8: E6 80		AND 80H	
25AA: 28 FA		JR Z,E1	
25AC: 7E		LD A,(HL)	
25AD: D3 01		OUT(01),A	
25AF: 23		INC HL	
25B0: FE 0F		CP 0FH	
25B2: 20 F2		JR NZ,E1	
25B4: C9		RET	
25B5: 0D 0A	EMESS	db DH, AH	
25B7: 45 4E 44 20		db 'END OF THE CYCLE'	
4F 46 20 54			
48 45 20 43			
59 43 4C 45			
25C7: 0D 0A 0F		db DH, AH, 0FH	

INTERRUPT ROUTINE

25CA: F5	INTERR	PUSH AF	
25CB: 05		PUSH BC	
25CC: 05		PUSH DE	
25CD: E5		PUSH HL	
25CE: CD E8 24		CALL TIMER	
25D1: 3A 3E 20		LD A,(TRC)	; LOAD TIMER REPEAT COUNTER (TRC)
25D4: 3C		INC A	
25D5: 32 3E 20		LD (TRC),A	; INCREMENT TRC
25D8: 6F		LD L,A	
25D9: 3A 46 20		LD A,(TRCS)	; LOAD TRC SET VALUE
25DC: 8D		CP L	
25DD: 20 36		JR NZ, JR3	
25DF: 2A 20 20		LD HL,(RCS)	; READING COUNTER (RC) SET VALUE
25E2: ED 5B 28 20		LD DE,(RCCR)	; CURRENT VALUE OF RC.
25E6: 37		SCF	
25E7: 3F		CCF	
25E8: ED 52		SBC HL,DE	
25EA: 30 04		JR NC, JR1	
25EC: 3E 01		LD A,01	
25EE: 18 02		JR JR2	
25F0: 3E 00	JR1	LD A,00	
25F2: 32 5D 20	JR2	LD (RSC),A	; READ/STORE CONTROL: 0=READ & STORE
25F5: CD 1B 26		CALL DATA	
25F8: 3A 58 20		LD A,(CSC)	; CONT. STAGE: 0=F, 1=H, 2=C
25FB: FE 02		CP 02	
25FD: CC E3 27		CALL Z, CCONT	
2600: 3A 58 20		LD A,(CSC)	
2603: FE 01		CP 01	
2605: CC B8 27		CALL Z, HCONT	
2608: 3A 58 20		LD A,(CSC)	
260B: FE 00		CP 00	
260D: CC CF 26		CALL Z, FCONT	
2610: 3E 00		LD A,00	
2612: 32 3E 20		LD (TRC),A	; RESET TRC AT ZERO
2615: E1	JR3	POP HL	
2616: D1		POP DE	
2617: C1		POP BC	
2618: F1		POP AF	
2619: ED 4D		RETI	
261B: DD 2A 2A 20	DATA	LD IX,(TSOSA)	; TEMP ADD. FOR THE START OF
261F:			; STORAGE ADDRESS (SOST)
261F: 3A 26 20		LD A,(FCN)	; NO OF THE 1ST. CHANN. TO BE READ
2622: 47		LD B,A	
2623: 0E 00	COUNT	LD C,00	
2625: 21 00 00		LD HL,0000	

2628: 3E F0	JR4	LD A,F0H	
262A: 80		ADD A,B	
262B: 03 16		OUT(16H),A	
262D: 0B 15	JR5	IN A,(15H)	
262F: 0B 13		IN A,(13H)	
2631: E6 02		AND 02	
2633: 20 F8		JR NZ,JR5	
2635: 3E F0		LD A,F0H	
2637: 80		ADD A,B	
2638: 03 16		OUT(16H),A	
263A: 3E 20		LD A,20H	
263C: 3D	JR6	DEC A	
263D: FE 00		CP 00	
263F: 20 FB		JR NZ, JR6	
2641: 3E 03		LD A,03	
2643: 03 13		OUT(13H),A	
2645: 0B 13		IN A,(13H)	
2647: 3E 10		LD A,10H	
2649: 80		ADD A,B	
264A: 03 16		OUT(16H),A	; ACTIVATE EN3 TO READ THE LSB
264C: 0B 15		IN A,(15H)	; A HAS XL
264E: E6 0F		AND 0FH	; TO DISCARD X
2650: 5F		LD E,A	; SAVE L IN E
2651: 3E 20		LD A,20H	
2653: 80		ADD A,B	
2654: 03 16		OUT(16H),A	; ACTIVATE EN1 & EN2 TO READ MSB &
2656: 0B 15		IN A,(15H)	; A HAS MSB & MB
2658: 57		LD D,A	; SAVE MSB & MB IN D TEMP.
2659: E6 0F		AND 0FH	; DISCARD MSB
265B: 17		RLA	
265C: 17		RLA	
265D: 17		RLA	
265E: 17		RLA	
265F: 83		ADD A,E	; A NOW HAS MB+LSB
2660: 5F		LD E,A	; E HAS MB+LSB
2661: 7A		LD A,D	; RELOAD MSB+MB INTO A
2662: E6 F0		AND F0H	; DISCARD MB
2664: 1F		RRA	
2665: 1F		RRA	
2666: 1F		RRA	
2667: 1F		RRA	; NOW A HAS 0+MSB
2668: 57		LD D,A	; LOAD 0+MSB INTO D. SO DE WILL HAVE
2669: 0C		INC C	
266A: 79		LD A,C	
266B: FE 03		CP 03	
266D: 20 89		JR NZ, JR4	
266F: 19		ADD HL,DE	
2670: 3A 5D 20		LD A,(RSC)	; SET READ/STORE CONTROL: 0=R&S, 1=R
2673: FE 01		CP 01	
2675: 28 08		JR Z, JR7	
2677: DD 74 00		LD (IX+00),H	
267A: DD 23		INC IX	
267C: DD 75 00		LD (IX+00),L	

267F: 3A 50 20	JR7	LD A, (FSCC) ; FILL STAGE CONT. CHANNEL (FSCC)
2682: B8		CP B
2683: 20 03		JR NZ, JR8
2685: 22 48 20		LD (TFSCCCR), HL ; TEMP ST. OF FSCC CURRENT READING
2688: 3A 51 20	JR8	LD A, (HSCC) ; HOLD STAGE CONT. CHANNEL (HSCC)
268B: B8		CP B
268C: 20 03		JR NZ, JR9
268E: 22 4A 20		LD (THSCCCR), HL ; TEMP ST. OF HSCC CURRENT READING
2691: 3A 52 20	JR9	LD A, (CSCC) ; COOL STAGE CONT. CHANNEL (CSCC)
2694: B8		CP B
2695: 20 03		JR NZ, JR10
2697: 22 4C 20		LD (TCSCCCR), HL ; TEMP ST. OF CSCC CURRENT READING
269A: 3A 26 20	JR10	LD A, (FCN) ; NO OF 1ST CHANN. TO BE READ
269D: B8		CP B
269E: 20 04		JR NZ, JR11
26A0: DD 22 2A 20		LD (TSOSA), IX ; TEMP ST. OF SOST
26A4: 3A 27 20	JR11	LD A, (LCN) ; NO OF LAST CHANN. TO BE READ
26A7: B8		CP B
26A8: 28 0C		JR Z, JR12
26AA: 04		INC B
26AB: DD 2B		DEC IX
26AD: ED 5B 24 20		LD DE, (DF) ; DISPLACEMENT FACTOR: 0001=128 READINGS
26B1: DD 19		ADD IX, DE
26B3: C3 23 26		JP COUNT
26B6: 3A 5D 20	JR12	LD A, (RSC) ; READ/STORE CONTROL
26B9: FE 01		CP 01
26BB: 28 0A		JR Z, JR13
26BD: DD 2A 2A 20		LD IX, (TSOSA)
26C1: DD 23		INC IX
26C3: DD 22 2A 20		LD (TSOSA), IX
26C7: 2A 28 20	JR13	LD HL, (RCCR)
26CA: 23		INC HL
26CB: 22 28 20		LD (RCCR), HL ; INCREMENT READING COUNTER RC
26CE: C9		RET
26CF: ED 53 2C 20	FCONT	LD (PC1CRTS), DE ; TEMP. ST. OF PC1 CURRENT READING
26D3: FD 2A C6 20		LD IY, (PC2CRAD) ; ADD. OF PC2 CURRENT READING
26D7: FD 66 00		LD H, (IY+00)
26DA: FD 6E 01		LD L, (IY+01)
26DD: FD 23		INC IY
26DF: FD 23		INC IY
26E1: FD 22 C6 20		LD (PC2CRAD), IY
26E5: 22 9E 20		LD (PC2CRTS), HL ; TEMP. ST. OF PC2 CURRENT READING
26E8: 2A 98 20		LD HL, (PNPCTP) ; PN/PC CONT. TRANSITION PRESSURE
26EB: AF		XOR A
26EC: ED 52		SBC HL, DE ; DE STILL HAS PC1 CURRENT READING
26EE: 38 2D		JR C, PCP6 ; IF PC1 \ PN/PC CONT. TRANSITION

26F0: FD 2A 70 20	LD IY,(PNCRAD)	; ADD. OF PN CURRENT READING
26F4: FD 66 00	LD H,(IY+00)	; LOAD PN C.R. INTO HL
26F7: FD 6E 01	LD L,(IY+01)	
26FA: FD 23	INC IY	
26FC: FD 23	INC IY	
26FE: FD 22 70 20	LD (PNCRAD),IY	
2702: 22 96 20	LD (PNCRTS),HL	; TEMP STORAGE OF PN C.R.
2705: 11 01 00	LD DE,0001H	
2708: AF	XOR A	
2709: ED 52	SBC HL,DE	
270B: 38 05	JR C, INCA	; IF PN < 0.0
270D: CD FB 28	CALL PNPICONT	
2710: 18 03	JR PCINC	
2712: CD 8D 31	CALL PNIAOR	
2715: CD 7F 32	CALL PCIAOR	
2718: CD 15 33	CALL PGIADR	
271B: 18 78	JR FILL	
271D: 2A 48 20	LD HL,(TFSCCCR)	
2720: FD 2A C4 20	LD IY,(PCICRAD)	
2724: FD 56 FE	LD D,(IY+-02)	
2727: FD 5E FF	LD E,(IY+-01)	
272A: AF	XOR A	
272B: ED 52	SBC HL,DE	; CALCULATE PC-t SLOPE @ t=t: dp(t)
272D: 22 D6 20	LD (DP1TS),HL	
2730: EB	EX DE,HL	
2731: FD 56 FC	LD D,(IY+-4)	
2734: FD 5E FD	LD E,(IY+-3)	
2737: AF	XOR A	
2738: ED 52	SBC HL,DE	; CALCULATE PC-t SLOPE @ t=t-1: dp(t-1)
273A: 22 D8 20	LD (DP2TS),HL	
273D: EB	EX DE,HL	; DE NOW HAS dp(t-1)
273E: 21 00 00	LD HL,0000	
2741: 01 00 00	LD BC,0000	
2744: 3A DA 20	LD A,(DPSL)	; LOAD DP SLOPE FACTOR SET THIS VALUE
2747: 19	ADD HL,DE	
2748: 03	INC BC	
2749: B9	CP C	
274A: 20 FB	JR NZ,FLP2	
274C: 3A DB 20	LD A,(DP5M)	; LOAD MSB OF DP SLOPE FACTOR
274F: B8	CP B	
2750: 20 F2	JR NZ,FLP1	
2752: 22 DC 20	LD (DPSTS),HL	; TEMP ST. OF DP2 * SLORE FACTOR
2755: EB	EX DE,HL	; DE NOW HAS dp(t-1)*SLORE FACTOR
2756: 2A D6 20	LD HL,(DP1TS)	
2759: AF	XOR A	
275A: ED 52	SBC HL,DE	
275C: 30 2C	JR NC,ENDF	; IF dp(t) - dp(t-1)*SF,END FILLING

275E: 2A 9C 20		LD HL,(PC1CRTS)	
2761: ED 5B 9E 20		LD DE,(PC2CRTS)	
2765: AF		XOR A	
2766: ED 52		SBC HL,DE	; HL NOW CONTAIN THE PRESS. GRAD.
2768: 22 44 21		LD (PGTS),HL	; TEMP. ST. OF PG
276B: ED 5B 9A 20		LD DE,(PCPGTP);	LOAD PC/PG CONTROL,TRANSITION POINT
276F: AF		XOR A	
2770: ED 52		SBC HL,DE	
2772: 38 0B		JR C,PCC	; IF PG < PC/PG TRANSITION, CALL PCCONT.
277A: CD 03 28		CALL PCUP	; TO UPDATE PC RELATED MEMORY SETTINGS
277D: 18 16		JR FILL	
277F: CD 07 2B	PCC	CALL PCPICONT	
2782: CD AB 28		CALL PNUP	
2785: CD 15 33		CALL PGIADR	
2788: 18 0B		JR FILL	
278A: 3E 01	ENDF	LD A,01	
278C: 32 58 20		LD (CSC),A	; STAGE CONTROL: 0=F, 1=H, 2=C
278F: CD 9D 27		CALL SERVOH	; SEND INIT. S.S.V.O. FOR HOLD
2792:			; STAGE (THIS IS = 0.0)
2792: CD 13 2D		CALL HCONTM	; CALL HOLD MASTER CONTROL PGM
2795: 2A 38 20	FILL	LD HL,(TFTC)	; TEMP ADD. FOR FILL TIME COUNTER
2798: 23		INC HL	
2799: 22 38 20		LD (TFTC),HL	; INCREMENT FILL TIME COUNTER
279C: C9		RET	
279D: 21 00 01	SERVOH	LD HL,0100H	
27A0: 3A 54 20		LD A,(SVOH)	; V.O FOR HOLD STAGE
27A3: 32 5C 20		LD (TSVO),A	
27A6: 16 00		LD D,00	
27A8: 5F		LD E,A	
27A9: ED 52		SBC HL,DE	
27AB: 7D		LD A,L	
27AC: D3 0A		OUT(0AH),A	
27AE: C9		RET	
27AF: 3E FF	CLOSESV	LD A,FFH	; CLOSE SSV
27B1: D3 04		OUT (04H),A	
27B3: 3E 00		LD A,00	
27B5: D3 0A		OUT (0AH),A	
27B7: C9		RET	
27B8: 2A 32 20	HCONT	LD HL,(HTCS)	; HOLD TIME CONT. SET POINT
27BB: ED 5B 3A 20		LD DE,(THTCR)	; TEMP ADD. FOR HOLD TIME COUNTER
27BF: 37		SCF	
27C0: 3F		CCF	
27C1: ED 52		SBC HL,DE	
27C3: 38 05		JR C,ENDH	; END HOLD
27C5: CD 13 2D		CALL HCONTM	; CALL THE HOLD CONTROL MASTER PGM.
27C8: 18 11		JR HOLD	; CONTINUE HOLDING
27CA: 3E FF	ENDH	LD A,FFH	
27CC: D3 17		OUT(17H),A	; STOP THE SOLENOIDS

270E: 3E FF		LD A,FFH	
2700: D3 04		OUT(04),A	
2702: 3E 00		LD A,00	; CLOSE THE S.S.V.
2704: D3 0A		OUT(0AH),A	
2706: 3E 02		LD A,02	
2708: 32 58 20		LD (CSC),A	; SET CONT. STAGE COUN. TO COOL
270B: 2A 3A 20	HOLD	LD HL,(THTCR)	
270E: 23		INC HL	
270F: 22 3A 20		LD(THTCR),HL	; INC HOLD TIME COUNTER
27E2: C9		RET	

27E3: 2A 34 20	CCONT	LD HL,(CTCS)	; COOLING TIME COUNTER SET POINT(CTCS)
27E6: ED 5B 3C 20		LD DE,(CTCR)	; COOLING TIME COUNTER CURRENT VALUE
27EA: 37		SCF	
27EB: 3F		CCF	
27EC: ED 52		SBC HL,DE	
27EE: 30 05		JR NC, JR26	
27F0: 3E 03		LD A,03	
27F2: 32 58 20		LD (CSC),A	; STAGE CONT.: 0=F, 1=H, 2=C
27F5: 2A 3C 20	JR26	LD HL,(CTCR)	
27F8: 23		INC HL	
27F9: 22 3C 20		LD (CTCR),HL	; INCREMENT COOLING TIME COUNTER
27FC: 2A 20 20		LD HL,(RCS)	; LOAD DATA READING COUNTER SETTING
27FF: ED 5B 28 20		LD DE,(RCCR)	
2803: AF		XOR A	
2804: EQ 52		SBC HL,DE	
2806: 38 68		JR C,RET	
2808: FD 2A 70 20		LD IY,(PNCRAD)	
280C: FD 66 00		LD H,(IY+00)	
280F: FD 66 01		LD L,(IY+01)	
2812: FD 23		INC IY	
2814: FD 23		INC IY	
2816: FD 22 70 20		LD (PNCRAD),IY	
281A: FD 2A 74 20		LD IY,(PNPSA)	; UPDATE PN SET POINT

2871: FD 2A 80 20	PGU	LD IY,(PCCRAD)	; ADD OF PC1 CR STORAGE
2875: FD 66 00		LD H,(IY+00)	
2878: FD 6E 01		LD L,(IY+01)	; LOAD PC1 CR INTO HL
287B: FD 23		INC IY	
287D: FD 23		INC IY	
287F: FD 22 80 20		LD (PCCRAD),IY	
2883: FD 2A C6 20		LD IY,(PC2CRAD)	; ADD OF PC2 CR STORAGE
2887: FD 56 00		LD D,(IY+00)	
288A: FD 5E 01		LD E,(IY+01)	; LOAD PC3 CR INTO DE
288D: FD 23		INC IY	
288F: FD 23		INC IY	
2891: FD 22 C6 20		LD (PC2CRAD),IY	

2895: AF	XOR A	
2896: ED 52	SBC HL,DE	
2898: FD 2A 30 21	LD IY,(PGCRAD)	; ADD. OF PG STORAGE
289C: FD 74 00	LD (IY+00),H	
289F: FD 75 01	LD (IY+01),L	; STORE PG
28A2: FD 23	INC IY	
28A4: FD 23	INC IY	
28A6: FD 22 30 21	LD (PGCRAD),IY	
28AA: C9	RET	
28AB: FD 2A 70 20 PNUP	LD IY,(PNCRAD)	
28AF: FD 66 00	LD H,(IY+00)	
28B2: FD 6E 01	LD L,(IY+01)	
28B5: FD 23	INC IY	
28B7: FD 23	INC IY	
28B9: FD 22 70 20	LD (PNCRAD),IY	
28BD: FD 2A 74 20	LD IY,(PNSPSA)	
28C1: FD 74 00	LD (IY+00),H	; COPY PN CURRENT READING AS
28C4: FD 75 01	LD (IY+01),L	; THE SET POINT PROFILE
28C7: FD 23	INC IY	
28C9: FD 23	INC IY	
28CB: FD 22 74 20	LD (PNSPSA),IY	
28CF: CD FE 31	CALL PNIADRI	
28D2: C9	RET	
28D3: FD 2A B0 20 PCUP	LD IY,(PCCRAD)	
28D7: FD 66 00	LD H,(IY+00)	
28DA: FD 6E 01	LD L,(IY+01)	
28DD: FD 23	INC IY	
28DF: FD 23	INC IY	
28E1: FD 22 B0 20	LD (PCCRAD),IY	
28E5: FD 2A B4 20	LD IY,(PCSPSA)	
28E9: FD 74 00	LD (IY+00),H	; COPY PN CURRENT READING AS
28EC: FD 75 01	LD (IY+01),L	; THE SET POINT PROFILE
28EF: FD 23	INC IY	
28F1: FD 23	INC IY	
28F3: FD 22 B4 20	LD (PCSPSA),IY	
28F7: CD 94 32	CALL PCIADRI	
28FA: C9	RET	
28FB: FD 2A 72 20 PNPICONT	LD IY,(PNSPP)	; ADD OF PN SET POINT PROFILE
28FF: FD 66 00	LD H,(IY+00)	
2902: FD 6E 01	LD L,(IY+01)	; LOAD PN SET POINT INTO HL
2905: FD 23	INC IY	
2907: FD 23	INC IY	
2909: FD 22 72 20	LD (PNSPP),IY	
290D: FD 2A 74 20	LD IY,(PNSPSA)	; ADD. OF PN SET POINT STORAGE
2911: FD 74 00	LD (IY+00),H	
2914: FD 75 01	LD (IY+01),L	; STORE PN SET POINT
2917: FD 23	INC IY	
2919: FD 23	INC IY	
291B: FD 22 74 20	LD (PNSPSA),IY	

291F: ED 5B 26 20		LD DE,(PNCRTS)	; LOAD PN C.R. INTO DE
2923: AF		XOR A	
2924: ED 52		SBC HL,DE	; CALCULATE THE ERROR
2926: 3E 00		LD A,00	
2928: 30 09		JR NC,PNES	; IF E IS +VE
292A: AF		XOR A	
292B: EB		EX DE,HL	
292C: 21 00 00		LD HL,0000	
292F: ED 52		SBC HL,DE	
2931: 3E 01		LD A,01	; IF E IS -VE
2933: 22 88 20	PNES	LD (PNETS),HL	; TEMP STORAGE FOR PN E1
2936: 32 8A 20		LD (PNETS),A	; TEMP STORAGE FOR PN E1 SIGN
2939: FD 2A 76 20		LD IY,(PNESA)	; ADD OF PN E STORAGE
293D: FD 74 00		LD (IY+00),H	
2940: FD 75 01		LD (IY+01),L	; STORE PN ERROR
2943: FD 23		INC IY	
2945: FD 23		INC IY	
2947: FD 22 76 20		LD (PNESA),IY	
2948: FD 2A 78 20		LD IY,(PNESSA)	; ADD OF PN E SIGN STORAGE
294F: FD 77 00		LD (IY+00),A	; STORE PN E SIGN
2952: FD 23		INC IY	
2954: FD 22 78 20		LD (PNESSA),IY	
2958: 01 00 00	PNMU1	LD BC,0000	
295B: 21 00 00		LD HL,0000	
295E: ED 5B 88 20		LD DE,(PNETS)	; LOAD THE MULTIPLICAND (PN E1)
2962: 3A 60 20	PNLPI	LD A,(PNA1L)	; LOAD PN A1 (THE LSB)
2965: 19	PNLP2	ADD HL,DE	
2966: 03		INC BC	
2967: 89		CP C	
2968: 20 FB		JR NZ,PNLP2	
296A: 3A 61 20		LD A,(PNA1M)	; LOAD MSB OF PN A1
296D: 88		CP B	
296E: 20 F2		JR NZ,PNLPI	
2970: 22 8C 20		LD (PNA1ETS),HL	; TEMP ST. OF PN A1 * E1
2973: FD 2A 76 20	PNMU2	LD IY,(PNESA)	; LOAD PN E(1-1) INTO DE
2977: FD 56 FC		LD D,(IY+-04)	; SUBTRACT 4 FFFCH
297A: FD 5E FD		LD E,(IY+-03)	; SUBTRACT 3 FFFDH
297D: 01 00 00		LD BC,0000	
2980: 21 00 00		LD HL,0000	
2983: 3A 62 20	PNLP3	LD A,(PNA2L)	; LOAD PN A2 (LSB)
2986: 19	PNLP4	ADD HL,DE	
2987: 03		INC BC	
2988: 89		CP C	
2989: 20 FB		JR NZ,PNLP4	
298B: 3A 63 20		LD A,(PNA2M)	; LOAD MSB OF PN A2
298E: 88		CP B	
298F: 20 F2		JR NZ,PNLP3	

2991: 22 8E 20		LD (PNAZETS),HL	; TEMP ST. OF PN A2 * E(1-1)
2994: 2A 8C 20		LD HL,(PNA1ETS)	; LOAD PN A1*E1 INTO HL
2997: ED 5B 8E 20		LD DE,(PNAZETS)	; LOAD PN A2*E(1-1) INTO DE
2998: FD 2A 78 20		LD IY,(PNESSA)	
299F: FD 46 FE		LD B,(IY+-02)	; LOAD PN E1-1 SIGN INTO B
29A2: 3A 8A 20		LD A,(PNESTS)	; LOAD PN E1 SIGN
29A5: FE 00		CP 00	; CHECK SIGN PN E1
29A7: 20 1C		JR NZ,PNNS1	
29A9: 78		LD A,B	
29AA: FE 00		CP 00	; CHECK SIGN PN E(1-1)
29AC: 20 12		JR NZ,PNNS2	
29AE: AF		XOR A	
29AF: ED 52		SBC HL,DE	
29B1: 3E 00		LD A,00	
29B3: 30 2B		JR NC,PNSR1	
29B5: EB		EX DE,HL	
29B6: 21 00 00		LD HL,0000	
29B9: AF		XOR A	
29BA: ED 52		SBC HL,DE	
29BC: 3E 01		LD A,01	
29BE: 18 20		JR PNSR1	
29C0: 19	PNNS2	ADD HL,DE	
29C1: 3E 00		LD A,00	
29C3: 18 1B		JR PNSR1	
29C5: 78	PNNS1	LD A,B	
29C6: FE 00		CP 00	
29C8: 20 05		JR NZ,PNNS12	
29CA: 19		ADD HL,DE	
29CB: 3E 01		LD A,01	
29CD: 18 11		JR PNSR1	
29CF: EB	PNNS12	EX DE,HL	
29D0: AF		XOR A	
29D1: ED 52		SBC HL,DE	
29D3: 3E 00		LD A,00	
29D5: 30 09		JR NC,PNSR1	
29D7: EB		EX DE,HL	
29D8: 21 00 00		LD HL,0000	
29DB: AF		XOR A	
29DC: ED 52		SBC HL,DE	
29DE: 3E 01		LD A,01	
29E0: 22 90 20	PNSR1	LD(PNRITS),HL	; TEMP ST. OF PN R1
29E3: 32 92 20		LD (PNRISTS),A	; TEMP ST. OF PN R1 SIGN
29E6: AF	PNLM1	XOR A	
29E7: 3A 64 20		LD A,(PNSF)	; LOAD PN SF
29EA: 47		LD B,A	
29EB: 7C		LD A,H	
29EC: 98		SBC A,B	
29ED: 38 05		JR C,PNLM2	
29EF: 21 FF 00		LD HL,00FFH	
29F2: 18 33		JR PNSR1	
29F4: AF	PNLM2	XOR A	
29F5: 7C		LD A,H	
29F6: DE 7F		SBC A,7FH	

29F8: 38 05		JR C,PNDIV	
29FA: 21 FF 00		LD HL,00FFH	
29FD: 18 28		JR PNSDR1	
29FF: 3A 64 20	PNDIV	LD A,(PNSF)	
2A02: 57		LD D,A	
2A03: 1E 00		LD E,00	
2A05: 06 08		LD B,08	
2A07: 2A 90 20		LD HL,(PNRITS)	
2A0A: 29	PNLP7	ADD HL,HL	
2A0B: AF		XOR A	
2A0C: ED 52		SBC HL,DE	
2A0E: 23		INC HL	
2A0F: 30 02		JR NC,PNNEXT	
2A11: 19		ADD HL,DE	
2A12: 2B		DEC HL	
2A13: 10 F5	PNNEXT	DJNZ PNLP7	
2A15: AF		XOR A	
2A16: 3A 66 20		LD A,(PNSF2)	; LOAD PN SF/2
2A19: 9C		SBC A,H	
2A1A: 30 09		JR NC,PNSDR	
2A1C: 3E FF		LD A,FFH	
2A1E: 80		CP L	
2A1F: 28 04		JR Z,PNSDR	
2A21: 3E 01		LD A,01	
2A23: 85		ADD A,L	
2A24: 6F		LD L,A	
2A25: 26 00	PNSDR	LD H,00	
2A27: 22 94 20	PNSDR1	LD (PNDRTS),HL	; TEMP ST. OF PN DR
2A2A: FD 2A 84 20		LD IY,(SSVOSA)	
2A2E: FD 56 FE		LD D,(IY+-02)	; GET THE PREVIOUS PN V.O.
2A31: FD 5E FF		LD E,(IY+-01)	
2A34: 3A 92 20		LD A,(PNR1STS)	
2A37: FE 01		CP 01	; CHECK SIGN OF PN R1
2A39: 28 0B		JR Z,PNSUB2	
2A3B: 19		ADD HL,DE	
2A3C: 7C		LD A,H	
2A3D: FE 00		CP 00	
2A3F: 28 1F		JR Z,PNSENDM	
2A41: 21 FF 00		LD HL,00FFH	
2A44: 18 1A		JR PNSENDM	
2A46: AF	PNSUB2	XOR A	
2A47: EB		EX DE,HL	
2A48: ED 52		SBC HL,DE	
2A4A: 30 14		JR NC,PNSENDM	
2A4C: 21 00 00		LD HL,0000	; IF M = 0 PUT M=0
2A4F: 3E FF		LD A,FFH	
2A51: 03 04		OUT (04),A	; SEND 0.0 SIGNAL TO THE VALVE,
2A53: 3E 00		LD A,00	; i.e. CLOSE THE VALVE
2A55: 03 0A		OUT (0AH),A	

2A57: 3E FF		LD A,FFH	; (7F LET MR=100 (IFMS=0.0 -->MR=100)
2A59: 03 0B		OUT (0BH),A	
2A5B: 16 00		LD D,00	
2A5D: 5F		LD E,A	
2A5E: 18 1D		JR PNSTM	
2A60: EB	PNSENDM	EX DE,HL	
2A61: 21 00 01		LD HL,0100H	
2A64: 3E 00		LD A,00	
2A66: 03 04		OUT (04),A	; +VE VALUE SIGNAL
2A68: AF		XOR A	
2A69: ED 52		SBC HL,DE	; HL NOW HAS THE ADJUSTED SIGNAL
2A6B:			; DE STILL HAS THE ACTUAL SIGNAL
2A6B: 7D		LD A,L	
2A6C: 03 0A		OUT (0AH),A	; SEND THE VALUE OF PN V.O.
2A6E: AF		XOR A	
2A6F: 21 FF 00		LD HL,00FFH	
2A72: ED 52		SBC HL,DE	; HL NOW HAS THE RSV OPENING
2A74: 30 03		JR NC,PNMR	
2A76: 21 00 00		LD HL,0000	
2A79: 7D	PNMR	LD A,L	
2A7A: 03 0B		OUT (0BH),A	
2A7C: EB		EX DE,HL	
2A7D: FD 2A 84 20	PNSTM	LD IY,(SSVOSA)	
2A81: FD 74 00		LD (IY+00),H	
2A84: FD 75 01		LD (IY+01),L	; STORE PN SSV OPENING
2A87: FD 23		INC IY	
2A89: FD 23		INC IY	
2A8B: FD 22 84 20		LD (SSVOSA),IY	
2A8F: FD 2A 86 20		LD IY,(RSVOSA)	
2A93: FD 72 00		LD (IY+00),D	
2A96: FD 73 01		LD (IY+01),E	; STORE PN RSV OPENING
2A99: FD 23		INC IY	
2A9B: FD 23		INC IY	
2A9D: FD 22 86 20		LD (RSVOSA),IY	
2AA1: 2A 8C 20		LD HL,(PNA1ETS)	
2AA4: FD 2A 7A 20		LD IY,(PNA1ESA)	; PN A1*E1 STORAGE ADD.
2AA8: FD 74 00		LD (IY+00),H	; STORE PN A1*E1
2AAB: FD 23		INC IY	
2AAD: FD 75 00		LD (IY+00),L	
2AB0: FD 23		INC IY	
2AB2: FD 22 7A 20		LD (PNA1ESA),IY	
2AB6: 2A 8E 20		LD HL,(PNA2ETS)	
2AB9: FD 2A 7C 20		LD IY,(PNA2ESA)	; PN A2*E1-1 STORAGE ADD.
2ABD: FD 74 00		LD (IY+00),H	; STORE PN A2*E(1-1)
2AC0: FD 23		INC IY	
2AC2: FD 75 00		LD (IY+00),L	
2AC5: FD 23		INC IY	
2AC7: FD 22 7C 20		LD (PNA2ESA),IY	
2ACB: 2A 90 20		LD HL,(PNRITS)	
2ACE: FD 2A 7E 20		LD IY,(PNRISA)	; PN R1=A1*E1-A2*E1-1 STORAGE ADD.
2AD2: FD 74 00		LD (IY+00),H	; STORE PN R1

2A05: FD 23	INC IY	
2A07: FD 75 00	LD (IY+00),L	
2ADA: FD 23	INC IY	
2ADC: FD 22 7E 20	LD (PNRISA),IY	
2AE0: 2A 94 20	LD HL,(PNDRTS)	
2AE3: FD 2A 82 20	LD IY,(PNDRSA)	; PN DR STORAGE ADD.
2AE7: FD 74 00	LD (IY+00),H	; STORE PN DR
2AEA: FD 23	INC IY	
2AEC: FD 75 00	LD (IY+00),L	
2AEF: FD 23	INC IY	
2AF1: FD 22 82 20	LD (PNDRSA),IY	
2AF5: 3A 92 20	LD A,(PNR1STS)	
2AF8: FD 2A 80 20	LD IY,(PNR1SSA)	; PN R1 SIGN STORAGE ADD.
2AFC: FD 77 00	LD (IY+00),A	; STORE PN R1 SIGN
2AFF: FD 23	INC IY	
2B01: FD 22 80 20	LD (PNR1SSA),IY	
2B05: AF	XOR A	
2B06: C9	RET	
2B07: FD 2A 82 20 PCPICONT	LD IY,(PCSPPP)	; ADD. OF PC1 SET POINT PROFILE
2B0B: FD 66 00	LD H,(IY+00)	
2B0E: FD 6E 01	LD L,(IY+01)	; LOAD PC1 SET POINT INTO HL
2B11: FD 23	INC IY	
2B13: FD 23	INC IY	
2B15: FD 22 82 20	LD (PCSPPP),IY	
2B19: FD 2A 84 20	LD IY,(PCSPSA)	; PC1 SET POINT STORAGE ADD.
2B1D: FD 74 00	LD (IY+00),H	
2B20: FD 75 01	LD (IY+01),L	; STORE PC1 SET POINT
2B23: FD 23	INC IY	
2B25: FD 23	INC IY	
2B27: FD 22 84 20	LD (PCSPSA),IY	
2B2B: ED 5B 48 20	LD DE,(TFSCCCR)	; LOAD PC1 CURRENT READING
2B2F: AF	XOR A	
2B30: ED 52	SBC HL,DE	; CALCULATE PC1 ERROR
2B32: 3E 00	LD A,00	
2B34: 30 09	JR NC,PCSE	; IF PC1 E IS +VE
2B36: AF	XOR A	
2B37: EB	EX DE,HL	
2B38: 21 00 00	LD HL,0000	
2B3B: ED 52	SBC HL,DE	
2B3D: 3E 01	LD A,01	; IF PC1 E IS -VE
2B3F: 22 C8 20 PCSE	LD(PCETS),HL	; TEMP STORAGE OF PC1 E1
2B42: 32 CA 20	LD (PCESTS),A	; TEMP STORAGE OF PC1 E1 SIGN
2B45: FD 2A 86 20	LD IY,(PCESA)	; PC1 E STORAGE ADD.
2B49: FD 74 00	LD (IY+00),H	
2B4C: FD 75 01	LD (IY+01),L	; STORE PC1 E
2B4F: FD 23	INC IY	
2B51: FD 23	INC IY	
2B53: FD 22 86 20	LD (PCESA),IY	
2B57: FD 2A 88 20	LD IY,(PCESSA)	; PC1 E SIGN STORAGE ADD.
2B5B: FD 77 00	LD (IY+00),A	; STORE PC1 E
2B5E: FD 23	INC IY	
2B60: FD 22 88 20	LD (PCESSA),IY	

2B64: 01 00 00	PCMU1	LD BC,0000	
2B67: 21 00 00		LD HL,0000	
2B6A: ED 5B C8 20		LD DE,(PCETS)	; LOAD THE MULTIPLICAND (PC1 E1)
2B6E: 3A A0 20	PCLP1	LD A,(PCAIL)	; LOAD PC1 A1 (THE LSB)
2B71: 19	PCLP2	ADD HL,DE	
2B72: 03		INC BC	
2B73: B9		CP C	
2B74: 20 FB		JR NZ,PCLP2	
2B76: 3A A1 20		LD A,(PCAIM)	; LOAD MSB OF PC1 A1
2B79: B8		CP B	
2B7A: 20 F2		JR NZ,PCLP1	
2B7C: 22 0C 20		LD (PCAIETS),HL	; TEMP ST. OF PC1 A1 * E1
2B7F: FD 2A B6 20	PCMU2	LD IY,(PCESA)	; LOAD PC1 E(1-1) INTO DE
2B83: FD 56 FC		LD D,(IY+-4)	
2B86: FD 5E FD		LD E,(IY+-3)	
2B89: 01 00 00		LD BC,0000	
2B8C: 21 00 00		LD HL,0000	
2B8F: 3A A2 20	PCLP3	LD A,(PCA2L)	; LOAD PC1 A2 (LSB)
2B92: 19	PCLP4	ADD HL,DE	
2B93: 03		INC BC	
2B94: B9		CP C	
2B95: 20 FB		JR NZ,PCLP4	
2B97: 3A A3 20		LD A,(PCA2M)	; LOAD MSB OF PC1 A2
2B9A: B8		CP B	
2B9B: 20 F2		JR NZ,PCLP3	
2B9D: 22 0E 20		LD (PCA2ETS),HL	; TEMP ST. OF PC1 A2 * E(1-1)
2BA0: 2A 0C 20		LD HL,(PCAIETS)	; LOAD PC1 A1 * E1 INTO HL
2BA3: ED 5B CE 20		LD DE,(PCA2ETS)	; LOAD PC1 A2 * E(1-1) INTO DE
2BA7: FD 2A B8 20		LD IY,(PCESSA)	
2BA8: FD 46 FE		LD B,(IY+-2)	; LOAD PC1 E1-1 SIGN INTO B
2BAE: 3A CA 20		LD A,(PCESTS)	; LOAD PC1 E1 SIGN
2BB1: FE 00		CP 00	; CHECK SIGN PC1 E1
2BB3: 20 1C		JR NZ,PCNS1	
2BB5: 78		LD A,B	
2BB6: FE 00		CP 00	; CHECK SIGN PC1 E(1-1)
2BB8: 20 12		JR NZ,PCNS2	
2BBA: AF		XOR A	
2BBB: ED 52		SBC HL,DE	
2BBD: 3E 00		LD A,00	
2BBF: 30 2B		JR NC,PCSR1	
2BC1: EB		EX DE,HL	
2BC2: 21 00 00		LD HL,0000	
2BC5: AF		XOR A	
2BC6: ED 52		SBC HL,DE	
2BC8: 3E 01		LD A,01	
2BCA: 18 20		JR PCSR1	
2BCC: 19	PCNS2	ADD HL,DE	
2BCD: 3E 00		LD A,00	
2BCF: 18 1B		JR PCSR1	

2BD1: 78	PCNS1	LD A,B	
2BD2: FE 00		CP 00	
2BD4: 20 05		JR NZ,PCNS12	
2BD6: 19		ADD HL,DE	
2BD7: 3E 01		LD A,01	
2BD9: 18 11		JR PCSR1	
2BD8: EB	PCNS12	EX DE,HL	
2BDC: AF		XOR A	
2BDD: ED 52		SBC HL,DE	
2BDF: 3E 00		LD A,00	
2BE1: 30 09		JR NC,PCSR1	
2BE3: EB		EX DE,HL	
2BE4: 21 00 00		LD HL,0000	
2BE7: AF		XOR A	
2BE8: ED 52		SBC HL,DE	
2BEA: 3E 01		LD A,01	
2BEC: 22 00 20	PCSR1	LD (PCRTS),HL	; TEMP ST. OF PC1 R1
2BEF: 32 02 20		LD (PCRTS),A	; TEMP ST. OF PC1 R1 SIGN
2BF2: AF	PCLM1	XOR A	
2BF3: 3A A4 20		LD A,(PCSF)	; LOAD PC SF
2BF6: 47		LD B,A	
2BF7: 7C		LD A,H	
2BF8: 98		SBC A,B	
2BF9: 38 05		JR C,PCLM2	
2BFB: 21 FF 00		LD HL,00FFH	
2BFE: 18 33		JR PCSDR1	
2C00: AF	PCLM2	XOR A	
2C01: 7C		LD A,H	
2C02: DE 7F		SBC A,7FH	
2C04: 38 05		JR C,PCDIV	
2C06: 21 FF 00		LD HL,00FFH	
2C09: 18 28		JR PCSDR1	
2C0B: 3A A4 20	PCDIV	LD A,(PCSF)	
2C0E: 57		LD D,A	
2C0F: 1E 00		LD E,00	
2C11: 06 08		LD B,08	
2C13: 2A D0 20		LD HL,(PCRTS)	
2C16: 29	PCLP7	ADD HL,HL	
2C17: AF		XOR A	
2C18: ED 52		SBC HL,DE	
2C1A: 23		INC HL	
2C1B: 30 02		JR NC,PCNEXT	
2C1D: 19		ADD HL,DE	
2C1E: 2B		DEC HL	
2C1F: 10 FS	PCNEXT	DJNZ PCLP7	
2C21: AF		XOR A	
2C22: 3A A6 20		LD A,(PCSF2)	; LOAD PC1 SF/2
2C25: 9C		SBC A,H	
2C26: 30 09		JR NC,PCSDR	
2C28: 3E FF		LD A,FFH	
2C2A: BD		CP L	
2C2B: 28 04		JR Z,PCSDR	

2C2D: 3E 01		LD A,01	
2C2F: 85		ADD A,L	
2C30: 6F		LD L,A	
2C31: 26 00	PCSDR	LD H,00	
2C33: 22 04 20	PCSDR1	LD (PCDRTS),HL	; TEMP ST. OF PC1 DR
2C36: FD 2A 84 20		LD IY,(SSVOSA)	; GET THE PREVIOUS PC1 V.O.
2C3A: FD 56 FE		LD D,(IY+-2)	
2C3D: FD 5E FF		LD E,(IY+-1)	
2C40: 3A D2 20		LD A,(PCR1STS)	
2C43: FE 01		CP 01	; CHECK SIGN OF PC1 R1
2C45: 28 0B		JR Z,PCSUB2	
2C47: 19		ADD HL,DE	
2C48: 7C		LD A,H	
2C49: FE 00		CP 00	
2C4B: 28 1F		JR Z,PCSENDM	
2C4D: 21 FF 00		LD HL,00FFH	
2C50: 18 1A		JR PCSENDM	
2C52: AF	PCSUB2	XOR A	
2C53: EB		EX DE,HL	
2C54: ED 52		SBC HL,DE	
2C56: 30 14		JR NC,PCSENDM	
2C58: 21 00 00		LD HL,0000	; IF M... 0 PUT M=0
2C5B: 3E FF		LD A,FFH	
2C5D: 03 04		OUT (04),A	; SEND 0.0 SIGNAL TO THE SUPPLY
2C5F: 3E 00		LD A,00	; i.e. CLOSE THE VALVE
2C61: 03 0A		OUT (0AH),A	
2C63: 3E FF		LD A,FFH	; (7F)
2C65: 03 0B		OUT (0BH)	; LET MR=100% (IF MS=0 --- MR=100)
2C67: 16 00		LD D,00	
2C69: 5F		LD E,A	
2C6A: 18 1D		JR PCSTM	
2C6C: EB	PCSENDM	EX DE,HL	; DE HAS THE ACTUAL VALVE SIGNAL
2C6D: 21 00 01		LD HL,0100H	
2C70: 3E 00		LD A,00	
2C72: 03 04		OUT (04),A	; +VE VALVE SIGNAL
2C74: AF		XOR A	
2C75: ED 52		SBC HL,DE	; HL NOW HAS THE ADJUSTED SIGNAL
2C77: 7D			; DE STILL HAS THE ACTUAL SIGNAL
2C78: 03 0A		LD A,L	
2C7A: AF		OUT (0AH),A	; SEND THE SUPPLY VALVE OPENING
2C7B: 21 FF 00		XOR A	
2C7E: ED 52		LD HL,00FFH	; (7F)
2C80: 30 03		SBC HL,DE	; HL NOW HAS THE RSV OPENING
2C82: 21 00 00		JR NC,PCMR	
2C85: 7D	PCMR	LD HL,0000	
2C86: 03 0B		LD A,L	
2C88: EB		OUT (0BH),A	; SEND SIGNAL TO RSV
		EX DE,HL	; HL HAS SSV0 & DE HAS RSV0

2C89: FD 2A 84 20	PCSTM	LD IY,(SSVOSA)	
2C8D: FD 74 00		LD (IY+00),H	
2C90: FD 75 01		LD (IY+01),L	; STORE PC1 SSV OPENING
2C93: FD 23		INC IY	
2C95: FD 23		INC IY	
2C97: FD 22 84 20		LD (SSVOSA),IY	
2C9B: FD 2A 86 20		LD IY,(RSVOSA)	
2C9F: FD 72 00		LD (IY+00),D	
2CA2: FD 73 01		LD (IY+01),E	; STORE RSV0
2CA5: FD 23		INC IY	
2CA7: FD 23		INC IY	
2CA9: FD 22 86 20		LD (RSVOSA),IY	
2CAD: 2A CC 20		LD HL,(PCA1ETS)	
2CB0: FD 2A BA 20		LD IY,(PCA1ESA)	; PC1 A1*E1 STORAGE ADD.
2CB4: FD 74 00		LD (IY+00),H	; STORE PC1 A1*E1
2CB7: FD 23		INC IY	
2CB9: FD 75 00		LD (IY+00),L	
2CBC: FD 23		INC IY	
2CBE: FD 22 BA 20		LD (PCA1ESA),IY	
2CC2: 2A CE 20		LD HL,(PCA2ETS)	
2CC5: FD 2A BC 20		LD IY,(PCA2ESA)	; PC1 A2*E1-1 STORAGE ADD.
2CC9: FD 74 00		LD (IY+00),H	; STORE PC1 A2*E(1-1)
2CCC: FD 23		INC IY	
2CCE: FD 75 00		LD (IY+00),L	
2CD1: FD 23		INC IY	
2CD3: FD 22 BC 20		LD (PCA2ESA),IY	
2CD7: 2A D0 20		LD HL,(PCRITS)	
2CDA: FD 2A BE 20		LD IY,(PCRISA)	; PC1 R1=A1*E1-A2*E1-1 STORAGE
2CDE: FD 74 00		LD (IY+00),H	; STORE PC1 R1
2CE1: FD 23		INC IY	
2CE3: FD 75 00		LD (IY+00),L	
2CE6: FD 23		INC IY	
2CE8: FD 22 BE 20		LD (PCRISA),IY	
2CEC: 2A D4 20		LD HL,(PCDRTS)	
2CEF: FD 2A C2 20		LD IY,(PCDRSA)	; PC1 DR STORAGE ADD.
2CF3: FD 74 00		LD (IY+00),H	; STORE PC1 DR
2CF6: FD 23		INC IY	
2CF8: FD 75 00		LD (IY+00),L	
2CFB: FD 23		INC IY	
2CFD: FD 22 C2 20		LD (PCDRSA),IY	
2D01: 3A D2 20		LD A,(PCRISTS)	
2D04: FD 2A C0 20		LD IY,(PCR1SSA)	; PC1 R1 SIGN STORAGE ADD.
2D08: FD 77 00		LD (IY+00),A	; STORE PC1 R1 SIGN
2D0B: FD 23		INC IY	
2D0D: FD 22 C0 20		LD (PCR1SSA),IY	
2D11: AF		XOR A	
2D12: C9		RET	
2D13: FD 2A F2 20	HCONTM	LD IY,(HSPP)	
2D17: FD 66 00		LD H,(IY+00)	; GET HOLD SET POINT PROFILE
2D1A: FD 6E 01		LD L,(IY+01)	

2D1D: FD 23	INC IY	
2D1F: FD 23	INC IY	
2D21: FD 22 F2 20	LD (HSPP),IY	
2D25: FD 2A B4 20	LD IY,(PCSPSA) ; HOLD SET POINT STORAGE ADDRESS	
2D29: FD 74 00	LD (IY+00),H	
2D2C: FD 75 01	LD (IY+01),L ; STORE SET POINT	
2D2F: FD 23	INC IY	
2D31: FD 23	INC IY	
2D33: FD 22 B4 20	LD (PCSPSA),IY	
2D37: ED 5B 4A 20	LD DE,(THSCCR) ; CURRENT HOLD PRESS.READING	
2D3B: AF	XOR A	
2D3C: ED 52	SBC HL,DE ; CALCULATE THE ERROR (SP-CR)	
2D3E: 3E 00	LD A,00 ; ERROR IS +ve	
2D40: 30 09	JR NC,HSAVE	
2D42: AF	XOR A	
2D43: EB	EX DE,HL	
2D44: 21 00 00	LD HL,0000	
2D47: ED 52	SBC HL,DE	
2D49: 3E 01	LD A,01 ; ERROR IS -ve	
2D4B: 22 0B 21 HSAVE	LD (HETS),HL ; SAVE E1 (TEMP)	
2D4E: 32 0A 21	LD (HESTS),A ; SAVE E1 SIGN (TEMP)	
2D51: FD 2A B6 20	LD IY,(PCESA) ; HESA SHOULD BE THE SAME AS PCESA	
2D55: FD 74 00	LD (IY+00),H	
2D58: FD 75 01	LD (IY+01),L ; STORE THE ERROR	
2D5B: FD 23	INC IY	
2D5D: FD 23	INC IY	
2D5F: FD 22 B6 20	LD (PCESA),IY	
2D63: FD 2A B8 20	LD IY,(PCESSA);HESSA SHOULD = PCESSA	
2D6C: FD 22 B8 20	LD (PCESSA),IY	
2D70: CD F0 2D	CALL HPICONT	
2D73: FD 2A 70 20	LD IY,(PNCRAD)	
2D77: FD 66 00	LD H,(IY+00) ; SET PN SET POINT WITH PN C.R.	
2D7A: FD 6E 01	LD L,(IY+01)	
2D7D: FD 23	INC IY	
2D7F: FD 23	INC IY	
2D81: FD 22 70 20	LD (PNCRAD),IY	
2D85: FD 2A 74 20	LD IY,(PNSPSA)	
2D89: FD 74 00	LD (IY+00),H	
2D8C: FD 75 01	LD (IY+01),L	
2D8F: FD 23	INC IY	
2D91: FD 23	INC IY	
2D93: FD 22 74 20	LD (PNSPSA),IY	
2D97: FD 2A B0 20	LD IY,(PCCRAD) ; ADD OF PC1 CR STORAGE	
2D9B: FD 66 00	LD H,(IY+00)	
2D9E: FD 6E 01	LD L,(IY+01) ; LOAD PC1 CR INTO HL	
2DA1: FD 23	INC IY	
2DA3: FD 23	INC IY	
2DA5: FD 22 B0 20	LD (PCCRAD),IY	
2DA9: FD 2A C6 20	LD IY,(PC2CRAD) ; ADD OF PC2 CR STORAGE	
2DAD: FD 56 00	LD D,(IY+00)	

2DB0:	FD 5E 01		LD E,(IY+01)	; LOAD PC2 CR INTO DE
2DB3:	FD 23		INC IY	
2DB5:	FD 23		INC IY	
2DB7:	FD 22 06 20		LD (PC2CRAD),IY	
2DBB:	AF		XOR A	
2DBC:	ED 52		SBC HL,DE	
2DBE:	3E 00		LD A,00	
2DC0:	30 09		JR NC,PGS2	; IF PG IS +VE
2DC2:	AF		XOR A	
2DC3:	EB		EX DE,HL	
2DC4:	21 00 00		LD HL,0000	
2DC7:	ED 52		SBC HL,DE	
2DC9:	3E 01		LD A,01	; IF PG IS -VE
2DCB:	FD 2A 30 21	PGS2	LD IY,(PGCRAD)	; ADD. OF PG STORAGE
2DCF:	FD 74 00		LD (IY+00),H	
2DD2:	FD 75 01		LD (IY+01),L	; STORE PG
2DD5:	FD 23		INC IY	
2DD7:	FD 23		INC IY	
2DD9:	FD 22 30 21		LD (PGCRAD),IY	
2DDD:	FD 2A 34 21		LD IY,(PGSPSA)	; ADD. OF PG SET POINT STORAGE
2DE1:	FD 74 00		LD (IY+00),H	
2DE4:	FD 75 01		LD (IY+01),L	; STORE PG SET POINT
2DE7:	FD 23		INC IY	
2DE9:	FD 23		INC IY	
2DEB:	FD 22 34 21		LD (PGSPSA),IY	
2DEF:	C9		RET	
2DF0:	01 00 00	HPICONT	LD BC,0000	
2DF3:	21 00 00		LD HL,0000	
2DF6:	ED 5B 08 21		LD DE,(HETS)	; LOAD THE MULTIPLICAND (E1)
2DFA:	3A E0 20	HLP1	LD A,(HAIL)	; LOAD A1 (THE LSB)
2DFD:	19	HLP2	ADD HL,DE	
2DFE:	03		INC BC	
2DFF:	B9		CP C	
2E00:	20 FB		JR NZ,HLP2	
2E02:	3A E1 20		LD A,(HA1M)	; LOAD MSB OF A1
2E05:	B8		CP B	
2E06:	20 F2		JR NZ,HLP1	
2E08:	22 0C 21		LD (HA1ETS),HL	; TEMP STORAGE OF A1 * E1
2E0B:	FD 2A B6 20	HMU2	LD IY,(PCESA)	; LOAD E(1-1) INTO DE
2E0F:	FD 56 FC		LD D,(IY+4)	
2E12:	FD 5E FD		LD E,(IY+3)	
2E15:	01 00 00		LD BC,0000	
2E18:	21 00 00		LD HL,0000	
2E1B:	3A E2 20	HLP3	LD A,(HA2L)	; LOAD A2 (LSB)
2E1E:	19	HLP4	ADD HL,DE	
2E1F:	03		INC BC	
2E20:	B9		CP C	
2E21:	20 FB		JR NZ,HLP4	
2E23:	3A E3 20		LD A,(HA2M)	; LOAD MSB OF A2

2E26: B8		CP B	
2E27: 20 F2		JR NZ,HLP3	
2E29: 22 0E 21		LD (HA2ETS),HL ; TEMP STORAGE OF SAVE A2 * E(1-1)	
2E2C: 2A 0C 21		LD HL,(HA1ETS) ; LOAD A1*E1 INTO HL	
2E2F: ED 5B 0E 21		LD DE,(HA2ETS) ; LOAD A2*E(1-1) INTO DE	
2E33: FD 2A B8 20		LD IY,(PCSSA)	
2E37: FD 46 FE		LD B,(IY+2)	
2E3A: 3A 0A 21		LD A,(HESTS)	
2E3D: FE 00		CP 00 ; CHECK SIGN E1	
2E3F: 20 1C		JR NZ,HNS1	
2E41: 78		LD A,B	
2E42: FE 00		CP 00 ; CHECK SIGN E(1-1)	
2E44: 20 12		JR NZ,HNS2	
2E46: AF		XOR A	
2E47: ED 52		SBC HL,DE	
2E49: 3E 00		LD A,00	
2E4B: 30 2B		JR NC,HSR1	
2E4D: EB		EX DE,HL	
2E4E: 21 00 00		LD HL,0000	
2E51: AF		XOR A	
2E52: ED 52		SBC HL,DE	
2E54: 3E 01		LD A,01	
2E56: 18 20		JR HSR1	
2E58: 19	HNS2	ADD HL,DE	
2E59: 3E 00		LD A,00	
2E5B: 18 1B		JR HSR1	
2E5D: 78	HNS1	LD A,B	
2E5E: FE 00		CP 00	
2E60: 20 05		JR NZ,HNS12	
2E62: 19		ADD HL,DE	
2E63: 3E 01		LD A,01	
2E65: 18 11		JR HSR1	
2E67: EB	HNS12	EX DE,HL	
2E68: AF		XOR A	
2E69: ED 52		SBC HL,DE	
2E6B: 3E 00		LD A,00	
2E6D: 30 09		JR NC,HSR1	
2E6F: EB		EX DE,HL	
2E70: 21 00 00		LD HL,0000	
2E73: AF		XOR A	
2E74: ED 52		SBC HL,DE	
2E76: 3E 01		LD A,01	
2E78: 22 10 21	HSR1	LD (HRITS),HL ; TEMP ST. OF R1	
2E7B: 32 12 21		LD (HRISTS),A ; TEMP ST. OF R1 SIGN	
2E7E: AF	HLM1	XOR A	
2E7F: 3A E4 20		LD A,(HSF) ; LOAD SF	
2E82: 47		LD B,A	
2E83: 7C		LD A,H	
2E84: 98		SBC A,B	
2E95: 38 05		JR C,HLM2	

2E87: 21 FF 00		LD HL,00FFH	
2E8A: 18 33		JR HSDR1	
2E8C: AF	HLM2	XOR A	
2E8D: 7C		LD A,H	
2E8E: DE 7F		SBC A,7FH	
2E90: 38 05		JR C,HDIV	
2E92: 21 FF 00		LD HL,00FFH	
2E95: 18 28		JR HSDR1	
2E97: 3A E4 20	HDIV	LD A,(HSF)	
2E9A: 57		LD D,A	
2E9B: 1E 00		LD E,00	
2E9D: 06 08		LD B,08	
2E9F: 2A 10 21		LD HL,(HRITS)	
2EA2: 29	HLP7	ADD HL,HL	
2EA3: AF		XOR A	
2EA4: ED 52		SBC HL,DE	
2EA6: 23		INC HL	
2EA7: 30 02		JR NC,HNEXT	
2EA9: 19		ADD HL,DE	
2EAA: 2B		DEC HL	
2EAB: 10 F5	HNEXT	DJNZ HLP7	
2EAD: AF		XOR A	
2EAE: 3A E6 20		LD A,(HSF2)	
2EB1: 9C		SBC A,H	
2EB2: 30 09		JR NC,HSDR	
2EB4: 3E FF		LD A,FFH	
2EB6: 8D		CP L	
2EB7: 28 04		JR Z,HSDR	
2EB9: 3E 01		LD A,01	
2EBB: 85		ADD A,L	
2EBC: 6F		LD L,A	
2EBD: 26 00	HSDR	LD H,00	
2EBF: 22 14 21	HSDR1	LD (HDIRTS),HL	; SAVE DIVISION RESULT (TEMP)
2EC2: FD 2A 84 20		LD IY,(SSVOSA)	
2EC6: FD 56 FE		LD D,(IY+2)	; GET THE PREVIOUS VALVE OPENING
2EC9: FD 5E FF		LD E,(IY+1)	
2ECC: 3A 12 21		LD A,(HRITS)	
2ECF: FE 01		CP 01	; CHECK SIGN OF R1
2ED1: 28 08		JR Z,HSUB2	
2ED3: 19		ADD HL,DE	
2ED4: 7C		LD A,H	
2ED5: FE 00		CP 00	
2ED7: 28 1F		JR Z,HSENDM	
2ED9: 21 FF 00		LD HL,00FFH	
2EDC: 18 1A		JR HSENDM	
2EDE: AF	HSUB2	XOR A	
2EDF: EB		EX DE,HL	
2EE0: ED 52		SBC HL,DE	
2EE2: 30 14		JR NC,HSENDM	
2EE4: 21 00 00		LD HL,0000	; IF MS = 0 PUT MS = 0

2EE7: 3E FF		LD A,FFH	
2EE9: D3 04		OUT (04),A	; SEND 0.0 SIGNAL TO THE SUPPLY VALVE
2EEB: 3E 00		LD A,00	; i.e. CLOSE THE VALVE
2EED: D3 0A		OUT (0AH),A	
2EEF: 3E FF		LD A,00FFH	; (7F)
2EF1: D3 0B		OUT (0BH),A	; LET MR = 100% (IF MS=0--MR=100)
2EF3: 16 00		LD D,00	
2EF5: 5F		LD E,A	
2EF6: 18 10		JR HSTM	
2EF8: EB	HSENDM	EX DE,HL	; DE HAS THE ACTUAL VALVE SIGNAL
2EF9: 21 64 00		LD HL,0100	
2EFC: 3E 00		LD A,00	
2EFE: D3 04		OUT (04),A	; +VE VALVE SIGNAL
2F00: AF		XOR A	
2F01: ED 52		SBC HL,DE	; HL HAS NOW THE ADJUSTED SIGNAL
2F03:			; DE STILL HAS THE ACTUAL SIGNAL
2F03: 7D		LD A,L	
2F04: D3 0A		OUT (0AH),A	; SEND THE SUPPLY VALVE OPENING
2F06: AF		XOR A	
2F07: 21 FF 00		LD HL,00FFH	; (7F)
2F0A: ED 52		SBC HL,DE	; HL NOW HAS THE RSV OPENING
2F0C: 30 03		JR NC,HMR	
2F0E: 21 00 00		LD HL,0000	
2F11: 7D	HMR	LD A,L	
2F12: D3 0B		OUT (0BH),A	; SEND SIGNAL TO RSV
2F14: EB		EX DE,HL	; HL HAS SSVO & DE HAS RSVO
2F15: FD 2A 84 20	HSTM	LD IY,(SSVOSA)	
2F19: FD 74 00		LD (IY+00),H	
2F1C: FD 75 01		LD (IY+01),L	; STORE S. VALVE OPENING
2F1F: FD 23		INC IY	
2F21: FD 23		INC IY	
2F23: FD 22 84 20		LD (SSVOSA),IY	
2F27: FD 2A 86 20		LD IY,(RSVOSA)	
2F2B: FD 72 00		LD (IY+00),D	
2F2E: FD 73 01		LD (IY+01),E	; STORE RELIEF VALVE OPENING
2F31: FD 23		INC IY	
2F33: FD 23		INC IY	
2F35: FD 22 86 20		LD (RSVOSA),IY	
2F39: 2A 0C 21		LD HL,(HA1ETS)	
2F3C: FD 2A BA 20		LD IY,(PCA1ESA)	
2F40: FD 74 00		LD (IY+00),H	; STORE A1 * E1
2F43: FD 23		INC IY	
2F45: FD 75 00		LD (IY+00),L	
2F48: FD 23		INC IY	
2F4A: FD 22 BA 20		LD (PCA1ESA),IY	
2F4E: 2A 0E 21		LD HL,(HA2ETS)	
2F51: FD 2A BC 20		LD IY,(PCA2ESA)	
2F55: FD 74 00		LD (IY+00),H	; STORE A2 * E(1-1)
2F58: FD 23		INC IY	

2F5A: FD 75 00	LD (IY+00),L	
2F5D: FD 23	INC IY	
2F5F: FD 22 BC 20	LD (PCA2ESA),IY	
2F63: 2A 10 21	LD HL,(HRITS)	
2F66: FD 2A BE 20	LD IY,(PCRISA)	
2F6A: FD 74 00	LD (IY+00),H	; STORE R1=A1+E1-A2*(1-1)
2F6D: FD 23	INC IY	
2F6F: FD 75 00	LD (IY+00),L	
2F72: FD 23	INC IY	
2F74: FD 22 BE 20	LD (PCRISA),IY	
2F78: 2A 14 21	LD HL,(HDIRTS)	
2F7B: FD 2A C2 20	LD IY,(PCDRSA)	
2F7F: FD 74 00	LD (IY+00),H	; STORE DIVISION RESULT
2F82: FD 23	INC IY	
2F84: FD 75 00	LD (IY+00),L	
2F87: FD 23	INC IY	
2F89: FD 22 C2 20	LD (PCDRSA),IY	
2F8D: 3A 12 21	LD A,(HRISTS)	
2F90: FD 2A C0 20	LD IY,(PCRISA)	
2F94: FD 77 00	LD (IY+00),A	; STORE SIGN OF R1
2F97: FD 23	INC IY	
2F99: FD 22 C0 20	LD (PCRISA),IY	
2F9D: AF	XOR A	
2F9E: C9	RET	
2F9F: ED 5B 44 21	LD DE,(PGTS)	; LOAD PG CURRENT PENDING
2FA3: FD 2A 30 21	LD IY,(PGCRAD)	; ADD OF PG STORAGE
2FA7: FD 72 00	LD (IY+00),D	
2FAA: FD 73 01	LD (IY+01),E	; STORE PG
2FAD: FD 23	INC IY	
2FAF: FD 23	INC IY	
2FB1: FD 22 30 21	LD (PGCRAD),IY	
2FB5: FD 2A 32 21	LD IY,(PGSPP)	; ADD OF PG SET POINT PROFILE
2FB9: FD 66 00	LD H,(IY+00)	
2FBC: FD 6E 01	LD L,(IY+01)	; LOAD PG SET POINT INTO HL
2FBF: FD 23	INC IY	
2FC1: FD 23	INC IY	
2FC3: FD 22 32 21	LD (PGSPP),IY	
2FC7: FD 2A 34 21	LD IY,(PGSPSA)	; ADD. OF PG SET POINT STORAGE
2FCB: FD 74 00	LD (IY+00),H	
2FCE: FD 75 01	LD (IY+01),L	; STORE PG SET POINT
2FD1: FD 23	INC IY	
2FDD: FD 23	INC IY	
2FDE: FD 22 34 21	LD (PGSPSA),IY	
2FD9: AF	XOR A	
2FDA: ED 52	SBC HL,DE	; CALCULATE PG ERROR
2FDC: 3E 00	LD A,00	
2FDE: 30 09	JR NC,SPGE	; IF E IS +VE
2FE0: AF	XOR A	
2FE1: EB	EX DE,HL	
2FE2: 21 00 00	LD HL,0000	

2FE5: ED 52		SBC HL,DE	
2FE7: 3E 01		LD A,01	; IF E IS -VE
2FE9: 22 48 21	SPGE	LD (PGETS),HL	; TEMP STORAGE FOR PG E1
2FEC: 32 38 21		LD (PGESSA),A	; TEMP STORAGE FOR PG E1 SIGN
2FEF: FD 2A 36 21		LD IY,(PGESA)	; ADD OF PG E STORAGE
2FF3: FD 74 00		LD (IY+00),H	
2FF6: FD 75 01		LD (IY+01),L	; STORE PG ERROR
2FF9: FD 23		INC IY	
2FFB: FD 23		INC IY	
2FFD: FD 22 36 21		LD (PGESA),IY	
3001: FD 2A 38 21		LD IY,(PGESSA)	; ADD OF PG E SIGN STORAGE
3005: FD 77 00		LD (IY+00),A	; STORE PG E SIGN
3008: FD 23		INC IY	
300A: FD 22 38 21		LD (PGESSA),IY	
300E: 01 00 00	PGMU1	LD BC,0000	
3011: 21 00 00		LD HL,0000	
3014: ED 5B 48 21		LD DE,(PGETS)	; LOAD THE MULTIPLICAND (PG E1)
3018: 3A 20 21	PGLP1	LD A,(PGAIL)	; LOAD PG A1 (THE LSB)
301B: 19	PGLP2	ADD HL,DE	
301C: 03		INC BC	
301D: B9		CP C	
301E: 20 FB		JR NZ,PGLP2	
3020: 3A 21 21		LD A,(PGA1M)	; LOAD MSB OF PG A1
3023: B8		CP B	
3024: 20 F2		JR NZ,PGLP1	
3026: 22 4C 21		LD (PGA1ETS),HL	; TEMP ST. OF PG A1 * E1
3029: FD 2A 36 21	PGMU2	LD IY,(PGESA)	
302D: FD 56 FC		LD D,(IY+-4)	; LOAD PG E(1-1) INTO DE
3030: FD 5E FD		LD E,(IY+-3)	
3033: 01 00 00		LD BC,0000	
3036: 21 00 00		LD HL,0000	
3039: 3A 22 21	PGLP3	LD A,(PGA2L)	; LOAD PG A2 (LSB)
303C: 19	PGLP4	ADD HL,DE	
303D: 03		INC BC	
303E: B9		CP C	
303F: 20 FB		JR NZ,PGLP4	
3041: 3A 23 21		LD A,(PGA2M)	; LOAD MSB OF PG A2
3044: B8		CP B	
3045: 20 F2		JR NZ,PGLP3	
3047: 22 4E 21		LD (PGA2ETS),HL	; TEMP ST. OF PG A2 * E(1-1)
304A: 2A 4C 21		LD HL,(PGA1ETS)	; LOAD PG A1 * E1 INTO HL
304D: ED 5B 4E 21		LD DE,(PGA2ETS)	; LOAD PG A2 * E(1-1) INTO DE
3051: FD 2A 56 21		LD IY,(PGSSA)	
3055: FD 46 FE		LD B,(IY+-2)	; LOAD PG E1-1 SIGN INTO B
3058: 3A 4A 21		LD A,(PGESTS)	; LOAD PG E1 SIGN
305B: FE 00		CP 00	; CHECK SIGN PG E1
305D: 20 1C		JR NZ,PGNS1	
305F: 78		LD A,B	

3060: FE 00		CP 00	; CHECK SIGN PG E(1-1)
3062: 20 12		JR NZ,PGNS2	
3064: AF		XOR A	
3065: ED 52		SBC HL,DE	
3067: 3E 00		LD A,00	
3069: 30 28		JR NC,PGSR1	
306B: EB		EX DE,HL	
306C: 21 00 00		LD HL,0000	
306F: AF		XOR A	
3070: ED 52		SBC HL,DE	
3072: 3E 01		LD A,01	
3074: 18 20		JR PGSR1	
3076: 19	PGNS2	ADD HL,DE	
3077: 3E 00		LD A,00	
3079: 18 18		JR PGSR1	
307B: 78	PGNS1	LD A,B	
307C: FE 00		CP 00	
307E: 20 05		JR NZ,PGNS12	
3080: 19		ADD HL,DE	
3081: 3E 01		LD A,01	
3083: 18 11		JR PGSR1	
3085: EB	PGNS12	EX DE,HL	
3086: AF		XOR A	
3087: ED 52		SBC HL,DE	
3089: 3E 00		LD A,00	
308B: 30 09		JR NC,PGSR1	
308D: EB		EX DE,HL	
308E: 21 00 00		LD HL,0000	
3091: AF		XOR A	
3092: ED 52		SBC HL,DE	
3094: 3E 01		LD A,01	
3096: 22 50 21	PGSR1	LD (PGRITS),HL	; TEMP ST. OF PG R1
3099: 32 52 21		LD (PGRISTS),A	; TEMP ST. OF PG R1 SIGN
309C: AF	PGLM1	XOR A	
309D: 3A 24 21		LD A,(PGSF)	; LOAD PG SF
30A0: 47		LD B,A	
30A1: 7C		LD A,H	
30A2: 98		SBC A,B	
30A3: 38 05		JR C,PGLM2	
30A5: 21 FF 00		LD HL,00FFH	
30A8: 18 33		JR PGSDR1	
30AA: AF	PGLM2	XOR A	
30AB: 7C		LD A,H	
30AC: DE 7F		SBC A,7FH	
30AE: 38 05		JR C,PGDIV	
30B0: 21 FF 00		LD HL,00FFH	
30B3: 18 28		JR PGSDR1	

30B5: 3A 24 21	PGDIV	LD A,(PGSF)	
30B8: 57		LD D,A	
30B9: 1E 00		LD E,00	
30BB: 06 08		LD B,08	
30BD: 2A 50 21		LD HL,(PGRITS)	
30C0: 29	PGLP7	ADD HL,HL	
30C1: AF		XOR A	
30C2: ED 52		SBC HL,DE	
30C4: 23		INC HL	
30C5: 30 02		JR NC,PGNEXT	
30C7: 19		ADD HL,DE	
30C8: 28		DEC HL	
30C9: 10 F5	PGNEXT	DJNZ PGLP7	
30CB: AF		XOR A	
30CC: 3A 26 21		LD A,(PGSF2)	; LOAD PG SF/2
30CF: 9C		SBC A,H	
30D0: 30 09		JR NC,PGSDR	
30D2: 3E FF		LD A,FFH	
30D4: BD		CP L	
30D5: 28 04		JR Z,PGSDR	
30D7: 3E 01		LD A,01	
30D9: 85		ADD A,L	
30DA: 6F		LD L,A	
30DB: 26 00	PGSDR	LD H,00	
30DD: 22 54 21	PGSDR1	LD (PGDRTS),HL	; TEMP ST. OF PG DR
30E0: FD 2A 84 20		LD IY,(SSVOSA)	
30E4: FD 56 FE		LD D,(IY+-2)	; GET THE PREVIOUS SSV.O.
30E7: FD 5E FF		LD E,(IY+-1)	
30EA: 3A 52 21		LD A,(PGRISTS)	
30ED: FE 01		CP 01	; CHECK SIGN OF PG R1
30EF: 28 0B		JR Z,PGSUB2	
30F1: 19		ADD HL,DE	
30F2: 7C		LD A,H	
30F3: FE 00		CP 00	
30F5: 28 1F		JR Z,PGSENDM	
30F7: 21 FF 00		LD HL,00FFH	
30FA: 18 1A		JR PGSENDM	
30FC: AF	PGSUB2	XOR A	
30FD: EB		EX DE,HL	
30FE: ED 52		SBC HL,DE	
3100: 30 14		JR NC,PGSENDM	
3102: 21 00 00		LD HL,0000	; IF M = 0 PUT M=0
3105: 3E FF		LD A,FFH	
3107: D3 04		OUT (04),A	; SEND 0.0 SIGNAL TO THE VALVE,
3109: 3E 00		LD A,00	; i.e. CLOSE THE VALVE
310B: D3 0A		OUT (0AH),A	
310D: 3E FF		LD A,FFH	; IF LET MR=100% (IFMS=0.0 -->MR=100)
310F: D3 0B		OUT (0BH),A	
3111: 16 00		LD D,00	
3113: 5F		LD E,A	
3114: 18 1D		JR PGSTM	

3116: EB	PGSENDM	EX DE,HL	
3117: 21 00 01		LD HL,0100H	
311A: 3E 00		LD A,00	
311C: D3 04		OUT (04),A	; +VE VALVE SIGNAL
311E: AF		XOR A	
311F: ED 52		SBC HL,DE	; HL NOW HAS THE ADJUSTED SIGNAL
3121:			; DE STILL HAS THE ACTUAL SIGNAL
3121: 7D		LD A,L	
3122: D3 0A		OUT (0AH),A	; SEND THE VALUE OF PG V.O.
3124: AF		XOR A	
3125: 21 FF 00		LD HL,00FFH	; /7F
3128: ED 52		SBC HL,DE	; HL NOW HAS THE RSV OPENING
312A: 30 03		JR NC,PGMR	
312C: 21 00 00		LD HL,0000	
312F: 7D	PGMR	LD A,L	
3130: D3 0B		OUT (0BH),A	
3132: EB		EX DE,HL	
3133: FD 2A 84 20	PGSTM	LD IY,(SSVOSA)	
3137: FD 74 00		LD (IY+00),H	
313A: FD 75 01		LD (IY+01),L	; STORE PG SSV OPENING
313D: FD 23		INC IY	
313F: FD 23		INC IY	
3141: FD 22 84 20		LD (SSVOSA),IY	
3145: FD 2A 86 20		LD IY,(RSVOSA)	
3149: FD 72 00		LD (IY+00),D	
314C: FD 73 01		LD (IY+01),E	; STORE PG RSV OPENING
314F: FD 23		INC IY	
3151: FD 23		INC IY	
3153: FD 22 86 20		LD (RSVOSA),IY	
3157: 2A 4C 21		LD HL,(PGA1ETS)	
315A: FD 2A 3A 21		LD IY,(PGA1ESA)	; ADD. OF PG A1*E1 STORAGE
315E: FD 74 00		LD (IY+00),H	; STORE PG A1*E1
3161: FD 23		INC IY	
3163: FD 75 00		LD (IY+00),L	
3166: FD 23		INC IY	
3168: FD 22 3A 21		LD (PGA1ESA),IY	
316C: 2A 4E 21		LD HL,(PGA2ETS)	
316F: FD 2A 3C 21		LD IY,(PGA2ESA)	; ADD. OF PG A2*E1-1 STORAGE
3173: FD 74 00		LD (IY+00),H	; STORE PG A2*E(1-1)
3176: FD 23		INC IY	
3178: FD 75 00		LD (IY+00),L	
317B: FD 23		INC IY	
317D: FD 22 3C 21		LD (PGA2ESA),IY	
3181: 2A 50 21		LD HL,(PGR1TS)	
3184: FD 2A 3E 21		LD IY,(PGR1SA)	; ADD. OF PG R1 STORAGE
3188: FD 74 00		LD (IY+00),H	; STORE PG R1
318B: FD 23		INC IY	
318D: FD 75 00		LD (IY+00),L	
3190: FD 23		INC IY	
3192: FD 22 3E 21		LD (PGR1SA),IY	
3196: 2A 54 21		LD HL,(PGDRTS)	
3199: FD 2A 42 21		LD IY,(PGDRSA)	; ADD. OF PG DR STOPAGE

319D: FD 74 00		LD (IY+00),H	; STORE PG DR
31A0: FD 23		INC IY	
31A2: FD 75 00		LD (IY+00),L	
31A5: FD 23		INC IY	
31A7: FD 22 42 21		LD (PGDRSA),IY	
31AB: 3A 52 21		LQ A,(PGRISTS)	
31AE: FD 2A 40 21		LD IY,(PGRISSA)	; ADD. OF PG R1 SIGN STORAGE
31B2: FD 77 00		LD (IY+00),A	; STORE PG R1 SIGN
31B5: FD 23		INC IY	
31B7: FD 22 40 21		LD (PGR1SSA),IY	
31BB: AF		XOR A	
31BC: C9		RET	
31BD: 3A 53 20	PNIADR	LD A,(ISVOF)	; SSV INITIAL OPENING FOR FILLING
31C0: FD 2A 84 20		LD IY,(SSVOSA)	; ADD. OF SSV OPENING STORAGE ADD.
31C4: FD 36 00 00		LD (IY+00),00	
31C8: FD 77 01		LD (IY+01),A	
31CB: FD 23		INC IY	
31CD: FD 23		INC IY	
31CF: FD 22 84 20		LD (SSVOSA),IY	
31D3: 3A 56 20		LD A,(IRSV0)	; RSU INITIAL OPENING
31D6: FD 2A 86 20		LD IY,(RSVOSA)	; ADD OF RSU OPENING STORAGE ADD.
31DA: FD 36 00 00		LD (IY+00),00	
31DE: FD 77 01		LD (IY+01),A	
31E1: FD 23		INC IY	
31E3: FD 23		INC IY	
31E5: FD 22 86 20		LD (RSVOSA),IY	
31E9: 2A 96 20		LD HL,(PNCRTS)	; PN CURRENT READING
31EC: FD 2A 74 20		LD IY,(PNSPSA)	; ADD. OF PN SET POINT STORAGE
31F0: FD 74 00		LD (IY+00),H	
31F3: FD 75 01		LD (IY+01),L	
31F6: FD 23		INC IY	
31F9: FD 23		INC IY	
31FA: FD 22 74 20		LD (PNSPSA),IY	
31FE: FD 2A 76 20	PNIADR1	LD IY,(PNESA)	; ADD. OF PN ERROR STORAGE
3202: FD 36 00 00		LD (IY+00),00	
3206: FD 36 01 00		LD (IY+01),00	
320A: FD 23		INC IY	
320C: FD 23		INC IY	
320E: FD 22 76 20		LD (PNESA),IY	
3212: FD 2A 78 20		LD IY,(PNESSA)	; ADD. OF PN ERROR SIGN STORAGE
3216: FD 36 00 00		LD (IY+00),00	
321A: FD 23		INC IY	
321C: FD 22 78 20		LD (PNESSA),IY	
3220: FD 2A 7A 20		LD IY,(PNA1ESA)	; ADD. OF PN A1*E1
3224: FD 36 00 00		LD (IY+00),00	
3228: FD 36 01 00		LD (IY+01),00	
322C: FD 23		INC IY	
322E: FD 23		INC IY	
3230: FD 22 7A 20		LD (PNA1ESA),IY	
3234: FD 2A 7C 20		LD IY,(PNA2ESA)	; ADD. OF PN A2*E(1-1)
3238: FD 36 00 00		LD (IY+00),00	

323C: FD 36 01 00	LD (IY+01),00	
3240: FD 23	INC IY	
3242: FD 23	INC IY	
3244: FD 22 7C 20	LD (PNA2ESA),IY	
3248: FD 2A 7E 20	LD IY,(PNRISA) ; ADD. OF PN R1=A1+E1-A2+E1-1	
324C: FD 36 00 00	LD (IY+00),00	
3250: FD 36 01 00	LD (IY+01),00	
3254: FD 23	INC IY	
3256: FD 23	INC IY	
3258: FD 22 7E 20	LD (PNRISA),IY	
325C: FD 2A 82 20	LD IY,(PNDRSA) ; ADD. OF PN DR STORAGE	
3260: FD 36 00 00	LD (IY+00),00	
3264: FD 36 01 00	LD (IY+01),00	
3268: FD 23	INC IY	
326A: FD 23	INC IY	
326C: FD 22 82 20	LD (PNDRSA),IY	
3270: FD 2A 80 20	LD IY,(PNRISSA) ; ADD. OF PN RI SIGN STORAGE	
3274: FD 36 00 00	LD (IY+00),00	
3278: FD 23	INC IY	
327A: FD 22 80 20	LD (PNRISSA),IY	
327E: C9	RET	
327F: 21 8C 01	LD HL,018CH	PCIADR
3282: FD 2A B4 20	LD IY,(PCSPSA) ; ADD. OF PCI SET POINT STORAGE	
3286: FD 74 00	LD (IY+00),H	
3289: FD 75 01	LD (IY+01),L	
328C: FD 23	INC IY	
328E: FD 23	INC IY	
3290: FD 22 B4 20	LD (PCSPSA),IY	
3294: FD 2A B6 20	LD IY,(PCESA) ; ADD. OF PCI ERROR STORAGE	PCIADR1
3298: FD 36 00 00	LD (IY+00),00	
329C: FD 36 01 00	LD (IY+01),00	
32A0: FD 23	INC IY	
32A2: FD 23	INC IY	
32A4: FD 22 B6 20	LD (PCESA),IY	
32A8: FD 2A B8 20	LD IY,(PCESSA) ; ADD. OF PCI ERROR SIGN STORAGE	
32AC: FD 36 00 00	LD (IY+00),00	
32B0: FD 23	INC IY	
32B2: FD 22 B8 20	LD (PCESSA),IY	
32B6: FD 2A BA 20	LD IY,(PCAIESA) ; ADD. OF PCI A1+E1	
32BA: FD 36 00 00	LD (IY+00),00	
32BE: FD 36 01 00	LD (IY+01),00	
32C2: FD 23	INC IY	
32C4: FD 23	INC IY	
32C6: FD 22 BA 20	LD (PCAIESA),IY	
32CA: FD 2A BC 20	LD IY,(PCA2ESA) ; ADD. OF PCI A2+E(1-1)	
32CE: FD 36 00 00	LD (IY+00),00	
32D2: FD 36 01 00	LD (IY+01),00	
32D6: FD 23	INC IY	
32D8: FD 23	INC IY	

32DA: FD 22 BC 20	LD (PCA2ESA), IY
32DE: FD 2A BE 20	LD IY, (PCRISA) ; ADD. OF PC1 R1=A1+E1-A2+E1-1
32E2: FD 36 00 00	LD (IY+00), 00
32E6: FD 36 01 00	LD (IY+01), 00
32EA: FD 23	INC IY
32EC: FD 23	INC IY
32EE: FD 22 BE 20	LD (PCRISA), IY
32F2: FD 2A C2 20	LD IY, (PCDRSA) ; ADD. OF PC1 DR STORAGE
32F6: FD 36 00 00	LD (IY+00), 00
32FA: FD 36 01 00	LD (IY+01), 00
32FE: FD 23	INC IY
3300: FD 23	INC IY
3302: FD 22 C2 20	LD (PCDRSA), IY
3306: FD 2A C0 20	LD IY, (PCR1SSA) ; ADD. OF PC1 R1 SIGN STORAGE
330A: FD 36 00 00	LD (IY+00), 00
330E: FD 23	INC IY
3310: FD 22 C0 20	LD (PCR1SSA), IY
3314: C9	RET
3315: 2A 9C 20 PGIADR	LD HL, (PC1CRTS) ; LOAD PC1 CURRENT READING
3318: ED 58 9E 20	LD DE, (PC2CRTS) ; LOAD PC2 CURRENT READING
331C: AF	XOR A
331D: ED 52	SBC HL, DE
331F: FD 2A 30 21	LD IY, (PGCRAD) ; ADD OF PG STORAGE
3323: FD 74 00	LD (IY+00), H
3326: FD 75 01	LD (IY+01), L ; STORE PG
3329: FD 23	INC IY
332B: FD 23	INC IY
332D: FD 22 30 21	LD (PGCRAD), IY
3331: FD 2A 34 21	LD IY, (PGSPSA) ; ADD. OF PG SET POINT STORAGE
3335: FD 74 00	LD (IY+00), H
3338: FD 75 01	LD (IY+01), L ; STORE PG SET POINT
333B: FD 23	INC IY
333D: FD 23	INC IY
333F: FD 22 34 21	LD (PGSPSA), IY
3343: FD 2A 36 21	LD IY, (PGESA) ; ADD. OF PG ERROR STORAGE
3347: FD 36 00 00	LD (IY+00), 00
334B: FD 36 01 00	LD (IY+01), 00
334F: FD 23	INC IY
3351: FD 23	INC IY
3353: FD 22 36 21	LD (PGESA), IY
3357: FD 2A 38 21	LD IY, (PGESSA) ; ADD. OF PG ERROR SIGN STORAGE
335B: FD 36 00 00	LD (IY+00), 00
335F: FD 23	INC IY
3361: FD 22 38 21	LD (PGESSA), IY
3365: FD 2A 3A 21	LD IY, (PGA1ESA) ; ADD. OF PG A1+E1
3369: FD 36 00 00	LD (IY+00), 00
336D: FD 36 01 00	LD (IY+01), 00
3371: FD 23	INC IY
3373: FD 23	INC IY
3375: FD 22 3A 21	LD (PGA1ESA), IY

```

21      LD IY,(PGA2ESA) ; ADD. OF PG  A2+E(1-1)
00      LD (IY+00),00
00      LD (IY+01),00
        INC IY
        INC IY
21      LD (PGA2ESA),IY
21      LD IY,(PGR1SA) ; ADD. OF PG  R1=A1+E1-A2+E1-1
00      LD (IY+00),00
00      LD (IY+01),00
        INC IY
        INC IY
21      LD (PGR1SA),IY
21      LD IY,(PGDRSA) ; ADD. OF PG  DR STORAGE
00      LD (IY+00),00
00      LD (IY+01),00
        INC IY
        INC IY
21      LD (PGDRSA),IY
21      LD IY,(PGR1SSA) ; ADD. OF PG  R1'SIGN STORAGE
00      LD (IY+00),00
        INC IY
21      LD (PGR1SSA),IY
        RET
        END

```